IOWA STATE UNIVERSITY
Digital Repository

Retrospective Theses and Dissertations

Iowa State University Capstones, Theses and Dissertations

1991

Dimerization kinetics and products of [alpha]-substituted o-quinodimethanes derived from benzene and furan

Man-kit Leung
Iowa State University

Follow this and additional works at: https://lib.dr.iastate.edu/rtd

Part of the Organic Chemistry Commons

3

92

07250

INFORMATION TO USERS

U·M·I

Dimerization kinetics and products of α-substituted
o-quinodimethanes derived from benzene and furan

Leung, Man-kit, Ph.D.

Iowa State University, 1991

Dimerization kinetics and products of α-substituted

o-quinodimethanes derived from benzene and furan

by

Man-kit Leung

A Dissertation Submitted to the

Graduate Faculty in Partial Fulfillment of the

Requirements for the Degree of

DOCTOR OF PHILOSOPHY

Department: Chemistry
Major: Organic Chemistry

Approved:

Signature was redacted for privacy.

In Charge of Major Work

Signature was redacted for privacy.

Fhr the Major Department

Signature was redacted for privacy.

For the Graduate College

Iowa State University
Ames, Iowa

1991

TABLE OF CONTENTS

iv

LIST OF FIGURES

LIST OF TABLES

1

GENERAL INTRODUCTION

For the last decade, the Trahanovsky research group has focused on the study of various reactive molecules such as benzocyclobutadiene and o-quinodimethanes (o-QDM's) derived from benzene, furan, thiophene, and ferrocene. These types of molecules are very reactive and dimerize or polymerize even at low temperature. One of our group's interests is to understand the dimerization mechanism of these molecules.

Section 1 describes the preparation and dimerization product analyses of α–methyl substituted 2,3-dimethylene-2,3-dihydrofurans. Insights provided by these results into the mechanism of the dimerization of 2,3-dimethylene-2,3-dihydrofuran are discussed.

In Section 2, the preparation of α–methyl, α–cyclopropyl, α–t-butyl, and α–mesityl substituted o-xylylenes, the kinetics and product analyses of their dimerizations and their Diels-Alder reactions with methyl methacrylate as a dienophile are described. On the basis of the trends of the regioselectivity, mechanisms for the Diels-Alder reaction and for the dimerization are proposed.

EXPLANATION OF DISSERTATION FORMAT

This dissertation has been written using the alternate dissertation format and consists of two sections as complete papers in the style suitable for publication in a journal published by the American Chemical Society. As such, each section has its own numbering system and each section's references follow it. The research described in the results and experimental sections were done by the author unless otherwise indicated.

SECTION 1:   THE EFFECTS OF α-METHYL GROUP SUBSTITUTION ON THE
DIMERIZATION PRODUCTS OF o-QUINODIMETHANES DERIVED
FROM FURAN [1]

INTRODUCTION

2,3-Dimethylene-2,3-dihydrofuran (1), the furan-based o-quinodimethane (o-QDM), has been studied extensively by our research group during the past decade.[2-5] Much of our work has focused on the mechanism of the dimerization of 1 which occurs readily in solution at temperatures above -30 °C. Of special interest is the fact that the dimerization gives almost quantitatively the head-to-head [4+4] dimer 2.[2] On the basis of a secondary deuterium kinetic isotope effect study, it was concluded
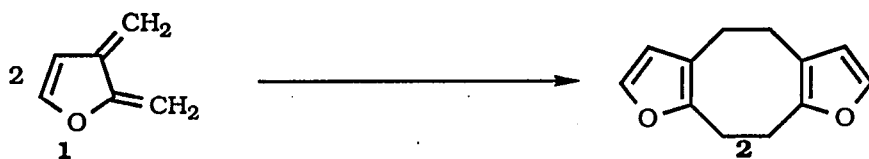
that the cyclization involves rate-determining formation of diradical 3, followed by rapid closure of the diradical to give the dimer.[3, 5a] Additional support for this
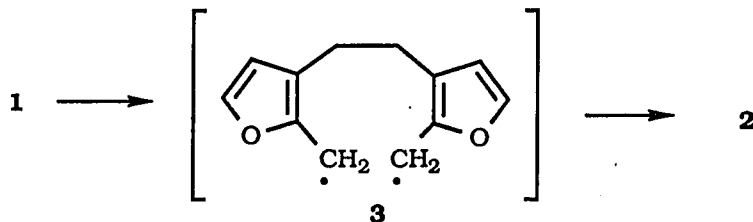
two-step mechanism was obtained from a study of the effects on the dimerization rates and products of a tert-butyl group on either the 3-methylene or 2-methylene group.[5b]

A question that has not yet been answered is why does the intermediate diradical 3 close to give predominantly the [4+4] dimer.[6] Some simple derivatives of 1, give a fair amount of the [4+2] dimers expected from closure of the intermediate diradical[5a,b] and many indole-based,[7] thiophene-based,[8] and benzene-based[9] o-QDM's give predominantly or exclusively [4+2] dimers. For example, the tert-butyl derivative 4[5b] gives a high yield of two stereoisomeric [4+2] dimers (5) and a small amount of [4+4] dimer 6, the dimers expected from diradical 7.
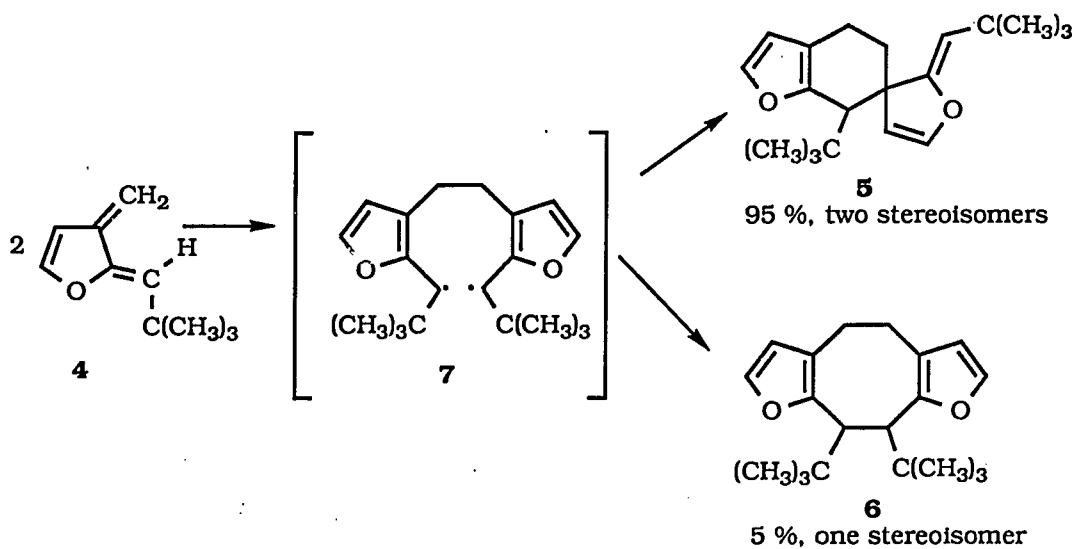
One of the possible factors affecting the mode of cyclization[10] is the conformation of the diradical which might be determined by the relative orientation of the o-QDM monomers in the transition state of the first step of dimerization. Collision of the monomers may lead to cisoid transition state **8** or transoid transition state **9** which develop to diradical conformations **10** and **11**, respectively, and each
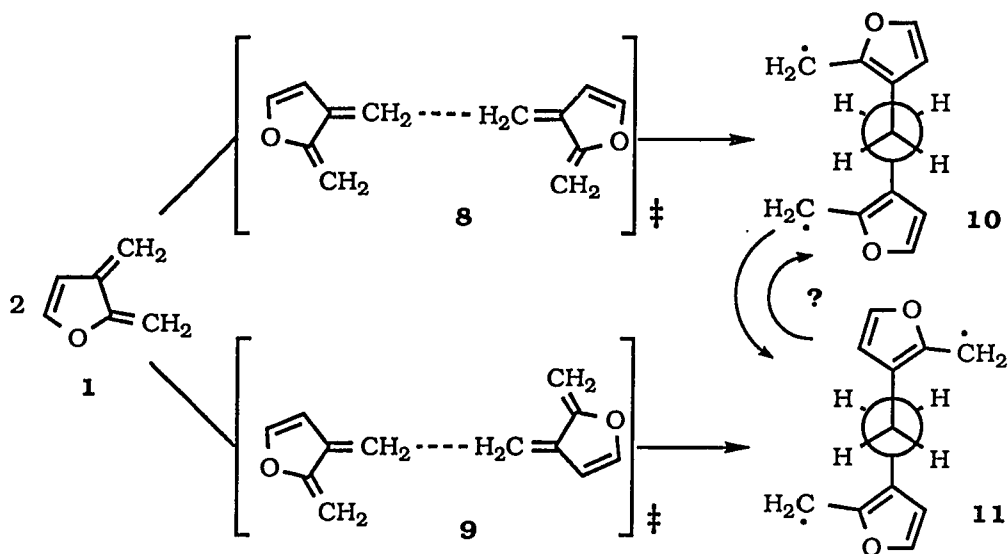
conformation may lead to different cyclization products. If cyclization of the diradicals occurs before **10** and **11** equilibrate, the relative rate of formation of **10** and **11** may control the distribution of cyclization products. On the other hand, if the equilibrium between **10** and **11** is established before cyclization occurs, the existence of two different transition states, **8** and **9**, will make no difference in the overall cyclization process.[11]

In an attempt to gain information about the formation of the intermediate diradical and its closure to products, we initiated a study of the derivatives of **1** with methyl groups on the termini of the reactive diene unit, o-QDM's **12**, **13**, and **14**. We
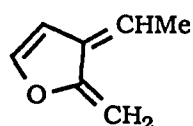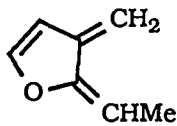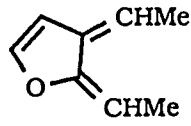
expected that a methyl group on the 3-methylene group would have the E configuration and this would allow us to probe the relative importance of transition states **8** and **9** by studying the stereochemistry of the final dimers. The results of this study are reported in this section of the dissertation.
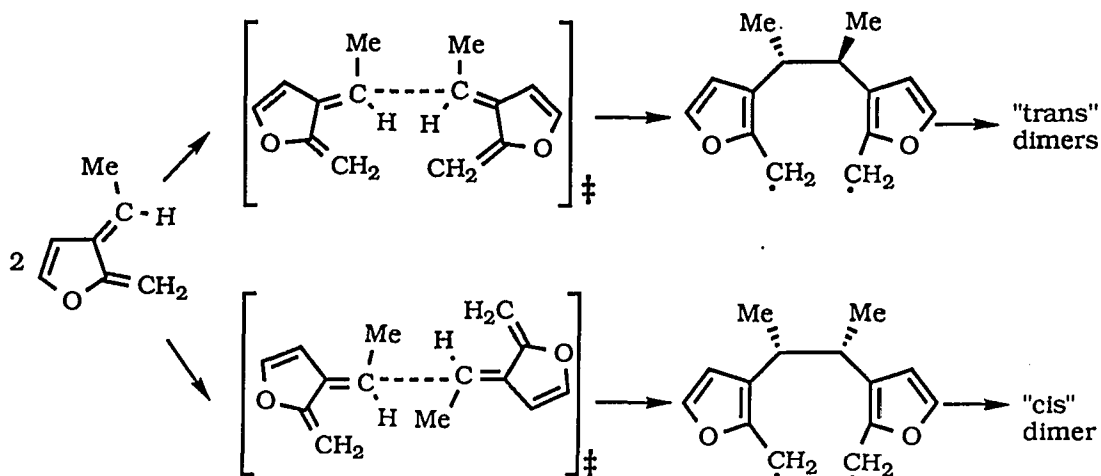
RESULTS

Although pyrolysis has been used extensively in the preparation of **1** and its derivatives, it could not.be used in the present study. The major problem arising from pyrolysis is the competitive [1,5] hydrogen shift which can occur at high
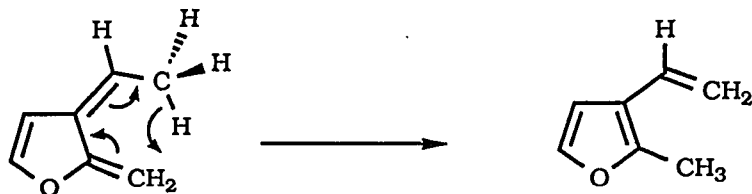
temperature.[12] To avoid this interference, substituted 2,3-dimethylene-2,3-dihydro-furans **12, 13,** and **14** were prepared in the solution phase at room temperature by the fluoride induced 1,4-conjugative elimination from the appropriate trimethylsilyl derivative.

For the generation of o-QDM's, the trimethylammonium group is the common leaving group[9b-e,13] but because of difficulty in preparation of the appropiate trimethylammonium salt, we switched to the acetate as the leaving group[14] Precursors **15, 16,** and **17** were synthesized as follows:

15   **16**   **17**
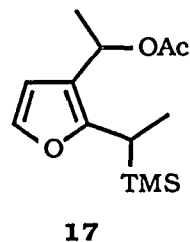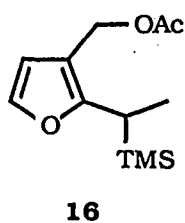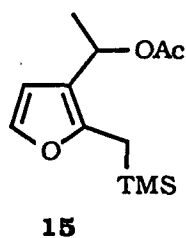
The synthesis of pecursor **15** is summarized in Scheme 1. Selective silylation of methyl furancarboxylate **18** at the 2-methyl group was achieved by use of chlorotrimethylsilane and two equivalents of lithium diisopropylamide at low temperature to give ester **19** without competitive methylation at the 5-position.[15,16] Direct reduction of ester **19** to alcohol **20** by LiAlH$_4$[17] followed by modified Collin's oxidation provided aldehyde **21**.[18] Addition of methyl lithium to aldehyde **21** followed by acylation of alcohol **22** gave precursor **15** .

The synthesis of **16** is outlined in Scheme 2. On treatment of **19** with LDA, followed by MeI in THF at -78°C, α–methylation adjacent to the trimethylsilyl group was achieved to afford **23**. However, co-generation of overmethylated product **24** could not be avoided. Purification of **23** from this mixture is necessary since the side products derived from **24** will interfere with the final dimerization product analyses. Purified **23** was then subjected to LiAlH$_4$ reduction followed by acetylation of **25** to provide **16**.

The synthesis of **17** is shown in Scheme 3. Alcohol **25** was oxidized by modified Collin's reagent to provide aldehyde **26**. Treatment of aldehyde **26** with methyl lithium followed by acetylation of alcohol **27** led to precursor **17**. Since the regio-structural assignments of the dimerization products cannot be obtained simply from their ^{1}H NMR spectra, the deuterium labelled dimers were desired. In our study, deuterated **17** was prepared from deuterated alcohol **25** which was derived from the reduction of **23** with LiAlD$_4$.

Scheme 1
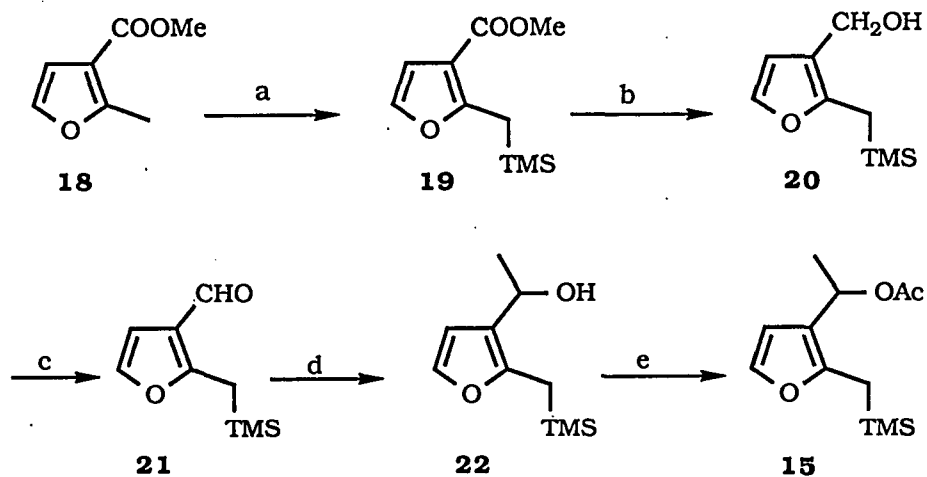
a, 2LDA, TMSCl, -78°C; b, LiAlH4; c, CrO3. 2Py; d, MeLi; e, AcCl. Py.

Scheme 2
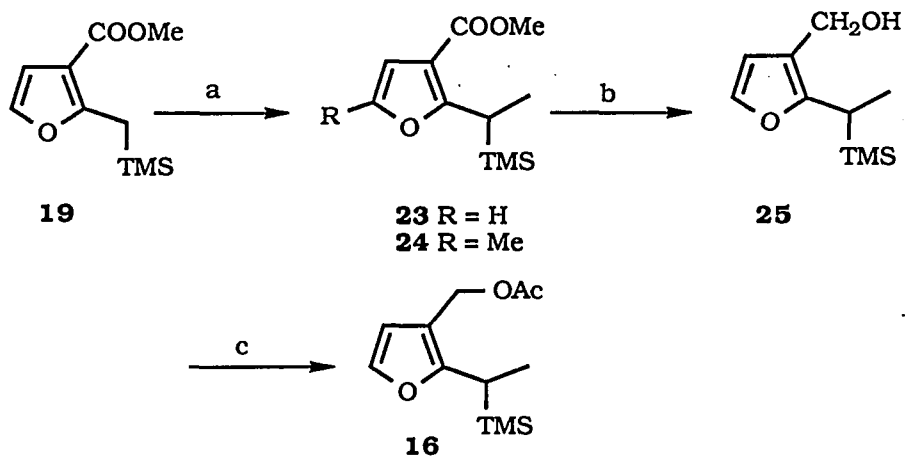
a, LDA, MeI; b, LiAlH4; c, AcCl. Py.

Scheme 3
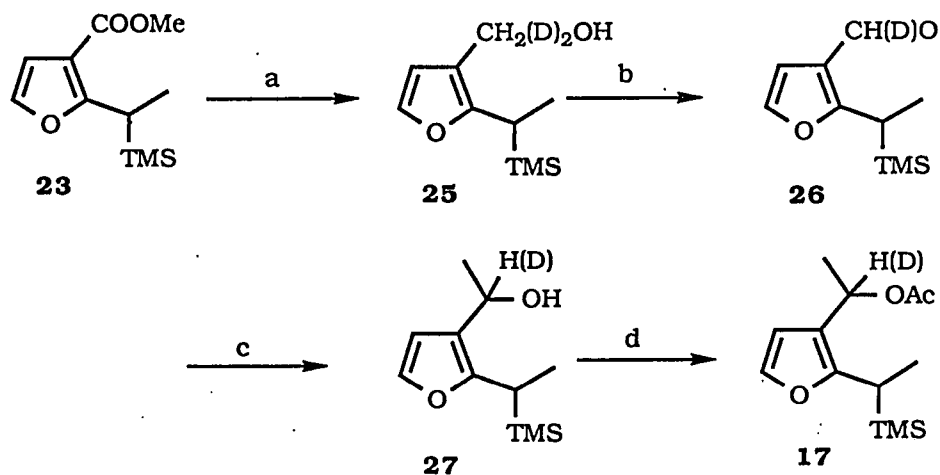
a, LiAlH$_4$ or LiAlD$_4$; b, CrO$_3$. 2Py; c, MeLi; d, AcCl. Py.

Generation and dimerization of 12. Fluoride induced 1,4-conjugative elimination of trimethylsilyl acetate from **15** was carried out in acetonitrile using an excess amount of tetrabutylammonium fluoride (TBAF) to give the reactive 3-ethylidene-2-methylene-2,3-dihydrofuran (**12**). The existence of **12** was first proved by a trapping experiment. In the presence of a large excess of methyl acrylate (10 eq.), **12** was trapped nearly quantitively to give a mixture of Diels-Alder adducts **28**.[5] By GC/MS and ^{1}H NMR analyses, four regio- and stereo-isomers were identified. Direct
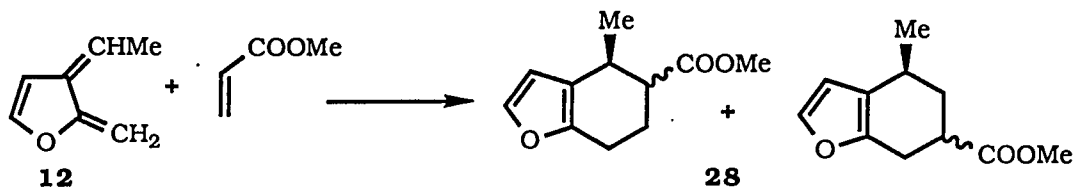
evidence for the existence of **12** was obtained by ^{1}H NMR spectroscopy. Due to its low molecular weight and high volatility, o-QDM **12** was generated and distilled immediately along with the deuterated solvent under vacuum at ambient temperature

and the mixture was condensed in a cold trap at -78°C. After the distillation, the condensate was warmed to room temperature and the ^{1}H NMR spectrum was obtained (Figure 1). Interestingly, o-QDM **12** is relatively stable and only dimerizes or polymerizes slowly at room temperature. The spectrum of **12** shows that only one stereoisomer was produced. Since both E and Z isomers of o-QDM **12** would give rise to the same ^{1}H NMR pattern, the pattern itself does not reveal the stereochemistry of **12**, but some stereochemical conclusions can be drawn from the chemical shifts of **12**. Fortunately, the very unreactive *tert*-butyl derivative o-QDM E-**29** was prepared by Huang[5b] by flash vacuum pyrolysis (FVP) [19] The chemical shifts of the olefinic protons of o-QDM's **12** and E-**29** are nearly identical and therefore we assign the E-configuration to o-QDM **12**.

E-12   **Z-12**   **29**
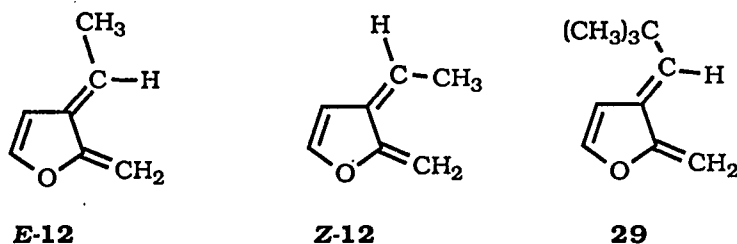
In the absence of a trapping reagent, **12** dimerizes to give a complicated mixture of dimers (~50%) and polymers. A similar yield of dimers was obtained in both a TBAF solution or in the distillate which suggests that polymerization of **12** is not a TBAF induced reaction.

GC/MS analysis of the product mixture shows that seven dimers were formed in the dimerization of **12** (Table 1). Five of them were readily separated and characterized by ^{1}H NMR spectroscopy. Two of these five are head-to-head [4+4]
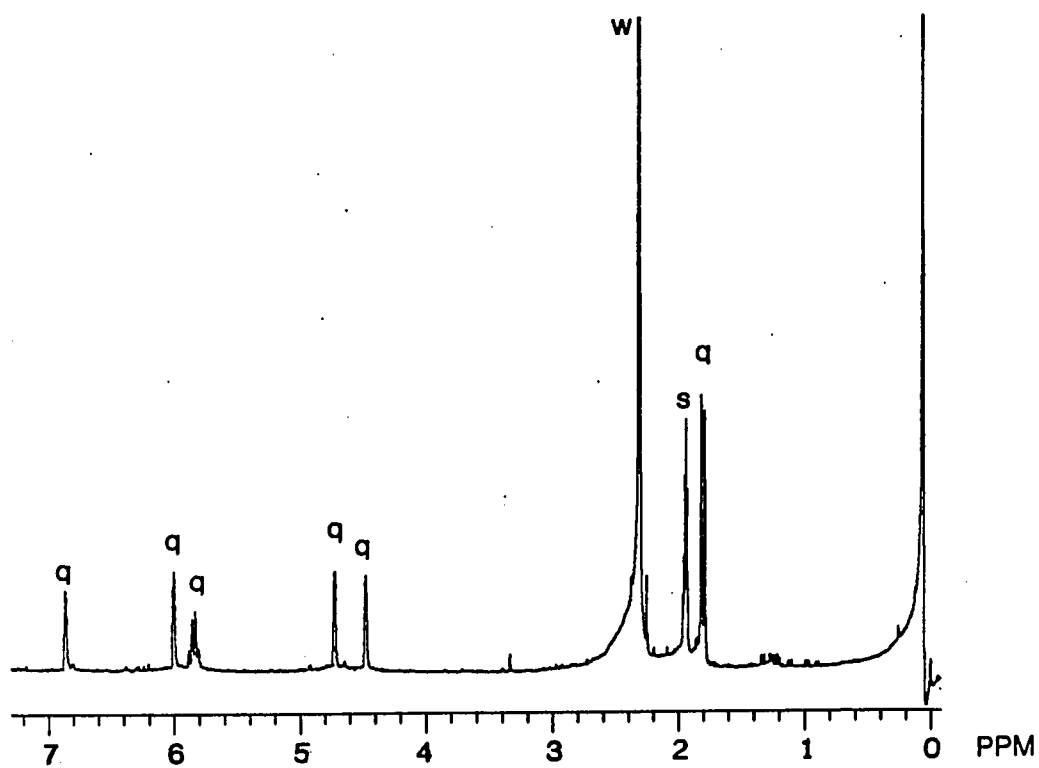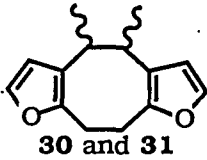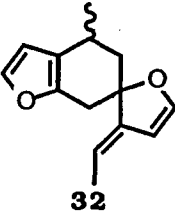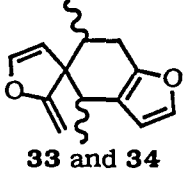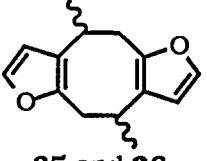
Figure 1. ^{1}H NMR spectrum (300 MHz, in CD$_3$CN) of 3-ethylidene-2-methyl-ene-2,3-dihydrofuran (**12**) recorded at room temperature (q: o-QDM **12**, w: H$_2$O from TBAF salt, s: CHD$_2$CN in d$_3$-acetonitrile). ·

Table 1. Dimerization products of 3-ethylidene-2-methylene-2,3-dihydrofuran
(**12**)

Dimer	Number of possible diastereomers	Mode of cyclization	Number of isolated dimers	GC retention time, (yield, %)
30 and 31	2	Head-to-head [4+4]	2	23.27 (32 %)[a] **30** 25.25 (10 %)[a] **31**
32	4	Head-to-tail [4+2]	1	23.94 (10 %)[a] **32**
33 and 34	4	Head-to-tail [4+2]	2	21.44 (24 %)[a] **33** 21.57 (18 %)[a] **34**
35 and 36	2	Head-to-tail [4+4]	1	22.79 (~4 %)[b] **35**
37		Unknown	-	22.61 (~2 %)[c] **37**

[a] The dimer was isolated and identified by ^{1}H NMR spectroscopy.
[b] The dimer was identified by the GC/MS and the ^{1}H NMR spectrum of the dimer mixture.
[c] The dimer was identified by the GC/MS anaylses.

adducts **30** and **31** (42 %) while the other three are head-to-tail [4+2] adducts **32-34** (52 %). The assignments of **30** and **31** were based on the AA'BB' pattern around δ 2.5 ppm in both of the ¹H NMR spectra. The structure of **32** was confirmed by both the characteristic quartet at δ 4.8 ppm which results from the signal for the exo-methide proton adjacent to a methyl group and the typical AB pattern around δ 3.0-2.2 ppm. The assignments of **33** and **34** were based on the observations of a typical signal for the exo-methylene protons with no AB quartet in their ¹H NMR spectra. In addition, these assignments were further confirmed by decoupling experiments. Dimer **35** could not be isolated and identified successfully until FVP of **34** was carried out. FVP of **34** gave rise to a mixture of **35** and **36** in a 2 to 1 ratio. They were identified by GC/MS, and ¹H NMR analyses. On the basis of the identical retention times, fragmentation patterns in the GC/MS and chemical shifts in the ¹H NMR spectra, **35** was identified as a minor product in the dimerization. Dimer **37** could not be isolated and identified, but the GC/MS analyses of **37** shows a fragmentation pattern very similar to those of the other dimers.

Generation and dimerization of o-QDM 13. Fluoride induced 1,4-conjug- ative elimination of trimethylsilyl acetate from **16** in acetonitrile led to reactive 2-ethylidene-3-methylene-2,3-dihydrofuran (**13**). By use of the same technique applied to o-QDM **12**, the ¹H NMR spectrum of **13** was obtained (Figure 2a). However, due to its higher reactivity towards dimerization, o-QDM **13** dimerized during the ¹H NMR acquisition process, and therefore small amounts of dimers also showed in the ¹H NMR spectrum. Interestingly, unlike o-QDM **12**, two different sets of olefinic proton signals, labelled **13a** and **13b**, are observed in the spectrum. The signals of the major isomer, **13a**, and the minor isomer, **13b**, disappeared with time leaving only signals
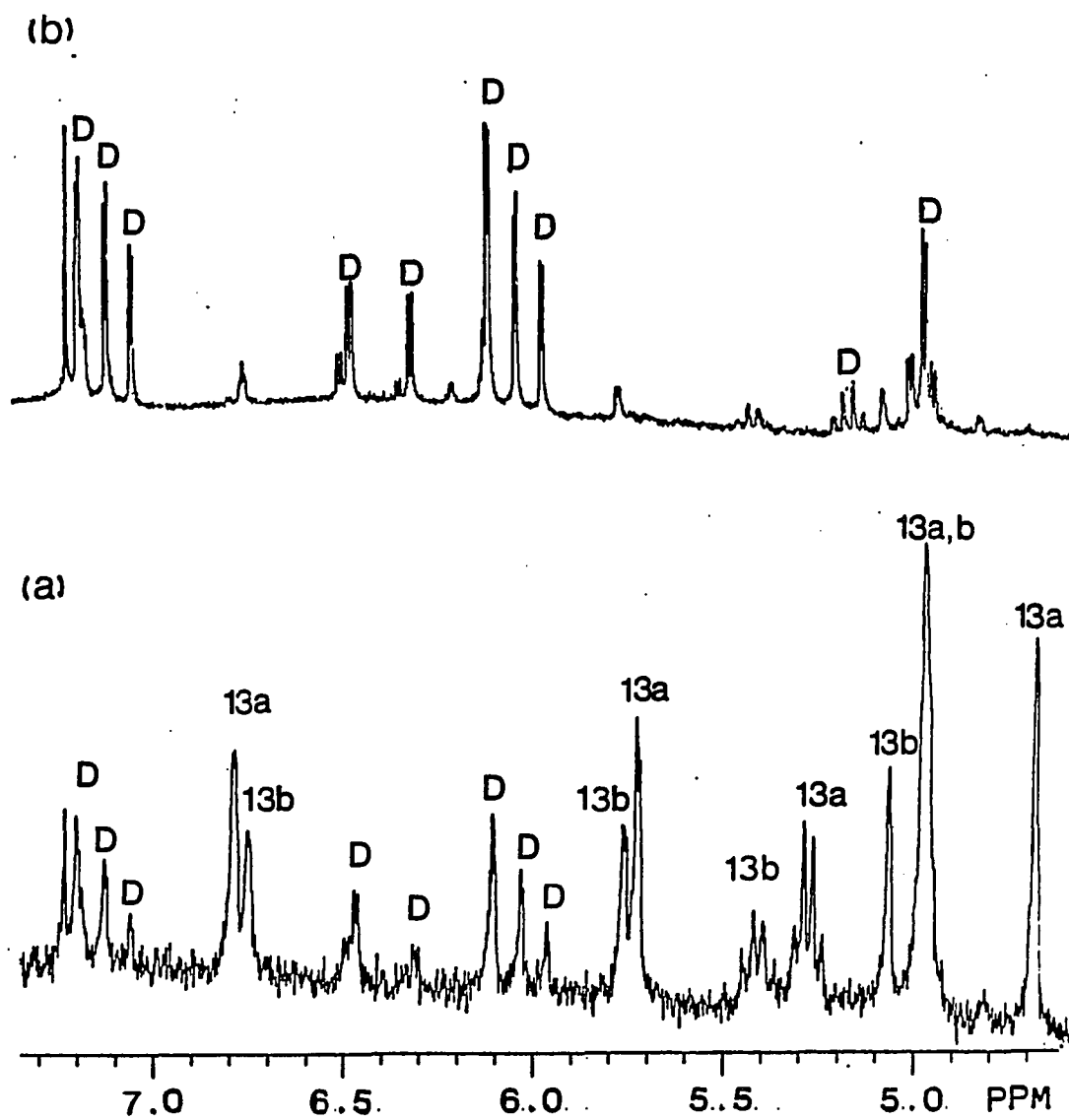
Figure 2. ^{1}H NMR spectrum (300 MHz, in CD$_3$CN) of 2-ethylidene-3-methyl-ene-2,3-dihydrofuran (**13**): (a) recorded right after the preparation of **13** (13a: 2Z-**13**, 13b: 2E-**13**, D: dimers); (b) recorded 24 h later (D: dimer).

from dimers (Figure 2b). Because of the nearly identical olefinic proton chemical shifts of **13a** and Z-**4**, which was prepared by FVP,[5b] we tentatively assign the Z-configuration to **13a** and the E-configuration to **13b**.

Z-13   **E-13**   **Z-4**
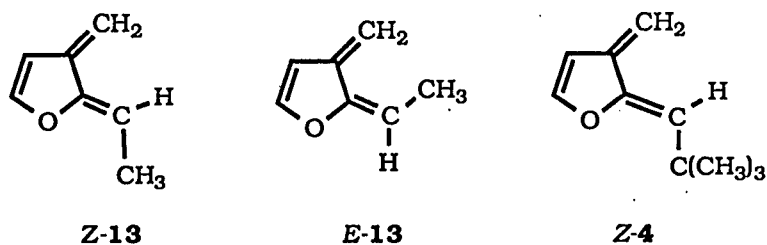
Dimerization of **13** led to a mixture of seven dimers. Six of these were isolated and identified as head-to-head dimers **38-43** (Table 2). Disportionation product **44** could not be identified until FVP of the dimer mixture was performed. The assignments of **38** and **39** were based on both the characteristic AA'BB' signals of the 3-ethylene bridge protons and the quartet which results from the 2-ethylene protons adjacent to the methyl group. On the other hand, the assignments of **40-43** were supported by the characteristic olefinic quartets resulting from the exo-methide protons adjacent to a methyl group and the quartets arising from the methylene bridge protons adjacent to the other methyl group. When the dimer mixture was subjected to FVP at 630 °C, a mixture of six components, **38, 39** and **44-47**, was obtained. Fragmentation product **45** was distilled along with deuterated solvent introduced after the pyrolysis and
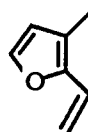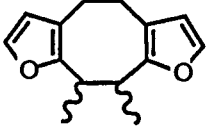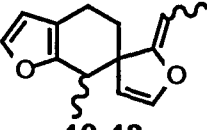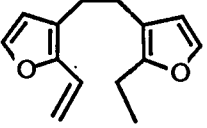
45   **46 and 47**

Table 2.   Dimerization products of 2-ethylidene-3-methylene-2,3-dihydrofuran (**13**)

Dimer	Number of possible diastereomers	Mode of dimerization	Number of isolated dimers	GC retention time, (yield, %)
38 and 39	2	Head-to-head [4+4]	2	16.36 (12 %)[a] 38 17.59 (18 %)[a] 39
40-43	4	Head-to-head [4+2]	4	15.90 (33 %)[a] 40 16.39 (12 %)[a] 41 17.14 (18 %)[a] 42 17.24 (4 %)[a] 43
44	1	Head-to-head disproportio-nation	1	16.04 (~2 %)[b] 44

[a] Compound was isolated and identified by ^{1}H NMR spectroscopy.
[b] Compound was identified by GC/MS analysis.

identified as the major product and significant amounts of disportionation products **44** (15 %) and **46** (10 %) were isolated. The assignment of **44** is supported by the observation of the signals of the ethyl group, four ethylene bridge protons (AA'BB' pattern) and three vinyl protons at δ 5.07, 5.55 and 6.41 ppm. Similar results were obtained in the pyrolysis of the mixture of [4+2] dimers **40** and **41**. We concluded that **44** is a minor component in the original dimer mixture because the GC retention time and mass spectra of one of the original products matched those of **44** obtained from the FVP of the dimer mixture. The structural assignment of **46** is based on the observation of the signals for the ethyl group and olefinic protons on the bridge at δ 6.52 ppm. The structural assignment of **47**, the cis-trans isomer of **46** is based on a mass spectrum which is very similar to that of **46**.

Generation and dimerization of o-QDM 14. Fluoride induced 1,4-conjug-ative elimination of trimethylsilyl acetate from **17** in acetonitrile led to the reactive 2,3-ethylidene-2,3-dihydrofuran (**14**). By utilizing the same vacuum distillation tech-nique, the ^{1}H NMR spectrum of the reactive intermediates was obtained (Figure 3). Again, two sets of olefinic signals are observed in the spectrum. Since we know that introduction of a methyl substituent at the 3-methylene position leads to a single isomer E-**12** while a methyl substituent at the 2-methylene position leads to a pair of cis-trans isomeric o-QDM's E-**13** and Z-**13**, we concluded that **14** is a mixture of ZE-**14** and EE-**14**.

ZE-14   EE-14
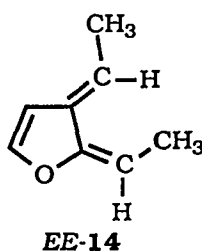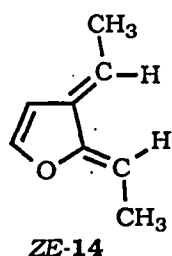
o-QDM's ZE-**14** and EE-**14**, condensed at low temperature, dimerized slowly at room temperature to give rise to a mixture of four separable major dimers **48-51** (Table 3) and fourteen minor dimers, which were identified by GC/MS analyses. Since the head-to-head, head-to-tail and tail-to-tail [4+2] dimers cannot be distinguished simply by ^{1}H NMR spectroscopy, deuterium isotope labelling experiments were performed. Separation of the deuterated dimers **48-51** on silica gel liquid chromatography afforded essentially pure dimers which were suitable for ^{1}H NMR analyses. The disappearance of the ethylene bridge proton signals on the ^{1}H NMR spectra of deuterated **49** and **50** strongly supports the head-to-head [4+2] assignments. The relative configuration between methyl substitutents on the ethylene
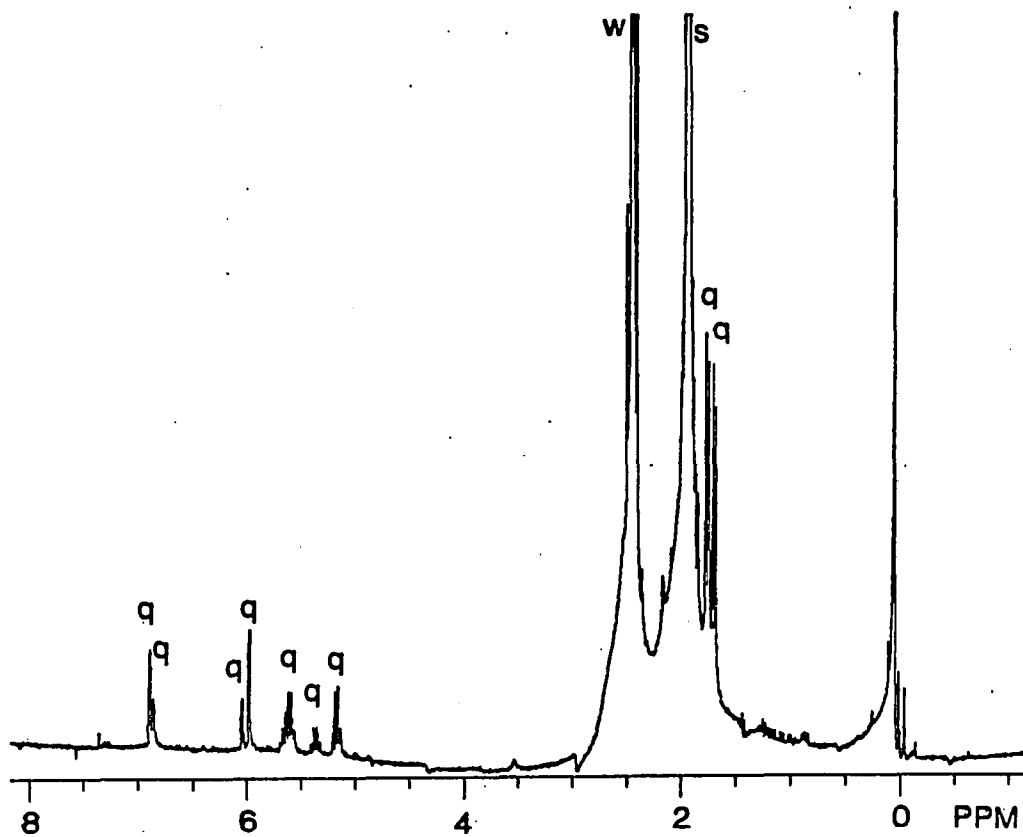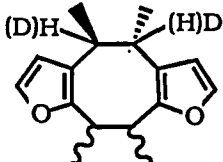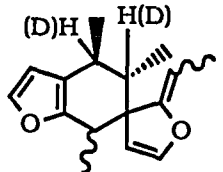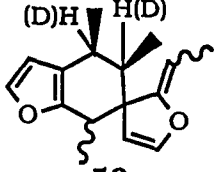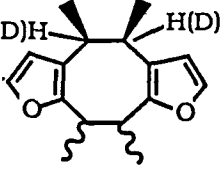
Figure 3. ^{1}H NMR spectrum (300 MHz, in CD$_3$CN) of 2,3-ethylidene-2,3-dihydro-furan (**14**) recorded at room temperature (q: diastereomeric o-QDM 2Z,3E-**14** and 2E,3E-**14**, w: H$_2$O from TBAF salt, s: CHD$_2$CN in d$_3$-acetonitrile).

Table 3.   Dimerization products of 2,3-diethylidene-2,3-dihydrofuran (14)

Dimer	Mode of cyclization	Retention time, (yield, %)
(D)H⟍ ⟋(H)D 48 and 54	Head-to-head [4+4]	52.24 (6 %)[a] 48 58.06 (2 %)[b] 54
(D)H H(D) 49	Head-to-head [4+2]	54.15 (42 %)[a]
(D)H H(D) 50	Head-to-head [4+2]	58.00 (39 %)[a]
(D)H⟍ ⟋H(D) 51	Head-to-head [4+4]	60.43 (6 %)[a]

[a]   The dimer was isolated and identified by ^{1}H NMR spectroscopy. The structure was further confirmed by deuterium isotope labelling experiment.

[b]   The dimer was identified by comparison the retention time and MS pattern with those of the pyrolysis products of 49

bridge of **49** was deduced from the spin-spin coupling constant between the methide protons on the bridge. The spin-spin coupling constant with J_{HCCH}=9.5 Hz indicates that the methide protons on the ethylene bridge are in the anti-position (with a dihedral angle ca. 180 °).[20] However, the moderate coupling constant (J_{HCCH} = 6.6Hz) of **50** does not lead to any definite assignment. In order to establish the stereochemistry of **50**, dimers **49** and **50** were subjected to FVP.

Pyrolysis of deuterated **49** generated a mixture of fragmentation products **52** and **53** along with three [4+4] dimers **48**, **54**, and **55**. On the other hand, pyrolysis of deuterated **50** under similar conditions led to the same fragmentation products **52**

52   **53**
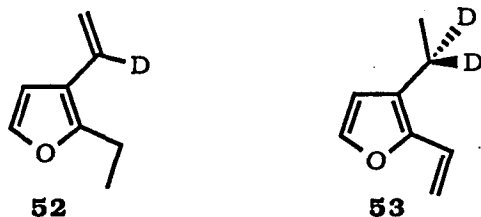
and **53** but totally different [4+4] dimers **51**, **56**, and **57**. The structures were assigned on the basis of GC/MS and ^{1}H NMR analyses and these assignments are simply illustrated by comparison of the ^{1}H NMR spectra (Figure 4a and 4b) of the pyrolysates. The common proton signals at δ 6.46 and 6.27 ppm were assigned to the furan ring proton at the 4-position of **52** and **53**, respectively. The down field shift of the signal at δ 6.46 ppm is due to the effect of the 3-vinyl substituent. The assignments were further confirmed by comparison of the chemical shifts with those of the signals of **45** and **46**. The doublets at δ 6.24, 6.07, and 6.03 ppm in Figure 4a and the doublets at δ 6.22, 6.18, and 6.14 ppm in Figure 4b indicate the existence of two different sets of [4+4] dimers, which are also suggested by their GC/MS fragmentation patterns. By chemical shifts and GC retention times, [4+4] dimer **48** was identified as one of the
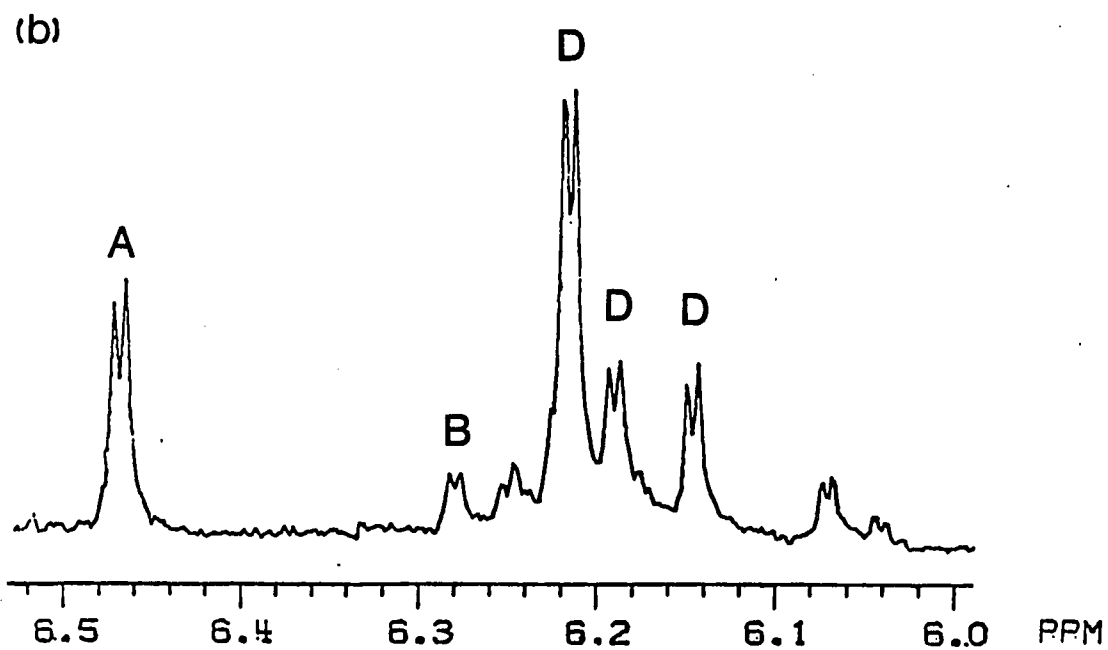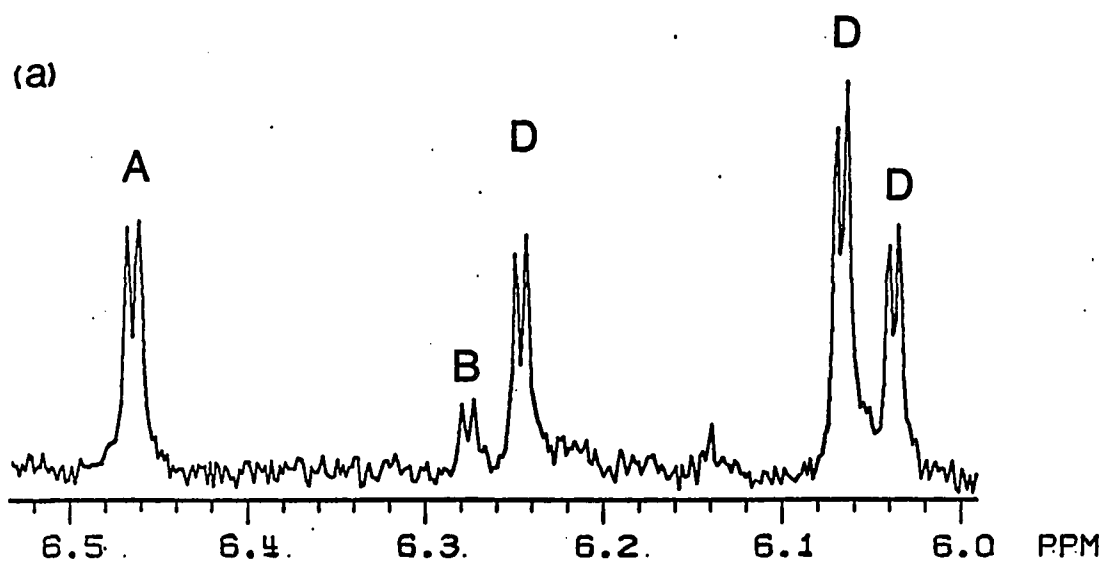
Figure 4. (a) ^{1}H NMR spectrum (300 MHz, CDCl$_3$) of the pyrolysate of [4+2] dimer **49** (A: 2-ethyl-3-ethylenyl-furan (**52**), B: 3-ethyl-2-ethyleneyl-furan (**53**), D:[4+4] dimers **48, 54** and **55**); (b) ^{1}H NMR spectrum (300 MHz, CDCl$_3$) of the pyrolysate of [4+2] dimer **50** (A: 2-ethyl-3-ethylenyl-furan (**52**), B: 3-ethyl-2-ethyleneyl-furan (**53**), D: [4+4] dimers **51, 56** and **57**).

components in the pyrolysate of **49** while [4+4] dimer **51** was assigned as one of the products in the pyrolysate of **50**.

To explain these pyrolysis results, we suggest that the stereochemistrie of the ethylene bridges of **49** and **50** are different. If both **49** and **50** have the same relative configuration on the ethylene bridge, we should have obtained the same [4+4] dimers in the pyrolyses. However, if these configurations are different, generation of the stereoisomeric diradical intermediates **58** and **59** are expected. Since the relative

| 49 | 58 | 48, 54 and 55 |

| 50 | 59 | 51, 56 and 57 |
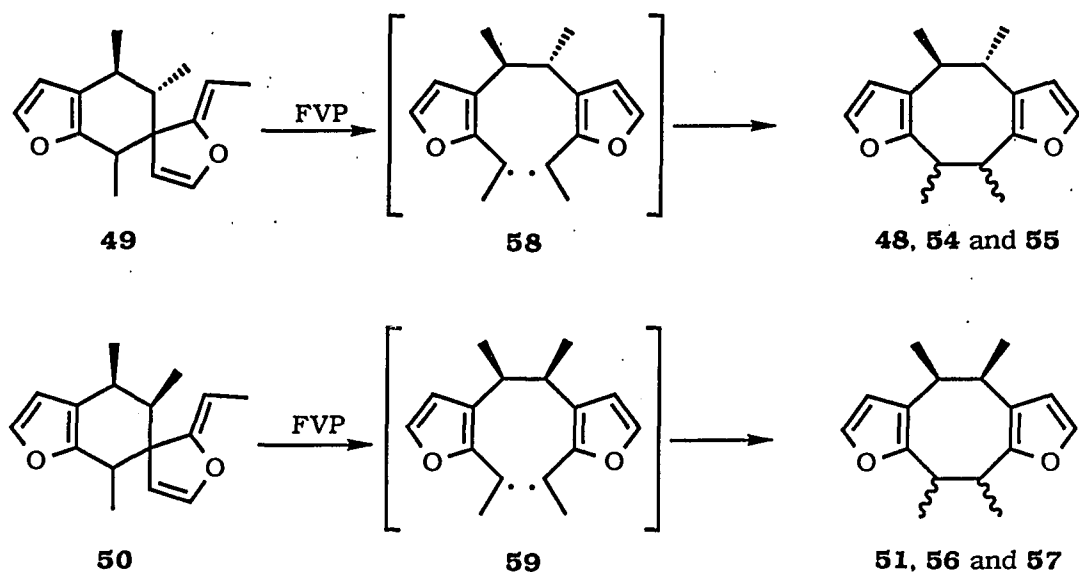
configuration of the ethylene bridge is maintained during the diradical formation process, there is no doubt that cyclization of the diradicals 58 and 59 afford two different sets of diastereomeric [4+4] dimers. Since the relative configuration of **49** was identified to be anti on the ethylene bridge, we assigned the syn-configuration to **50**. Also, because we identified **48** and **54** as pyrolysis products of **49**, and **51** as one of the pyrolysis products of **50**, their relative configurations of the 3-ethylene bridges are determined.

DISCUSSION

Recent kinetic and product studies are consistent with the proposal that 2,3-dimethylene-2,3-dihydrofuran (1) dimerizes by a two-step diradical mechanism which involves rate-determinating formation of a diradical intermediate followed by rapid cyclization of the diradical.[3] On the basis of deuterium kinetic isotope studies, Chou and Trahanovsky concluded that only the 3-methylene carbon is involved in the rate-determinating step while the 2-methylene carbon is involved only in the diradical ring-closure process and attributed these results to the relative stability of the furfuryl diradicals. This arguement is consistent with the fact that the 2-furfuryl radical is more stable than the 3-furfuryl radical.[21] In the present study introduction of methyl substituents on the reactive diene unit of furan-based o-QDM's indeed affects both the diradical formation step and the diradical cyclization step. We now discuss these effects.

On the basis of the proposed diradical mechanism, we expected to see retardation of furan-based o-QDM dimerizations by introduction of a bulky substituent on the 3-methylene position. In fact, the trend of the relative reactivity of 2,3-dimethylene-2,3-dihydrofuran (1), 3-ethylidene-2-methylene-2,3-dihydrofuran (12), and 2-methylene-3-tert-butyl-methylene-2,3-dihydrofuran (29) towards dimerization is strongly consistent with this expectation. The parent o-QDM 1 is so reactive that it dimerizes at -20 °C, the 3-methyl derivative (12) dimerizes slowly within several hours at room temperature, and the 3-tert-butyl derivative (29) is unreactive at room temperature and no dimer was isolated even after all of the monomer disappeared at higher temperature.[5b]

The shielding of the reactive 3-methylene position of o-QDM 12 by the methyl substituent apparently retards the head-to-head dimerization process enough to allow

the head-to-tail dimerization to become competitive. In the dimerization of **12**, significant amounts of head-to-tail dimers **32-35** were isolated along with the head-to-head [4+4] dimers **30** and **31**. These results are attributed to the competitive formation of the head-to-tail diradical **61** which further cyclizes to head-to-tail dimers **32-35**. The head-to-head [4+4] dimers **30** and **31** are the dimers expected from the head-to-head diradical **60**, but the possibility of the involvement of tail-to-tail diradical **62** cannot be eliminated. However, the assumption that the head-to-head diradical **60** is involved is consistent with the fact that the head-to-head dimerization of the dimethyl *o*-QDM **14** still occurs even though **14** has a methyl group on the 3-methylene position.
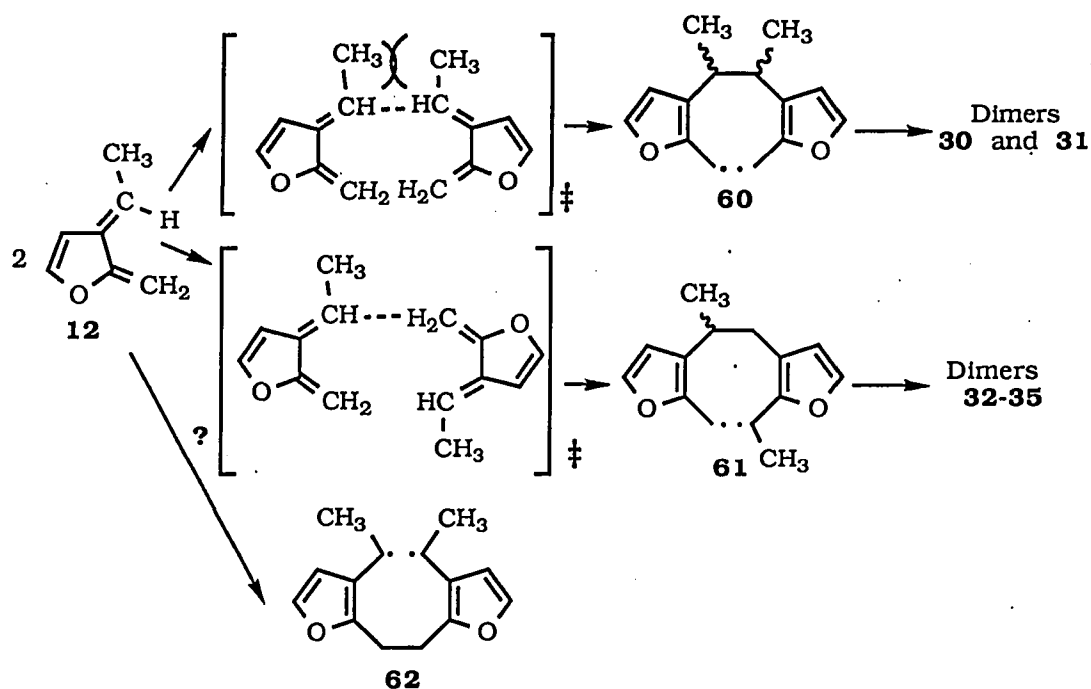
Introduction of a methyl substituent on the 2-methylene carbon, instead of the 3-methylene position, does not retard the head-to-head dimerization. In fact, *o*-QDM **13** dimerizes exclusively in the head-to-head fashion to give rise to (4+4) and

(4+2) dimers **38-43**. Importantly, identification of the disproportionation product **44** in this case strongly supports the diradical mechanism.[22]
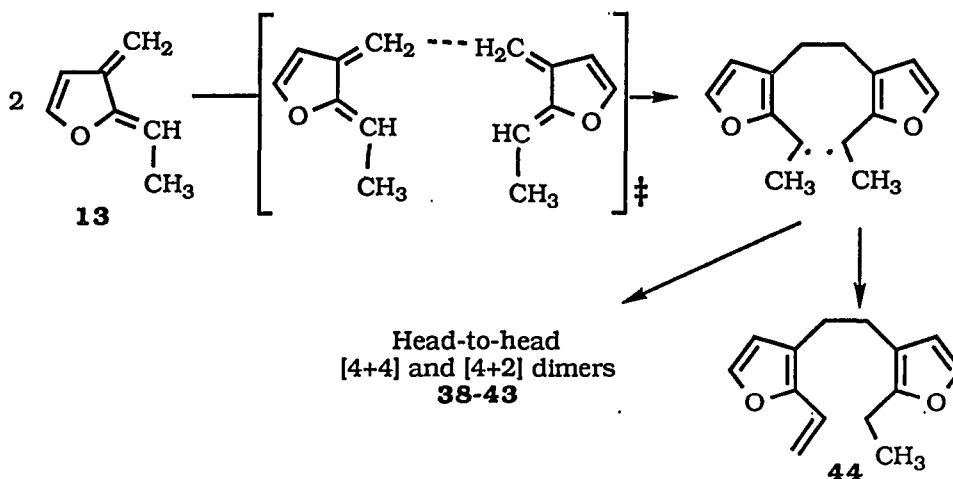
In contrast to the dimerization of **12**, o-QDM **14** dimerizes mainly in a head-to-head fashion. Introduction of methyl substituents at the 2-methylene and 3-methylene positions indeed enhances steric retardation of both head-to-head and head-to-tail dimerization processes. As the discrepancy of the steric hindrance disappears, electronic influences predominate and, like the parent o-QDM **1**, o-QDM **14** dimerizes again in the head-to-head fashion.
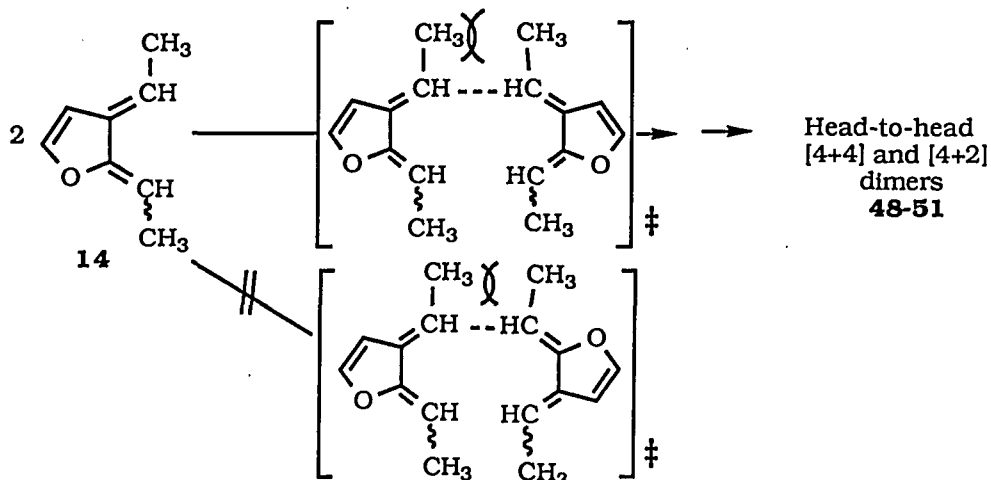
Formation of both head-to-head [4+4] dimers **30** and **31** in the dimerization of **12** indicates the existence of two distinct diradical intermediates **63** and **64**.[23] However, both diradical, cisoid **63** and transoid **64**, cyclize in a [4+4] fashion. These results indicate that the second step of the head-to-head dimerization is uninfluenced by the relative orientation of the monomers in transition states **65** and **66** and that both the cisoid and transoid diradicals derived from these transition state cyclize in the same fashion.

Head-to-head
[4+4] dimers
30 and **31**
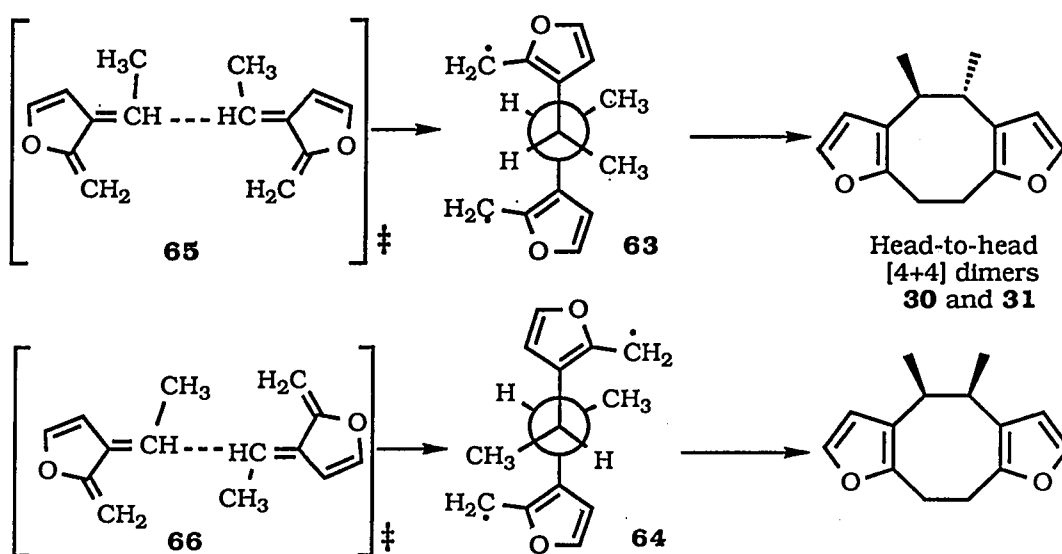
On the other hand, a methyl group on at the 2-methylene position changes the preference of cyclization of the diradical. Dimerization of **13** provides the head-to-head [4+2] and head-to-head [4+4] dimers in a 2.3 to 1 ratio. This observation is consistent with the result of *o*-QDM *Z*-4 dimerization.[5b] *o*-QDM *Z*-4 was generated by FVP and is reported to dimerize mainly in a head-to-head [4+2] fashion.

Z-4
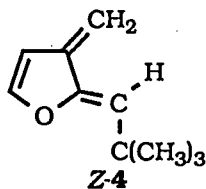
Pyrolysis of the [4+2] dimers of o-QDM **13** led to a series of thermodynamically stable products. On the basis of the FVP experiment, we concluded that the [4+4] dimers are thermodynamically more stable than the [4+2] dimers which means that the cyclization of diradical **67** indeed is a kinetically controlled process. Increasing steric hindrance at the 2-methylene position by introduction of a substituent appears to retard the [4+4] cyclization which enhances the competitiveness of the [4+2] cyclization.
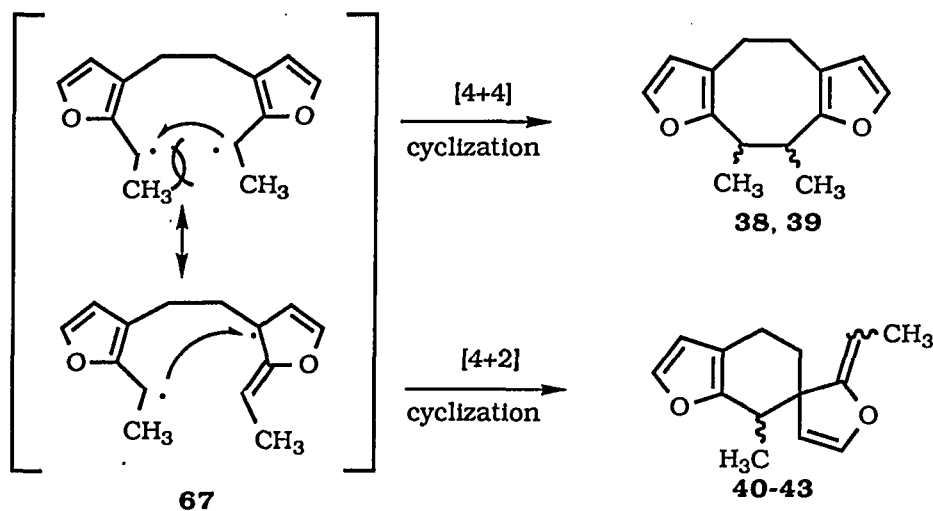
The combined features of the dimerization of o-QDM **12** and of o-QDM **13** can be seen in the dimerization of o-QDM **14**. Similar to o-QDM **12**, o-QDM **14** dimerized to two series of head-to-head dimers which possess different relative configurations of their 3-ethylene bridges. On the basis of our analyses, dimers **48, 49,** and **54** are

originally derived from cisoid diradical **68** and dimers **50** and **51** are derived from transoid diradical **69**. These results again implicate the existence of the cisoid and transoid monomer encounters in the diradical formation step. On the other hand, the methyl substituents on the 2-furfuryl radical sites of **68** and **69** again make a
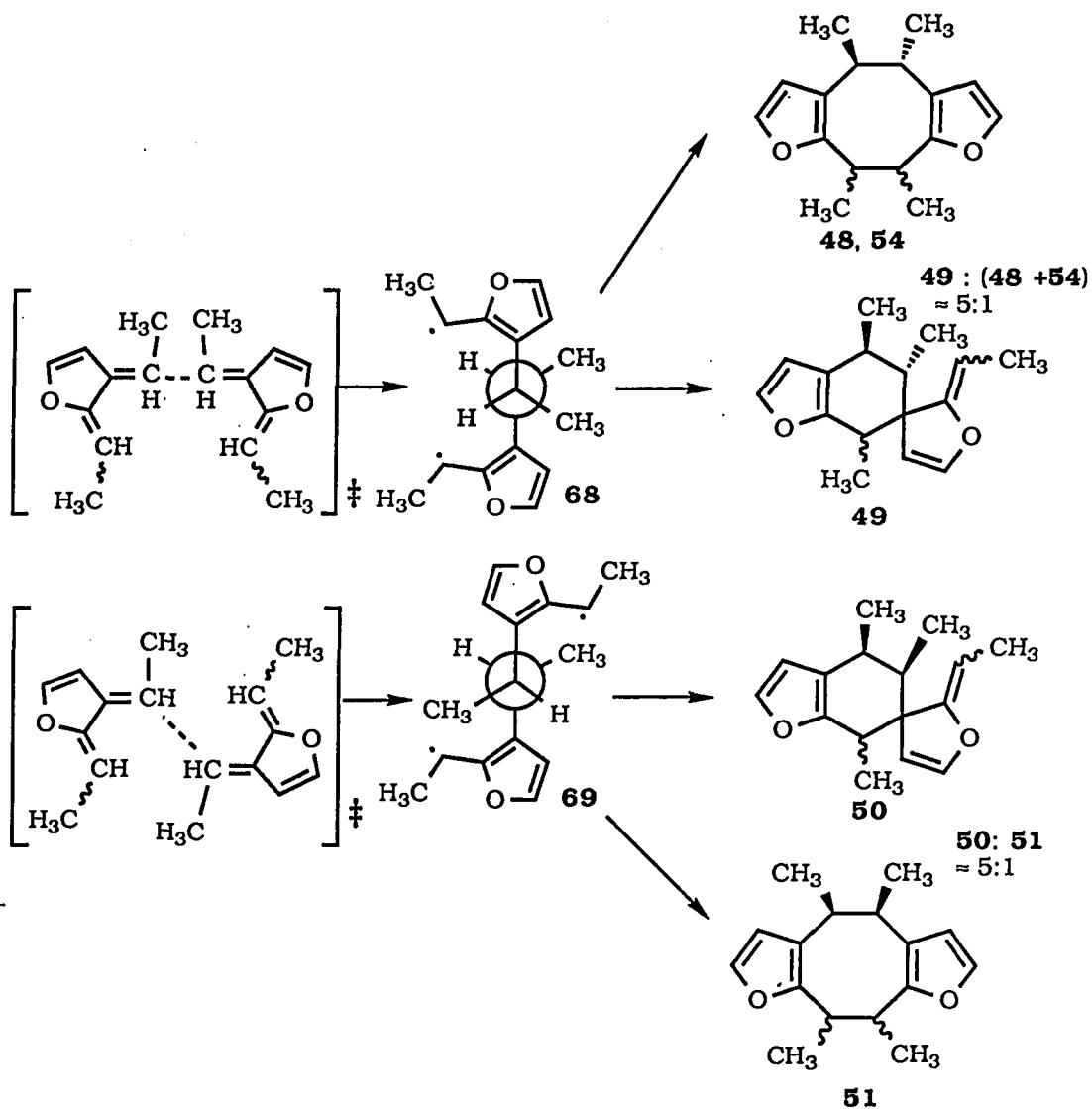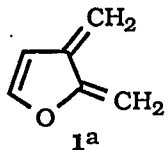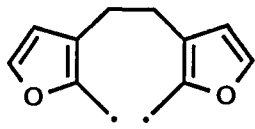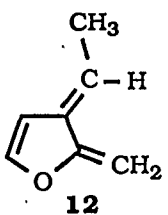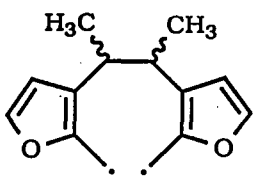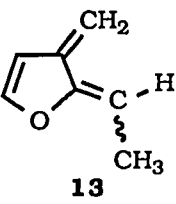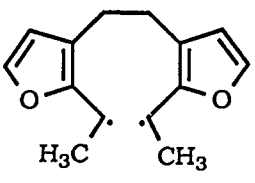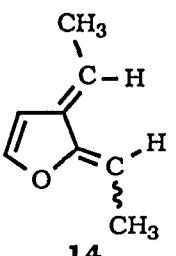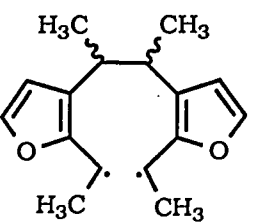
distinct change in the mode of cyclization. Unlike the head-to-head diradical intermediate of the parent o-QDM **1** and those of o-QDM **12**, but similar to that of o-QDM **13**, diradicals **68** and **69** prefer to cyclize in a [4+2] fashion. More interestingly, both **68** and **69** cyclized to give rise to a mixture of [4+2] and [4+4] dimers in a similar ratio of 5 to 1. This observation suggests that the preference for the cyclization mode of the diradical intermediates in the dimerization is insensitive to the initial conformation of the radicals or the relative orientation of the monomers in the transition states of the diradical formation step.

To summarize our studies, a comparison of the dimerization results is shown in Table 4. The cisoid and transoid monomer encounters in the diradical formation step were successfully labelled by introducing a methyl group at the 3-methylene position of the furan-based o-ODM's. Once the diradical intermediate is formed, the methyl substituents on the 3-ethylene bridge do not show any significant effect on the mode of cyclization of the diradical. On the other hand, the mode of cyclization is strongly affected by a methyl substituent on the 2-methylene position. This result indicates that steric retardation of bond formation between two 2-furfuryl radical sites of the diradical intermediate may slow down the [4+4] cyclization and enhance the competitiveness of the [4+2] cyclization.

In general, cyclization of a reactive species involves an internal bond rotation step as well as the intramolecular bond formation step between the active sites on the chain.[10] A general idea about the cyclization reaction is depicted in Scheme 4. Conformational motion of the carbon chain brings the intermediate to reactive conformation **70** or **71** which can further cyclize to form cyclization products **72** and **73**, respectively. In principle, any factor that can affect the internal rotation or the intramolecular bond formation of the intermediate can be crucial in the

Table 4. Cyclization regioselectivity of the diradical intermediates in the dimerization of furan-based o-quinodimethanes.

Entry	o-QDM	Head-to-head diradical intermediate	Cyclization regioselectivity [4+4] : [4+2]
1	CH_2 / CH_2 1^a		> 20
2	CH_3 / C–H / CH_2 **12**	H_3C CH_3	> 20
3	CH_2 / C–H / CH_3 **13**	H_3C CH_3	< 0.5
4	CH_3 / C–H / C–H / CH_3 **14**	H_3C CH_3 / H_3C CH_3	< 0.25

a, See reference 2

regioselectivity of the cyclization[10,24]. However, in view of this studing of the results of the furan-based o-QDM dimerizatons, we believed that the bond formation step between the actives sites on two furan moieties of the diradical intermediate is the key step in controlling the regioselectivity in the diradical cyclization process. The first

Scheme 4

* reactive site
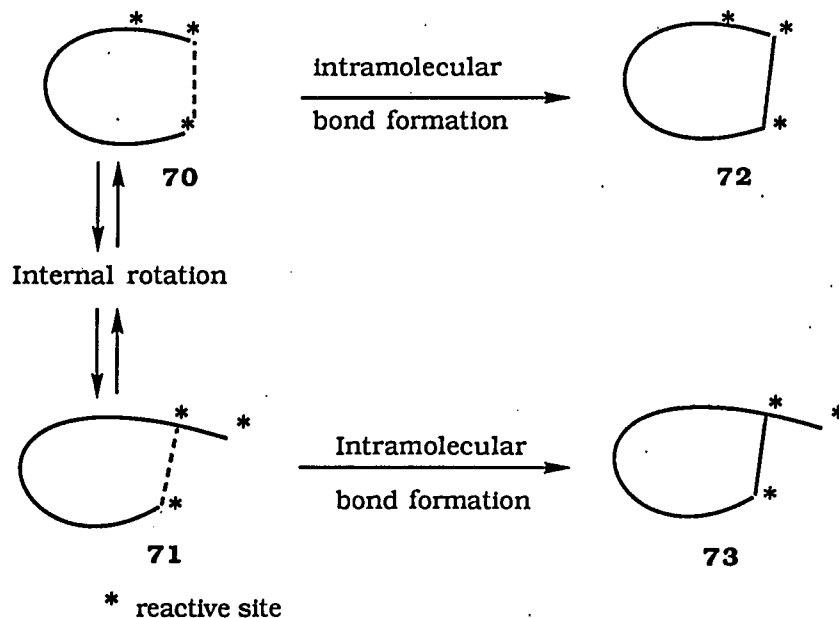
insight we obtained from our experiments is the successfully labelling of the cisoid and transoid transition states, which lead to cisoid and transoid diradicals, in the dimerization. On the basis of these results, we reasonably extrapolate this conclusion to the dimerization of the parent 2,3-methylene-2,3-dihydrofuran (2) and suggest the co-existence of cisoid and transoid diradicals 7 and 8 in the dimerization. Since both cisoid and transoid diradicals lead to the same kind of cyclization products in all the cases we studied, we believed that the initial conformation of the diradical is unimportant in the regioselectivity of the diradical cyclization and diradical conformations 7 and 8 will lead to the same [4+4] dimer. Moreover, although the methyl substituents on the 3-ethylene bridge restrict the bond rotation of the diradical intermediates, they do not strongly interfere with the regioselectivity of the diradical cyclization (Table 4, entries 2 and 4). This observation is consistent with the results reported by Huang.[5b] Huang discovered that a *tert*-butyl substituent at the 4-position

on the furan ring does not alter the mode of cyclization of o-QDM **74** which gives rise to the major [4+4] dimer **75**, eventhough retardation of the ethylene bridge rotation is expected. These results again indicated that the regioselectivity of the diradical

74   **75**
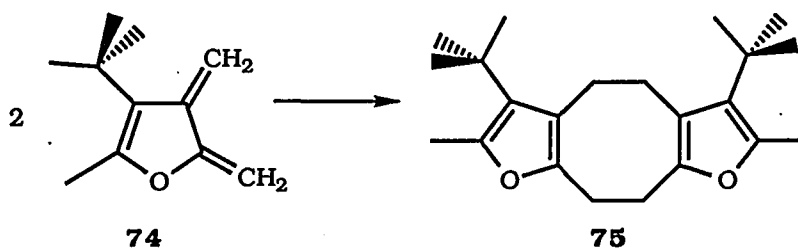
cyclization, the product determinating step, is not controlled by the motion of the bridge. However, increasing steric shielding around the furfuryl radical site can alter the regioselectivity of the cyclization to favor the [4+2] cyclization.

EXPERIMENTAL SECTION

The pyrolysis apparatus has been previously described.[19] ^{1}H NMR spectra were obtained on a Nicolet NT-300 spectrometer. Chemical shifts are reported in parts per million (δ) from tetramethylsilane (TMS). Gas chromatographic analyses were performed on a Hewlett-Packard model 5840A gas chromatograph (GC) equipped with a 30 meter, DB-1 capillary column from J&W scientific and a flame ionization detector. Combined gas chromatographic/mass spectra (GC/MS) analyses were performed on a Finnigan 4000 GC/MS with Incos data system. High resolution mass spectra were measured with an Associated Electronics Industries MS-902 instrument or MS 50 mass spectrometer. Infrared spectra (IR) were recorded on a Beckman Acculab II spectrometer. Tetrahydrofuran (THF) was distilled from sodium/benzophenone immediately before use. Acetonitrile was deaerated immediately before use. Diisopropylamine was distilled from calcium hydride (CaH_2). Commercial methyl lithium (in ether), n-butyl lithium (in hexane), chlorotrimethylsilane, tetrabutyl-ammonium fluoride (TBAF) and methyl 2-[(trimethylsilyl)methyl]-3-furancarboxylate were purchased from Aldrich Chemical Company.

Methyl 2-[(trimethylsilyl)methyl]-3-furancarboxylate (19). To a stirred solution of diisopropylamine (29.6 g, 293 mmol) in THF (200 mL) at -78°C was added n-butyllithium (115 mL, 288 mmol) under nitrogen. The mixture was stirred for 1 h and a solution of chlorotrimethylsilane (17.0 g, 157 mmol) and methyl 2-methyl-3-fu-rancarboxylate (18) (19.0 g, 136 mmol) in THF (200 mL) was added dropwise over 90 min. After addition, the solution was further stirred for 1 h and the reaction was quenched at low temperature by addition of water. The solution was then warmed to room temperature and extracted with 3 x 150mL of CH_2Cl_2. The combined organic phases was treated with 100 mL of brine and dried over anhydrous Na_2SO_4. Removal

of the solvent left an oil which was distilled under reduced pressure to give essentially pure ester **19** (22.4 g, 78%): bp 105-110°C (20 mmHg); IR (neat, NaCl) 2850-2980 (C-H), 1720 (C=O), 1250 (Si-CH$_3$) cm^{-1}; ^{1}H NMR (CDCl$_3$) δ 0.03 (s, 9H), 2.56 (s, 2H), 3.78 (s, 3H), 6.58 (d,1H, J=1.9 Hz), 7.14 (d, 1H, J=1.9 Hz); mass spectrum m/e (relative intensity) 212 (10), 197 (20), 181 (7), 108 (84), 89 (160), 80 (22), 73 (100), 59 (20), 45 (31); exact mass, m/e 212.08727, calculated for C$_{10}$H$_{16}$O$_3$Si 212.08688.

3-(Hydroxymethyl)-2-[(trimethylsilyl)methyl]furan (20). To a stirred LiAlH$_4$ suspension (2.0 g, 53 mmol) in anhydrous diethyl ether (30 mL) at 0°C was added an etheral solution of carboxylic ester **19** (6.8 g, 32 mmol in 30 mL of anhydrous ether) dropwise over 20 min. After addition of the ester, the mixture was further stirred for 3 h and then worked up as usual[17] to provide the crude alcohol **20**. Distillation of the crude oil under vacuum gave essentially pure alcohol **20** (5.4 g, 29 mmol, 91%) : bp=103-105°C (17 mmHg); IR (neat, NaCl) 3280 (O-H), 2900-2980 (C-H), 1260 (Si-CH$_3$), 1050 (C-OH) cm^{-1}; ^{1}H NMR (CDCl$_3$) δ 0.03 (s, 9H), 1.22 (t, 1H, J=4.6 Hz), 2.06 (s, 3H), 4.41 (d, 2H, J=4.6 Hz), 6.34 (d, 1H, J=1.9 Hz), 7.20 (d, 1H, J=1.9 Hz); mass spectrum m/e (relative intensity) 184 (7), 94 (100), 75 (32), 73 (66), 45 (24); exact mass, m/e 184.09234, calcd for C$_9$H$_{16}$O$_2$Si 184.09196.

3-(1-Hydroxyethyl)-2-[(trimethylsilyl)methyl]furan (22). To a solution of pyridine (12.4 g, 156 mmol) in dichloromethane (200 mL), protected by a drying tube, was added chromium trioxide (7.8 g, 78 mmol). The solution was stirred for 15 min at room temperature and then a solution of alcohol **20** (2.4 g, 13 mmol) in dichloromethane (10 mL) was added in one portion. A tarry, black deposit separated immediately. After stirring an additional 15 min at room temperature, the solution was decanted from the residue and worked up in the same manner as reported by Ratcliffe[18] to afford the crude aldehyde **21**. Distillation of the crude oil under reduced

pressure provided essentially pure aldehyde **21** (1.6 g, 62%) : bp 68-70 °C (0.5 mmHg); ^{1}H NMR (CDCl$_3$) δ 0.06 (s, 9H), 2.45 (s, 2H), 6.63 (d, 1H, J=2.1 Hz), 7.20 (d, 1H, J=2.1 Hz), 9.81 (s, 1H); mass spectrum m/e (relative intensity) 182 (13), 167 (12), 73 (100), 45 (17).

To a stirred solution of aldehyde **21** (1.6 g, 8.8 mmol) in THF (80 mL) was added dropwise an etheral solution of methyl lithium (6.5 mL, 1.4 M, 9.1 mmol) at -78 °C. After addition, the solution was further stirred for 30 min and was then quenched with water at low temperature. The mixture was extracted with 3 x 100 mL of diethyl ether. The combined organic phases was washed with 100 mL of brine and dried over anhydrous MgSO$_4$. Removal of the solvent left the crude oil which was further distilled under reduced pressure to give essentially pure alcohol **22** (1.4 g, 80%): bp 65-67 °C (0.35 mmHg); IR (neat, NaCl) 3360 (broad, O-H), 2900-2980 (C-H), 1250 (Si-CH$_3$) cm^{-1}; ^{1}H NMR (CDCl$_3$) δ 0.04 (s, 9H), 1.43 (d, 3H, J=6.5 Hz), 1.53 (bs, 1H), 2.06 (s, 2H), 4.74 (q, 1H, J=6.5 Hz), 6.35 (d, 1H, J=1.7 Hz), 7.18 (d, 1H, J=1.7 Hz); mass spectrum m/e (relative intensity) 198 (20), 108 (90), 75 (46), 73 (100), 45 (19); exact mass, m/e 198.10794, calcd for C$_{10}$H$_{18}$O$_2$Si 198.10761.

3-(1-Acetoxyethyl)-2-[(trimethylsilyl)methyl]furan (15). To a stirred solution of acetyl chloride (1.2 g, 15 mmol) in benzene (10 mL), protected by a drying tube, at room temperature was added a solution of pyridine (1.2 g, 15 mmol) in benzene (5 mL). After addition, a white precipitate formed immediately. The solution was stirred for 10 min and a solution of alcohol **22** (1.4 g, 7 mmol) in benzene (5 mL) was added. The mixture was stirred for additional 2 h, and then quenched with water and extracted with 2 x 50 mL of dichloromethane. The combined organic phases was washed with 100 mL of brine, dried over anhydrous Na$_2$SO$_4$ and concentrated to provide a colorless crude oil. Distillation of the crude oil under reduced pressure

afforded essentially pure ester **15** (1.5 g, 88 %): bp 81-83 °C (1.4 mmHg); IR (neat, NaCl) 2900-2990 (C-H), 1740 (C=O), 1250 (Si-CH$_3$) cm^{-1}; ^{1}H NMR (CDCl$_3$) δ 0.02 (s, 9H), 1.45 (d, 3H, J=6.5 Hz), 2.00 (s, 3H), 2.02-2.11 (AB q, 2H, J=14.8 Hz), 5.74 (q, 1H, J=6.5 Hz), 6.35 (d, 1H, J=1.9 Hz), 7.18 (d, 1H, J=1.9 Hz); GC/MS (70eV) m/e (relative intensity) 240 (6), 181 (11), 117 (17), 108 (100), 73 (83), 43 (56); exact mass m/e 180.09720, calculated for C$_{10}$H$_{16}$OSi (M-CH$_3$COOH) 180.09705.

Methyl 2-[1(trimethylsilyl)ethyl]furan-3-carboxylate (23). To a solution of diisopropylamine (4.8 g, 47.5 mmol) in THF (40 mL) at -78°C under nitrogen was added 19 mL of 2.5 M n-BuLi solution in hexanes (47.1 mmol). After 2h at -78°C, a solution of trimethylsilylated methyl furancarboxylate **19** in THF (5 mL) was added. The reaction mixture was further stirred at -78°C for 8 h and a solution of MeI (10.0 g, 71 mmol) in THF (5 mL) was then added. After being further stirred for 30 min, the reaction mixture was quenched by addition of water at low temperature. The quenched solution was warmed to room temperature and extracted with diethyl ether twice. The combined extracts was washed with brine, dried over anhydrous MgSO$_4$, and concentrated under reduced pressure and fractional distilled under vacuum to provide a mixture of **23** and overmethylated product **24** in a 10:1 ratio. The mixture was further purified on a silica gel flash chromatography with a mixture of benzene and hexanes (1:3) as the eluent. The purity of **23** was checked by GC/MS analysis: bp 72-73°C (0.9 mmHg); IR (neat, NaCl) 2900-3000 (C-H), 1720 (s, C=O) 1250 (Si-CH$_3$) cm^{-1}; ^{1}H NMR (CDCl$_3$) δ -0.01 (s, 9H), 1.32 (d, J=7.3 Hz, 3H), 3.25 (q, J=7.3 Hz, 1H), 3.78 (s, 3H), 6.58 (s, 1H), 7.18 (s, 1H); mass spectrum, m/e (relative intensity) 226 (M$^+$, 17), 211 (15), 197 (5), 195 (5), 167 (3), 151 (8), 123 (9), 122 (100), 121 (30), 94 (30), 73 (60); exact mass, m/e 226.10266, calcd for C$_{11}$H$_{18}$O$_3$Si 226.10253.

3-(Hydroxymethyl)-2-[1-(trimethylsilyl)ethyl]furan (25). To a suspension of LiAlH$_4$ (1g, 26 mmol) in diethyl ether (50 mL) at 0°C was added dropwise a solution of ester **23** (1.8g, 8.0 mmoL). The reaction mixture was stirred overnight at ambient temperature and worked up as usual[17] to provide the crude oil which was subjected to vacuum distillation to provide essentially pure alcohol **25** (1.1g, 70%): bp 74-75°C (1 mmHg); IR (neat, NaCl) 3700-3100 (broad, O-H), 2880-2960 (C-H), 1250 (Si-CH$_3$) cm^{-1}; ^{1}H NMR (CDCl$_3$) δ -0.14 (s, 9H), 1.30 (d, J=7.5 Hz, 3H), 1.54 (broad s, 1H), 2.25 (q, J=7.5 Hz, 1H), 4.44-4.38 (AB q, J=12.1 Hz, 2H), 6.33 (d, J=1.7 Hz, 1H), 7.22 (d, J=1.7 Hz, 1H); mass spectrum, m/e (relative intensity) 198 (M$^+$, 5) 183 (4), 167 (5), 124(5), 109 (13), 108 (100), 107 (18), 79 (22), 75 (50), 73 (89), 45 (33), 43 (20); exact mass, m/e 198.10759, calcd for C$_{10}$H$_{18}$O$_2$Si 198.10761.

Deuterated **25** was prepared in the same manner except that LiAlD$_4$ was used as the reducing agent: IR (neat, NaCl) 3700-3000 (broad, C-H) 2200, 2120 (C-D), 1250 (Si-CH$_3$) cm^{-1}; ^{1}H NMR (CDCl$_3$) δ -0.07 (s, 9H), 1.19 (s, 1H), 1.30 (d, J=7.5 Hz, 3H), 2.25 (q, J=7.5 Hz, 1H), 6.34 (d, J=1.9 Hz, 1H), 7.22 (d, J=1.9 Hz, 1H); mass spectrum, m/e (relative intensity) 200 (M$^+$, 4), 185 (3), 167 (6), 110 (100), 81 (11), 75 (33), 73 (73); exact mass, m/e 200.12034, calcd. for C$_{10}$H$_{16}$D$_2$O$_2$Si 200.12017.

3-(Acetoxymethyl)-2-[1-(trimethylsilyl)ethyl]furan (16). Ester **16** was prepared following the procedure described previously in the preparation of **15** from a solution of acetyl chloride (0.9 g, 11.5 mmol) in benzene (20 mL) and a solution of pyridine (0.9 g, 11.1 mmol) in benzene (5 mL), and a solution of alcohol **25** (1.1g, 5.6 mmol) to afford essentially pure **16** (1.1 g, 82 %): bp 82-83 °C (0.75 mmHg); IR (neat, NaCl) 2800-2960 (C-H), 1750 (C=O) 1250, 1230 (Si-CH$_3$) cm^{-1}; ^{1}H NMR (CDCl$_3$) δ -0.02 (s, 9H), 1.29 (d, J=7.4 Hz, 3H), 2.04 (s, 3H), 2.28 (q, J=7.4 Hz, 1H), 4.80-4.93 (AB q, J=12.3 Hz, 2H), 6.31 (d, J=1.9 Hz, 1H), 7.22 (d, J=1.9 Hz, 1H); mass spectrum, m/e

(relative intensity) 240 (M$^+$, 9), 225 (1), 198 (8), 183 (14), 117(23), 109 (10), 108 (100), 107 (20), 79 (20), 75 (32), 73 (81), 45 (25), 43 (56); exact mass, m/e 240.11813, calcd for $C_{12}H_{20}O_3Si$ 240.11818.

2-[1-(Trimethylsilyl)ethyl]-3-furaldehyde (26). To a vigorously stirred suspension of CrO_3 (0.9 g, 9 mmol) in P_2O_5 dried CH_2Cl_2 (50 mL) cooled in an ice-bath, was added 5 g of pyridine slowly. The reaction mixture turned a deep red. After 15 min a solution of alcohol **25** (300 mg, 1.5 mmol) in CH_2Cl_2 (10 mL) was added in one portion. A tarry black deposit precipitated immediately. The deep brownish solution was further stirred for 15 min, decanted and worked up as reported by Ratcliffe[18] to give a crude oil. Distillation of the crude oil under vacuum provided essentially pure aldehyde **26**: IR (CCl_4, NaCl) 2800-2970 (C-H), 2740 (O=C-H), 1670 (s, C=O) 1250 (Si-CH$_3$) cm^{-1}; ^{1}H NMR (CDCl$_3$) δ 0.01 (s, 9H), 1.38 (d, J=7.3 Hz, 3H), 2.85 (q, J=7.3 Hz, 1H), 6.64 (d, J=2.0 Hz, 1H), 7.23 (d, J=2.0 Hz, 1H), 9.85 (s, 1H); mass spectrum, m/e (relative intensity) 196 (m$^+$, 88), 181 (9), 167 (11), 151 (13), 147 (21), 138 (5), 124 (12), 107 (11), 95 (5), 75 (45), 73 (100); exact mass, m/e 196.09168, calcd for $C_{10}H_{16}O_2Si$ 196.09196.

Deuterated **26** was prepared from deuterated **25** in the same manner. The product was purified on a silica gel column with a mixture of hexanes and ethyl acetate (8:1) as the eluent: IR (neat, NaCl) 2900-2980 (C-H), 2100 (C-D), 1670 (C=O) 1250 (Si-CH$_3$) cm^{-1}; ^{1}H NMR (CDCl$_3$) δ 0.02 (s, 9H), 1.40 (d, J=7.3 Hz, 3H), 2.86 (q, J= 7.3 Hz, 1H), 6.66 (d, J=2.0 Hz, 1H), 7.24 (d, J=2.0 Hz, 1H); mass spectrum, m/e (relative intensity) 197 (M$^+$, 98), 182 (10), 168 (8), 147 (22), 125 (11), 108 (10), 75 (51), 73 (100); exact mass, m/e 197.09859, calcd for $C_{10}H_{15}DO_2Si$ 197.09824.

3-[-(Hydroxyethyl)]-2-[1-(trimethylsilyl)ethyl]furan (27). To a stirred solution of aldehyde **26** (130 mg, 0.67 mmol) in THF (20 mL) was added dropwise an

ethereal solution of methyl lithium (0.6 mL, 0.82 mmol) at -78°C. After addition of the reagent, the solution was further stirred for 30 min and was quenched with water at low temperature and worked up as mentioned previously in the preparation of **22** to give a diastereomeric mixture of alcohols **27** (135 mg, 95 %): IR of the diastereomeric mixture (neat), 3700-3100 (broad, O-H), 2890-2900 (C-H), 1260 (Si-CH$_3$) cm^{-1}; ^{1}H NMR of the diastereomeric mixture (CDCl$_3$) δ -0.01 and 0.02, (two s, 9H), 1.32-1.25 (two d, J=7.7 Hz, 3H), 1.43 (d, J=6.4 Hz, 3H), 2.23-2.28 (m, 1H), 4.75-4.82 (m, 1H), 6.36 (d, J=1.9 Hz, 1H), 7.21 (d, J=1.9 Hz, 1H); GC/MS, temperature program, initial temperature (time), rate, final temperature (time), 120 °C (5 min), 10 °C/min, 200 °C (5 min). Component 1: GC retention time (relative intensity) 9.68 min (65 %), mass spectrum, m/e (relative intensity) 212 (M$^+$, 2), 197 (3), 194 (3), 167 (5), 123 (10), 122 (52), 121 (5), 108 (3), 107 (41), 105 (3), 75 (35), 73 (100), 45 (29), 43 (33). Component 2: mass spectrum, m/e (relative intensity) 212 (M$^+$, 2), 197 (2), 194 (3), 167 (6), 123 (9), 122 (50), 121 (5), 108 (3), 107 (41), 105 (3), 75 (35), 73 (100), 45 (29), 43 (33); exact mass of the diasteromeric mixture m/e 212.12297, calcd for C$_{11}$H$_{20}$O$_2$Si 212.12326.

Deuterated **27** was prepared from deuterated **26** in the the same manner: bp ~100 °C (5.2 mmHg), IR of the diastereomeric mixture (neat, NaCl) 3700-3100 (broad, O-H), 2890-2990 (C-H), 2160 (C-D), 1260 (Si-CH$_3$) cm^{-1}; ^{1}H NMR (CDCl$_3$) δ 0.02-0.12 (two s, 9H), 1.26-1.32 (two d, J=7.5 Hz, 3H), 1.43 (s, 3H), 2.24 (m, 1H), 6.36 (d, J=1.9 Hz, 1H), 7.21 (d, 1.9 Hz, 1H); GC/MS, temperature program, initial temperature (time), rate, final temperature (time), 120 °C (5 min), 10 °C/min, 200 °C (5 min). Component 1: GC retention time (relative intensity) 9.30 min (62 %), mass spectrum, m/e (relative intensity), 213 (2), 198 (3), 167 (4), 123 (100), 108 (54), 75 (31), 73 (82), 45 (31), 43 (42). Component 2: GC retention time (relative intensity) 9.86 min (33 %), mass

spectrum m/e (relative intensity) 213 (2), 198 (3), 167 (5), 123 (100), 108 (55), 75 (33), 73 (88), 45 (32), 43 (41); exact mass m/e 213.12925, calcd for $C_{11}H_{19}DO_2Si$ 213.12954.

3-[1-(Acetoxyethyl)]-2-[1-(trimethylsilyl)ethyl]furan (17). Acetoxy furan **17** was prepared following the procedure described previously in the preparation of **15** from a solution of acetyl chloride (400 mg, 5.12 mmol) and pyridine (400 mg 5.06 mmol) in benzene (10 mL), and a solution of alcohol **27** (130 mg, 0.61 mmol) in benzene (5 mL) to provide a diastereomeric mixture of esters **17** (105 mg, 68 %). IR of the mixture (NaCl, neat) 2860-2980 (O-H), 1740 (C=O), 1250 (Si-CH$_3$) cm^{-1}; ^{1}H NMR of the major component (66 %) (CDCl$_3$) δ -0.04 (s, 9H), 1.24 (d, J=7.5 Hz, 3H), 1.45 (d, J=6.5 Hz, 3H), 1.99 (s, 3H), 2.28 (q, J=7.5 Hz, 1H), 5.83 (q, J=6.6 Hz, 1H), 6.34 (d, J=1.9 Hz, 1H), 7.21 (d, J=1.9 Hz, 1H). GC/MS of the major component, temperature program, initial temperature (time), rate, final temperature (time), 120 °C (5 min), 10 °C/min, 200 °C (10 min), retention time 11.21 min; mass spectrum, m/e (relative intensity) 254 (M$^+$, 5), 212 (6), 197 (8), 195 (9), 194 (6), 122 (100), 177 (24), 107 (59), 75 (30), 73 (95), 45 (26), 43 (43). ^{1}H NMR spectrum of the minor component (32 %) (CDCl$_3$) δ. -0.04 (s, 9H), 1.26 (d, J=7.4 Hz, 3H), 1.44 (d, J=6.6 Hz, 1H), 1.99 (s, 3H), 2.33 (q, J=7.4 Hz, 1H), 5.76 (q, J=6.6 Hz, 1H), 6.33 (d, J=1.9 Hz, 1H), 7.21 (d, J=1.9 Hz, 1H); GC/MS of the minor component, temperature program, initial temperature (time), rate, final temperature (time), 120 °C (5 min), 10 °C/min, 200 °C (10 min), GC retention time 11.35 min; mass spectrum, m/e (relative intensity) 254 (M$^+$, 5) 212 (6), 197 (8), 195 (9), 194 (6), 122 (100), 117 (24), 107 (59), 75 (30), 73 (95), 45 (26), 43 (43). Exact mass of the diastereomeric mixture, m/e 254.13394. calcd for $C_{13}H_{22}O_3Si$ 254.13383.

The diastereomeric deuterated derivatives of **17** were prepared from deuterated alcohol **27** in the same manner: IR (neat, NaCl) 2860-2970 (C-H), 1740 (C=O), 1250

(Si-CH$_3$) : The ^{1}H NMR spectra and GC/MS of both diastereomers were obtained from their mixture: ^{1}H NMR of the major component (64 %) (CDCl$_3$) δ -0.16 (s, 9H), 1.29 (d, J=7.4Hz, 3H), 1.46 (s, 3H), 2.01 (s, 3H), 2.30 (q, J=7.4 Hz, 1H), 6.35 (d, J=1.9 Hz, 1H), 7.21 (d, J=1.9 Hz, 1H); GC/MS of the major component, temperature program, initial temperature (time), rate, final temperature (time), 120 °C (5 min), 10 °C/min, 200 °C (10 min), retention time 11.23 min; mass spectrum, m/e (relative intensity) 255 (M$^+$, 4), 213 (4), 198 (8), 196 (8), 123 (100), 108 (47), 75 (29), 73 (85), 45 (30), 43 (56). ^{1}H NMR spectrum of the minor component (36 %), (CDCl$_3$) δ -0.16 (s, 9H), 1.26 (d, J=7.4Hz, 3H), 1.46 (s, 3H), 2.01 (s, 3H), 2.38 (q, J=7.4 Hz, 1H), 6.34 (d, J=1.9 Hz, 1H), 7.21 (d, J=1.9 Hz, 1H). GC/MS of the minor component, temperature program, initial temperature (time), rate, final temperature (time), 120 °C (5 min), 10 °C/min, 200 °C (10 min), retention time 11.37 min; mass spectrum 255 (M$^+$, 6), 213 (5), 198 (9), 196 (9), 123 (91), 108 (52), 75 (27), 73 (100), 40 (30), 43 (56). Exact mass of the diastereomers, m/e 255.13974, calcd for C$_{13}$H$_{21}$DO$_3$Si 255.14011.

Diels-Alder trapping reaction of 12 with methyl acrylate. To a solution of 3-(1-acetoxyethyl)-2-[(trimethylsilyl)methyl]furan **12** (100 mg, 0.42 mmol) and methyl acrylate (360 mg, 4.2 mmol) in acetonitrile (8.0 mL) under nitrogen at reflux temperature was added dropwise a solution of TBAF (180 mg, 5.7 mmol) in acetonitrile (5.0 mL). After addition, the solution was stirred for additional 30 min, and then was quenched with water. The mixture was extracted with 2 x 30 mL of diethyl ether. The combined organic phase was washed with 2 x 50 mL of distilled water, 50 mL of brine and dried over anhydrous MgSO$_4$. Removal of the solvent provided a slightly yellowish crude oil (80 mg). By use of the GC/MS and ^{1}H NMR analyses, four major components in the crude oil were identified as regio- and stereo-isomers of Diels-Alder adducts of **28** with methyl acrylate. GC/MS, initial temperature (time), rate, final temperature

(time), 120 °C (5 min), 5 °C/min, 250 °C (5min).   Diels-Alder adduct 1: retention

time (20.33 min); mass spectrum, m/e (relative intensity) 194 (40), 179 (5), 163 (10), 135

(100), 134 (45), 119 (41), 108 (35), 91 (34), 79 (20).   Diels-Alder adduct 2: retention

time (20.42), mass spectrum, m/e (relative intensity) 194 (54), 179 (16), 163 (16), 135

(68), 134 (100), 119 (86), 108 (53), 91 (56), 79 (38).   Diels-Alder adduct 3: retention

time (20.87), mass spectrum, m/e (relative intensity) 194 (55), 179 (4), 163 (14), 135

(55), 134 (95), 119 (83), 108 (100), 91 (48), 79 (33).   Diels-Alder adduct 4: retention

time (20.95), mass spectrum, m/e (relative intensity) 194 (42), 179 (9), 163 (10), 135

(41), 134 (100), 119 (84), 108 (57), 91 (55), 79 (24).

Preparation and direct observation of 3-ethylidene-2-methylene-2,3-dihydrofuran (12).   To a deaerated solution of 3-(1-acetoxyethyl)-2-[(trimethylsilyl)methyl]furan **15** (0.2 g, 0.8 mmol) in d_3-acetonitrile (3.0 mL) under nitrogen was

added TBAF (1.1 g, 3.5 mmol). The solution was stirred for 5 min and then was distilled

under reduced pressure (5-8 mmHg) at ambient temperature which was regulated by

use of a water bath. The distillate was trapped in a cold-trap at -78°C. After distillation,

the solidified distillate was warmed to room temperature and the ^{1}H NMR spectrum of

the solution was obtained: ^{1}H NMR (CD$_3$CN) δ 1.79 (d, 3H, J=7.6 Hz) 4.47 (s, 1H), 4.72

(s, 1H), 5.84 (q, 1H, J=7.6 Hz), 6.00 (bs, 1H), 6.85 (bs, 1H). The ^{1}H NMR spectrum of E-

29[5b] reported by Huang: (CDCl$_3$) δ 1.16 (s, 9H), 4.52 (d, J=2 Hz, 1H), 4.68 (J=2 Hz, 1H),

5.81 (s, 1H), 6.06 (d, J=2.7 Hz, 1H), 6.77 (m, 1H).

Preparation and direct observation of 2-ethylidene-3-methylene-2,3-dihydrofuran (13).   o-QDM **13** was prepared following the procedure described in the

preparation of o-QDM **12** from a deaerated solution of 3-(1-acetoxyethyl)-2-[(trimethylsilyl)methyl]furan **16** (0.3 g, 1.3 mmol) in d_3-acetonitrile (3.0 mL) and TBAF

(1.4 g, 4.4 mmol) and the ^{1}H NMR spectrum of **13** was obtained. On the basis of ^{1}H

NMR spectrum, we concluded that a mixture of cis-trans isomers in a ratio ca. 2 to 1 was obtained. We assigned the Z-configuration to the major dimer. Since **13** is relatively reactive and dimerized effectively during the data acquisition process, the ^{1}H NMR signals of **13** were mixed with the signals of the dimers. Only the signals of the vinylic protons of **13** can be clearly identified.   The major isomer of **13**: ^{1}H NMR (CD$_3$CN) δ 4.60 (s, 1H), 5.00 (s, 1H), 5.30 (q, J=8 Hz, 1H), 5.76 (s, 1H), 6.90 (s, 1H).   The minor isomer of **13**: ^{1}H NMR (CD$_3$CN) δ 5.00 (s, 1H), 5.10 (s, 1H), 5.43 (q, J=8 Hz, 1H), 5.80 (s, 1H), 6.77 (s, 1H). The ^{1}H NMR spectrum of Z-**4** reported by Huang[5b]: (CDCl$_3$), δ 1.15(s, 9H), 4.74 (d, J=1 Hz, 1H), 4.96 (d, J=1 Hz, 1H), 5.25 (s, 1H), 5.75 (d, J=3 Hz, 1H), 6.77 (br, 1H).

Preparation and direct observation of 2,3-ethylidene-2,3-dihydrofuran (14).   o-QDM **14** was prepared following the procedure described in the preparation of o-QDM **12** from a deaerated solution of 3-(1-acetoxyethyl)-2-[1-(trimethylsilyl)-ethyl]furan **17** (0.1 g, 0.4 mmol) in d$_3$-acetonitrile (2 mL) and TBAF (0.5 g, 1.6mmol) and the ^{1}H NMR spectrum of o-QDM **14** was obtained. In this experiment, we obtained two cis-trans isomers in a ratio of 2:1 in the solution. We assigned them as EE-**14** and ZE-**14**.   The major isomer of **14**: ^{1}H NMR (CD$_3$CN) δ 1.68(d, J=7.3 Hz, 3H), 1.74 (d, J=8.0 Hz, 3H), 5.16 (q, J=7.3 Hz, 1H), 5.59 (q, J=8 Hz, 1H), 5.97 (d, J=2.7 Hz, 1H), 6.88 (broad s, 1H).   The minor isomer of **14**: 1.74 (d, J=8 Hz, 3H), 1.84 (d, J=8Hz, 1H), 5.30 (q, J=8 Hz, 1H), 5.64 (q, J=8 Hz, 1H), 6.03 (m, 1H), 6.85 (broad s, 1H).

Deuterated EE-**14** and ZE-**14** were generated in the same manner. Their spectra were obtained from the spectrum of the distillate. The product ratio is ca. 2:1. The major cis-trans isomer of d-**14**: 1.67 (d, J=7.3 Hz, 3H), 1.73 (s, 3H), 5.14 (q, 7.3 Hz, 1H), 5.96 (d, J=2.6 Hz, 1H), 6.88 (d, J=2.6 Hz, 1H). The minor cis-trans isomer of d-**14**:

1.74 (d, J=8 Hz, 3H), 1.83 (s, 3H), 5.34 (q, J=8 Hz, 1H), 6.02 (d, J=2.8 Hz, 1H), 6.84 (d, J=2.8 Hz, 1H).

Dimerization of 3-ethylidene-2-methylene-2,3-dihydrofuran (12). To a deaerated solution of 3-(1-acetoxyethyl)-2-[(trimethylsilyl)methyl]furan **(15)** (489 mg, 2.08 mmol) in acetonitrile (130 mL) under nitrogen was added a deaerated solution of TBAF (2.5 g, 7.9 mmol) in acetonitrile (20 mL). The solution was stirred for 72 h, and then the solvent was removed in vacuo. The residue was taken up with a small amount of diethyl ether and chromatographed on neutral alumina (Brockman activity grade 1) with a mixture of hexanes and diethyl ether (1:1) as the eluent. The isolated yield of the dimer mixture was 78 mg (35%). GC analysis showed that seven components were present in the mixture. The mixture was chromatographed on silica gel (60-200 mesh, 22x48 cm, flow rate 6-8 mL/min) with hexanes. This provided a mixture which contained **35** and **31** as the major components in the first band, partially resolved **34** in the second band and completely resolved **30** in the third band. The forth band was collected effectively by changing the eluent to a mixture of hexanes and ether (1:1) and this gave essentially pure **33**. The mixture from the first band was further chromatographed on basic alumina (150 g, Brockman activity grade 1) with hexanes as the eluent. This afforded pure **35** in earlier fractions of the first band and completely resolved **31** in the second band. Finally, the partially resolved **34** was chromatographed on neutral alumina (Brockman activity grade 1) with hexanes as the eluent and essentially pure **34** was obtained: GC/MS, temperature program, initial (time), rate, final (time), 100 °C (5 min), 4 °C/min, 200 °C (10 min). Dimer **30** (GC retention time 23.27 min): ¹H NMR (CDCl₃) δ 1.29-1.27 (2d, 6H), 2.85-2.83 (m, 2H), 3.14-2.97 (m, ABCD , 4H), 6.14 (d, J=1.6 Hz, 2H), 7.14 (d, J=1.6 Hz, 2H); mass spectrum, m/e (relative intensity) 216 (19), 210 (4), 187 (8), 108 (100), 79 (18). Dimer

31 (GC retention time 25.52 min): ^{1}H NMR (CDCl$_3$) δ 1.13 (d, J=7.0 Hz, 6H), 2.92-3.02 and 3.16-3.26 (two m, AA'BB', 4H), 3.30 (q, J=7.0 Hz, 2H), 6.21 (d, J=1.8 Hz, 2H), 7.19 (d, J=1.8 Hz, 2H); mass spectrum, m/e (relative intensity) 216 (18), 210 (3), 187 (7), 108 (100), 79 (18).   Dimer **32** (GC retention time 23.94 min): ^{1}H NMR (CDCl$_3$) δ 1.20 (d, J=6.9 Hz, 3H),1.26 (m, 1H), 1.72 (d, J=6.9 Hz, 3H), 1.94-2.00 (dd, J$_1$=1.51 Hz, J$_2$=13.6 Hz, 1H), 2.57-2.86 (AB q, J=17.2 Hz, 2H), 2.93 (m, 1H), 4.81 (q, J=6.9 Hz, 1H), 5.72 (m, 1H), 6.30 (d, J=1.8Hz, 1H), 6.65 (bs, 1H), 7.28 (d, J=1.8 Hz, 1H); mass spectrum, m/e (relative intensity) 216 (20), 201(4), 187 (11), 108 (100), 79 (14).   **33** (GC retention time 21.44 min): ^{1}H NMR (CDCl$_3$) δ 1.00 (d, J=6.8 Hz, 3H), 1.13 (d, J=7.1Hz, 3H), 2.08 (m, 1H), 2.30 (dd, J$_1$=6.4 Hz, J$_2$=16.7 Hz, 1H), 2.66 (q, 7.1 Hz, 1H), 2.97 (dd, J$_1$=6.0 Hz, J$_2$ =16.6 Hz, 1H), 3.87 (d, J=2.0 Hz, 1H), 4.69 (d, J=2.0 Hz, 1H), 5.09 (d, J=2.9 Hz, 1H), 6.20 (d, J=1.8 Hz, 1H), 6.47 (d, J=2.9 Hz, 1H), 7.26(d, J=1.8 Hz, 1H); mass spectrum, m/e (relative intensity) 216 (12), 201 (4), 187 (9), 108 (100), 79 (19).   **34** (GC retention time 21.57 min): ^{1}H NMR (CDCl$_3$) δ 0.93 (d, J=6.6 Hz, 3H), 1.01 (d, J=7.0 Hz, 3H), 1.96 (m, 1H), 2.31 (m, J$_1$=2.8 Hz, J$_2$=11.4 Hz, J$_3$=16.6 Hz, 1H), 2.58 (m, 1H), 2.70 (dd, J$_1$=5.4 Hz, J$_2$=16.7 Hz, 1H), 4.04 (d, J=2.4 Hz, 1H), 4.70 (d, J=2.4 Hz, 1H), 4.78 (d, J=2.9 Hz, 1H), 6.22 (d, J=1.8 Hz, 1H), 6.54 (d, J= 2.9 Hz, 1H), 7.24 (d, J=1.8 Hz, 1H); mass spectrum, m/e (relative intensity) 216 (15), 201 (4), 187 (10), 108 (100), 79 (19).   **35** (GC retention time 22.79 min): mass spectrum m/e (relative intensity) 216 (18), 201 (5), 187 (10), 108 (100), 79 (18).   **37** (GC retention time 22.61 min): mass spectrum, m/e (relative intensity) 216 (19), 210 (5), 187 (15), 108 (100), 79 (19).

Pyrolysis of [4+2] dimer 34.   Dimer **34** (retention time 21.57) (~10 mg) was flash vacuum pyrolyzed (oven 658-665°C; sample chamber 55-60°C; pressure 2.1x10^{-5} torr) in a normal manner[19] to give a crude mixture with two major components. The mixture was taken up with hexanes and chromatographed on silica gel with hexanes

to give a relatively pure mixture. GC/MS and ^{1}H NMR analyses showed that both of them are [4+4] dimers **35** and **36** in a 2:1 ratio.: GC/MS, (70 eV) m/e (relative intensity) **35** (retention time 22.75 min) 216 (30), 201 (5), 187 (14), 108 (100), 79 (17). **36** (retention time 22.23 min) 216 (30), 201 (5), 187 (14), 108 (100), 79 (17).

Dimerization of 2-ethylidene-3-methylene-2,3-dihydrofuran (13). To a deaerated solution of **16** (220 mg, 0.92 mmol) in acetonitrile (10 mL) under nitrogen was added a solution of TBAF (1.3 g, 4 mmol) in acetonitrile (10 mL). The solution was stirred overnight and the solvent was removed under reduced pressure. The residue was taken up with a small amount of water and the aqueous layer were extracted with hexanes. The extracts were combined, dried over anhydrous Na_2SO_4 and concentrated under reduced pressure (98.4 mg, 98 %). A sample of the crude products was subjected to ^{1}H NMR and GC/MS analyses. Seven dimers were identified by GC/MS analyses. The crude dimer mixture was then chromatographed on a silica gel column with hexanes as the eluent. Six dimer samples of **38-43**, pure enough for ^{1}H NMR analyses, were obtained. The disproportionation product **44** could not be isolated and identified directly. However, sufficient evidence to support the structural assignment was obtained after pyrolysis of the dimer mixture was performed. The temperature program used for GC/MS analyses: initial temperature (time), rate, final temperature (time), 120°C (5 min), 5 °C/min, 200 °C (5 min). [4+4] Dimer **38**: GC retention time (relative intensity) 16.36 min (12 %); ^{1}H NMR (CDCl3) δ 1.32-1.35 (m, 6H), 2.69-2.85 (m, AA'BB', 4H), 3.12-3.17 (m, 2H), 6.03 (d, J=1.8 Hz, 2H), 7.14 (d, J=1.8 Hz, 2H); mass spectrum, m/e (relative intensity) 216 (M[+], 31), 201 (11), 187 (16), 159 (5), 109 (28), 108 (100), 107 (17), 79 (25), 77 (13). [4+4] Dimer **39**: GC retention time (relative intensity) 17.59 min (18 %); ^{1}H NMR (CDCl3) δ 1.22 (d, J=7.0 Hz, 6 H), 2.55-2.66 and 2.96-3.05 (m, AA'BB', 4H), 3.48 (q, J=7 Hz, 2H), 6.10 (J=1.7 Hz, 2H), 7.20 (d, J=1.7 Hz, 2H); mass

spectrum, m/e (relative intensity) 216 (M$^+$, 30), 201 (10), 187 (15), 109 (27), 108 (100), 107 (17), 79 (24), 77 (12).   [4+2] Dimer **40**: GC retention time (relative intensity) 15.90 min (33 %), ^{1}H NMR (CDCl$_3$) δ 1.12 (d, J=7.0 Hz, 3H), 1.61 (d, J=6.8 Hz, 3H), 1.80-1.84 (m, 2H), 2.36-2.48 (m, 1H), 2.64-2.75 (m, 1H), 2.79 (q, J=7.0 hz, 1H), 4.24 (q, J=6.8 Hz, 1H), 5.00 (d, J=2.8 Hz, 1H), 6.17 (d, J=1.8 hz, 1H), 6.52 (broad s, 1H), 7.26 (broad s, 1H); mass spectrum, m/e (relative intensity) 216 (M$^+$, 26), 201 (10), 187 (15), 109 (25), 108 (100), 107 (21), 79 (30), 77 (15).   [4+2] Dimer **41**: GC retention time (relative intensity) 16.39 min (12 %); ^{1}H NMR (CDCl$_3$) δ 1.05 (m, J=6.9 Hz, 1H), 1.69 (d, J=6.8 Hz, 3H), 1.72-1.80 (m, 2H), 2.68 (q, J=6.9 Hz, 1H), 4.43 (q, J=6.8 Hz, 1H), 5.02 (d, J=2.9 Hz, 1H), 6.18 (d, J=1.9 Hz, 1H), 6.53 (d, J=2.9 Hz, 1H), 7.26 (d, J=1.9 Hz, 1H); mass spectrum, m/e (relative intensity) 216 (M$^+$, 24), 201 (10), 187 (14), 159 (44), 109 (25), 108 (100), 107 (19), 79 (28), 77 (13).   [4+2] Dimer **42**: GC retention time (relative intensity) 17.14 min (18 %); ^{1}H NMR (CDCl$_3$) δ 1.23 (d, J=7.12 Hz, 3H), 1.60 (d, J=7.7 Hz, 3H), 1.72-1.81 (m, 1H), 2.28-2.42 (m, 1H), 2.43-2.58 (m, 2H), 2.81 (q, J=7.1 Hz, 1H), 5.10 (dd, J_1=2.9 Hz, J_2=0.9 Hz, 1H), 5.32 (q, J=7.7 Hz, 1H), 6.17 (d, J=1.8 Hz, 1H), 6.36 (d, J=2.9 Hz, 1H), 7.26 (d, J=1.8 Hz, 1H); mass spectrum, m/e (relative intensity) 216 (M$^+$, 16), 201 (7), 187 (11), 109 (23), 108 (100), 107 (18), 79 (26), 77 (13).   [4+2] Dimer **43**: GC retention time (relative intensity) 17.24 min (4 %); ^{1}H NMR (CDCl$_3$) δ 1.13 (d, J=6.8 Hz, 1H), 1.73 (d, J=7.6 Hz, 1H), 1.88-1.94 (m, 1H), 2.33-2.43 (m, 1H), 2.47-2.53 (m, 2H), 3.30 (q, J=6.8 Hz, 1H), 4.92 (d, J=2.9 Hz, 1H), 5.16 (q, J= 7.7 Hz, 1H), 6.20 (d, J= 1.7 Hz, 1H), 6.39 (d, J=2.9 Hz, 1H), 7.26 (d, J=1.7 Hz, 1H); mass spectrum, m/e (relative intensity) 216 (M$^+$, 24), 201 (10), 187 (13), 109 (22), 108 (100), 107 (16), 79 (19), 77 (10).   Disproportionation product **44**: GC retention time (relative intensity) 16.04 min (2 %); mass spectrum. m/e (relative intensity) 216 (M$^+$, 22), 201 (5), 187 (9), 159 (4), 109 (100), 108 (20), 107 (23), 94 (4), 81 (16), 79 (17), 77 (20), 65 (6), 53 (10).

Flash vacuum pyrolysis of the dimer mixture of 38-44. FVP of a dimer mixture of **38-44** (~20 mg) was performed at 614-620 °C under vacuum (2.1x10^{-5} torr). The pyrolysate was collected in a liquid nitrogen cold trap. After the pyrolysis was finished, 1 to 2 mL of CDCl$_3$ was introduced into the trap. The trap was then allowed to warm to room temperature. The ^{1}H NMR spectrum of the pyrolysate was collected as a record of the original pyrolysate and a sample of the solution was subjected to GC/MS analyses. The deuterated solvent of the solution was then distilled under vacuum at ambient temperature. The distillate was trapped in a cold trap immersed in dry ice-acetone bath. Since the fragmentation product **45** has a low molecular weight, it was distilled along with the deuterated solvent. The trapped distillate was warmed to room temperature and the ^{1}H NMR spectrum of **45** was obtained The residue of the distillation was then subjected to a silica gel column and chromatographed with hexanes as the eluent to provide dimer samples of **38, 39, 44** and **46** pure enough for ^{1}H NMR analyses. By combining the information from the ^{1}H NMR and mass spectra, pyrolysis product **47** was identified (Table 5). Pyrolysis

Table 5. FVP of the dimer mixtures of 2-ethylidene-3-methylene-2,3-di-hydrofuran (**13**)

	Precursor	
	Mixture of **38-44**^{a}	Mixture of **40** and **41**^{b}
Pyrolysis product	Retention time, min (yield, %)	Retention time, min (yield, %)
45	4.05 (5.0)	4.05 (42.9)
47	13.27 (0.5)	13.32 (3.2)
44	13.65 (11.2)	13.68 (14.6)
38	13.86 (41.7)	13.89 (16.1)
39	14.79 (39.8)	14.82 (12.9)
46	15.53 (2.1)	15.58 (10.3)

a FVP at 614-620 °C under vacuum (2.1x10^{-5} torr).
b FVP at 625-638 °C under vacuum (1.4x10^{-4} torr).

of a mixture of [4+2] dimers **40** and **41** also gave rise to the same products. However, their distributions are different.   Disportionation product **44**: ^{1}H NMR (CDCl$_3$) δ 1.10 (t, J=7.5 Hz, 3H), 2.46 (q, J=7.5 Hz, 2H), 2.56-2.64 (m, AA'BB', 4H), 5.07 (d of d, J$_1$=11.4 Hz, J$_2$=1.5 Hz, 1H), 5.55 (d of d, J$_1$=17.4 Hz, J$_2$=1.5 Hz, 1H), 6.15 (d, J=1.7 Hz, 1H), 6.20 (d, J=1.8 Hz, 1H), 6.41 (d of d, J$_1$=17.4 Hz, J$_2$=11.4 Hz, 1H), 7.22 (m, 2H); mass spectrum, m/e (relative intensity) 216 (M$^+$, 16), 201 (5), 187 (9), 159 (4), 109 (100), 108 (19), 107 (25), 81 (18), 79 (18), 78 (4), 77 (21).   Fragmentation product **45**: ^{1}H NMR (CDCl$_3$) δ 2.05 (s, 3H)), 5.10 (d of d, J$_1$=11.3 Hz, J$_2$= 1.3 Hz, 1H), 5.55 (d of d J$_1$=17.4 Hz, J$_2$=1.3 Hz, 1H), 6.52 (d of d, J$_1$=17.4 Hz, J$_2$=11.3 Hz, 1H), 7.25 (d, J=1.7 Hz, 1H); mass spectrum, m/e (relative intensity), 108 (M$^+$, 100), 108 (32), 79 (78), 77 (50), 55 (11), 53 (23), 51 (22), 50 (12), 39 (32).   Compound **47**: mass spectrum m/e (relative intensity), 216 (M$^+$, 100), 201 (10), 187 (38), 173 (9), 171 (10), 159 (23), 155 (10), 145 (18), 131 (23), 129 (10), 128 (14), 115 (23), 108 913), 93 (41), 91 (17), 77 (16), 69 (14), 65 (12), 64 (15), 57 (35), 55 (41), 51 (19), 43 (33), 41 (16), 39 (22).   Product **46**: ^{1}H NMR (CD$_3$CN) δ 1.21 (t, J=7.5 Hz, 6H), 2.68 (q, J=7.5 Hz, 4H), 6.52 (s, 2H), 6.55 (d, J=2.0 Hz, 2H), 7.25 (d, J=2.0 Hz, 2H); mass spectrum, m/e (relative intensity) 216 (M$^+$, 100), 201 (10), 187 (36), 173 (8), 171 (10), 159 (22), 155 (10), 145 (17), 131 (22), 129 (10), 128 (15), 115 (18), 108 (15), 93 (30), 91 (14), 77 (14), 69 (10), 65 (10), 64 (14), 57 (34), 55 (34), 51 (14), 43 (27), 41 (11), 39 (17).

Dimerization of 2,3-diethylene-2,3-dihydrofuran (14).   To a deaerated solution of 3-(1-acetoxyethyl)-2-[1-(trimethylsilyl)ethyl]furan **(17)** (300mg, 1.2 mmol) in acetonitrile (10 mL) under nitrogen was added a solution of TBAF (1.5 g, 4.8 mmol) in acetonitrile (10 mL). The solution was stirred for 72 h and the solvent was removed under reduced pressure. Water was added to the residue, and the solution was

extracted with hexanes twice. The extracts were combined and washed with brine, dried over anhydrous Na_2SO_4, and concentrated under reduced pressure. A sample of the mixture was subjected to GC/MS analyses, and four major dimers and ten minor dimers were identified. The mixture was then subjected to a silica gel liquid chromatography with hexanes as the eluent, and the major dimers were separated and identified as **48-51**. However, the minor [4+4] dimer **54** could not be identified until pyrolysis of **48** was performed. [4+4] dimer **48**: ^{1}H NMR (CDCl3) δ 1.32 (d, J=6.4 Hz, 3H), 1.37 (d, J=6.5 Hz, 3H), 2.62 (m, 2H), 2.99 (m, 2H), 6.03 (d, J=1.8 Hz, 2H), 7.07 (d, J=1.8 Hz, 2H); mass spectrum m/e (relative intensity) 244 (M^+, 16), 215 (4), 187 (3), 123 (13), 122 (100), 121 (5), 107 (38), 79 (5), 77 (9). [4+2] dimer **49**: ^{1}H NMR (CDCl3) δ 0.87 (d, J=6.6 Hz, 3H), 1.18 (d, J=7.0 Hz, 3H), 1.21 (d, J=6.8 Hz, 3H), 1.47 (m, 1H), 1.74 (d, J=6.9 Hz, 3H), 2.20 (m, 1H), 2.65 (q, J=7.0 Hz, 1H), 4.35 (q, J=6.9 Hz, 1H), 4.99 (d, J=2.8 Hz, 1H), 6.22 (d, J=1.8 Hz, 1H), 6.48 (d, J=2.8 Hz, 1H), 7.24 (merged with CHCl3); mass spectrum, m/e (relative intensity) 244 (M^+, 13), 215 (4), 187 (3), 123 (12), 122 (100), 121 (6), 107 (42), 79 (6), 77 (8). [4+2] dimer **50**: ^{1}H NMR (CDCl3) δ 0.90 (d, J=7.0 Hz, 3H), 1.05 (d, J=6.9 Hz, 3H), 1.09 (d, J=7.3 Hz, 3H), 1.71 (d, J=6.8 Hz, 3H), 1.93 (m, 1H), 2.62 (d, J=7.3 Hz, 1H), 2.75 (m, 1H), 4.34 (q, J=6.8 Hz, 1H), 4.86 (d, J=2.9 Hz, 1H), 6.25 (d, J=1.8 Hz, 1H), 6.56 (d, J=2.9 Hz, 1H), 7.27 (d of d, J_1=1.8 Hz, J_2=1.0 Hz, 1H); mass spectrum, m/e (relative intensity) 244 (M^+, 14), 215 (4), 187 (3), 123 (11), 122 (100), 121 (5), 107 (40), 79 (5), 77 (8). [4+4] dimer **51**: ^{1}H NMR (CDCl3) δ 1.09 (d, J=6.8 Hz, 6H), 1.19 (d, J=6.8 Hz, 6H), 3.28 (m, 2H), 3.50 (m, 2H), 6.21 (d, J=1.7 Hz, 2H), 7.23 (d, J=1.7 Hz, 2H), mass spectrum m/e (relative intensity), 244 (M^+, 16), 215 (4), 187 (2), 123 (10), 122 (100), 121 (4), 107 (35), 79 (5), 77 (8).

Dimerization of deuterated *o*-QDM **14** was performed in the same manner and deuterated dimers **48-51** were isolated. [4+4] dimer d2-**48**: ^{1}H NMR (CDCl3) δ 1.30 (s,

3H), 1.37 (d, J=6.6 Hz, 3H), 2.83-3.03 (m, 2H), 6.03 (d, J=1.8 Hz, 2H), 7.07 (d, J=1.7 Hz, 2H); mass spectrum m/e (relative intensity) 246 (M$^+$, 20), 124 (13), 123 (100), 122 (4), 109 (2), 108 (26), 107 (8). [4+2] dimer d$_2$-49: ^{1}H NMR (CDCl$_3$) δ 0.86 (s, 3H), 1.18 (d, J=7.0 Hz, 3H), 1.25 (s, 3H), 1.74 (d, J=6.9 Hz, 3H), 2.65 (q, J=7.0 Hz, 1H), 4.35 (q, J=6.8 Hz, 1H), 4.99 (d, J=2.9 Hz, 1H), 6.22 (d, J=1.9 Hz, 1H), 6.48 (d, J=2.9 Hz, 1H), 7.24 (merged with CHCl$_3$); mass spectrum, m/e (relative intensity) 246 (M$^+$, 19), 124 (16), 123 (100), 109 (3), 108 (40), 107 (13). [4+2] dimer d$_2$-50: ^{1}H NMR (CDCl$_3$) δ 0.90 (s, 3H), 1.05 (d, J=7.0 Hz, 3H), 1.08 (s, 3H), 1.71 (d, J=6.8 Hz, 3H), 2.62 (d, J=7.0 Hz, 1H), 4.34 (q, J=6.8 Hz, 1H), 4.86 (d, J=3.0 Hz, 1H), 6.25 (d, J=1.8 Hz, 1H), 6.55 (d, J=2.9 Hz, 1H), 7.26 (m, 1H); mass spectrum, m/e (relative intensity) 246 (M$^+$, 18), 215 (6), 124 (14), 123 (100), 108 (24), 107 (7). [4+4] dimer d$_2$-51: ^{1}H NMR (CDCl$_3$) δ 1.11 (s, 6H), 1.24 (d, J=7.1 Hz, 6H), 3.48-3.52 (m, 2H), 6.22 (d, J=1.7 Hz, 2H), 7.23 (merged with CHCl$_3$ in the deuterated solvent), mass spectrum, m/e (relative intensity) 246 (M$^+$, 18), 124 (11), 123 (100), 109 (2), 108 (25).

Pyrolysis of deuterated [4+2] dimers d$_2$-49 and d$_2$-50. FVP of dimer d$_2$-49 (4 mg, 0.02 mmol) was performed at 616-627 °C under vacuum (0.7x10^{-5} torr). The sample chamber was warmed to 40 °C during the pyrolysis. The pyrolysate was collected in a liquid nitrogen cold trap. After the pyrolysis was finished, 1 mL of CDCl$_3$ was introduced into the cold trap. The trap was then warmed to room temperature and the ^{1}H NMR spectrum of the pyrolysate was collected (Figure 4a). In addition, a sample of the solution was subjected to GC/MS analyses. Two fragmentation products d$_2$-52, d$_2$-53 and three [4+4] dimers d$_2$-48, d$_2$-54 and d$_2$-55 were identified by GC/MS analyses (Table 6). The temperature program used in the GC/MS analyses: initial temperature (time), rate, final temperature (time), 80 °C (10 min), 1.5 °C/min, 160 °C (30 min). Fragmentation products d$_2$-52: GC retention time (relative intensity)

4.84 min (16 %); mass spectrum, m/e (relative intensity) 123 (M$^+$, 75), 109 (7), 108 (100), 107 (10), 94 (4), 93 (1), 92 (12), 92 (16), 91 (5), 80 (58), 79 (22), 78 (71), 77 (36). Fragmentation product d$_2$-**53**: GC retention time (relative intensity) 5.18 min (4 %); mass spectrum, m/e (relative intensity) 123 (M$^+$, 87), 109 (7), 108 (100), 107 (39), 94 (10), 93 (2), 92 (16), 91 (5), 80 (58), 79 (22), 78 (71), 77 (36). [4+4] dimer d$_2$-**54**: GC retention time (relative intensity) 51.46 min (15 %) ; mass spectrum, m/e (relative intensity) 246 (M$^+$, 19), 124 (15), 123 (100), 122 (4), 108 (28), 107 (10). [4+4] dimer d$_2$-**48**: GC retention time (relative intensity) 52.25 min (21 %) ; mass spectrum, m/e (relative intensity) 246 (M$^+$, 16), 124 (13), 123 (100), 122 (4), 108 (29), 107 (10). [4+4] dimer d$_2$-**55**: GC retention time (relative intensity) 58.06 min (36 %) ; mass spectrum, m/e (relative intensity) 246 (M$^+$, 19), 124 (11), 123 (100), 122 (4), 108 (28), 107 (9).

FVP of dimer d$_2$-**50** (4 mg, 0.02 mmol) was performed at 614-622 °C under vacuum (0.7x10^{-5} torr). The sample chamber was warmed to 40 °C during the pyrolysis. The pyrolysate was collected in a liquid nitrogen cold trap. After the pyrolysis was finished, 1 mL of CDCl$_3$ was introduced into the cold trap. The trap was then warmed to room temperature. The ^{1}H NMR spectrum of the pyrolysate was collected (Figure 4b). In addition, a sample of the solution was subjected to GC/MS analyses. Two common fragmentation products d$_2$-**52** and d$_2$-**53** were identified by GC/MS analyses . However, only two major peaks for the [4+4] dimers, instead of three as in the pyrolysis of d$_2$-**49**, were observed. This observationis rationalized by suggesting that the retention times of dimers **56** and **57** are nearly the same and the signals overlap. The dimer with a retention time of 60.46 min was identified as [4+4] dimer d$_2$-**51**. This assignment was further confirmed by the chemical shifts in the ^{1}H NMR of the pyrolysate. [4+4] dimer d$_2$-**56** and d$_2$-**57**: GC retention time (relative intensity) 58.36 min (28 %); mass spectrum, m/e (relative intensity) 246 (M$^+$, 16), 124

(11), 123 (100), 122 (4), 109 (2) 108 (27), 107 (9).   [4+4] dimer d_2-51: GC retention time

(relative intensity) 60.46 min (42 %) ; mass spectrum, m/e (relative intensity) 246 (M^+,

15), 124 (10), 123 (100), 122 (4), 109 (2) 108 (28), 107 (9).

Table 6. GC/MS analyses of the original dimers of deuterated o-QDM 14 and the major components in the pyrolysates of the deuterated [4+2] dimers 49 and 50

	GC retention time , min (yield %)		
Assigned structure	Dimer of o-QDM 14	Pyrolysate of 49	Pyrolysate of 50
Fragmentation Product 52	-	4.84 (17)	4.85 (16)
Fragmentation Product 53	-	5.18 (4)	5.19 (4)
[4+4] dimer 54	-	51.46 (15)	_b_
[4+4] dimer 48	52.42 (6.5)	52.25 (21)	-
[4+2] dimer 49	54.15 (38.6)	-	-
[4+2] dimer 50	58.00 (36.0)	-	-
[4+4] dimer 55	58.06 (~ 2)	58.06 (37)	_b_
[4+4] dimer 56 and 57	-	_a_	58.36 (27)
[4+4] dimer 51	60.43 (6.5)	_a_	60.40 (40)

a The minor components, which are less than 3 %, may be generated from the impurity in the pyrolyzed sample of 49
b The minor components, which are less than 4 %, may be generated from the impurity in the pyrolyzed sample of 50

REFERENCES

(1)   Based on work by M.-k. Leung in partial fulfillment of the requirements for the Ph.D. Degree at Iowa State University.

(2)   Trahanovsky, W. S.; Cassady, T. J.; Woods, T. L. *J. Am. Chem. Soc.* **1981**, *103*, 6691.

(3)   Chou, C. H.; Trahanovsky, W. S. *J. Am. Chem. Soc.* **1986**,*1108*, 4138.

(4)   Chou, C. H. and Trahanovsky, W. S. *J. Org. Chem,* **1986**, *51*, 4208.

(5)   (a) Chou. C. H. Ph. D. dissertation, Iowa State University, 1986. (b) Huang, Y. C. J. Ph. D. dissertation, Part I, Iowa State University, 1986. (c) Lee, S. K. Ph. D. dissertation, Part I, Iowa State University, 1987.

(6)   Chauhan P. M. S.; Crew, A. P. A.; Jenkins, G.; Storr, R. C.; Walker, S. M.; Yelland, M. *Tetraherdon Lett.* **1990**, *31*, 1487.

(7)   (a) Marinelli, E. R. *Tetrahedron lett.* **1982**, *23*, 2745 (b) Vice, S. F.; Nandin de Carvalno, H.; Taylor, N. G.; Dmitrienku, G. I. *Tetrahedron lett,* **1989**, *30*, 7289. (c) Haber, M.; Pindur, U. *Tetrahedron,* **1991**, *47*, 1925.

(8)   Huang, Y. C. J. MS. Thesis, Iowa State University, 1984. (e) van den Berg, K. J. Ph. D. dissertation, Groningen Univeristy, 1990.

(9)   Errede, L. A. *J. Am. Chem. Soc.* **1961**, *83*, 949. (b) Macias, J. R. Ph.D. Dissertation, Iowa State University, 1987. (c) Fischer, D. R. Ph. D. Dissertation, Iowa State University, 1990. (d) Trahanovsky, W. S. Macias, J. R. *J. Am. Chem. Soc.* **1986**, *108*, 6820. (e) Trahanovsky, W. S.; Chou, C. H.; Fischer, D. R.; Gerstein, B. C. *J. Am. Chem. Soc.* **1988**, *110*, 6579.

(10)   Winnik, M. A. *Chem. Rev.* **1981**, *81*, 491; *Acc. Chem. Res.* **1985**, *18*, 73.

(11)   See Curtin-Hammett Principle: Carey, F. A.; Sundberg, R. J. *Advanced Organic Chemistry 2 ed.* Plenum: New York, **1984**, part A, p 219-220.

(12) Lee observed significant amounts of [1, 5] hydrogen shift products in the gas phase pyrolytic preparation of α-alkenyl furan-based o-quinodimethanes.[5c]

(13) (a) Ito, Y.; Nakatsuka, M.; Saegusa, T. *J. Am. Chem. Soc.* **1980**, *102*, 863. (b) Ito, Y.; Nakatsuka, M.; Saegusa, T *J, Am. Chem. Soc.* **1982**, *104*, 7609. (c) Ito, Y.; Nakajo, E. ; Sho, K.; Saegusa, T. *Synthesis* **1985**, 698. (d) Chauhan P. M. S.; Jenkins, G.; Walker, S. M.; Storr , R. C. *Tetrahedron Lett.* **1988**, *29*, 117.

(14) (a) Sieber, P. *Helv. Chim. Acta* **1977**, *60*, 2711. (b) Gerlach, H. *Helv. Chim. Acta* **1977**, *60*, 3039.

(15) Su, H.-W.; Hirose, K.; Shirai, K; Kumamoto, T. *Bull. Chem. Soc. Jpn.* **1989**, *62*, 2725.

(16) Clark, R. D.; Jahangir, *J. Org. Chem.* **1987**, *52*, 5378.

(17) Fieser, L. F. and Fieser, M. *Reagents for Organic Synthesis*; John Wiley and Sons: New York, **1967**; Vol 1, pp 581-595.

(18) Ratcliffe, R.; Rodehorst, R. *J. Org. Chem.* **1970**, *35*, 4000.

(19) (a) Trahanovsky, W. S.; Ong, C. C.; Pataky, J. G.; Weitl, F. J.; Mullen, P. W.; Clardy, J. C.; Hansen, R. S. *J. Org. Chem.* **1971**, *36*, 3575. (b) For review, see Brown, R. C. F. *Pyrolysis Methods in Organic Chemistry*; Academic: New York, **1980**, Chapter 2.

(20) The vicinal Karplus correlation relationship. See Silverstein, R. M.; Bassler, G. C.; Morrill, T. C. *Spectrometric Identification of Organic Compounds*; John Wiley and Sons: **1981**, 209-211.

(21) Strom, E. T. P.; Russell, G. A.; Schoeb, J. H. *J. Am. Chem. Soc.* **1966**, *88*, 2004.

(22) Scaiano, J. C.; Johnston, L. J. *Chem. Rev.* **1989**, 81, 521.

(23) No evidence for the other isomer (the Z isomer) was obtained under any

conditions; the dimerization was followed by ^{1}H NMR spectroscopy and as the

signals for the dimers increased, the signals for *E*-**12** disappeared with the

development of no signals that could be attributed to *Z*-**12**.

(24) One of the common examples is the exo-endo cyclization regioselectivity of

alkenyl radicals. See Laird, E. R.; Jorgensen, W. L. *J. Org. Chem.* **1990**, *55*, 9

and references cited therein.

APPENDIX
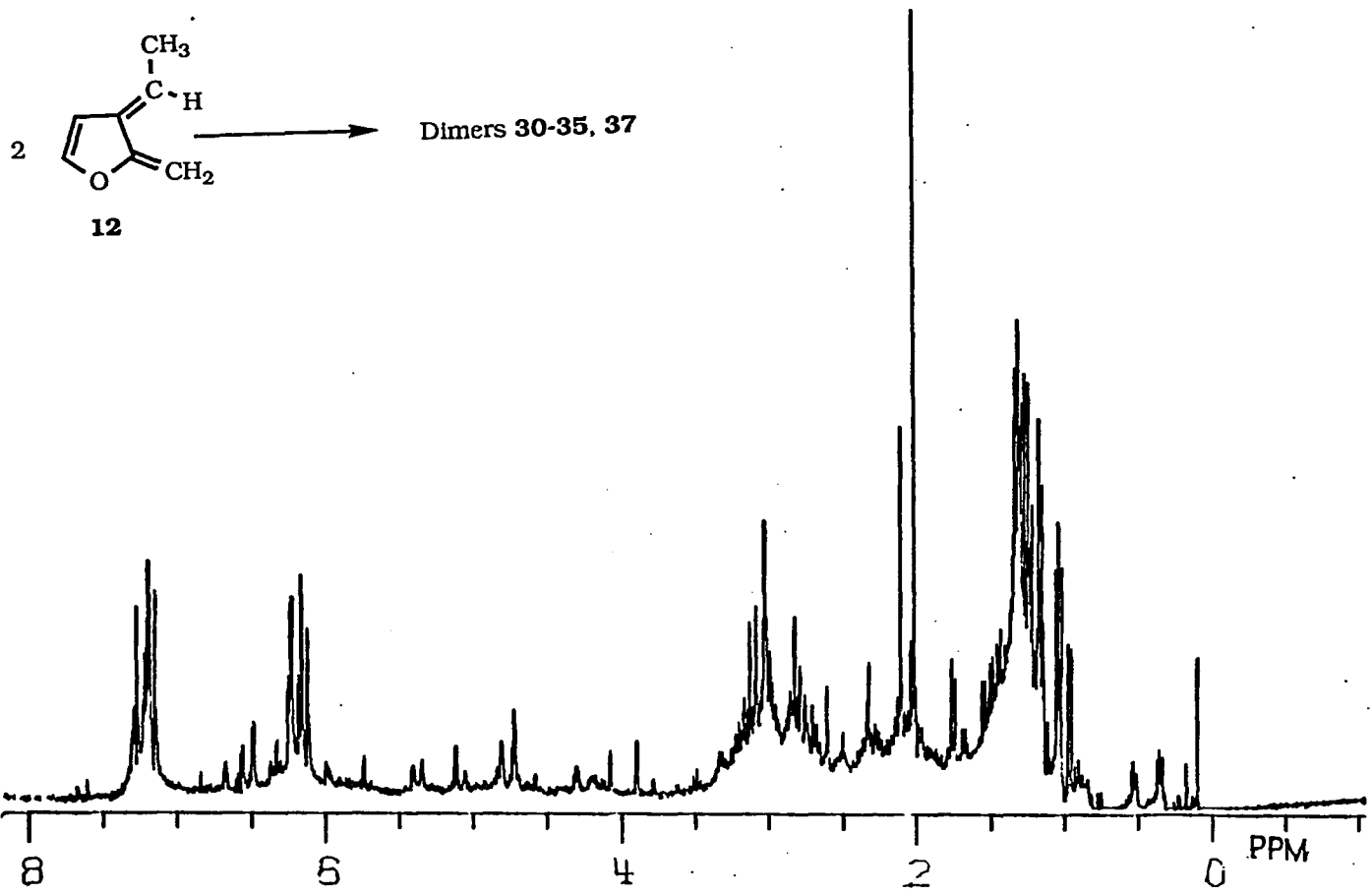
Figure A-1. ^{1}H NMR spectrum (300 MHz, CDCl$_3$) of the dimer mixture of 3-ethylidene-2-methylene-2,3-di-hydrofuran (**12**).
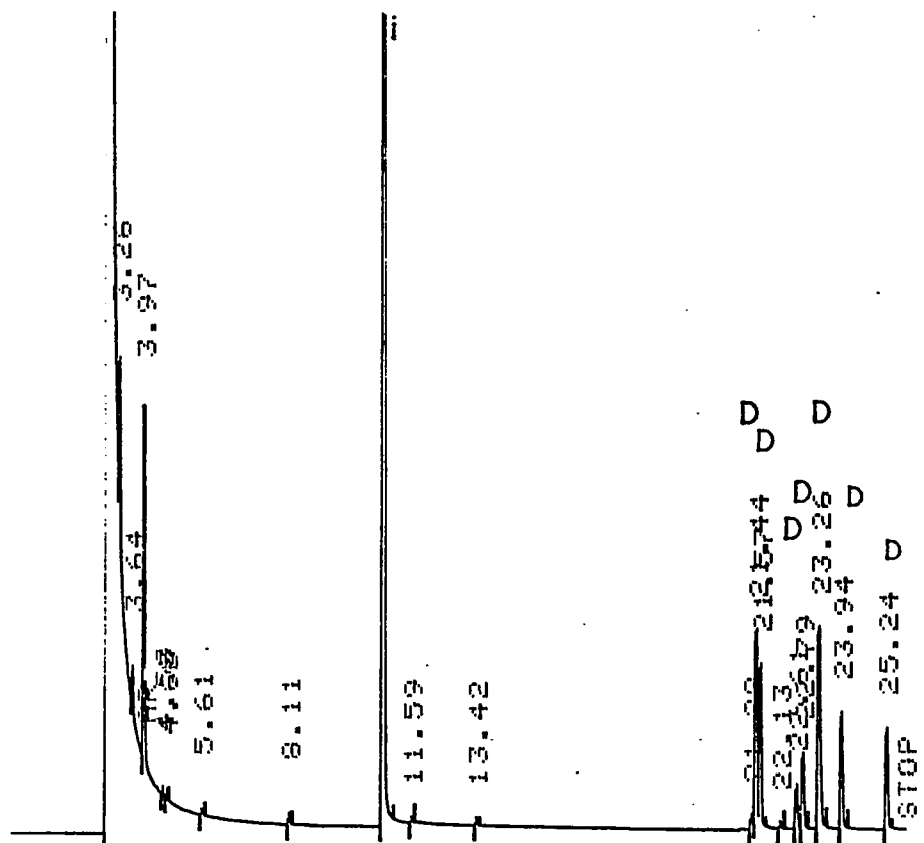
Figure A-2.   Gas chromatograph (DB1,temperature program 100 °C, 5 min, 4 °C/min, 200 °C, 10 min) of the dimer mixture of 3-ethylidene-2-methylene-2,3-dihydrofuran (**12**) (i: internal standard diphenylmethane, D: dimers).
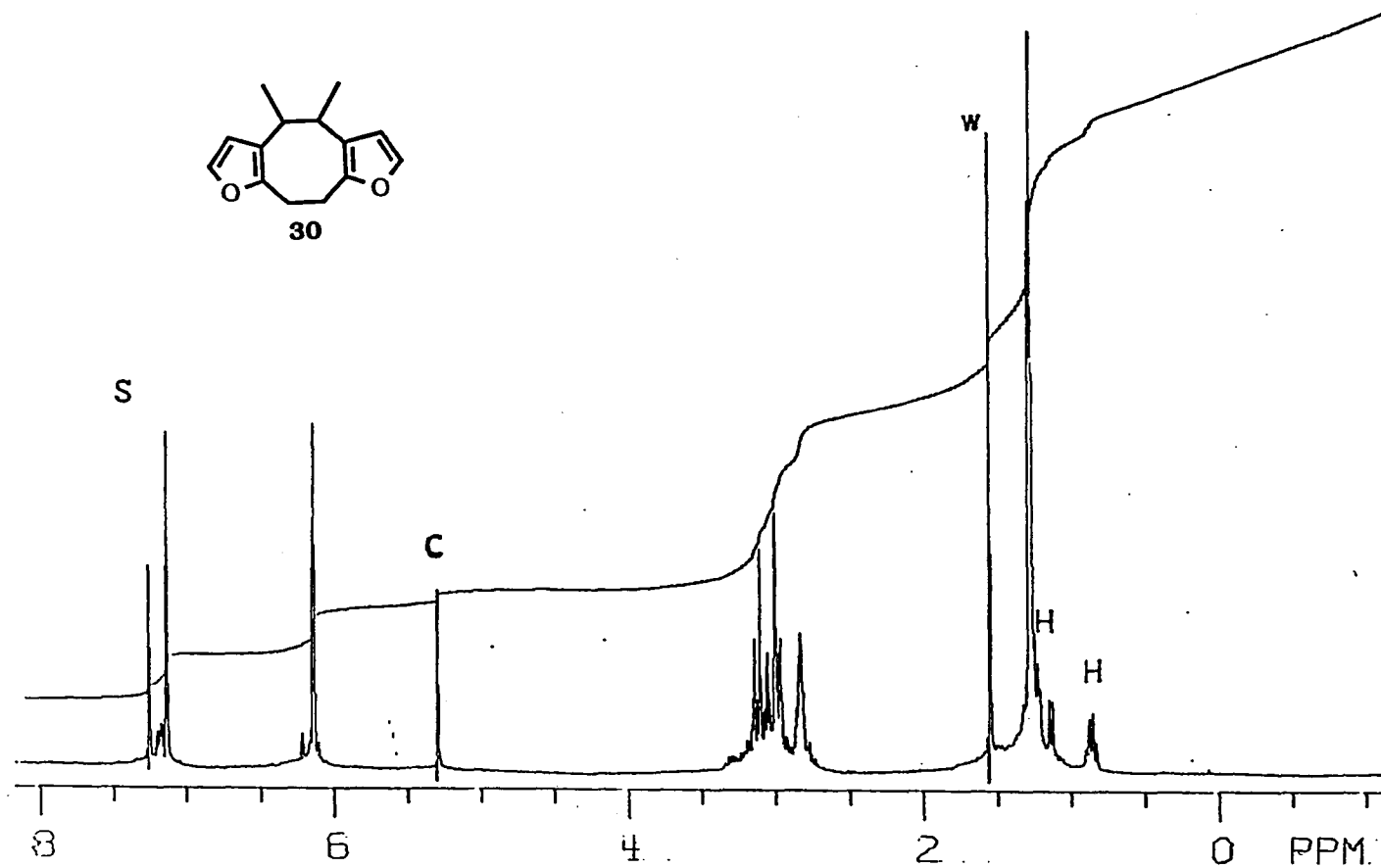
Figure A-3. ^{1}H NMR spectrum (300 MHz, CDCl$_3$) of the [4+4] dimer **30** of 3-ethylidene-2-methylene-2,3-dihydrofuran (**12**) (s: chloroform, c: dichloromethane, w: H$_2$O, H: high boiling residue from hexanes, the eluent).
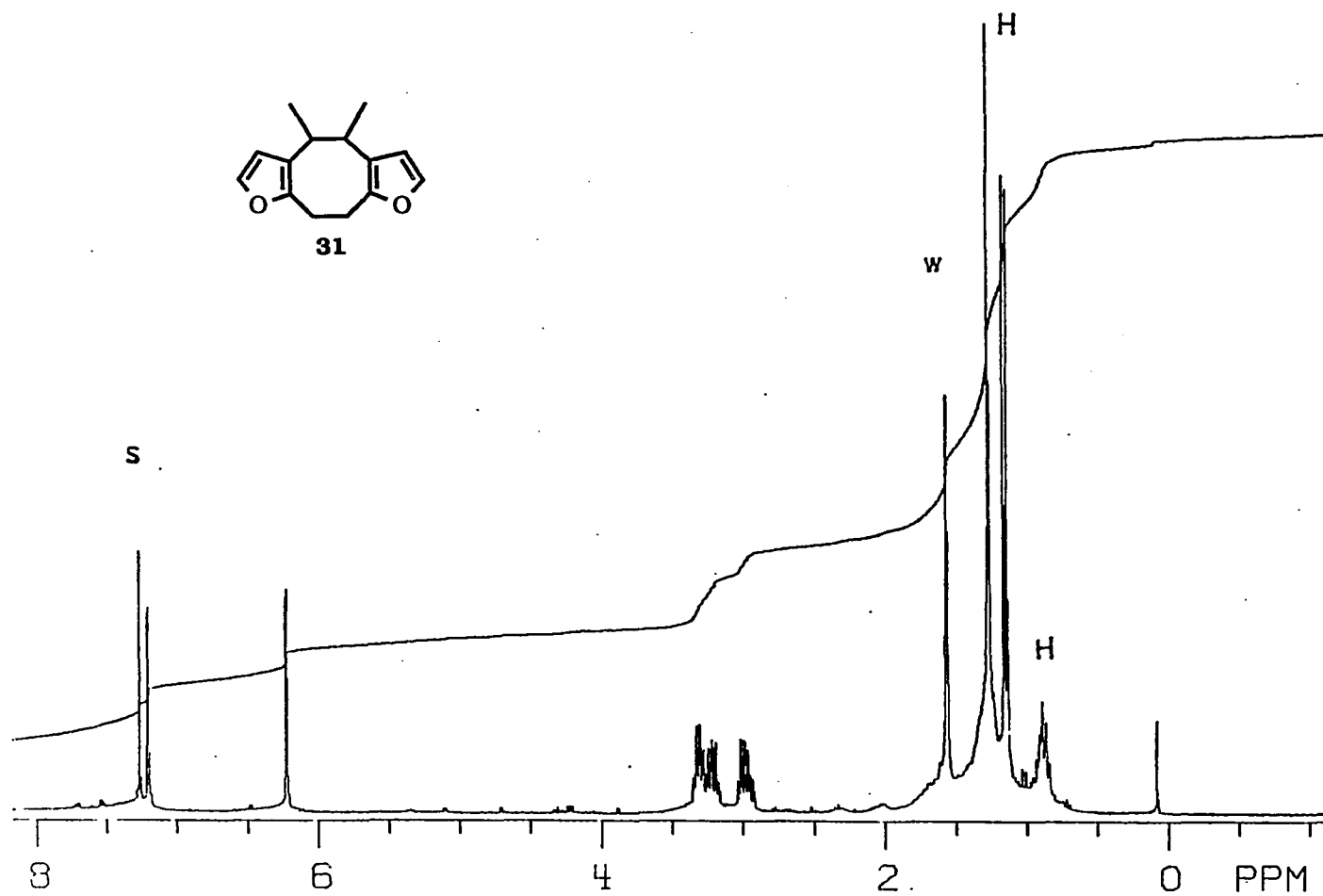
Figure A-4. ^{1}H NMR spectrum (300 MHz, CDCl$_3$) of the [4+4] dimer **31** of 3-ethylidene-2-methylene-2,3-dihydrofuran (**12**) (s: chloroform, w:H$_2$O, H: high boiling residue from hexanes, the eluent).
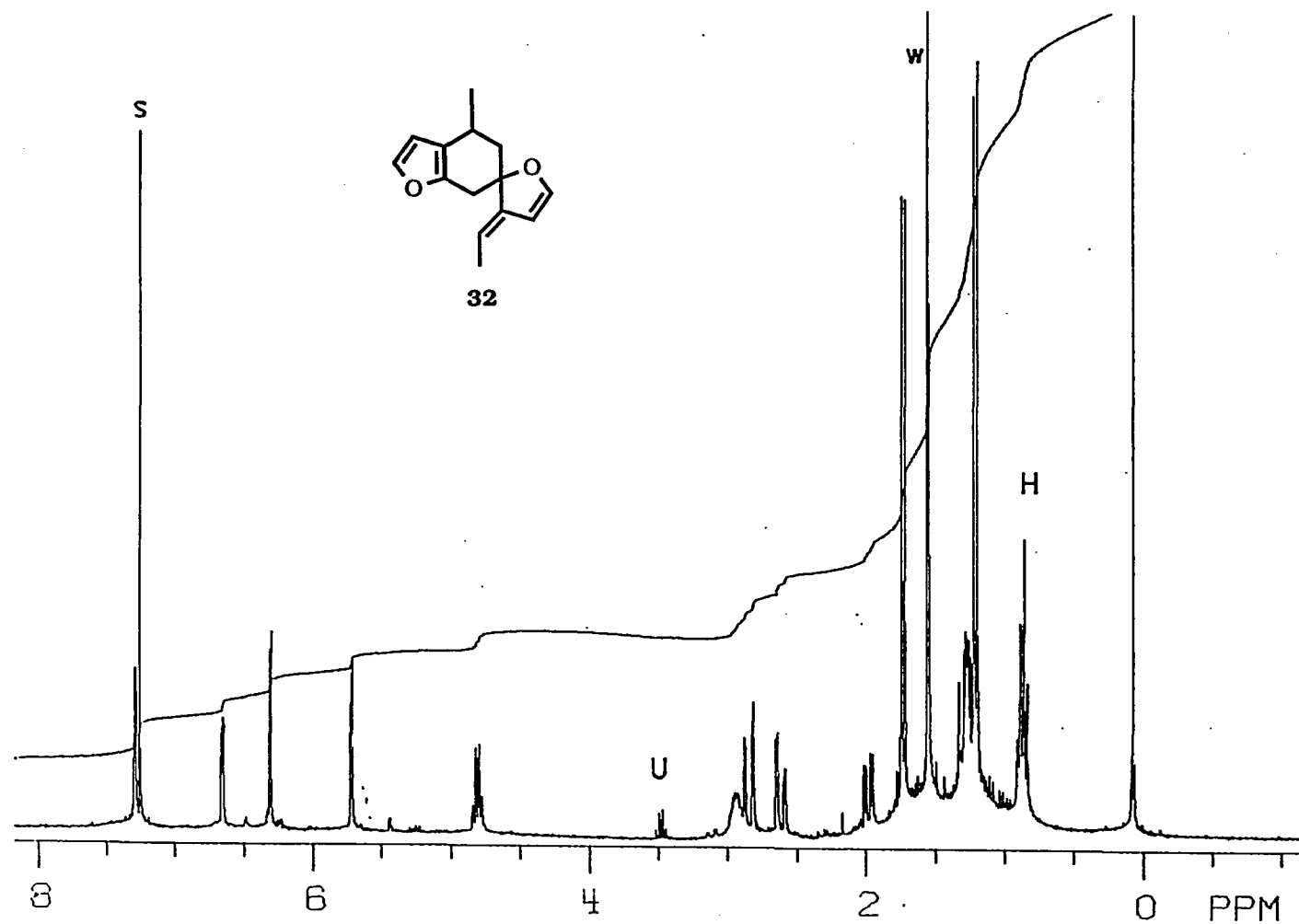
Figure A-5. ^{1}H NMR spectrum (300 MHz, CDCl$_3$) of the [4+2] dimer 32 of 3-ethylidene-2-methylene-2,3-di-hydrofuran (12) (s: chloroform, w: H$_2$O, H: high boiling residue from hexanes, the eluent, U: diethyl ether).
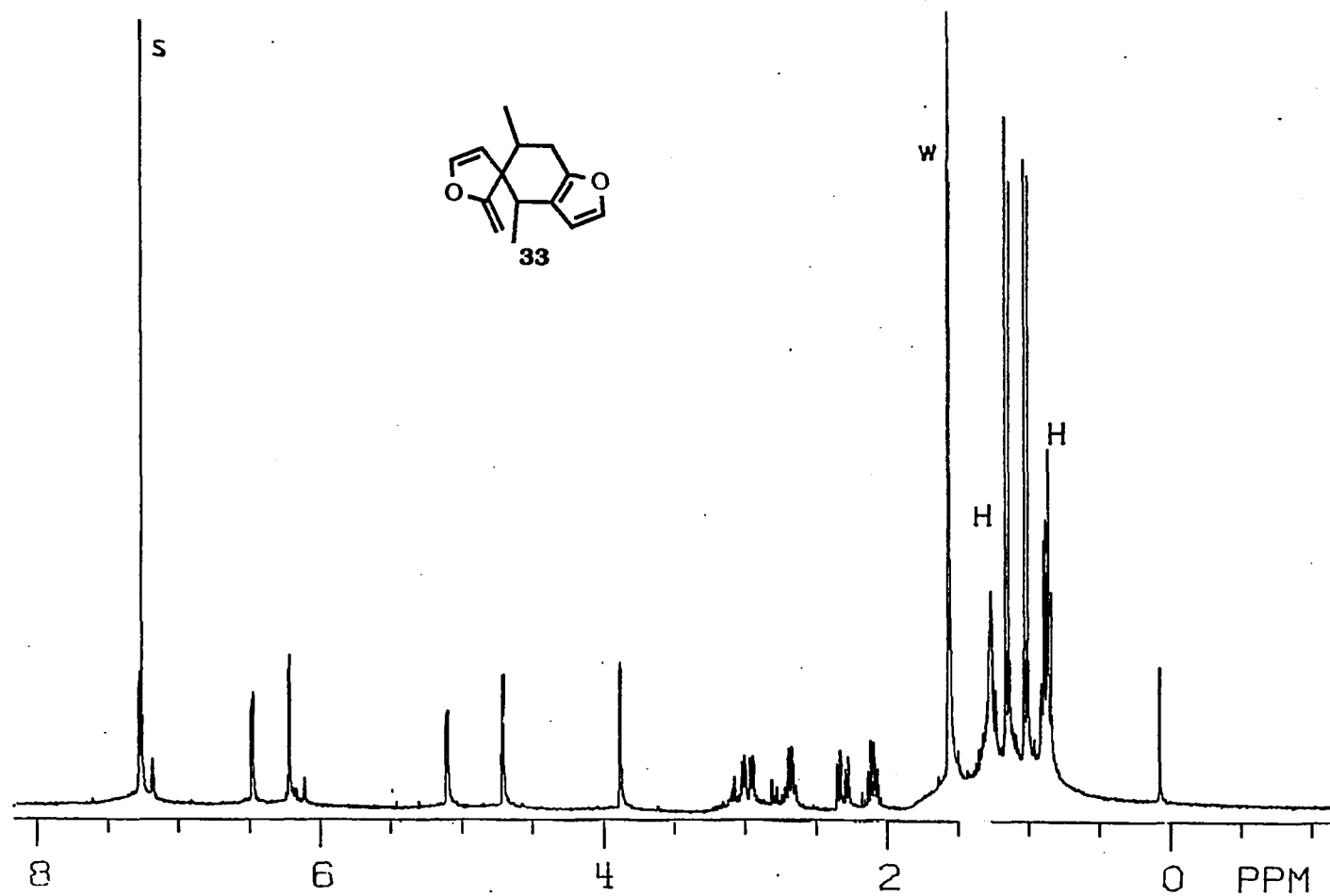
Figure A-6. ^{1}H NMR spectrum (300 MHz, CDCl$_3$) of the [4+2] dimer **33** of 3-ethylidene-2-methylene-2,3-di-hydrofuran (**12**) (s: chloroform and one furan proton of the dimer, w: H$_2$O, H: high boiling residue from hexanes, the eluent).
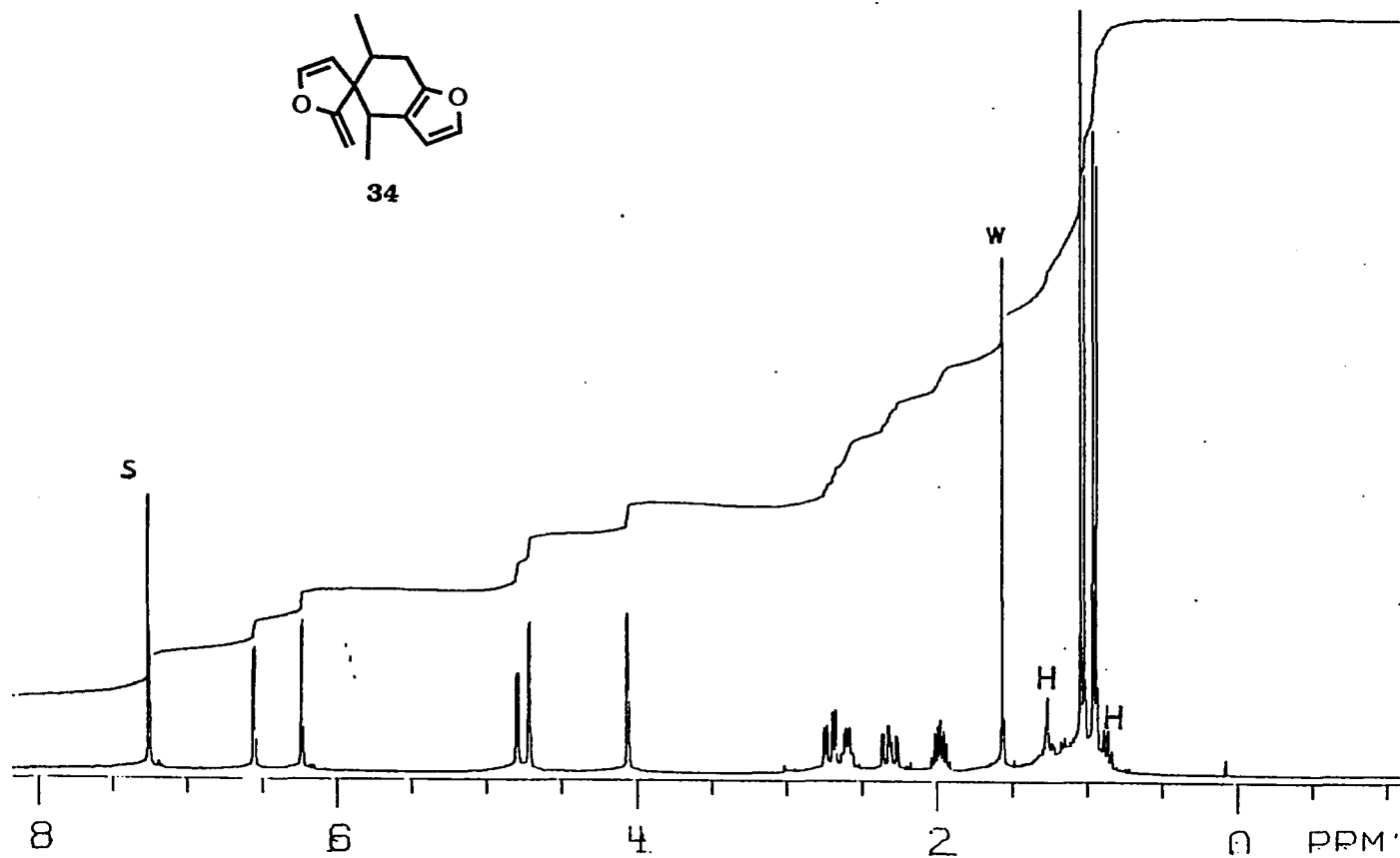
Figure A-7. ¹H NMR spectrum (300 MHz, CDCl₃) of the [4+2] dimer **34** of 3-ethylidene-2-methylene-2,3-di-hydrofuran **(12)** (s: chloroform and one furan proton of the dimer, w: H₂O, H: high boiling residue from hexanes, the eluent).
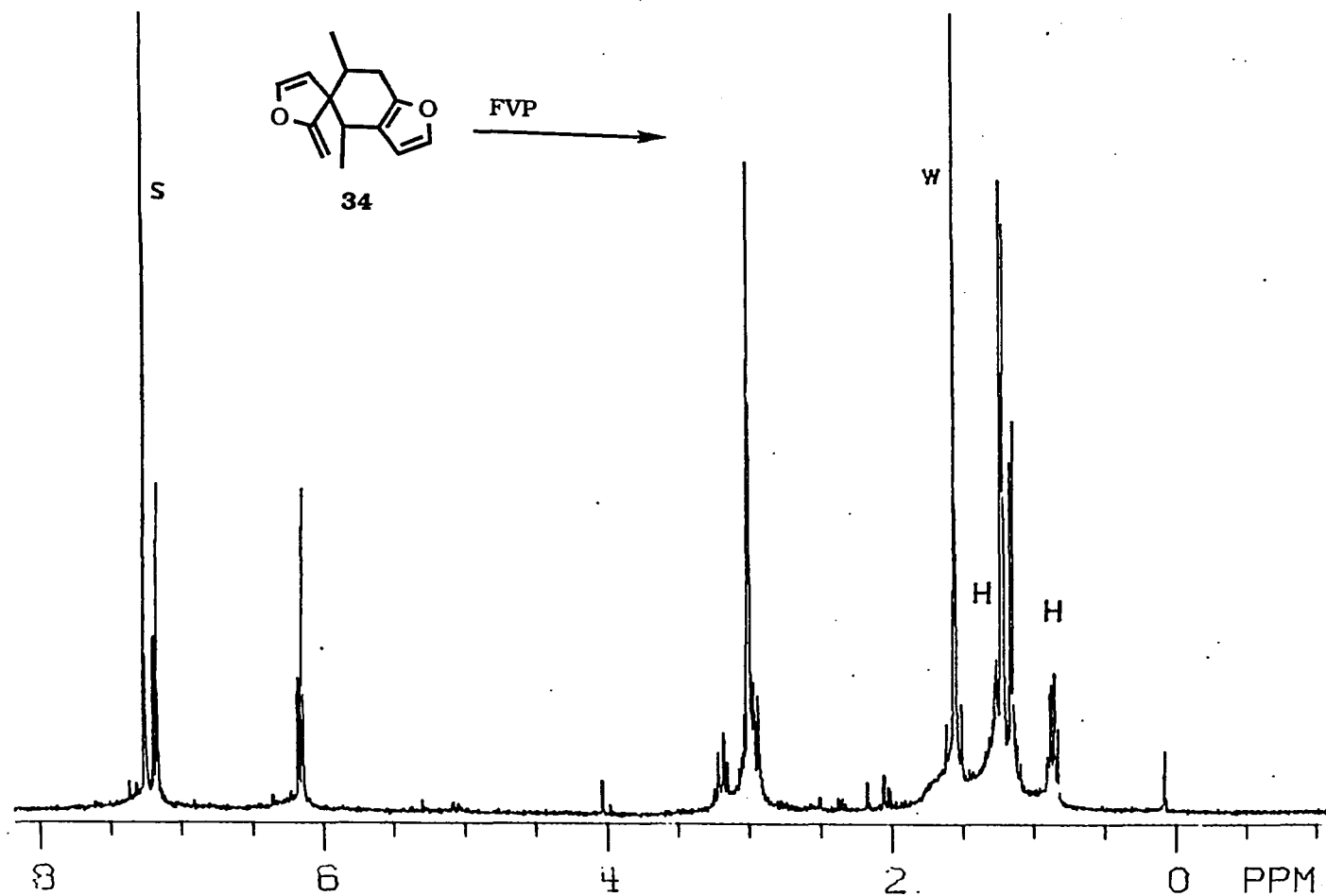
Figure A-8. ^{1}H NMR spectrum (300 MHz, CDCl$_3$) of the pyrolysate of the [4+2] dimer **34** of 3-ethylid-ene-2-methylene-2,3-dihydrofuran (**12**) (s: chloroform, w: H$_2$O, H: high boiling residue from hexanes, the eluent).
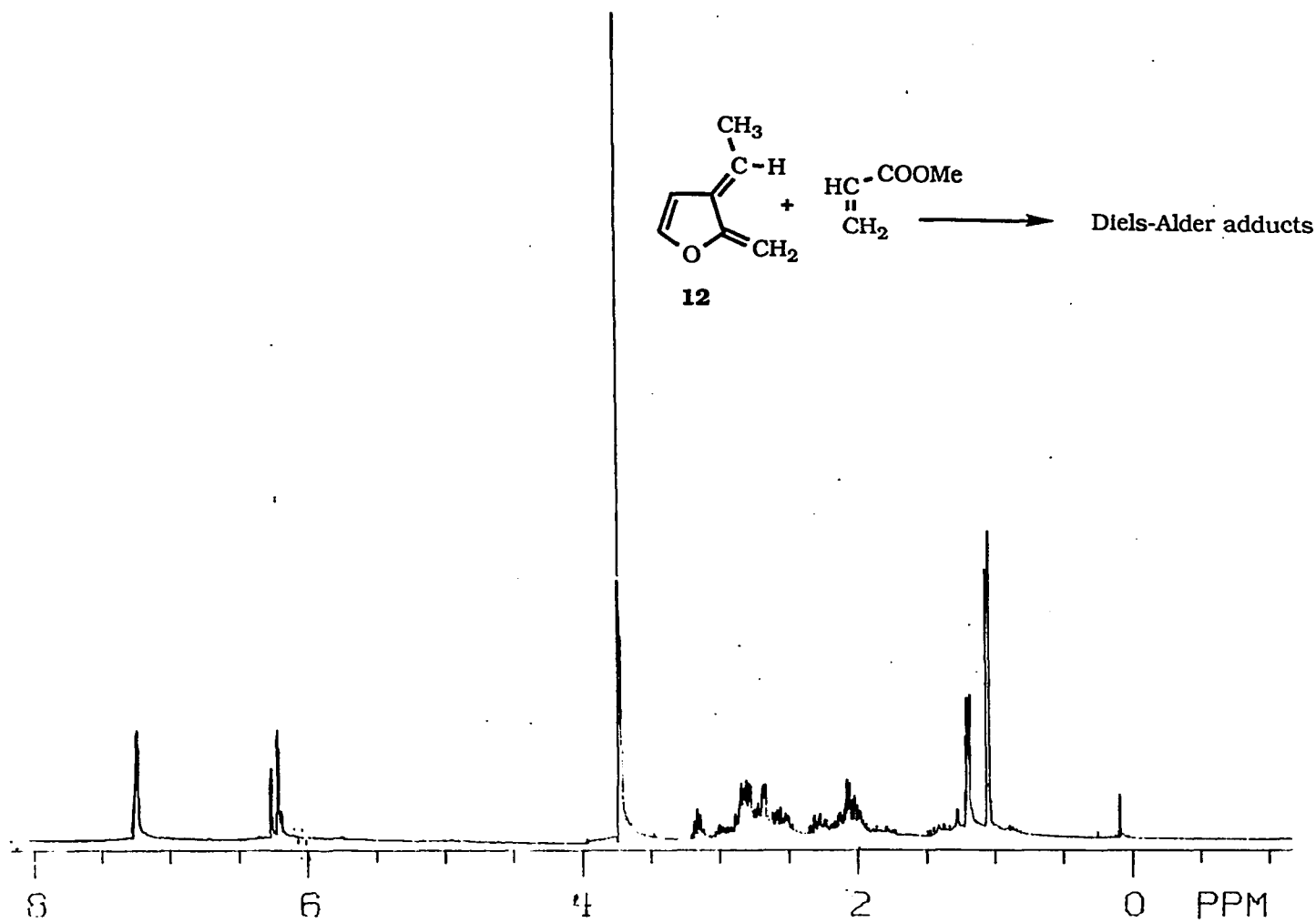
Figure A-9. ^{1}H NMR spectrum (300 MHz, CDCl$_3$) of the Diels-Alder adducts (**28**) of methyl acrylate and 3-ethylidene-2-methylene-2,3-dihydrofuran (**12**).
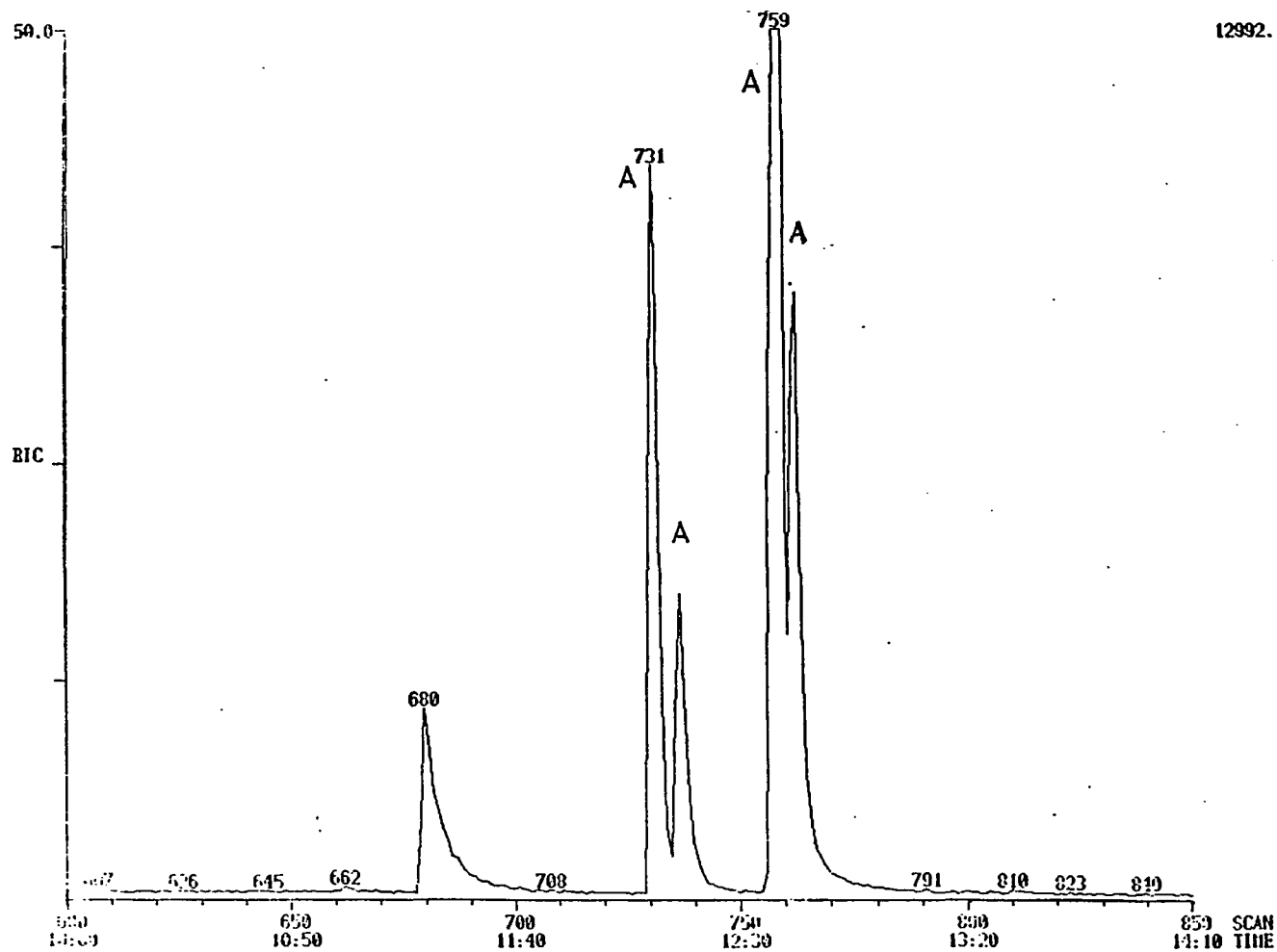
Figure A-10.   Gas chromatograph (DB1, temperature program, 80 °C (5 min), 5 °C/min, 200 °C) of the Diels-Alder adducts **(28)** of methyl acrylate and 3-ethylidene-2-methylene-2,3-dihydrofuran **(12)** (A: Diels-Alder adducts).
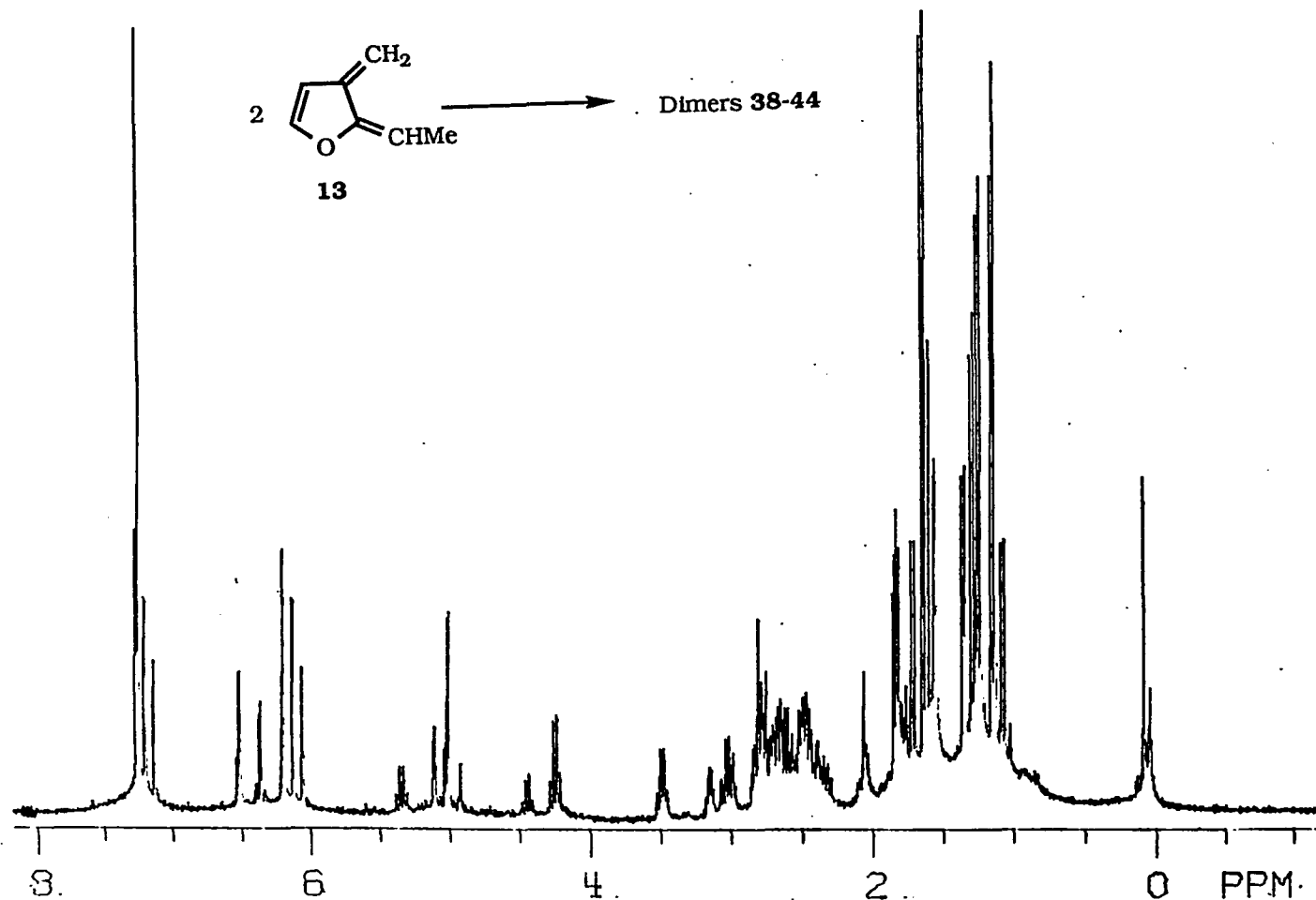
Figure A-11. ^{1}H NMR spectrum (300 MHz, CDCl$_3$) of the dimer mixture of 2-ethylidene-3-methylene-2,3-di-hydrofuran (13).
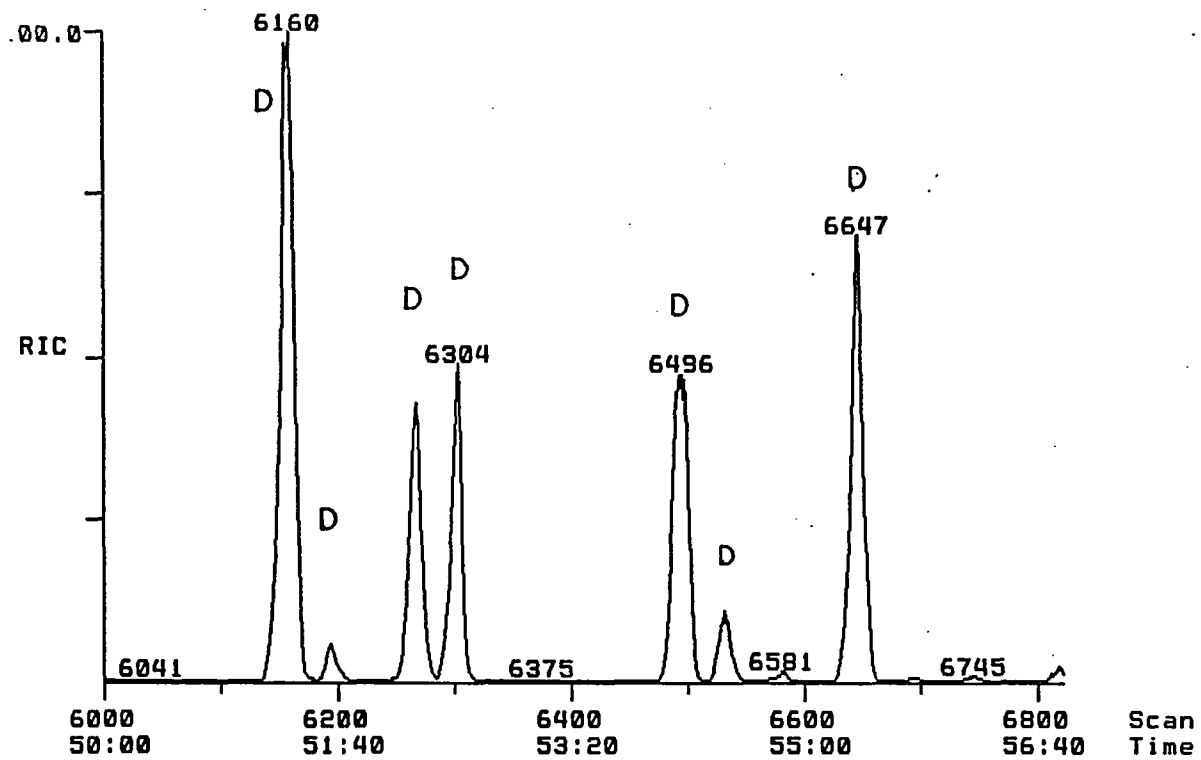
Figure A-12.   Gas chromatograph (DB1, temperature program, 60 °C, 5 min, 2 °C/min 180°C) of the dimer mixture of 2-ethylidene-3-methylene-2,3-dihydrofuran (**13**) (D: dimer).
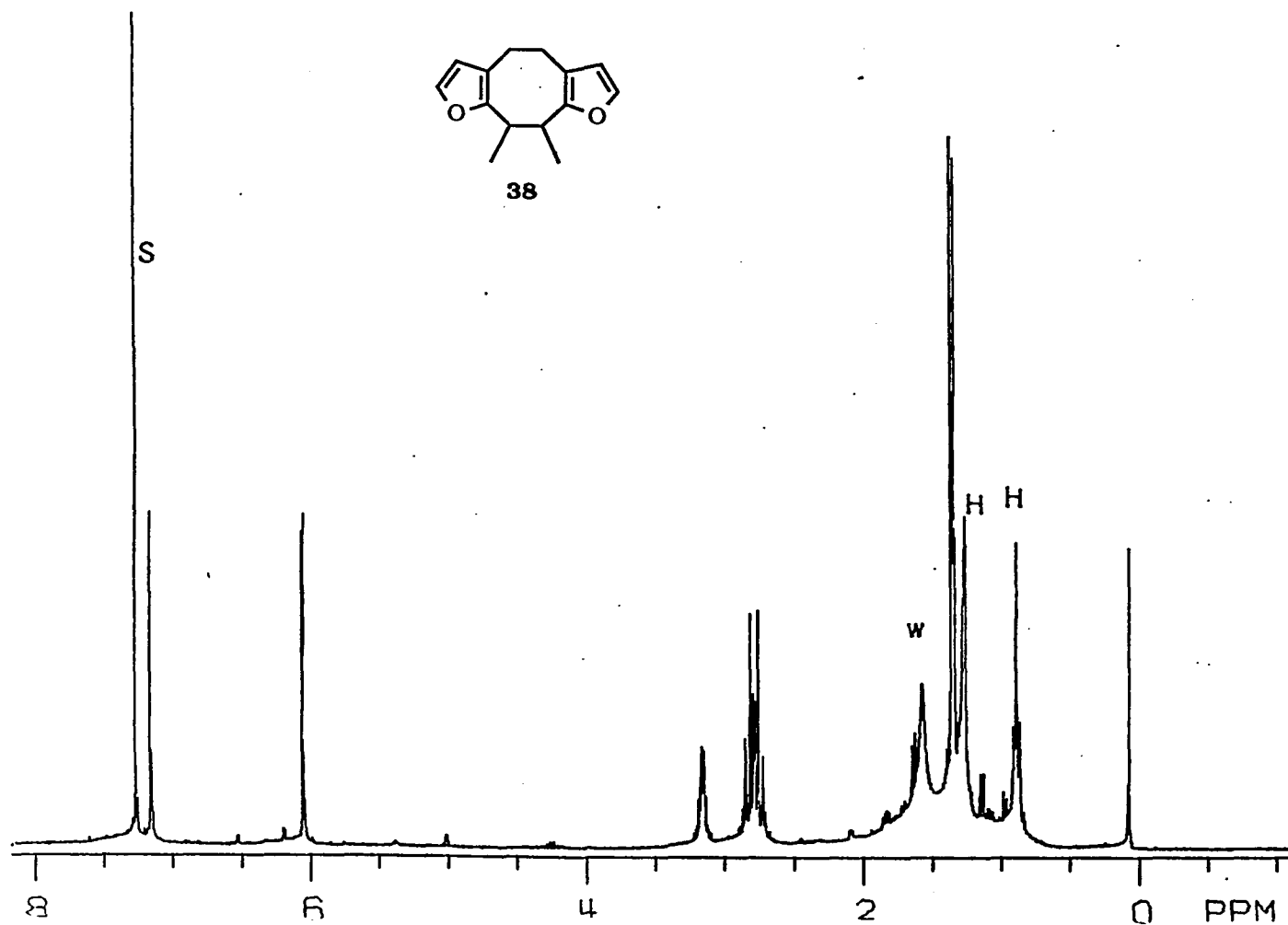
Figure A-13. ^{1}H NMR spectrum (300 MHz, CDCl${}_3$) of the [4+4] dimer **38** of 2-ethylidene-3-methylene-2,3-di-hydrofuran (**13**) (s: chloroform, w: H${}_2$O, H: high boiling residue from hexanes, the eluent).
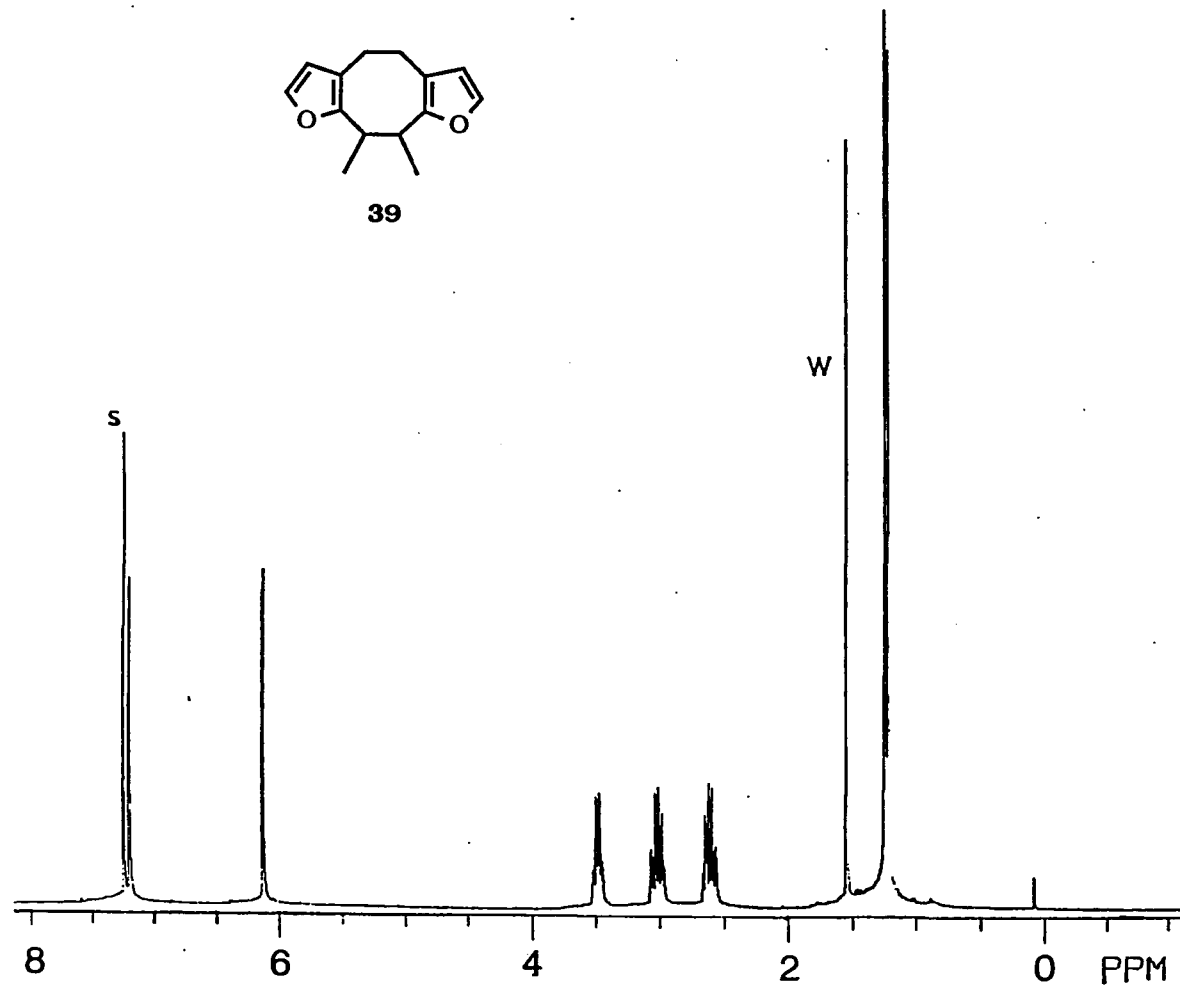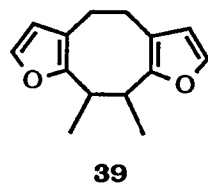
Figure A-14. ^{1}H NMR spectrum (300 MHz, CDCl$_3$) of the [4+4] dimer **39** of 2-ethylidene-3-methylene-2,3-di-hydrofuran (**13**)(s: chloroform, w H$_2$O, H: high boiling residue from hexanes, the eluent).

40
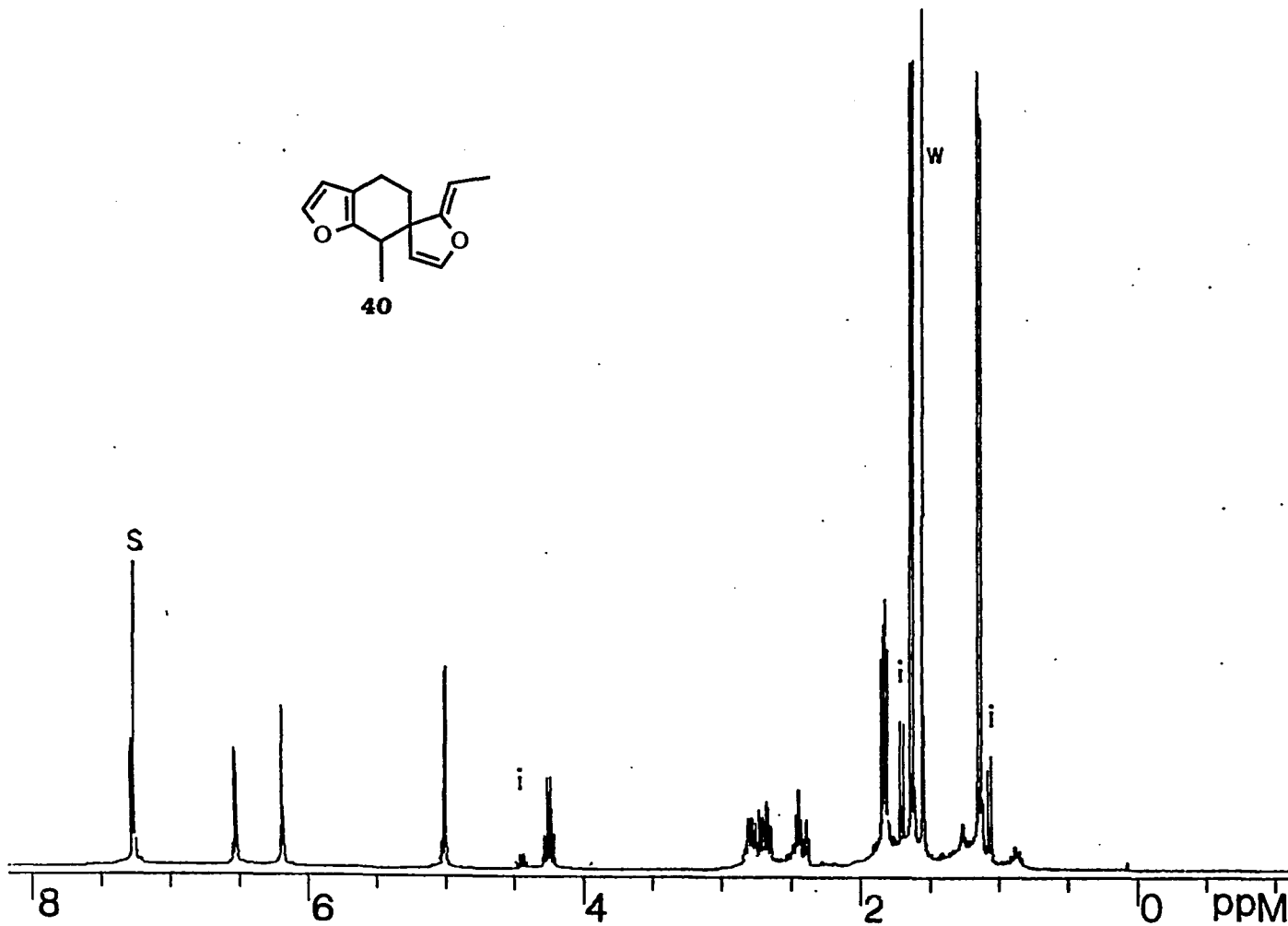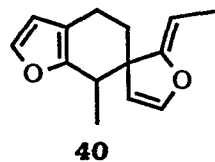
Figure A-15. ^{1}H NMR spectrum (300 MHz, CDCl$_3$) of the [4+2] dimer **40** of 2-ethylidene-3-methylene-2,3-di-hydrofuran (**13**) (s: chloroform, w: H$_2$O, H: high boiling residue from hexanes, the eluent, i: dimer **41**).
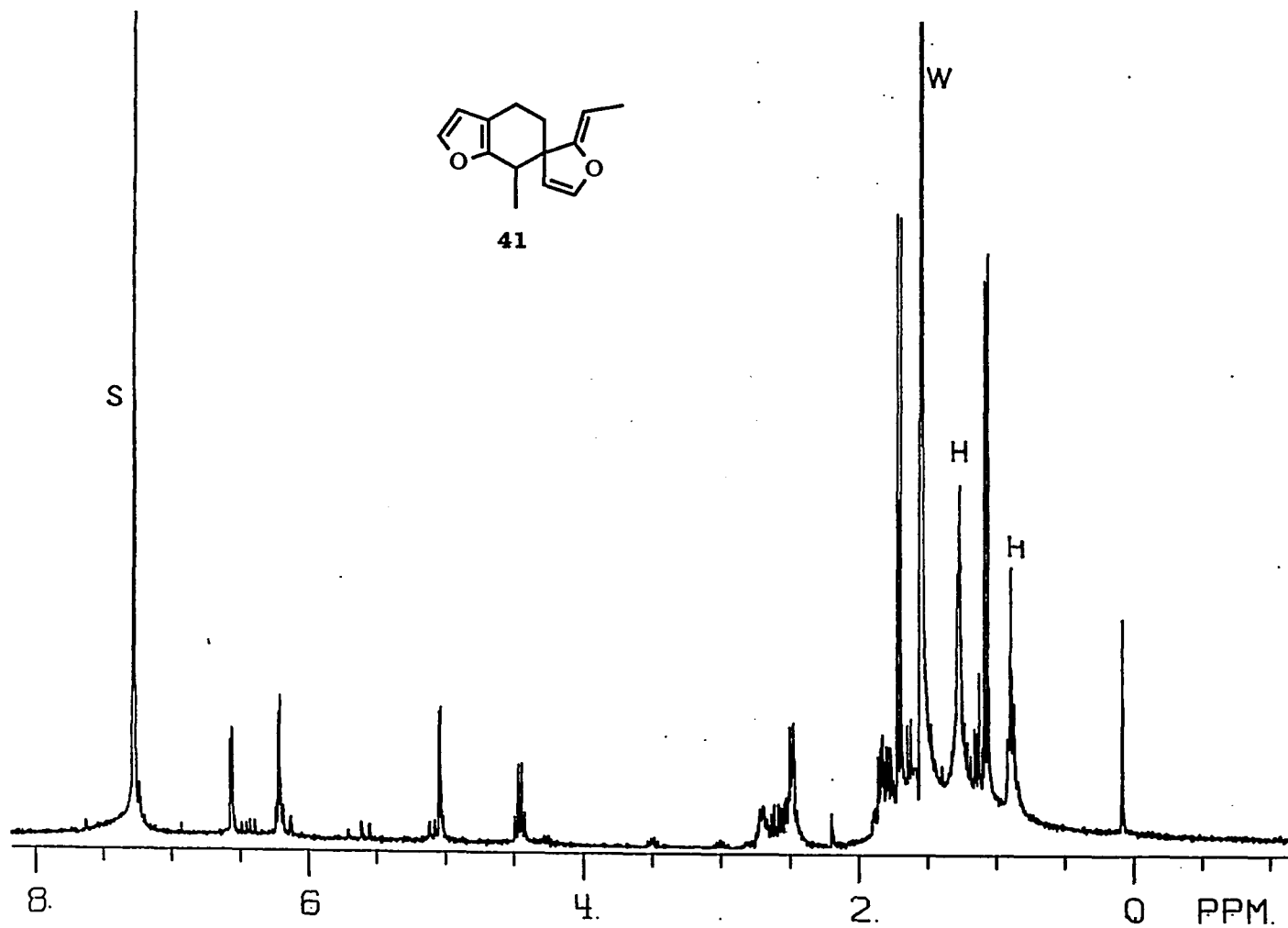
Figure A-16. ^{1}H NMR spectrum (300 MHz, CDCl$_3$) of the [4+2] dimer **41** of 2-ethylidene-3-methylene-2,3-di-hydrofuran (**13**) (s: chloroform and one furan proton of the dimer, w: H$_2$O, H: high boiling residue from hexanes, the eluent).
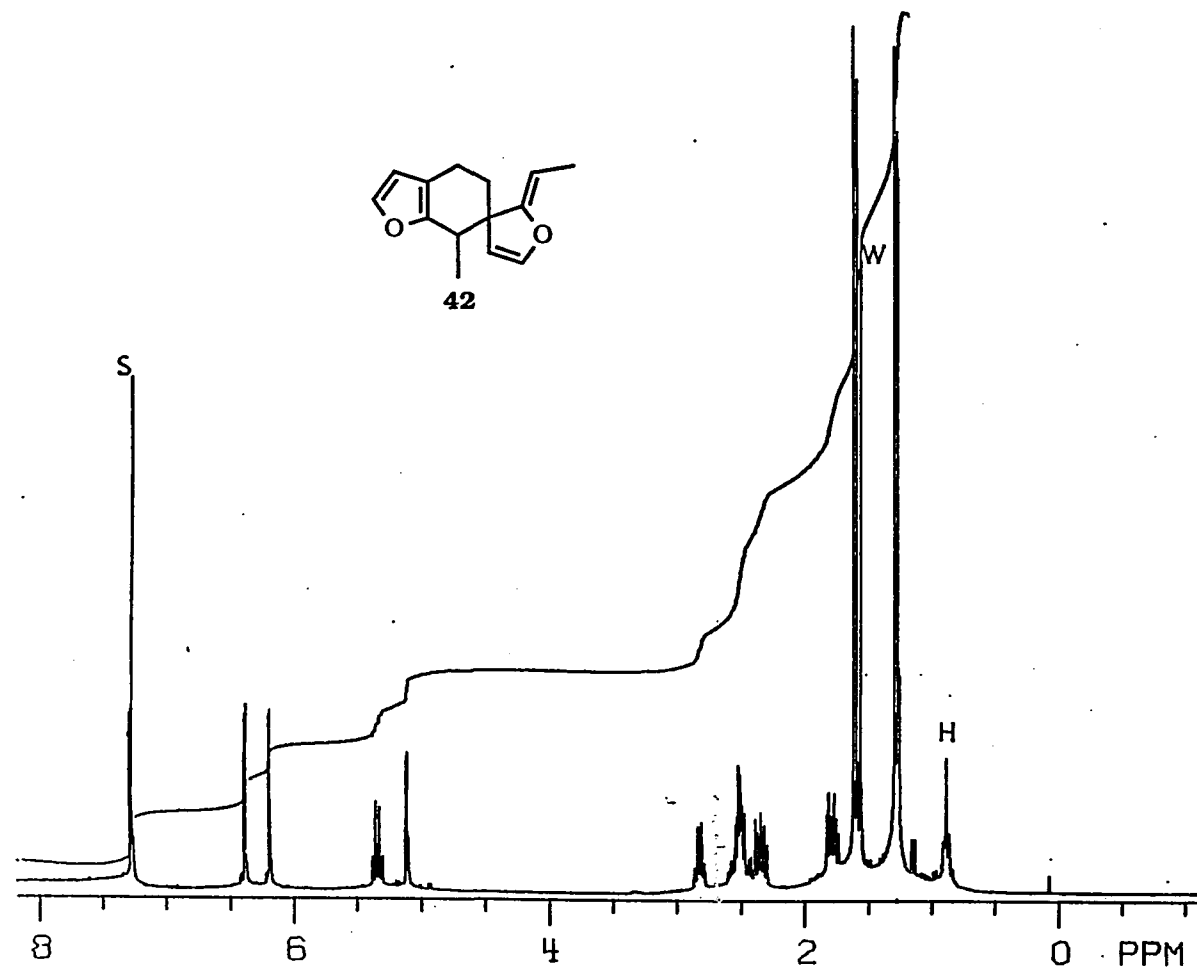
Figure A-17. ^{1}H NMR spectrum (300 MHz, CDCl$_3$) of the [4+2] dimer **42** of 2-ethylidene-3-methylene-2,3-dihydrofuran **(13)** (s: chloroform and one furan proton of the dimer, w: H$_2$O, H: high boiling residue from hexanes, the eluent).
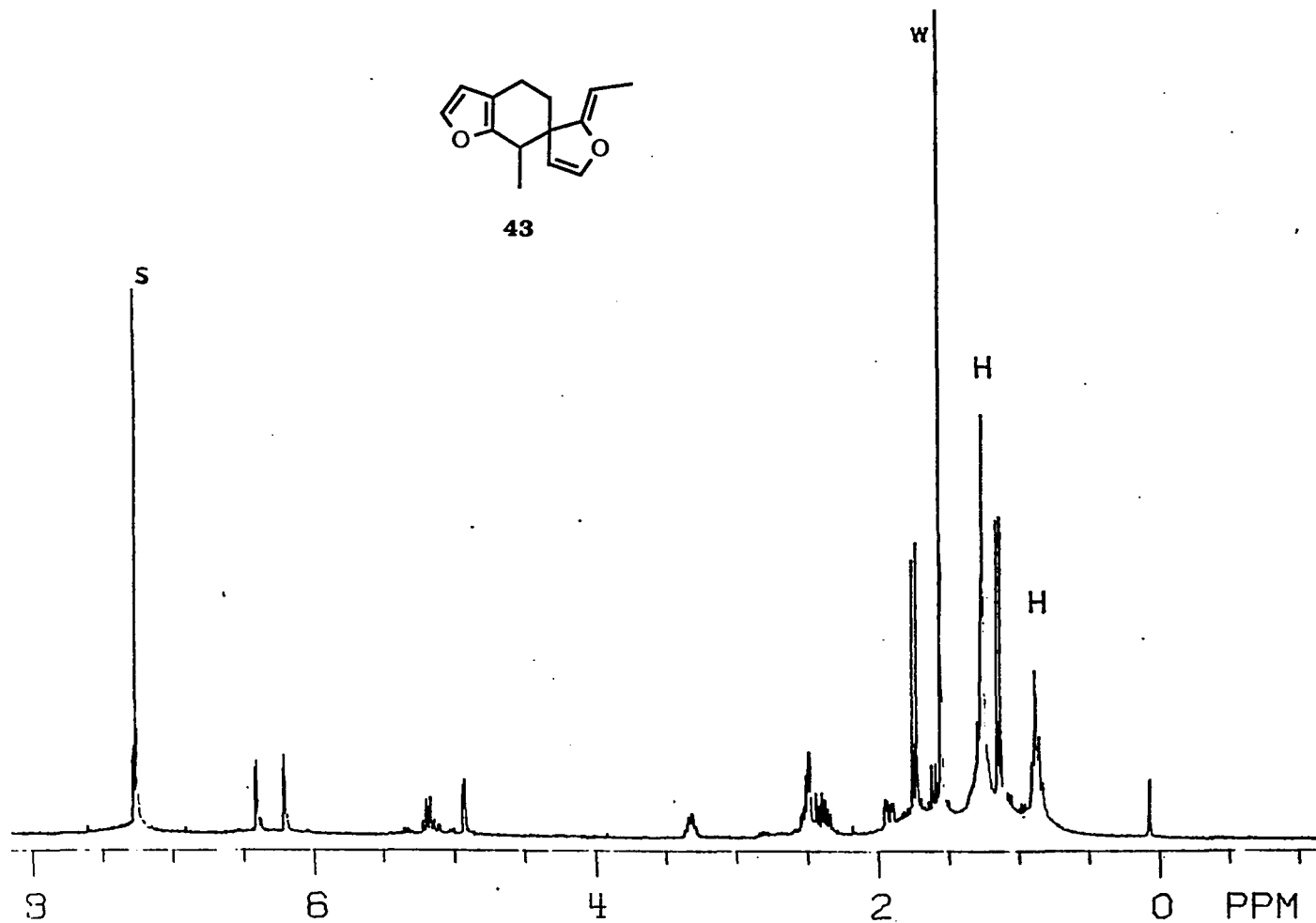
Figure A-18. ^{1}H NMR spectrum (300 MHz, CDCl$_3$) of the [4+2] dimer **43** of 2-ethylidene-3-methylene-2,3-di-hydrofuran **(13)** (s: chloroform, w: H$_2$O, H: high boiling residue from hexanes, the eluent).
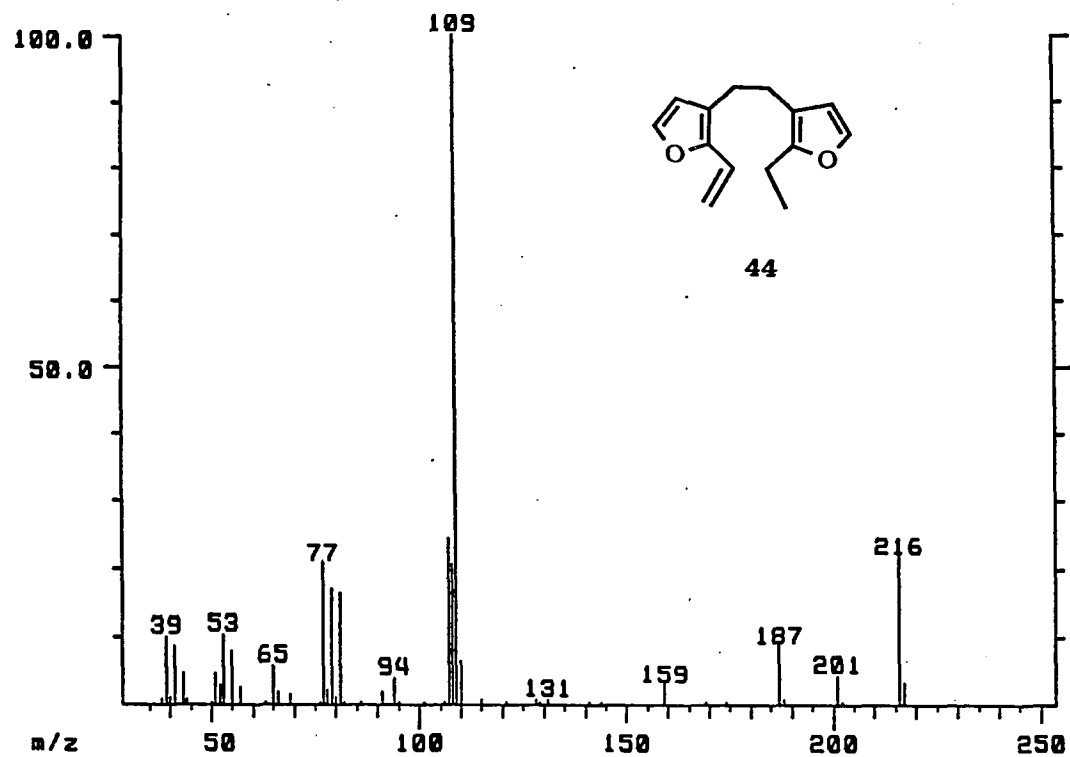
Figure A-19.   GC/ MS of the disproportionation dimer (44) of 2-ethylidene-3-methyl-ene-2,3-dihydrofuran (13).
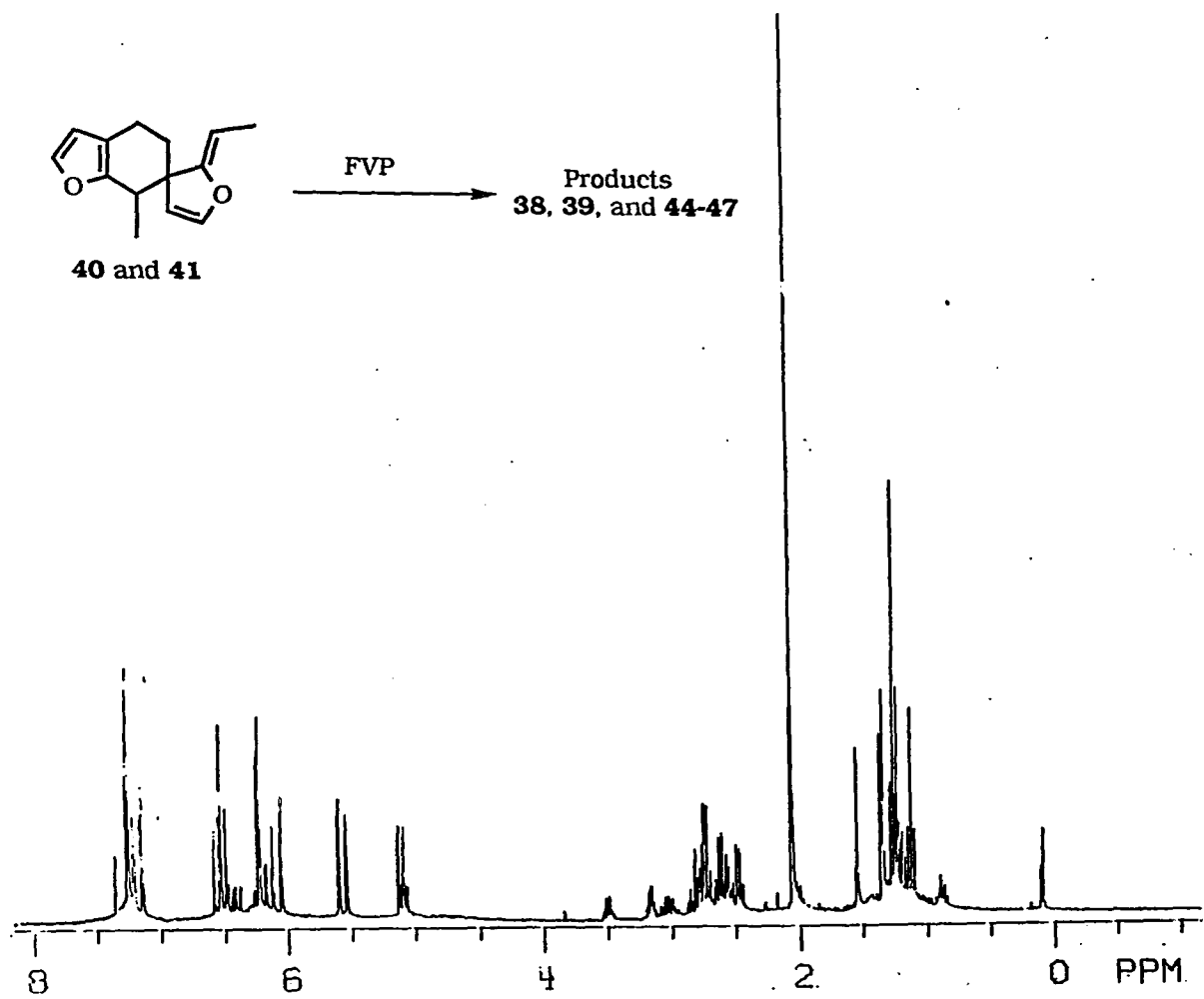
FVP

Products
38, 39, and **44-47**

40 and **41**

Figure A-20.   ^{1}H NMR spectrum (300 MHz, CDCl$_3$) of the pyrolysate of the [4+2] dimer mixture of **40** and **41**.

Figure A-21. Gas chromatograph (DB1, temperature program 120 °C, 15 °C/min, 310 °C) of the pyrolysate of the [4+2] dimer mixture of **40** and **41**.

44
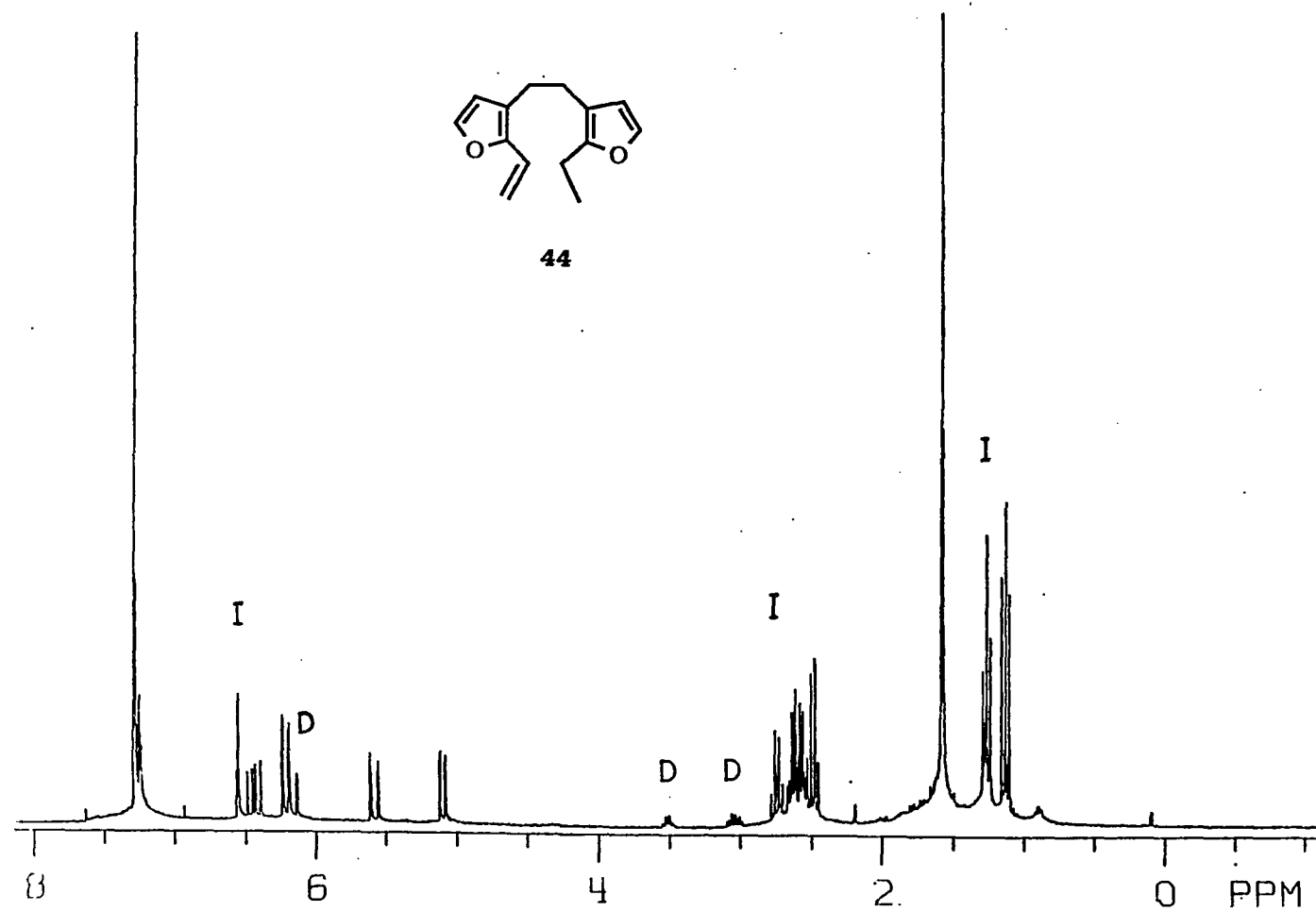
Figure A-22. ^{1}H NMR spectrum (300 MHz, CDCl$_3$) of product **44** from the pyrolysis of the [4+2] dimer mixture of **40** and **41**(s: chloroform, w: H$_2$O, I: **46**, D: **39**).
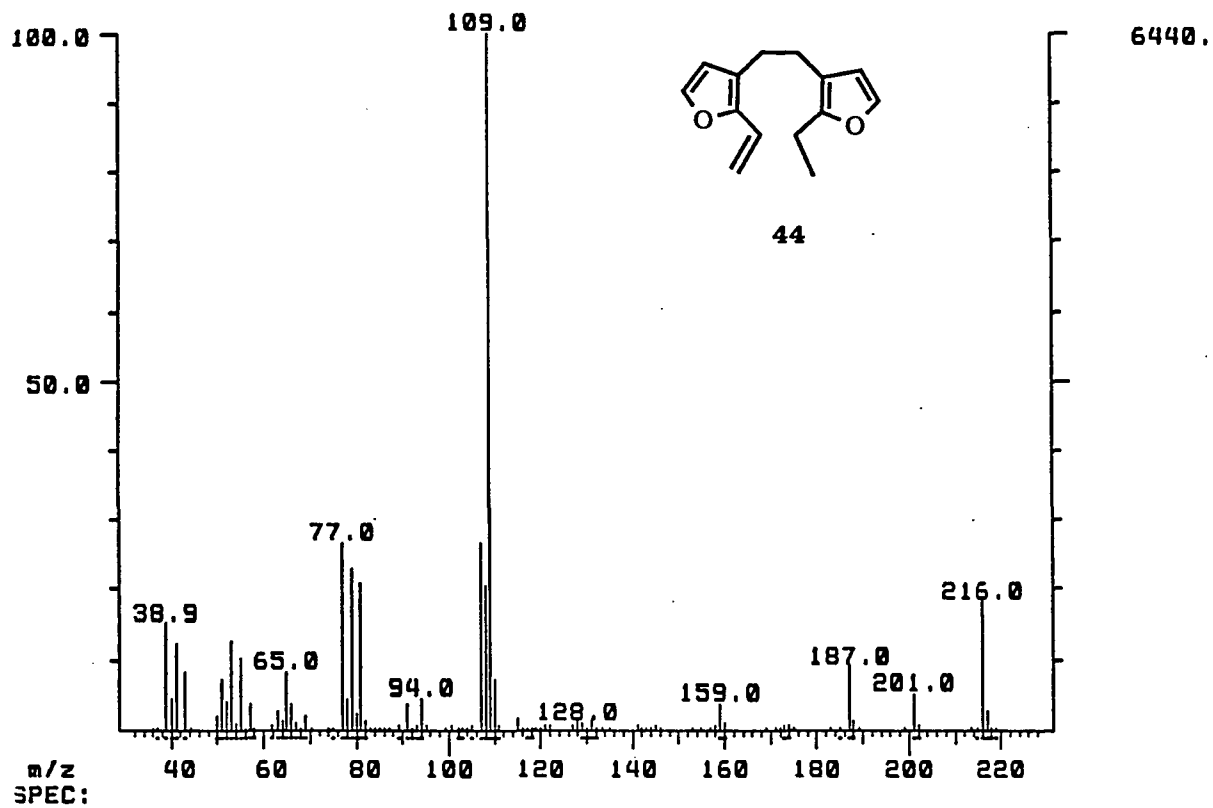
Figure A-23.   GC/MS of product **44** from the pyrolysis of the [4+2] dimer mixture of **40** and **41**.

45
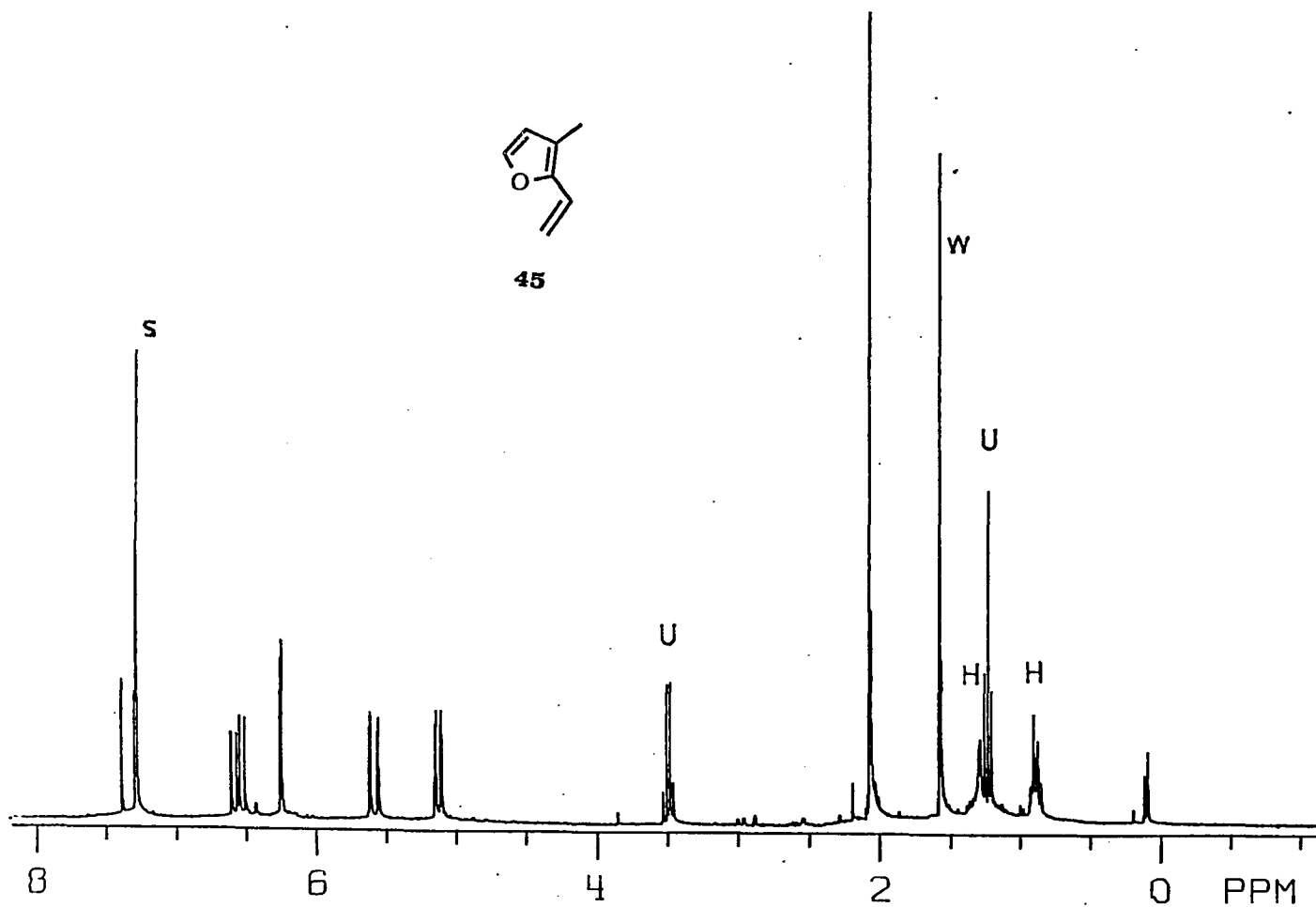
Figure A-24. ^{1}H NMR spectrum (300 MHz, CDCl$_3$) of fragmentation product **45** from the pyrolysis of the [4+2] dimer mixture of **40** and **41**(s: chloroform and one furan proton of the dimer, w: H$_2$O, U: diethyl ether H: high boiling residue from hexanes, the eluent).
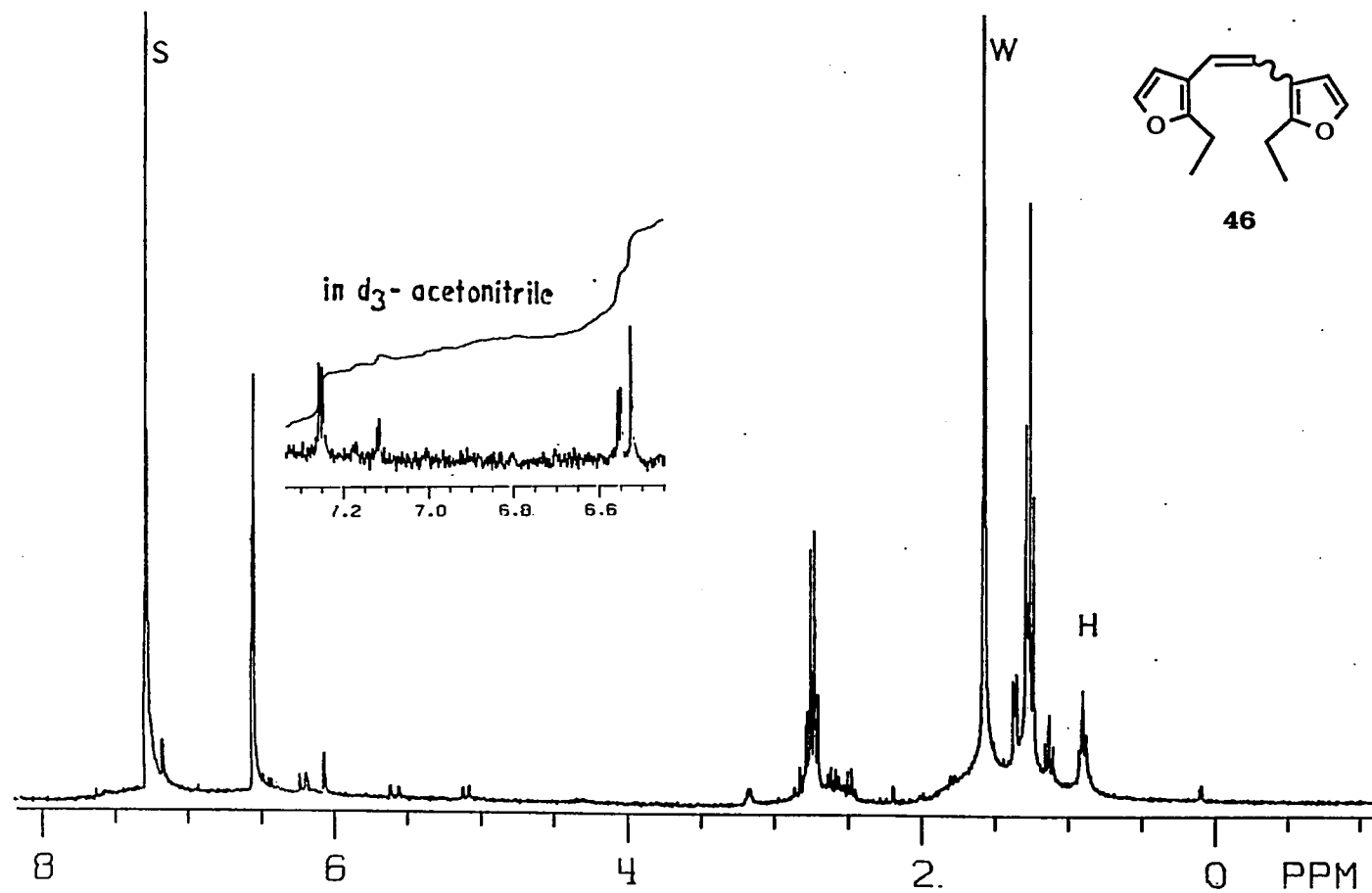
Figure A-25. ^{1}H NMR spectrum (300 MHz, CDCl3) of product **46** from the pyrolysis of the [4+2] dimer mixture of **40** and **41**(s: chloroform and one furan proton of the dimer, w: H2O, H: high boiling residue from hexanes, the eluent).
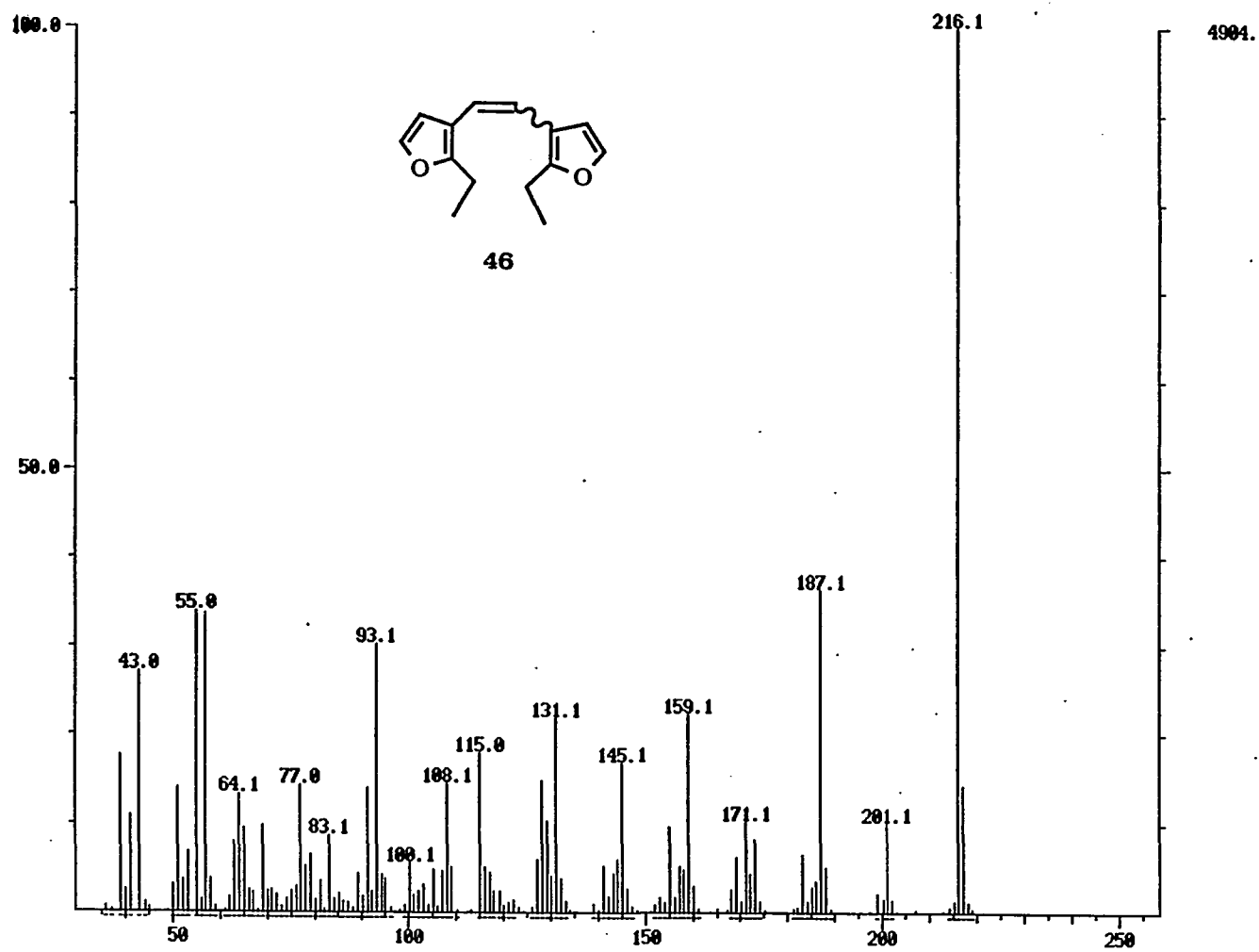
Figure A-26. GC/MS of product **46** from the pyrolysis of the [4+2] dimer mixture of **40** and **41**.

100.0 ⌐   216.1   ┌ 1204.

47

50.0 ⌐

43.0   55.0   93.1

64.1   77.0   115.0   131.1   159.1   187.1
                                            145.1
              83.0   108.1   171.1   201.1
                   100.4

50   100   150   200   250
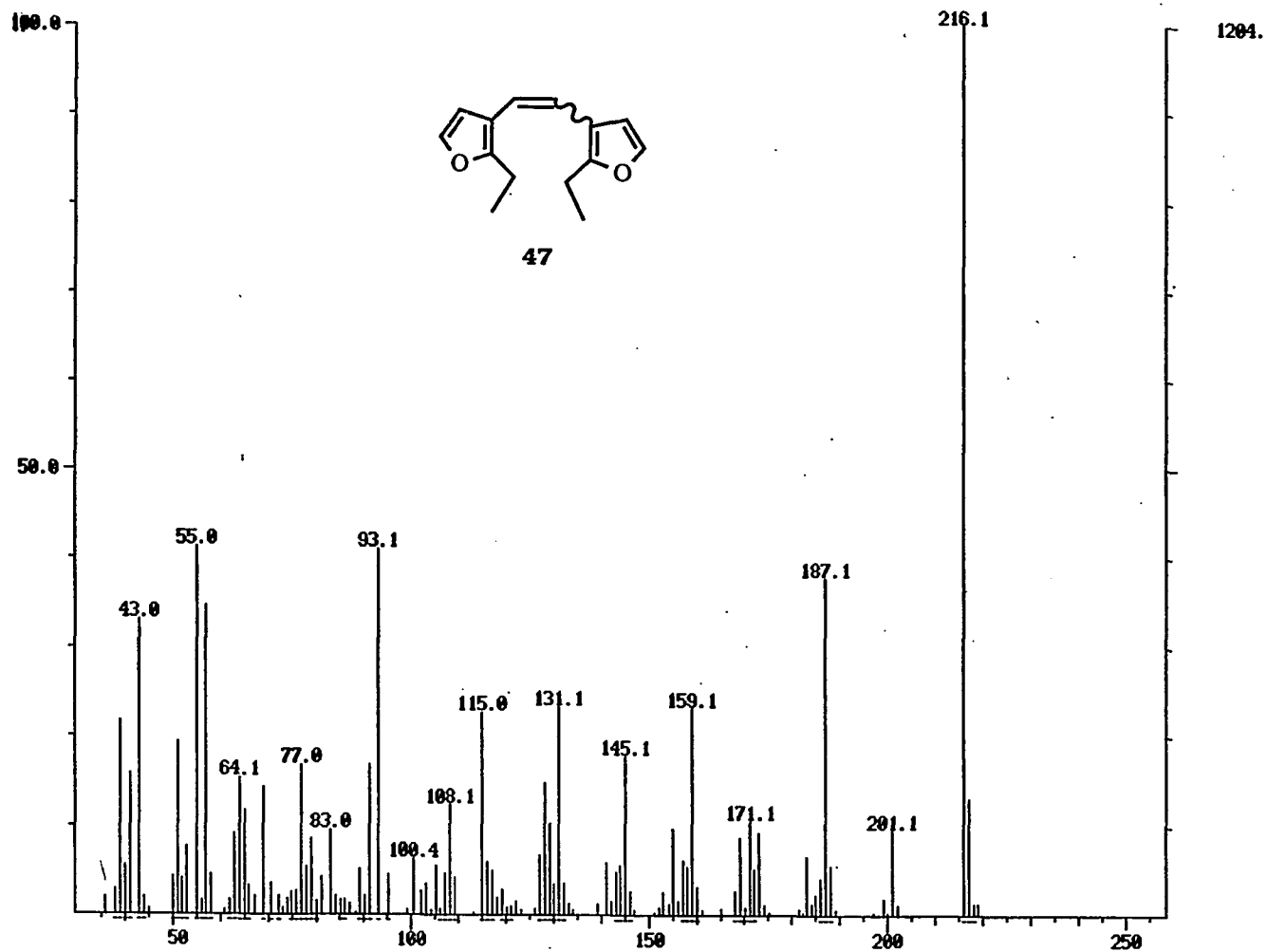
Figure A-27.   GC/MS of product **47** from the pyrolysis of the [4+2] dimer mixture of **40** and **41.**
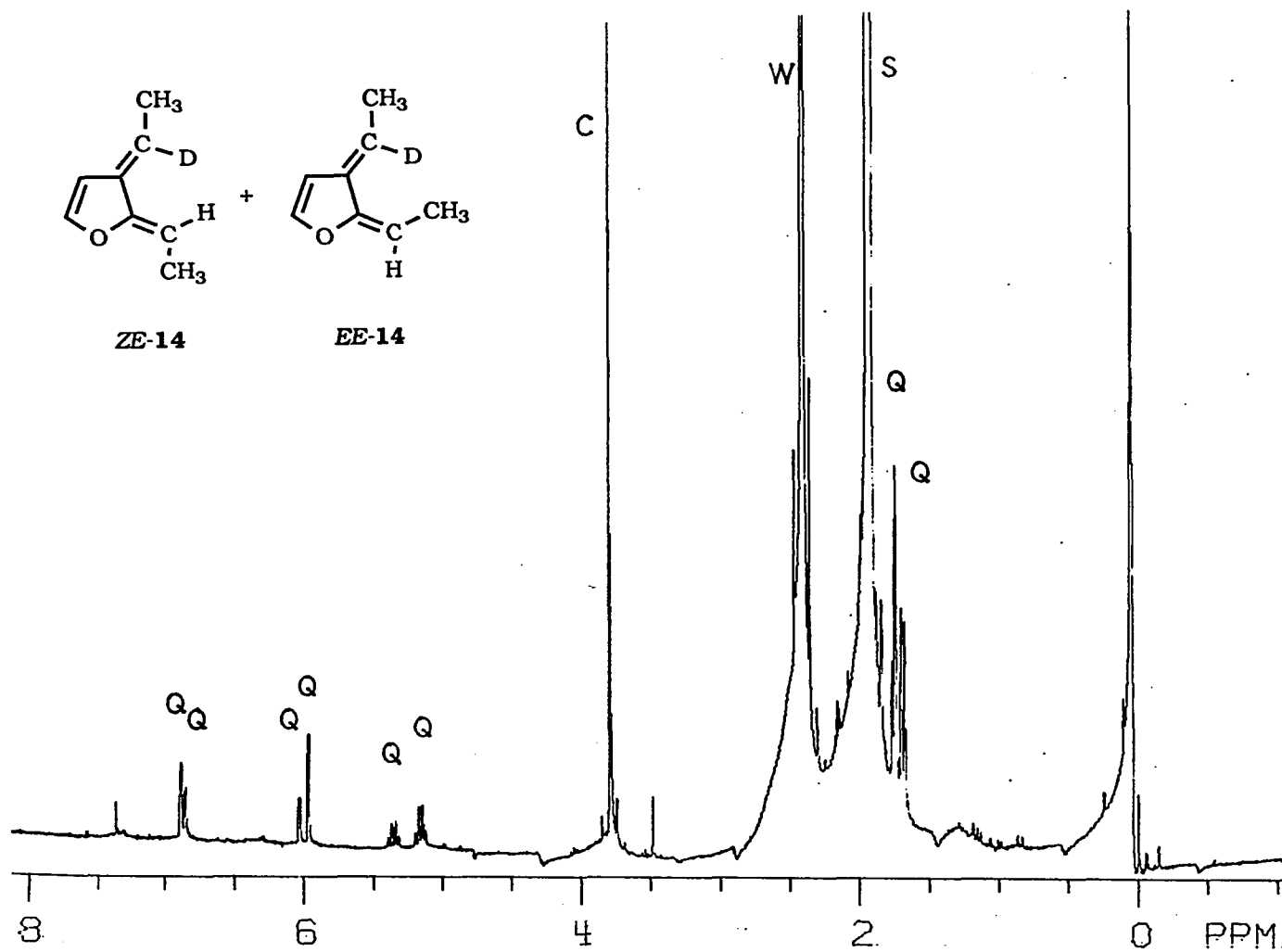
Figure A-28. ^{1}H NMR spectrum (300 MHz, CDCl$_3$) of 2-ethylidene-3-(d_1-ethylidene)-2,3-dihydrofuran (d_1-14) (C: internal standard 1,2-dichloroethane, w: H$_2$O, s: CD$_2$HCN, Q: *EE-14* and *ZE-14*).
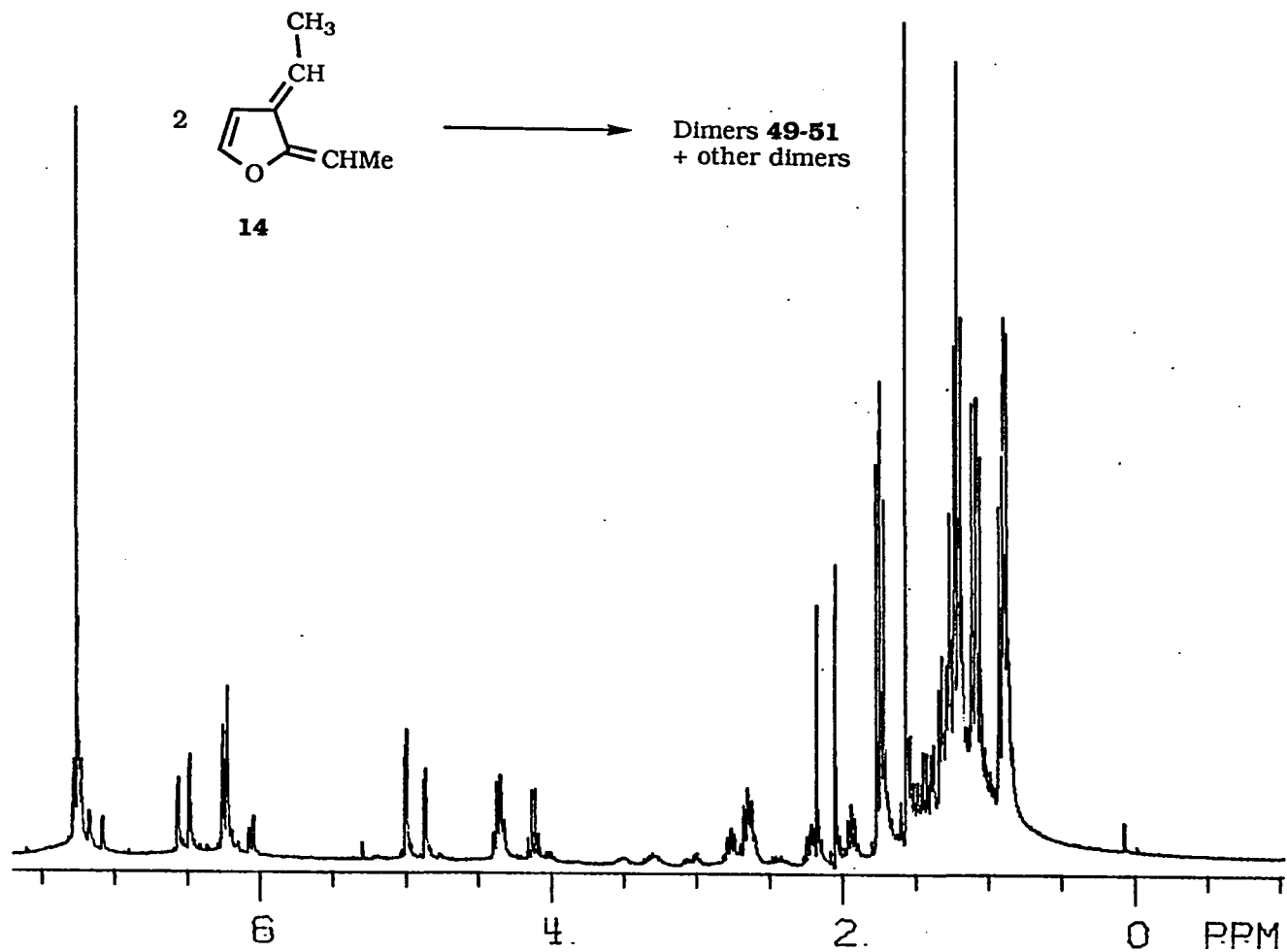
Figure A-29. ^{1}H NMR spectrum (300 MHz, CDCl$_3$) of the dimer mixture of 2,3-diethylidene-2,3-dihydrofuran (14).
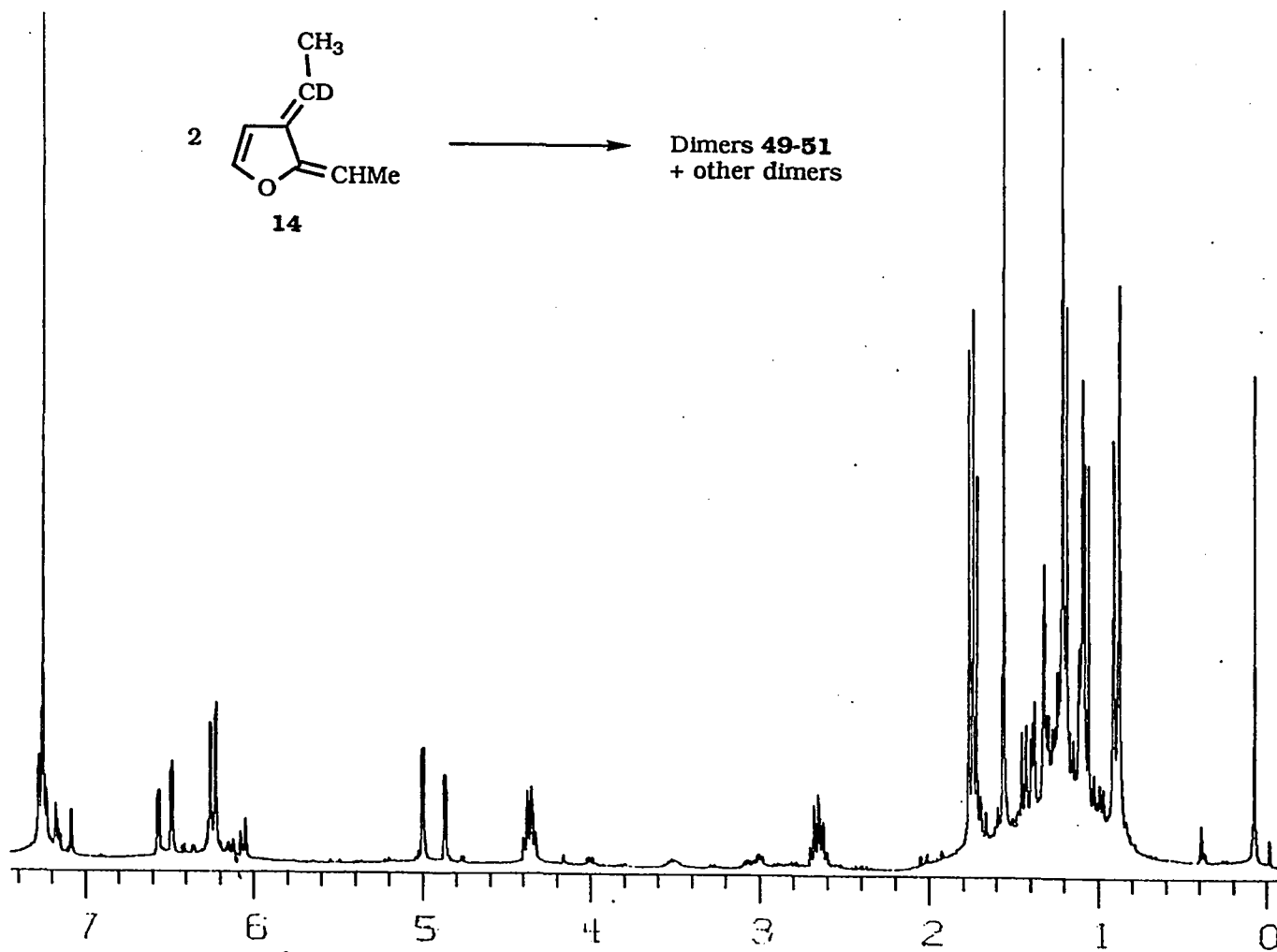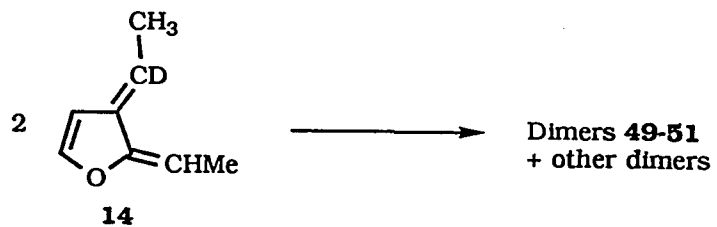
Figure A-30. ^1H NMR spectrum (300 MHz, CDCl$_3$) of the dimer mixture of 2-ethylidene-3-d_1-ethylidene-2,3-dihydrofuran (d_1-**14**).
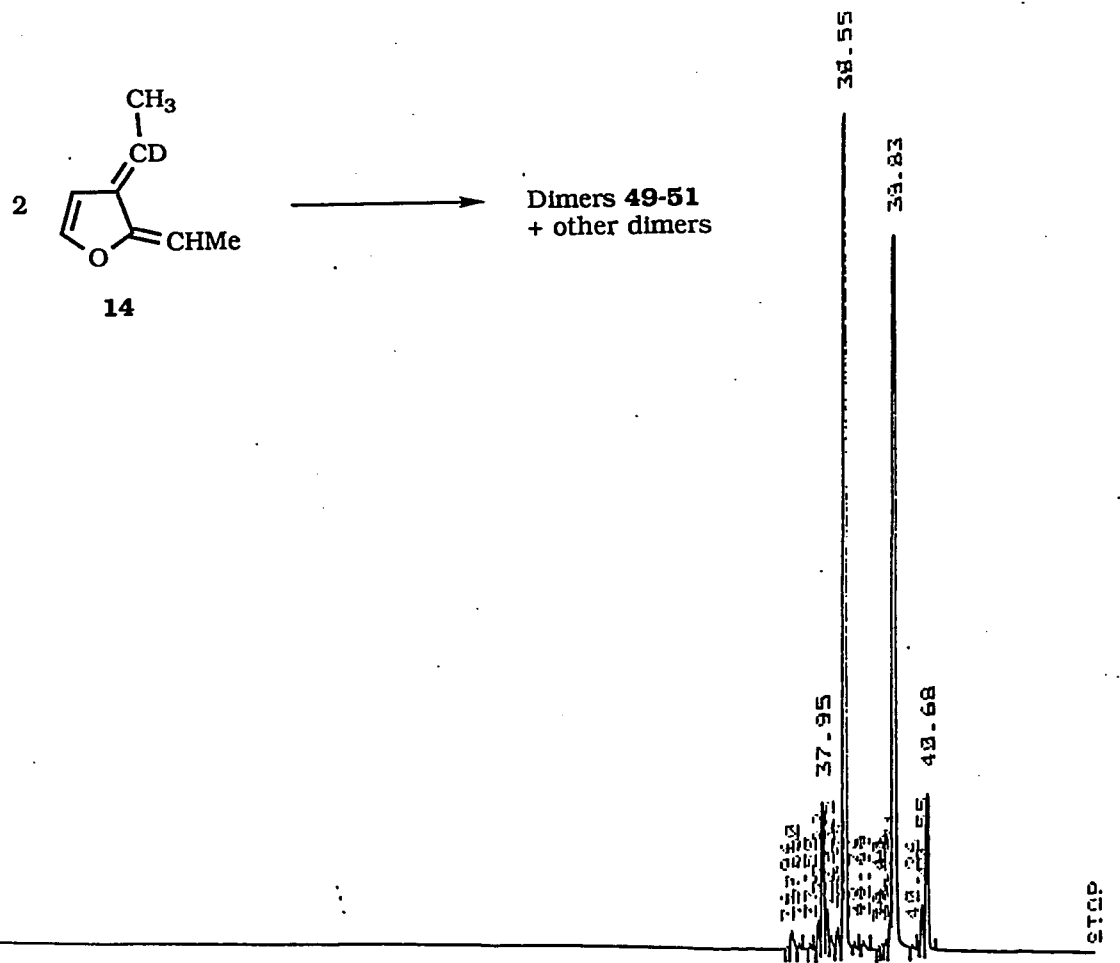
Figure A-31. Gas chromatograph (DB1, temperature program, 60 °C, 5 min, 2 °C/min 180°C) of the dimer mixture of 2-ethylidene-3-(d_1-ethylidene)-2,3-dihydrofuran (d_1-**14**).
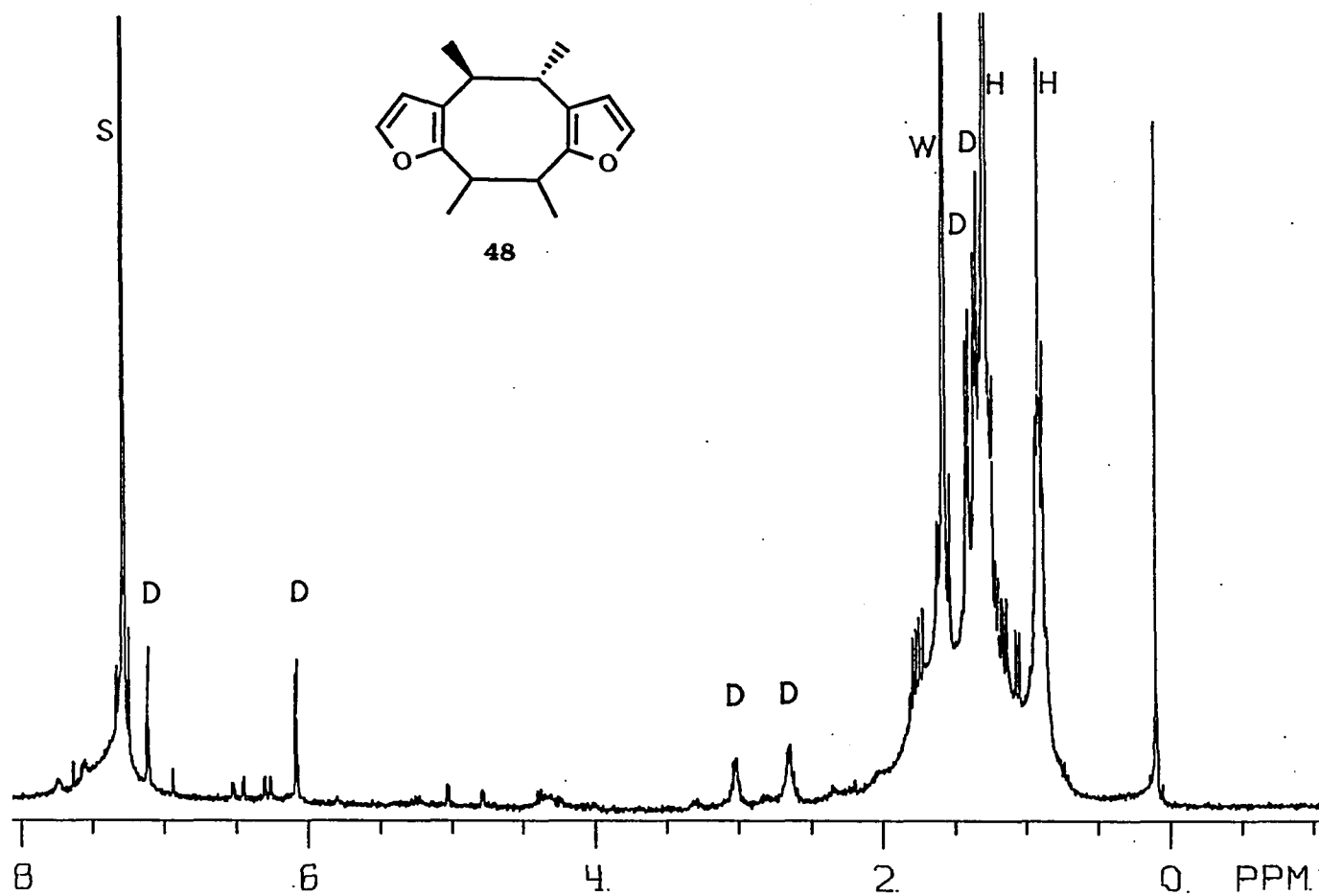
Figure A-32. ^{1}H NMR spectrum (300 MHz, CDCl₃) of the [4+4] dimer **48** of 2,3-diethylidene-2,3-di-hydrofuran (**14**) (D: dimer **48**, s: chloroform, w: H₂O, H: high boiling residue from hexanes, the eluent).
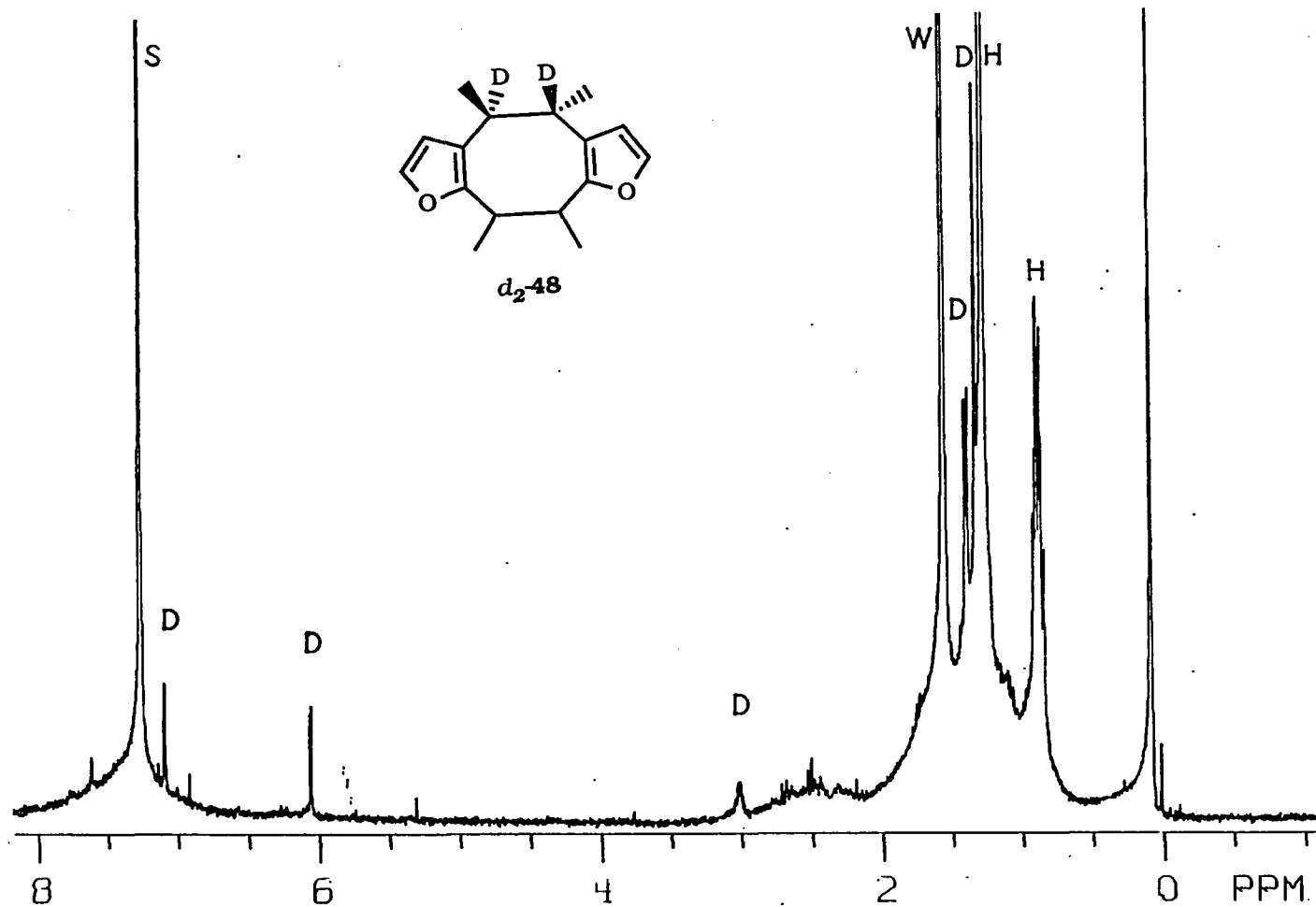
Figure A-33. ^{1}H NMR spectrum (300 MHz, CDCl$_3$) of the [4+4] dimer **48** of 2-diethylidene-3-d_1-ethylidene-2,3-dihydrofuran (d_1-**14**) (D: dimer d_2-**48**, s: chloroform, w: H$_2$O, H: high boiling residue from hexanes, the eluent).
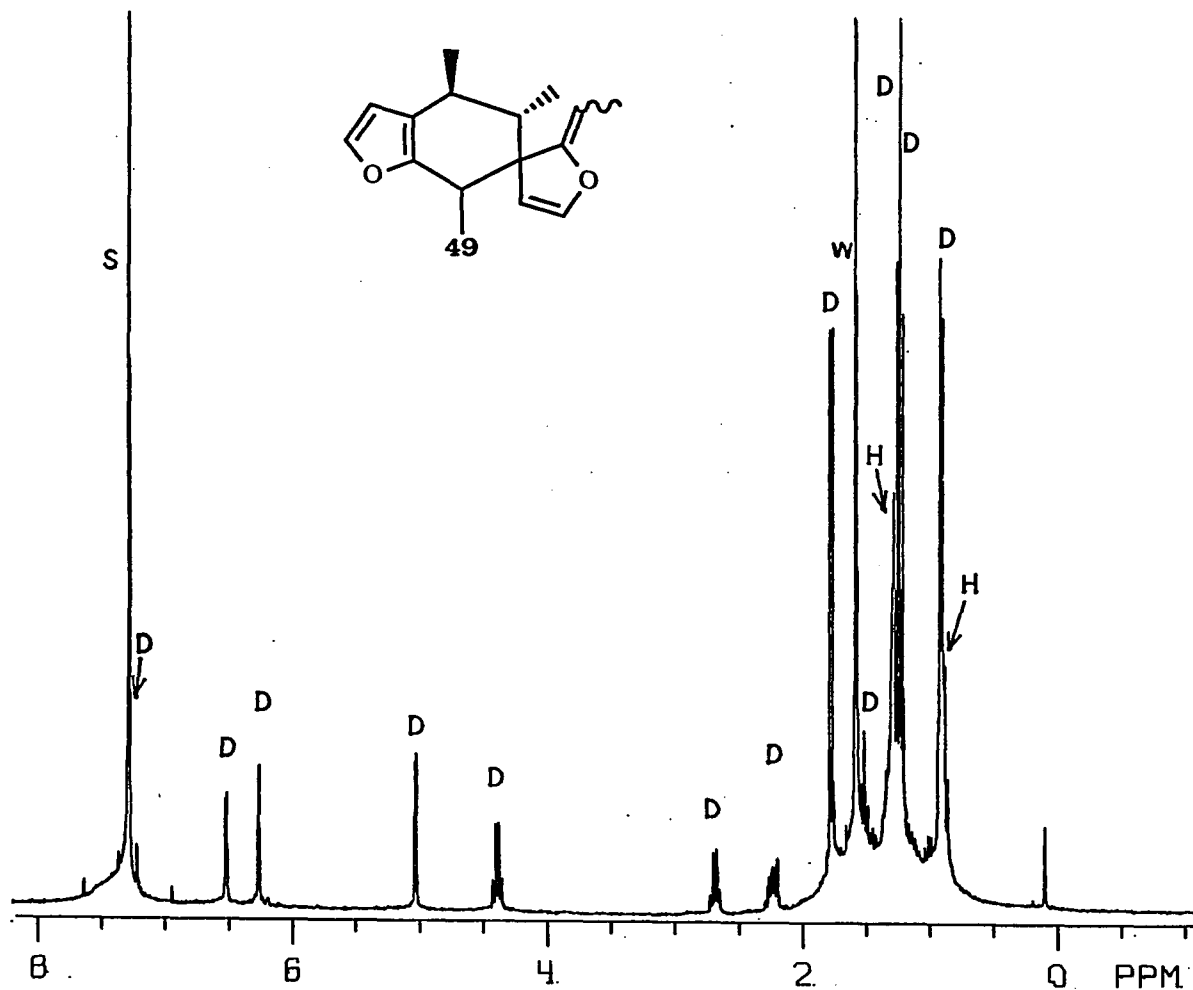
Figure A-34. ^1H NMR spectrum (300 MHz, $CDCl_3$) of the [4+2] dimer **49** of 2,3-diethylidene-2,3-dihydrofuran **(14)** (D: dimer **49**, s: chloroform, w: H_2O, H: high boiling residue from hexanes, the eluent) .
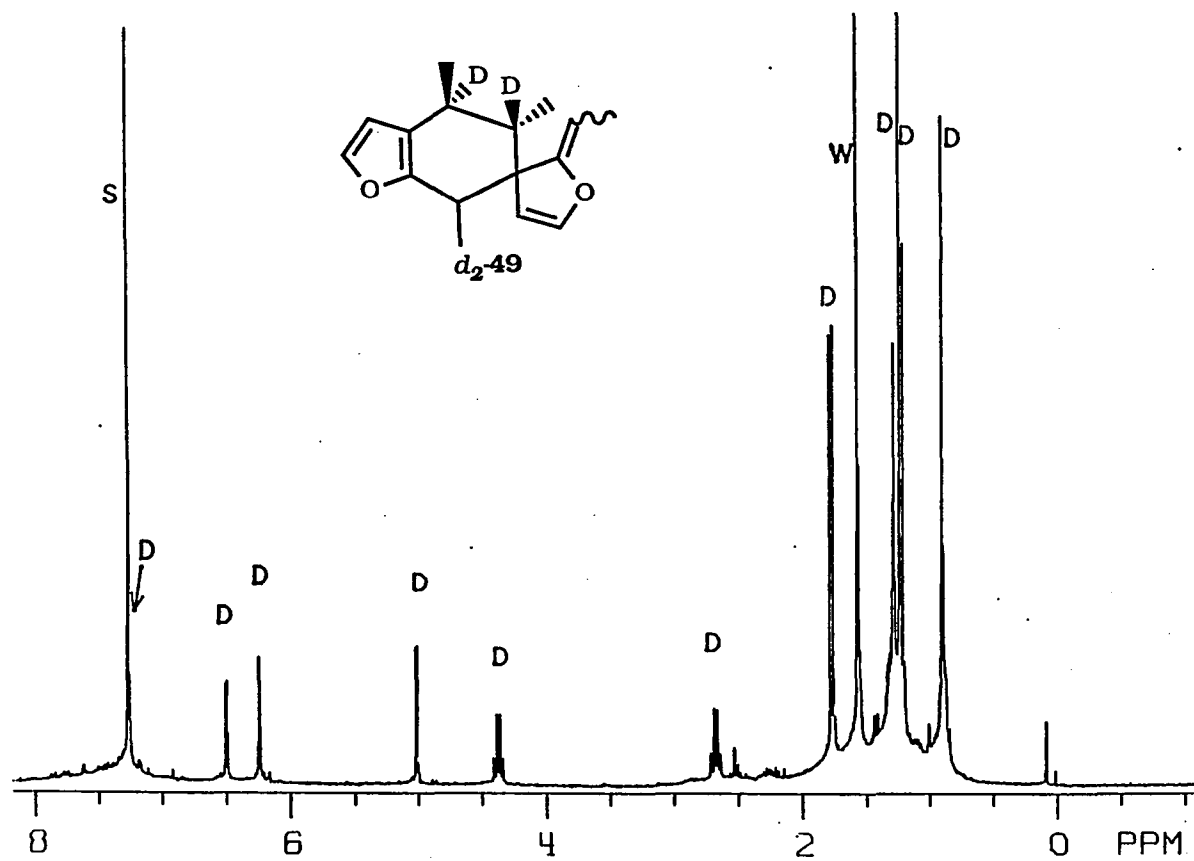
Figure A-35. ^{1}H NMR spectrum (300 MHz, CDCl$_3$) of the [4+2] dimer **49** of 2-diethylidene-3-d_1-ethylid-ene-2,3-dihydrofuran (d_1-**14**) (D: dimer d_2-**49**, s: chloroform, w: H$_2$O).
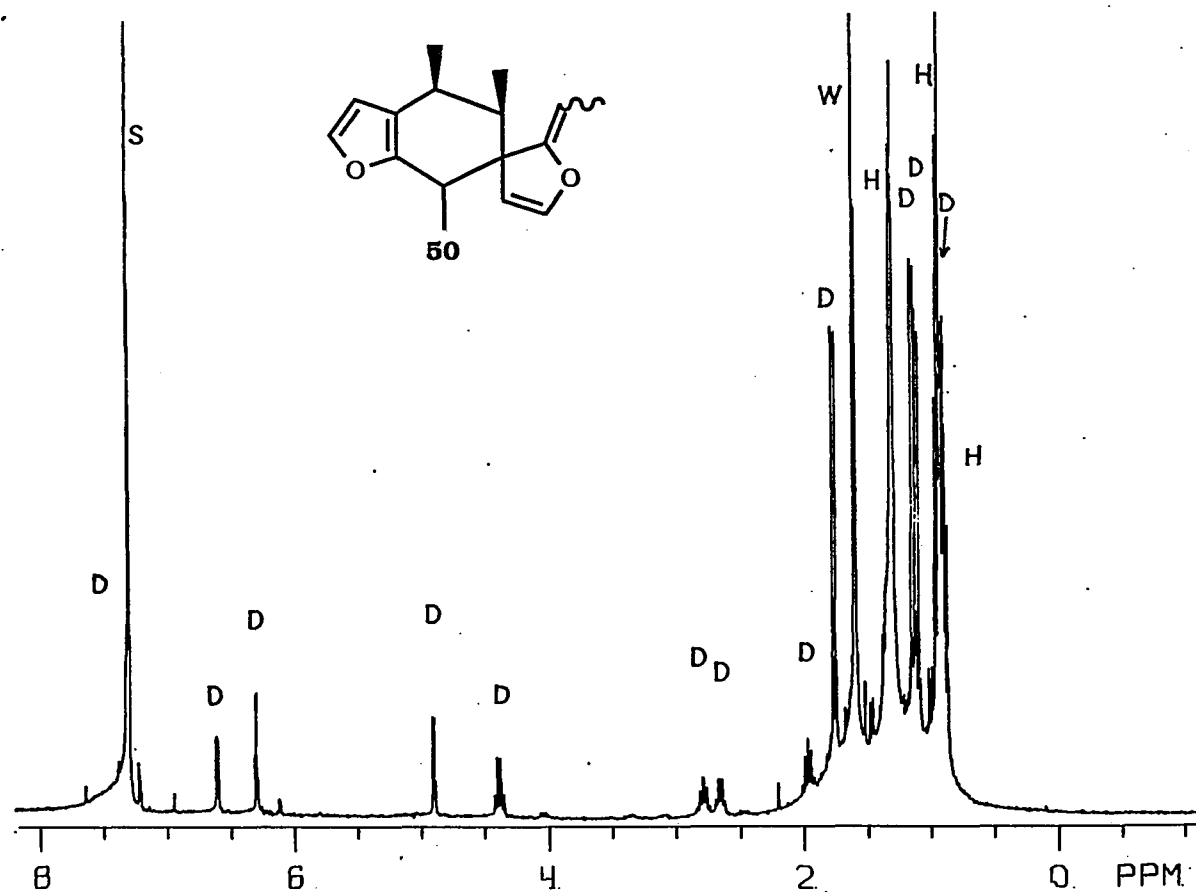
Figure A-36. ^{1}H NMR spectrum (300 MHz, CDCl$_3$) of the [4+2] dimer **50** of 2,3-diethylidene-2,3-dihydrofuran (**14**) (D: dimer **50**, s: chloroform, w: H$_2$O, H: high boiling residue from hexanes, the eluent).
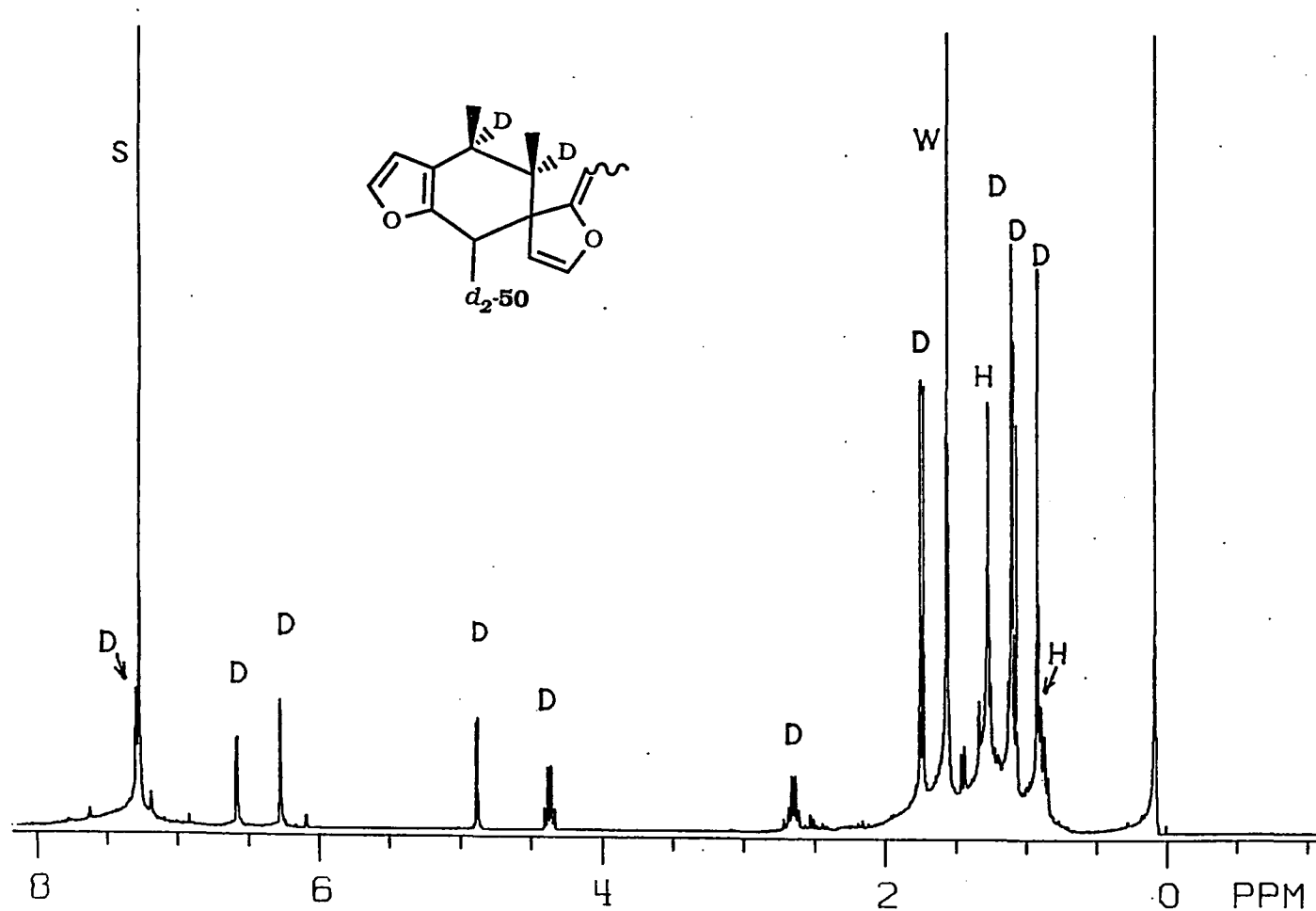
Figure A-37. ^{1}H NMR spectrum (300 MHz, CDCl$_3$) of the [4+2] dimer **50** of 2-diethylidene-3-d_1-ethylid-ene-2,3-dihydrofuran (d_1-**14**) (D: dimer d_2-**50**, s: chloroform, w: H$_2$O, H: high boiling residue from hexanes, the eluent).
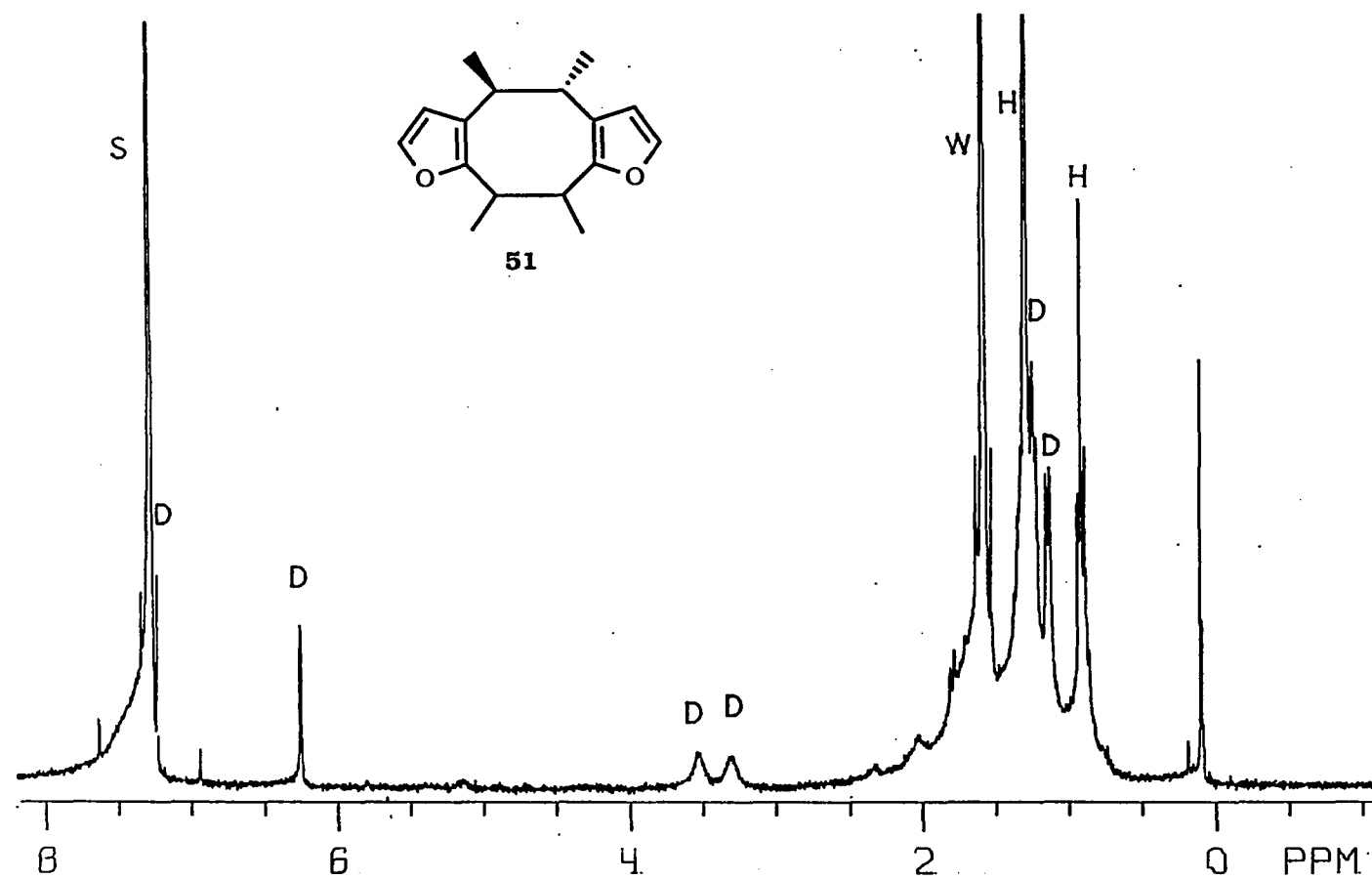
Figure A-38. ^{1}H NMR spectrum (300 MHz, CDCl$_3$) of the [4+4] dimer **51** of 2,3-diethylidene-2,3-di-hydrofuran **(14)** (D: dimer **51**, s: chloroform, w: H$_2$O, H: high boiling residue from hexanes, the eluent).
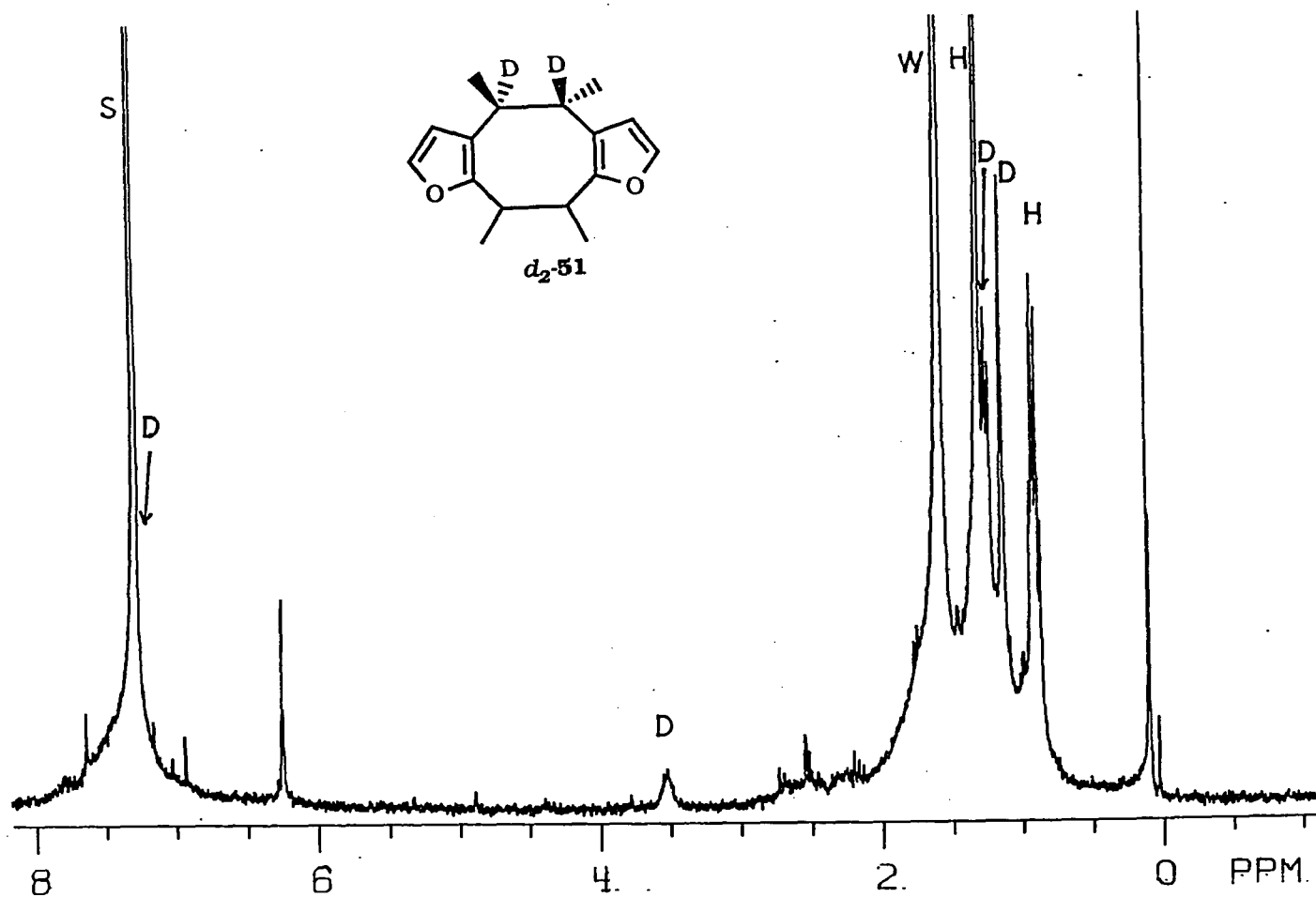
Figure A-39. ^1H NMR spectrum (300 MHz, CDCl$_3$) of the [4+4] dimer **51** of 2-diethylidene-3-d_1-ethylidene-2,3-dihydrofuran (d_1-14) (D: dimer d_2-51, s: chloroform, w: H$_2$O, H: high boiling residue from hexanes, the eluent).
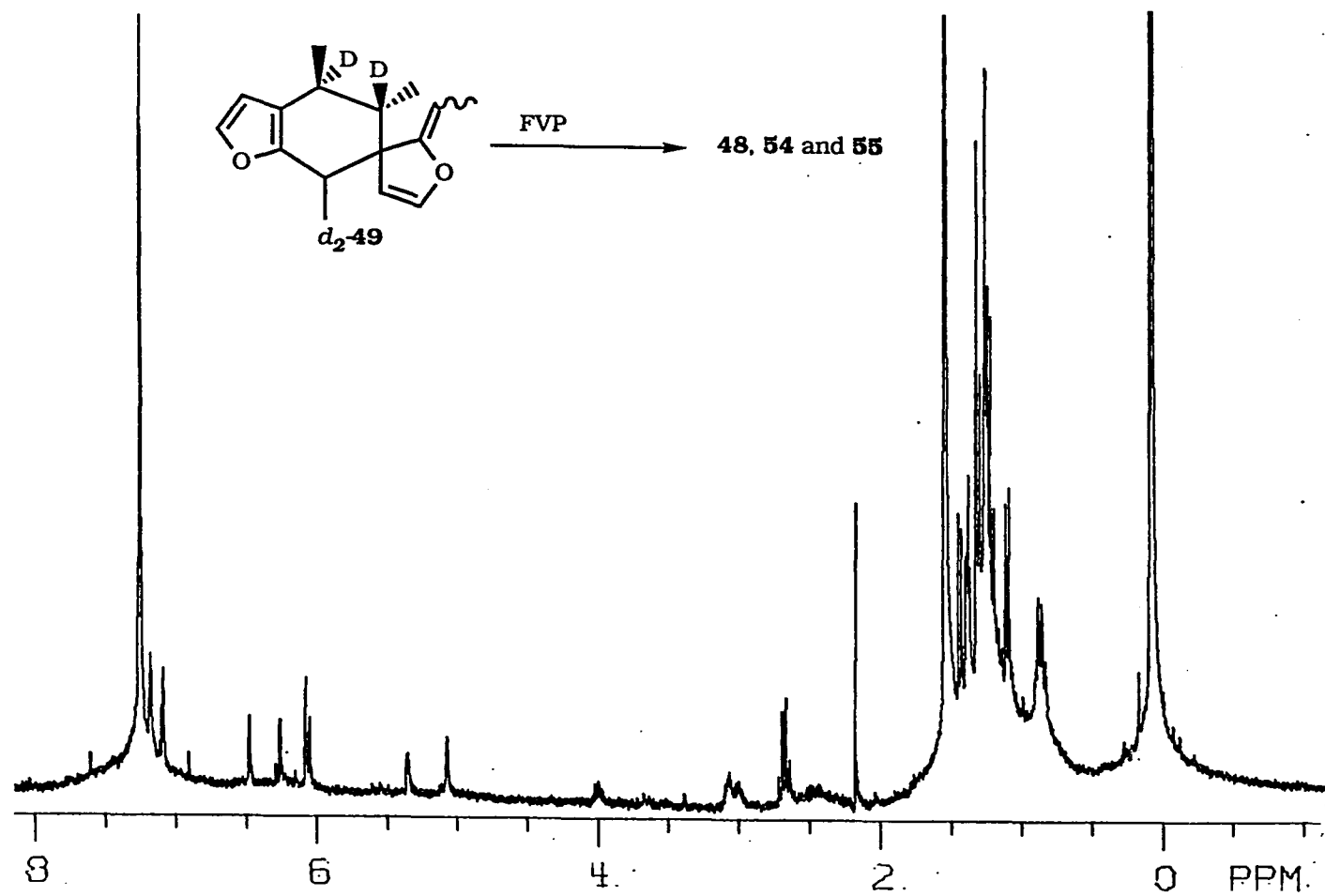
Figure A-40. ^{1}H NMR spectrum (300 MHz, CDCl$_3$) of the pyrolysate of the [4+2] dimer d_2-49.
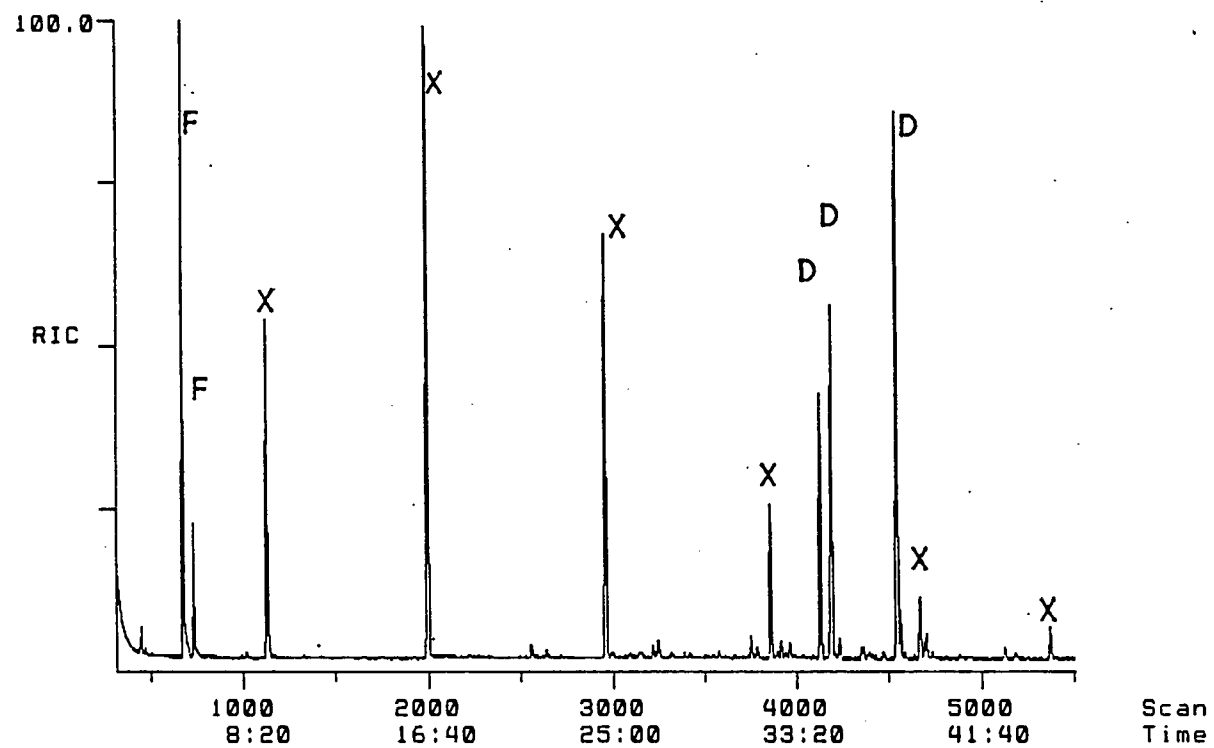
Figure A-41. Gas chromatograph (DB1, temperature program, 80 °C, 10 min, 1.5 °C/min, 200 °C, 30 min) of the pyrolysate of the [4+2] dimer d_2-**49** (X: silicon grease, F: fragmentation product, D: [4+4] dimer).
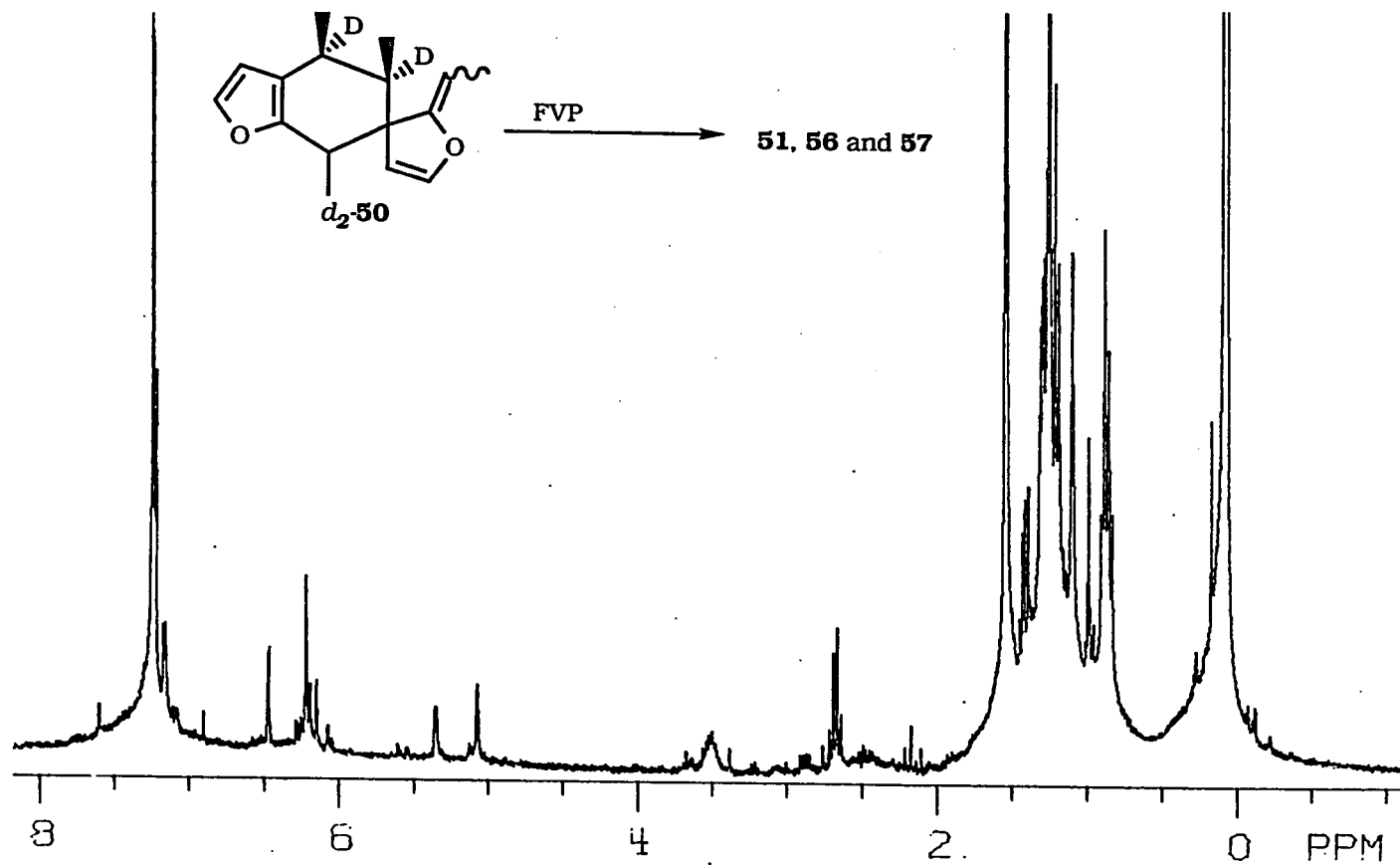
Figure A-42. ^{1}H NMR spectrum (300 MHz, CDCl$_3$) of the pyrolysate of the [4+2] dimer d_2-50.
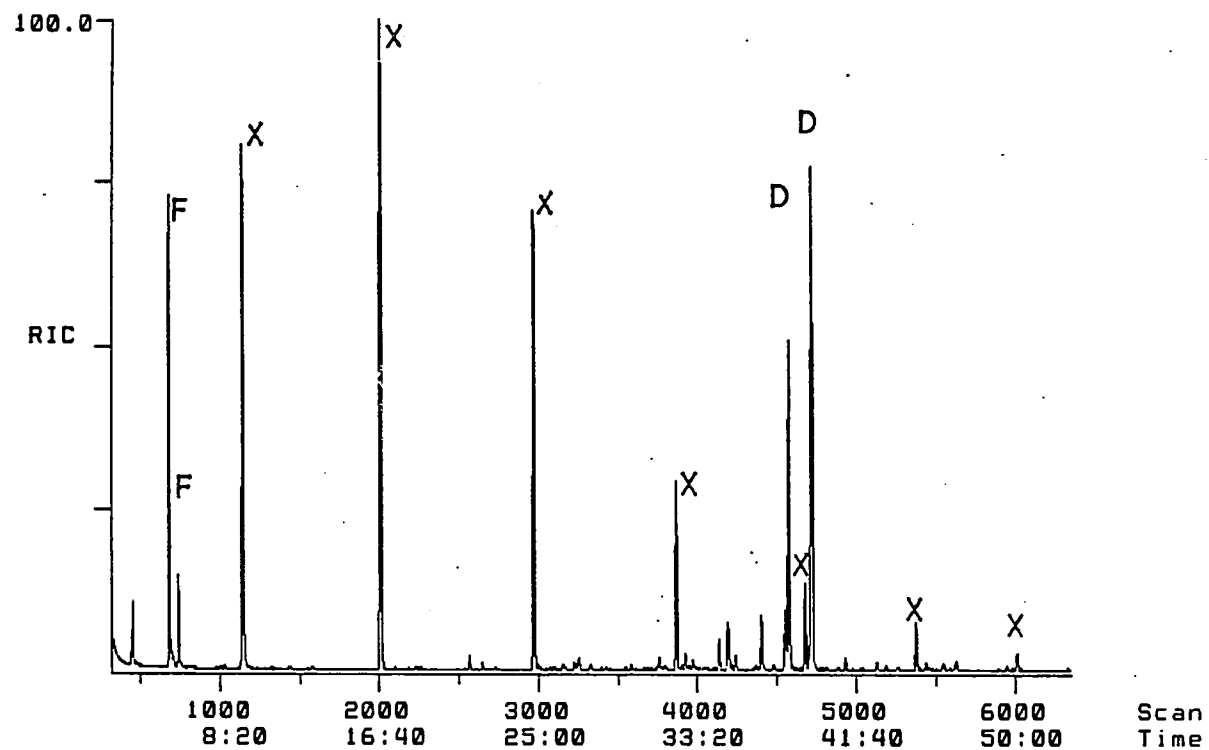
Figure A-43. Gas chromatograph (DB1, temperature program, 80 °C, 10 min, 1.5 °C/min, 200 °C, 30 min) of the pyrolysate of the [4+2] dimer d_2-**50** (X: silicon grease, F: fragmentation product, D: [4+4] dimer).

SECTION 2. THE DIMERIZATION KINETICS AND PRODUCTS ANALYSES, AND THE DIELS-ALDER REACTION KINETICS AND PRODUCT ANALYSES OF α-METHYL-o-XYLYLENE, α–CYCLOPROPYL-o-XYLYLENE, α–tert-BUTYL-o-XYLYLENE AND α–MESITYL-o-XYLYLENE.

INTRODUCTION

Benzene-based *o*-quinodimethanes (*o*-QDM's), such as the parent *o*-xylylene (**1**),

1

have been a subject of much interest and have been used extensively as reactive dienes in organic synthesis during past three decades.[1] Although it has been known for a long time that *o*-QDM's dimerize rapidly,[2] the mechanisms of these dimerizations have not been completely elucidated. Recently, we have shown that the dimerization of the furan-based *o*-QDM, **2**, which gives a high yield of the head-to-head [4+4] dimer **3**, proceeds by a stepwise mechanism via a diradical intermediate **4**.[3] This mechanism is strongly supported by the results of a secondary deuterium kinetic isotope effect

study[4] and by the results of a study of the effects of *t*-butyl substitution on the ends of the reactive diene system.[5]

Unlike the furan-based *o*-QDM **2**, **1** dimerizes to give mostly the [4+2] dimer **5** as well as a small amount of the [4+4] dimer **6**.[2] Having obtained firm support for the mechanism of the dimerization of the furan based *o*-QDM **2**, we set out to probe the

1   **5 (90 %)**   **6 (~10 %)**

mechanism of the dimerization of the benzene-based *o*-QDM's. Since the main mode of dimerization of **1** is the [4+2] mode, a concerted mechanism following Woodward-Hoffmann[6] rules, is a reasonable possibility.
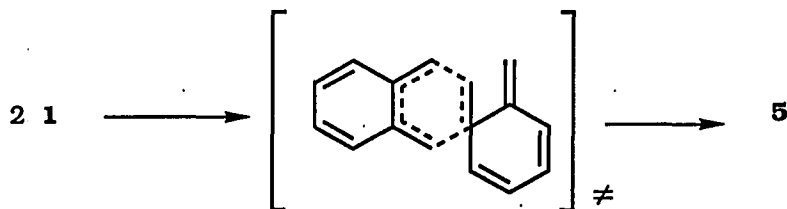
In spite of the high reactivity towards dimerization, benzene-based *o*-QDM's have been observed directly by UV-visible spectroscopy both in solution[7] and in a low temperature matrix,[8] by IR, Raman, fluorescence and fluorescence excitation spectroscopy in a low-temperature matrix,[9] and by UV-photoelectron spectroscopy in the gas phase.[10] Recently, our research group has published the ^{1}H NMR spectrum of **1**[11] and has measured the activation parameters of the dimerization of **1** and other reactive *o*-QDM's **7** and **8** by using the stopped-flow technique.[12] Because the

7   **8**
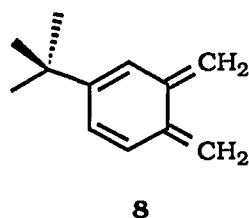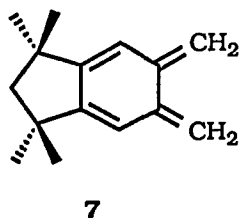
differences in the rate constants for dimerization of **1**, **7**, and **8** are small, it was suggested that the approach of monomers during dimerization is non-endo. Indeed, this observation does not rule out either the concerted or stepwise mechanism. Unfortunately, because of the low enthalpy of activation ($\Delta H^{\neq}= $ 3-5 kcal/mol) of dimerization, which is consistent with an early transition state, the secondary kinetic isotope effect would be expected to be significantly reduced.[13] In this situation, it is difficult to draw any firm conclusion from the kinetic isotope experiments. Moreover, the lack of a precise method to determine the relative dimerization rate constants for deuterated and non-deuterated o-QDM **1** further discouraged us from attempting the study.

We thus decided to probe the dimerization mechanism by studying a series of α-substituted o-QDM's **9** to **12**. We anticipated that comparison of the regioselectivity of this series in the Diels-Alder reaction, a [4+2] cycloaddition that is thought to be a concerted (one-step) reaction, with the regioselectivity obtained in the dimerizations would allow us to draw some conclusions about the mechanism of the dimerization of benzene-based o-QDM's.
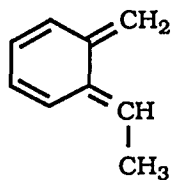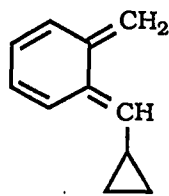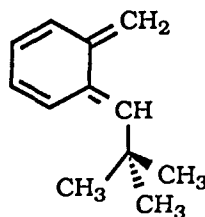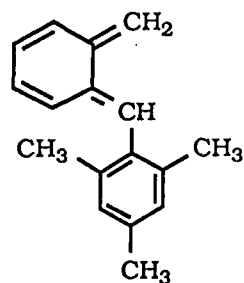
9	**10**	**11**	**12**

RESULTS

Preparation of precursors for generation of o-quinodimethane inter-mediates. o-QDM's **9, 10** and **11** were generated in solution by fluoride ion induced 1,4-elimination from the quaternary ammonium salt precursors **13, 14,** and **15**. The
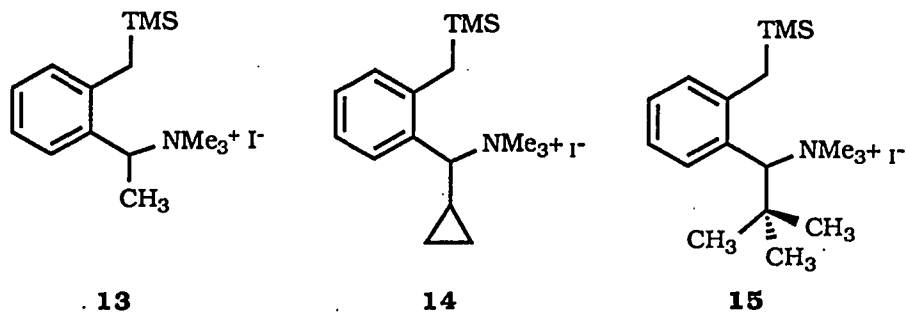
preparation of precursor **13** has been reported by Ito.[14] The syntheses of **14** and **15** are based on a similar strategy and are shown in Scheme 1. Silylation of benzoate **16** provided α-silylated ester **17**[15,16] which was reduced by LiAlH$_4$[17] to give alcohol **18**, followed by modified Collin's oxidation[18] to give aldehyde **19**. Imination[19] of **19** followed by treatment of **20** with cyclopropyllithium[20] at -10 °C or with *tert*-butyl-lithium at -78 °C gave rise to secondary amines **21** and **22**. The amines were methylated by reductive amination[21] to provide tertiary amines **23** and **24** which were further quaternized with methyl iodide to give **14** and **15**, respectively.

However, due to the steric hindrance introduced by the mesityl substituent, the preparation of the corresponding quaternary ammonium salt precursor failed. In order to solve this problem, other kinds of leaving groups were investigated. The problem was finally overcome by employing trichloroacetate as the leaving group. The synthesis of **25**, the precursor of **12**, is shown in Scheme 2. Since compound **25** is unstable on silica gel and hydrolysed quickly to give back alcohol **26**, precursor **25** was used in the following studies without further purification.

Scheme 1

c ⎧ **18** R' = CH$_2$OH
  ⎩ **19** R' = CHO
d ⎧ **20** R' = CH=NCH$_3$

21 R = c-C$_3$H$_5$
22 R = C(CH$_3$)$_3$

23 R = c-C$_3$H$_5$
24 R = C(CH$_3$)$_3$

14 R = c-C$_3$H$_5$
15 R = C(CH$_3$)$_3$
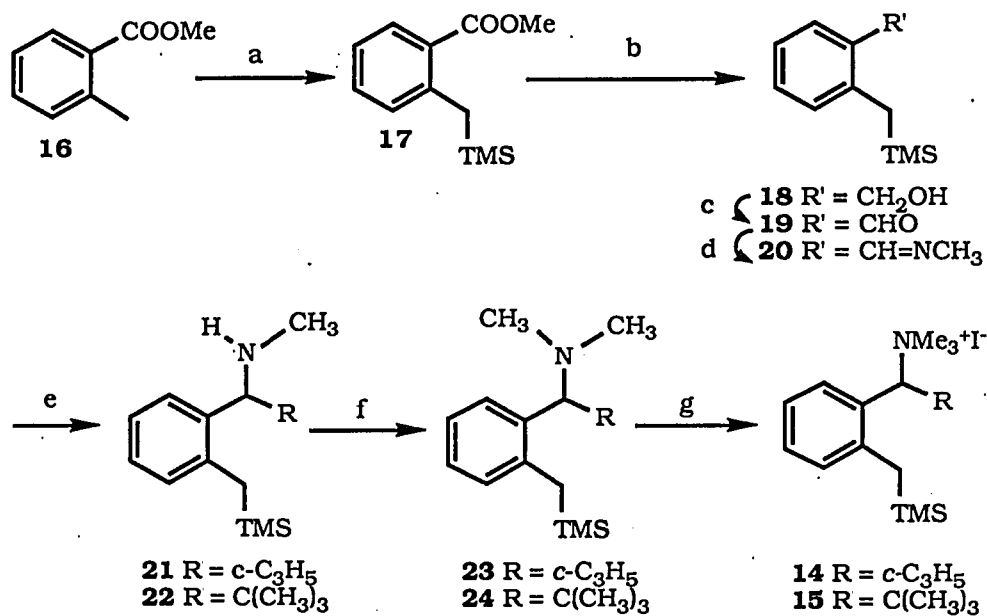
a, 2 LDA, TMSCl; b, LiAlH$_4$; c, CrO$_3$· 2Py; d, MeNH$_2$ in benzene; e, RLi; f, NaBH$_3$CN, CH$_2$O, HOAc; g, MeI in acetonitrile.

Scheme 2

19   **26**   **25**
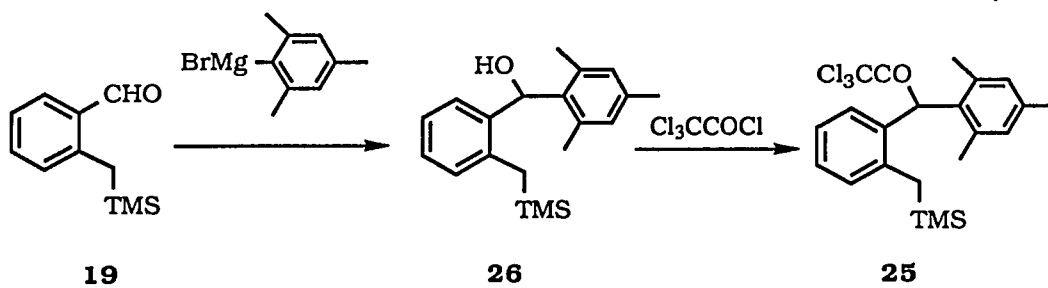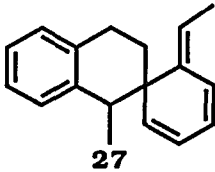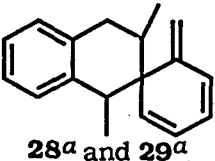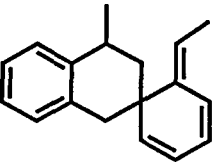
Product analyses of dimerizations of o-quinodimethanes. In the absence
of dienophiles, generation of o-QDM's **9, 10, 11,** and **12** in acetonitrile with TBAF led
to a variety of dimers in all cases. However, these product mixtures could not be
analyszed by GC/MS due to the thermal instability of the [4+2] dimers. The dimers
were separated by liquid chromatography and analysed by ^{1}H NMR spectroscopy. In
order to make sure that the dimers were coming from the original product mixtures,
the ^{1}H NMR spectra of the isolated dimers were compared with the ^{1}H NMR spectrum
of the original product mixture. The results of the dimerization product analyses and
their relative percentages are summarized in Table 1, 2, 3 and 4. Details about the
structural assignment of the dimers are presented in the Experimental Section.

In the dimerization of o-QDM **9,** [4+2] dimer **27** was isolated as the only major
product (Table 1). Three other minor dimers were identified as **28, 29,** and **30.** In
contrast to o-xylylene (**2**) dimerization, no evidence for [4+4] dimers could be found by
^{1}H NMR spectroscopy. However, an unknown compound (~5 %), which may also be a
dimer, was observed in the NMR spectrum of the dimer mixture.

The dimerization of o-QDM **10** provided at least seven dimers which were
identified as dimers **31-37** (Table 2). Not surprisingly, the [4+2] dimers **31-35** were
formed predominately. However, two [4+4] dimers **36** and **37** were found in this case.
The structure of **31** was confirmed by ^{1}H NMR spectroscopy. Thermolysis of **31** in
1,4-cyclohexadiene at 80 °C for 2 h provided **36** and **37** in a ratio of 19:1. According to
the GC/MS analysis, no other products such as cyclopropane ring opening products
or diradical trapping products were found in the thermolysis. When dimer **31** was
subjected to flash vacuum pyrolysis (FVP)[22] at 540 °C, a mixture of **36** and **37** was
obtained but in a different ratio, a ratio of 5:1. In addition, two minor components (0.7
% and 2 %) were found in the GC/MS. Unfortunately, their structures could not be

Table 1. Dimerization products of α–methyl-o-xylylene (9)

Product[b]	Mode of cyclization	Yield , %
27	Head-to-head [4+2]	67
28[a] and **29**[a]	Head-to-tail [4+2]	9 (**28**) 10 (**29**)
30[a]	Head-to-tail [4+2]	9
Unknown compound	---	5

[a] Compound was isolated from the dimer mixture and identified by ^{1}H NMR spectroscopy.
[b] Each product number represents a single diastereomer.

determined from the GC/MS data. The ^{1}H NMR spectrum of **32** is consistent with the assigned structure but firmer evidence was obtained from the FVP of **32** which produced, as did **31**, a mixture of head-to-head [4+4] dimers **36** and **37**. The structure

31 or 32 → FVP → **36 and 37**
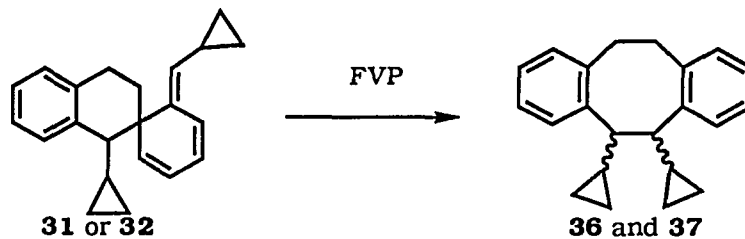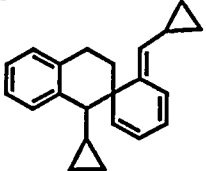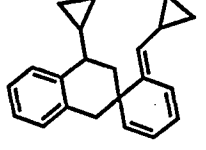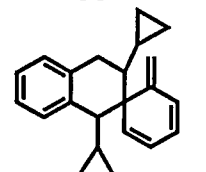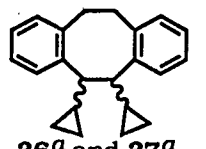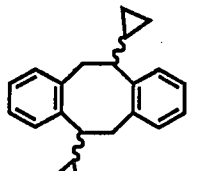
Table 2. Dimerization products of α–cyclopropyl-o-xylylene (**10**)

Product[c]	Mode of cyclization	Yield , %
31[a] and **32**[a]	Head-to-head [4+2]	53 (**31**) 13 (**32**)
33[a]	Head-to-tail [4+2]	11 (**33**)
34[b] and **35**[b]	Head-to-tail [4+2]	4 (**34**) 3 (**35**)
36[a] and **37**[a]	Head-to-head [4+4]	< 16 (**36** and **37**)
38 and **39**[d]	Head-to-tail [4+4]	---

a Compound was isolated from the dimer mixture and identified by ^{1}H NMR spectroscopy.

b Structures were identified on the basis of the ^{1}H NMR spectroscopy of a mixture of **34** and **35**.

c Each structure number represents a single diastereomer.

d Dimers **38** and **39** were obtained as a mixture from the FVP of **33**.

of **33** is based ori several key ^{1}H NMR signals, the benzylic AB quartet and the vinyl

doublet, which is coupled to a cyclopropyl ring proton. FVP of **33** led to a pair of [4+4]

dimers which are different from **36** and **37**. These were assigned as the head-to-tail

dimers **38** and **39**. [4+2] Dimers **34** and **35** could not be separated and their
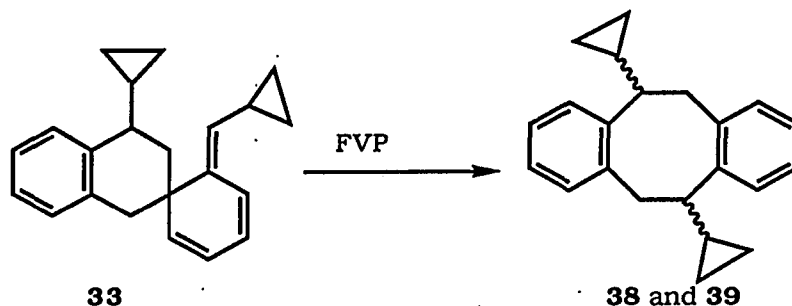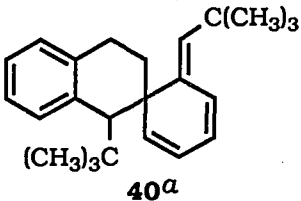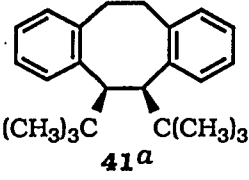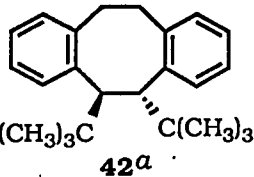
33   **38 and 39**

structural assignments are based on the ^{1}H NMR signals from the exo-methylene

protons and benzylic proton (a doublet) which is coupled to a cyclopropyl ring proton.

FVP of a mixture of **34** and **35** gave **38** and **39** in a ratio of 1.3:1. This result further

$$\mathbf{34 + 35} \quad \xrightarrow{\text{FVP}} \quad \mathbf{38 + 39}$$
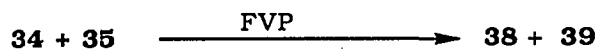
supports the head-to-tail [4+2] assignment of **34** and **35**.

The dimerization of o-QDM **11** at room temperature in acetonitrile provided a

mixture of three dimers which were identified as head-to-head [4+2] dimer **40** and

head-to-head [4+4] dimers **41** and **42** (Table 3). The identity of the [4+2] dimer **40** was

simply established by ^{1}H NMR spectroscopy and a ^{1}H-^{1}H NOESY experiment. On the

other hand, the NMR spectra of the [4+4] dimers indicated that one of the [4+4] dimers

possesses an asymmetric conformation while the other possesses a symmetric

conformation. Since the steric repulsion between the two adjacent cis tert-butyl groups

of **41** tends to force the conformation of the eight-membered ring away from σ_v

Table 3.   Dimerization products of α–*tert*-butyl-*o*-xylylene (**11**)

Product[b]	Mode of cyclization	Yield, %
 40[a]	Head-to-head [4+2]	80
 41[a]	Head-to-head [4+4]	12
 42[a]	Head-to-head [4+4]	8

[a]   Compound was isolated from the dimer mixture and identified by ^{1}H NMR spectroscopy.

[b]   Each compound number represents a single diastereomer.

symmetry, this structure was assigned to the compound having the ^{1}H NMR spectrum with an asymmetric pattern. The steric repulsion of the two trans *tert*-butyl groups of the [4+4] dimer **42** does not affect the C$_2$ symmetry of the structure and therefore this structure was assigned to the compound with the symmetrical ^{1}H NMR spectrum. Interestingly, the compound formed in the dimerization at room temperature in acetonitrile to which we assigned structure **42** is thermally labile and converts to another symmetrical conformation in boiling acetonitrile. We attribute this observation to the interconversion of di-equatorial **42** and di-axial **42** which are

separated by a sufficiently high rotational energy barrier that interconversion at room temperature is slow.[23] Clearly, one conformation is significantly more stable than the other. An MM-X[24] calculation indicated that di-axial skewed form of **42** is the most stable conformation.

di-axial **42**   di-equatorial **42**
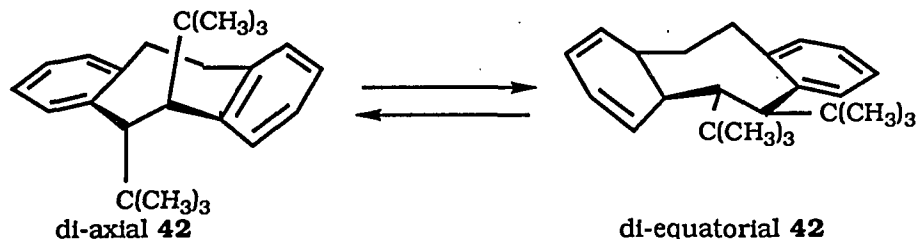
FVP of [4+2] dimer **40** at 550 °C provided a mixture of thermally stable symmetric [4+4] dimer **42** and asymmetric [4+4] dimer **41**. Indeed, **40** is thermally unstable and undergoes an unimolecular rearrangement with a half-life of 27 min at 63 °C in acetonitrile to give rise to the same mixture of the [4+4] dimers.

o-QDM **12** generated from the trichloroacetate precursor **25** in TBAF solution dimerized to two head-to-head dimers **43** and **44** (Table 4). As expectedly, [4+2] dimer **43** is also thermally unstable and rearranges to **44** under mild conditions. When **43** was subjected to thermolysis in thiophenol or in 2-diiodopropane at 80 °C, the rearrangement product, [4+4] dimer **44**, was isolated. But interestingly, thermolysis of **43** in thiophenol at 180 °C in a sealed tube generated the reduction product **45** and phenyl disulfide in a ratio of 1:1.

43   PhSH, at 180°C   **45**
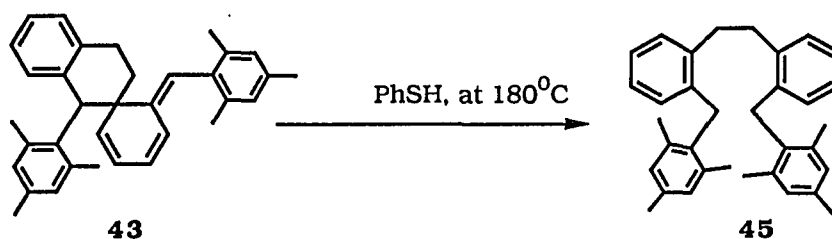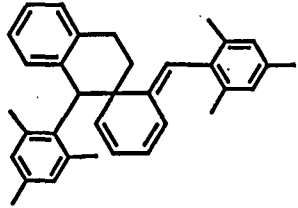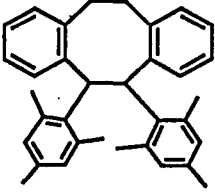
Table 4. Dimerization products of α–mesityl-*o*-xylylene (12)

Product[b]	Mode of cyclization	Yield, %
43[a]	Head-to-head [4+2]	58
44[a]	Head-to-head [4+4]	42
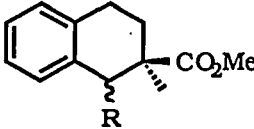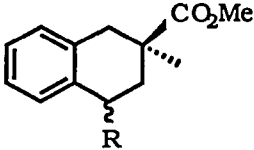
[a] Compound was isolated and identified by ^{1}H NMR spectroscopy.
[b] Each structure number represents a single diastereomer.

Regioselectivity in the Diels-Alder reactions of o-quinodimethanes. In the presence of a dienophile, the α-substituted *o*-QDM's were trapped to produce Diels-Alder[14] adducts (Table 5). In our investigation, methyl methacrylate was used as the dienophile in the regioselectivity study.

When *o*-QDM's **9, 10, 11,** and **12** were generated in acetonitrile in the presence of an excess of methyl methacrylate, four types of Diels-Alder adducts were identified by GC/MS and ^{1}H NMR spectroscopy and the results are summarized in Table 5. In all the cases, the "ortho" isomers are the major products.[14] However, the relative ratio of "ortho" to "meta" isomers is affected significantly by the specific α-substituent on the *o*-QDM.

Table 5. The Diels-Alder adducts of methyl methacrylate and o-QDM's **9, 10, 11** and **12**

Diels-Alder adducts · R =	**5** CH$_3$ [a]	**6** c-C$_3$H$_5$ [b]	**7** C(CH$_3$)$_3$ [c]	**8** Mesityl [c]
"ortho"	8.8[d] (39:34)[e]	4.3[d] (26:25)[e]	2.2[d] (13:6)[e]	5.8[d] (38:11)[e]
"meta"	1 (4.6:3.7)[e]	1 (6.2:5.7)[e]	1 (4.3:4.2)[e]	1 (4.4:4.0)[e]

[a] The regiochemistry was determined by means of applying the [1]NMR decoupling technique to the product mixture directly.

[b] The major "ortho" isomers were separated from the "meta" isomers and the regiochemistry was determined by means of applying the ^{1}H NMR decoupling technique to the "ortho" isomer mixture directly.

[c] The isomers were separated and identified by ^{1}H NMR spectroscopy.

[d] The "ortho" to "meta" ratio.

[e] The diastereomeric ratio.

Stopped-flow kinetics and competitive kinetics experiments. The stopped-flow technique is a well known method which has been used to study the kinetics of reactive intermediates such as o-QDM's.[11,12] The very rapid formation of an o-QDM, followed by its second order decay is monitored by UV-visible spectroscopy. From the measured second order decay curve, the rate of the dimerization of the o-QDM is determined. Since the dimerization is a second-order process, determination of the rate constant, k_2, requires knowledge of the concentration of the o-QDM and this can be obtained by knowing the ε_{max} of the o-QDM. In our experiments, the ε_{max} for o-QDM's **9** and **11** were determined in the following manner. Several runs

were carried out in which the optimum fluoride ion concentration was kept constant but the concentration of the quaternary ammonium salt precursor was varied. In each experiment, we obtained a maximum absorbance of the o-QDM intermediate. Assuming that the quaternary ammonium salt precursor was converted quantitatively to the corresponding o-QDM before much of the o-QDM intermediate had dimerized, we obtained the initial concentration of o-QDM. By using Beer's Law, the ε_{max} of the o-QDM was determined from the linear plot of the absorbances against the concentrations of the o-QDM.

Rate constants for the dimerizations of **9** and **11** from 10-50 °C were measured and these are reported in Table 6. The activation parameters evaluated from the rate constants and the ε_{max}'s of **9** and **11** are summarized in Table 7. The dimerization rate constant, k_2, for **9** and **11** at 25 °C are close to that for the parent o-xylylene (**1**) within one order of magnitude.[12] All their activation enthalpies are around 3 to 4 kcal/mol while the activation entropies are around ~29 to ~30 eu.

Table 6. Second-order rate constants for the dimerization of **9** and **11**

Temperature, °C	k_2 ($\times 10^{-3}$) for **9**, $M^{-1}s^{-1}$	k_2 ($\times 10^{-3}$) for **11**, $M^{-1}s^{-1}$
14.75	---	0.782 ± 0.01
15.50	6.80 ± 0.07	---
23.80	8.29 ± 0.01	---
23.85	---	1.03 ± 0.01
29.65	---	1.16 ± 0.01
30.40	9.49 ± 0.07	---
37.10	---	1.45 ± 0.01
38.40	11.1 ± 0.06	---
44.45	---	1.72 ± 0.05
45.60	13.1 ± 0.11	---

Table 7.   Extinction coefficients and activation parameters for the dimerization
of **1, 9,** and **11**

o-QDM	Extinction coefficient	k_2,[e] $M^{-1}s^{-1}(x10^{-3})$	$\Delta H^{\neq}$, kcal mol^{-1}	$\Delta S^{\neq}$, eu
1[a]	3015[b]	9.94 ± 0.32	3.5 ± 0.1	-29.0 ± 1.1
9	3320[c]	8.69 ± 0.30	3.3 ± 0.1[f]	-29.6 ± 0.2[f]
11	4234[d]	1.05 ± 0.04	4.2 ± 0.1	-30.5 ± 0.4

[a]   see ref. 15
[b]   The ε_{max} was measured at 367nm.
[c]   The ε_{max} was measured at 377nm.
[d]   The ε_{max} was measured at 378nm.
[e]   Dimerization rate constant at 25 °C.
[f]   Since we could not resolve the rate constants for the head-to-head and
head-to-tail dimerization processes, the activation parameter reported here was
determined from the total k_2.

Competition experiments[25] can be used to evaluate the rate constants for the

Diels-Alder reactions of o-QDM's with dienophiles. For the two competitive reactions

shown in equations (1) and (2), with the assumptions that the stoichiometric

relationship $2[M_2]_\infty + [MD]_\infty = [M]_0$ holds and $[D]$ ($>>$ $[M]_0$) is a constant during the

reaction, the product ratio is given by equation (3) where $A=2k_2 / (k_{DA} \cdot [D])$.

$$M \ + \ M \ \xrightarrow{\ k_2\ } \ M_2 \tag{1}$$

$$M \ + \ D \ \xrightarrow{\ k_{DA}\ } \ MD \tag{2}$$
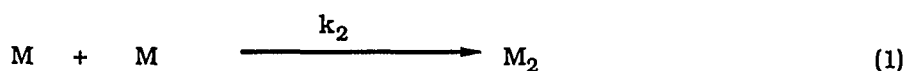
$$R_\infty = \frac{[M_2]_\infty}{[MD]_\infty} = \frac{[M]_0 - A^{-1} \ln([M]_0 A + 1)}{2A^{-1} \ln([M]_0 A + 1)} \tag{3}$$

In our experiments, several runs were carried out in which the initial concentration of o-QDM, $[M_0]$, was kept constant but the concentration of the dienophile $[D]$ was varied. In each run with different $[D]$, a final product ratio $R_\infty=[M_2]_\infty/[MD]_\infty$ was obtained. On the basis of the $[M]_0$, $[D]$ and R_∞, the rate constant ratio k_2/k_{DA} was estimated by means of a non-linear curve fitting technique.[25b] Relative rate constants k_2/k_{DA} of 9 and 11 from 0-40 ^oC were measured and these are reported in Table 8. The activation parameters evaluated from the rate constants are summarized in Table 9.

Table 8. Relative rate constants k_2 / k_{DA} for competition experiments of dimerization and Diels Alder reaction of o-QDM 9 and 11

Temperature, ^oC	k_2 /k_{DA} ($\times 10^{-2}$) of 9, M^{-1}	k_2/k_{DA} ($\times 10^{-3}$) of 11, M^{-1}
0.20	4.72 ± 0.16	---
2.90	---	2.69 ± 0.06
3.40	---	2.62 ± 0.08
8.40	4.40 ± 0.18	---
10.10	---	2.13 ± 0.03
15.80	---	2.03 ± 0.02
17.70	3.85 ± 0.13	---
21.30	3.67 ± 0.11	---
23.10	---	1.70 ± 0.02
29.00	3.32 ± 0.23	---
32.50	3.15 ± 0.11	---
32.90	---	1.37 ± 0.02
33.55	---	1.33 ± 0.03

Table 9. The rate constant ratio and activation parameters of o-QDM's **9** and **11** for competition between the dimerizations and Diels-Alder reactions

o-QDM	k_2/k_{DA}, M^{-1} [a]	$\Delta\Delta H^{\neq}$, kcal^{-1}mol^{-1} [b,c]	$\Delta\Delta S^{\neq}$, eu [b,c]
9	349 ± 8	-2.1 ± 0.1	4.5 ± 0.4
11	1607 ± 65	-3.7 ± 0.1	2.2 ± 0.5

[a] The rate constant ratio at 25 °C.

[b] The activation parameter at 25 °C.

[c] Since we could not resolve the rate constants for each regio- and stereo-isomeric pathway, in the Diels-Alder reaction, the activation parameter reported here was determined from the total k_2/k_{DA}.

DISCUSSION

It is well known that benzene-based o-QDM's are important intermediates in many kinds of reactions including ones used in natural product syntheses.[1] In general, o-QDM's can be prepared from the electrocyclic ring opening of benzocyclobutene derivatives photochemically or thermally or from 1,4-conjugative elimination of α,α'-substituted o-xylene derivatives.[1] Ito and Saegusa first reported the fluoride induced 1,4-conjugative elimination from trimethylsilyl quaternary ammonium salt precursors to generate o-QDM's[14] and applied it to natural product syntheses.[1f] However, some of the quaternary ammonium salt presursors, especially sterically congested ones, are difficult to prepare and thus application of this method is limited. In this investigation, we have found that trichloroacetate can be employed as an effective leaving group in fluoride induced 1,4-conjugative elimination. This discovery leads to a new and convenient method for preparing α-substituted o-QDM's from the corresponding secondary alcohols. In addition, the successful generation of o-QDM **12** demonstrates that this method can be applied to sterically hindered alcohols.

o-QDM's are reactive enough to be trapped by a variety of dienophiles at room temperature to form Diels-Alder adducts. In this study, we have found that although the cycloaddition of α-substituted o-QDM's with dienophiles shows a strong preference for the formation of the "ortho" regioisomers, the ratios between the "ortho" and "meta" isomers are dependent on the size of the substituents. In principle, the regioselectivity of the Diels-Alder reaction is controlled by a combination of electronic and steric factors, but electronic factors usually predominate.[26] Recently, it has been reported [27] that both **46** and **47** undergo a Diels-Alder reaction more rapidly than the unsubstituted compound which indicates that rate-accelerating electronic effects of
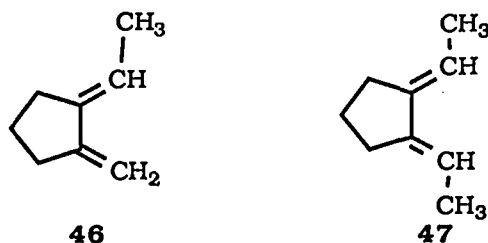
the methyl groups are more important than rate-retarding steric effects. However, since the electronic donating ability of the methyl, cyclopropyl, *tert*-butyl, and mesityl substituents of α-substituted *o*-QDM's **9, 10, 11,** and **12** should be similar, we attribute the regioselectivity differences in these cases to steric factors. In the following discussion, the mechanistic implications of the regioselectivity differences are presented.

For all four of the α–substituted *o*-QDM's **9** to **12**, the Diels-Alder reaction with methyl methacrylate gives more of the "ortho" than the "meta" isomer. This is easily explained by the similar electron donating ability of each of the four substituents. However, the change from methyl **(9),** to cyclopropyl **(10),** to *tert*-butyl **(11)** *o*-QDM results in a decrease of this ratio from 8.8 to 4.3 to 2.2, respectively (see Table 5). This regioisomer ratio shift can be rationalized in terms of steric hindrance in the "ortho" and "meta" transition states **48** and **49.** Since the α–substituent of the *o*-QDM's and
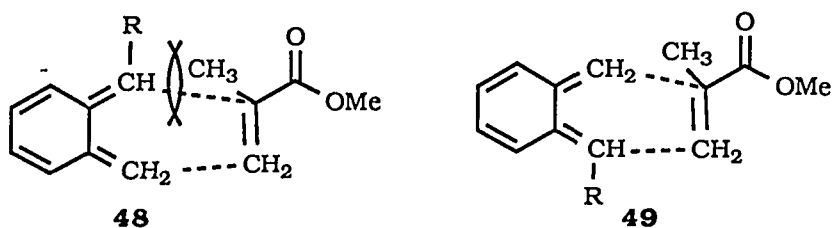
that of the olefins are adjacent to each other in the "ortho" transition state **(48),** this pathway should be more sensitive to the size of the substituent R at the α-position of

the o-QDM's. Thus increasing the size of the α-substituent will retard the "ortho" pathway more effectively than the "meta" pathway and hence reduce the "ortho" to "meta" regioisomer ratio.

The regioselectivity of **12** deviates from the trend of the other o-QDM's. Since the terminal methylene position of **12** is shielded by the o-methyl groups of the mesityl substituent, the concerted Diels-Alder reaction may be retarded completely and the reaction might become stepwise. In fact, the Diels-Alder trapping reaction of **12** is

12
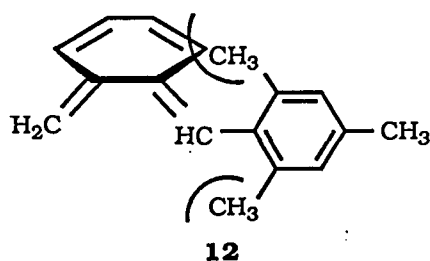
relatively slow. By using high dilution to retard the dimerization and by increasing the dienophile to monomer ratio to enhance the extent of the trapping reaction, we isolated the Diels-Alder adducts in reasonable yield. The reaction gives predominately one "ortho" adduct along with three other minor regioisomers.

The endo-exo selectivity of the "ortho" adducts is also sensitive to the size of the α-substituent. Increasing the size of the substituent from methyl to mesityl enhances the selectivity from a ratio of 1:1 to a ratio of 3:1.[28] However, the endo-exo selectivity of the meta adducts is insensitive to the size of the substituent, and does not show any preference at all in the Diels-Alder cycloaddition reactions.

In contrast to the Diels-Alder reaction, the regioselectivity of the o-QDM dimerizations cannot be explained by a concerted mechanism. In Scheme 3 the isomeric concerted transition states **50-53** are presented. Clearly, **50** is more

Scheme 3

50

54

59
Head-to-head

51

55

60
Head-to-tail

52

56

53

57

61
Tail-to-tail

58

59 or 61
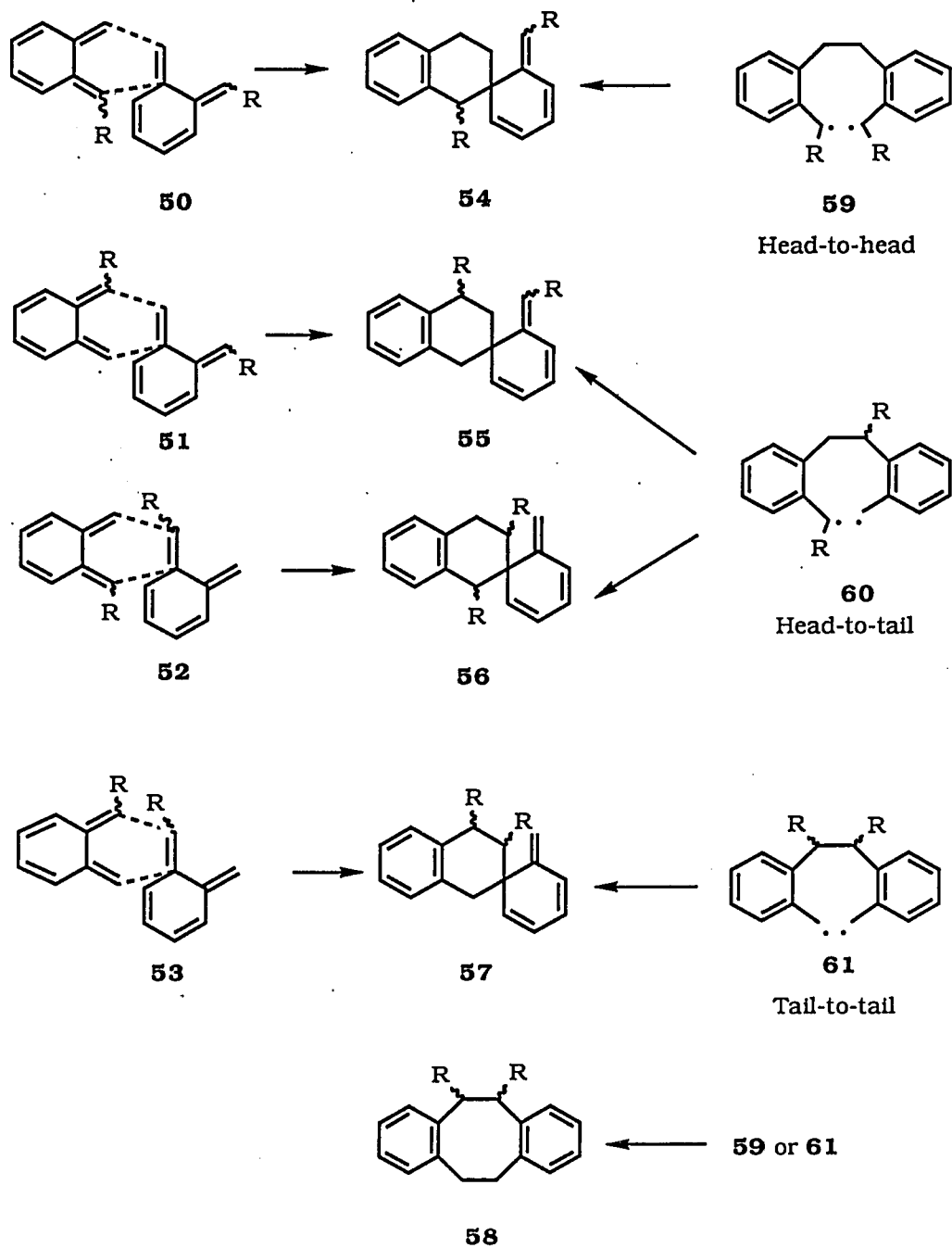
congested than **51**. If the o-QDM's dimerize through a concerted pathway, the product

ratio of **54:55** should be reduced by increasing the size of the α-substituent, but this is

opposite to that observed (see Table 10). In fact, when the substituent is the very large

tert-butyl or mesityl group, the only [4+2] dimer produced is the head-to-head dimer

54.

Table 10. Regioselectivity of the dimerization of α–substituted o-QDM's **9, 10, 11,** and **12** in dimerization reaction

	Yield of the dimerization product , %			
Dimer	o-QDM **9** -CH$_3$	o-QDM **10** -c-C$_3$H$_5$	o-QDM **11** -C(CH$_3$)$_3$	o-QDM **12** -Mesityl
54	67	66	80	53
55	9	11	---	---
56	19	7	---	---
57	---	---	---	---
Head-to-head [4+4] dimer **58**	---	16	20	47
Suspected dimer	5	---	---	---

Although the [4+2] dimerization results do not fit those predicted by the

concerted mechanism, the results are readily rationalized by a stepwise, diradical

mechanism. Of the three possible diradicals of the stepwise mechanism, **59, 60,** and

61, formation of the head-to-head diradical **59** should be favored because steric

repulsion arising from the α-substituent R should be minimal in the transition state

leading to diradical **59**. Thus, on the basis of the stepwise mechanism, dimer **54**

should be the major [4+2] dimer produced. In fact, head-to-head dimer **54** is predominant in the dimerization of all four o-QDM's. Moreover, since increasing the size of the α–substituent should not significantly affect formation of head-to-head diradical **59**, but should retard formation of head-to-tail diradical **60** and tail-to-tail diradical **61**, increasing the size of α–substituent should enhances the contribution of the head-to-head diradical pathway. In fact, when R is equal to the methyl or cyclopropyl group, small amounts of head-to-tail dimers **55** and **56** can still be identified from the dimerization products, but when R is as large as the tert-butyl or mesityl group, formation of diradicals **60** and **61** are inhibited and therefore only the [4+2] dimers **54** were isolated along with some head-to-head [4+4] dimers **58**.

The suggestion of diradical formation in o-QDM dimerization was also reported by Ito.[14] When he studied the dimerization of o-QDM **62**, a disproportio-nation product **63** was isolated as the major product. He proposed diradical intermediate **64** as the precursor of **63**.
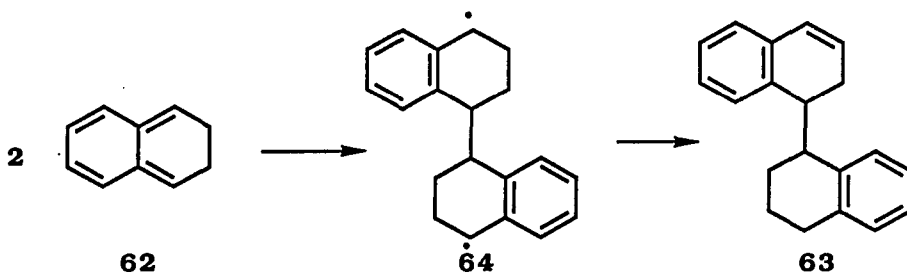
Comparsion of the rate of dimerization of o-xylylene (**1**) and o-QDM **8** reveals that the introduction of a methyl substituent at the α-position does not show any significant retardation of the dimerization reaction (see Table 7). This result is consistent with the observation that significant amounts of head-to-tail [4+2] dimers **28**, **29**, and **30** are formed. On the other hand, introduction of a tert-butyl substituent

(o-QDM **11**) retards the dimerization significantly. Since the *tert*-butyl substituent inhibits formation of the head-to-tail and tail-to-tail dimers **55-57**, the dimerization rate constant of o-QDM **11** should be reduced at least by a statistical factor of four. In fact, the dimerization rate constant of **11** is actually reduced by a factor of ten relative to that of the parent o-xylylene (**1**) and a factor of eight relative to that of o-QDM **9**. This extra retardation arises from a slight increase in the activation enthalpy (see Table 6). Because the activation parameters for o-xylylene (**1**) are very similar to those of **9** and **11**, we conclude that dimerization of the parent o-QDM, o-xylylene (**1**), also proceeds through a diradical mechanism.

The rate of the Diels-Alder reactions of **9** and **11** are relatively sensitive to the size of the α-substituent. The reaction rate constant of **11** is found to be 38 times slower than that of **9** (see Table 9). In addition, the steric repulsion increment from methyl to *t*-butyl group increases the reaction activation enthalpy by 2.5 kcal/mol in contrast to the small increment of 0.9 kcal/mol in the dimerization. These results further support the concertedness of the Diels-Alder reactions and implicate the stepwise process in the dimerization reactions.

Table 11. Activation parameters for the Diels-Alder reaction of **9** and **11**

o-QDM	k_{DA}, $M^{-1}S^{-1}$ [a]	$\Delta H^{\neq}$, kcal mol^{-1} [b]	$\Delta S^{\neq}$, eu
9	$(2.5 \pm 0.1) \times 10^{1}$	5.4 ± 0.2	-34.1 ± 0.6
11	$(6.5 \pm 0.4) \times 10^{-1}$	7.9 ± 0.2	-32.7 ± 0.9

[a] The calculated rate constant for the Diels-Alder reaction at 25 °C.
[b] The ratio of the regio-isomers is nearly independent of the temperature

It is well known that cyclization of diradicals is a fast process.[29] The lifetime of a triplet diradical is in the nanosecond range.[29a] Moreover, singlet diradicals are expected to cyclize even faster than triplet diradicals.[29b] One of the common methods to determine diradical cyclization rate constants is the internal clock technique. In our investigation, we employed the cyclopropyl benzyl radical ring opening reaction of **65** as an internal clock to monitor the cyclization rate constant of the intermediate.[30]

$$k=2.7 \times 10^5 \, s^{-1}$$

65 **66**
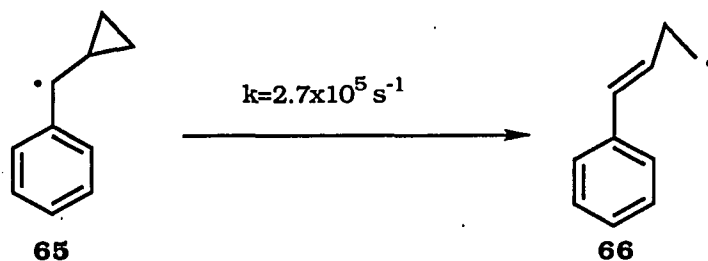
However, there is no evident for the existence of ring opening products in the dimerization of o-QDM **10**. Thermolysis of the [4+2] dimer **31** in 1,4-cyclohexadiene at 80 °C for 2 h only provides the rearrangement [4+4] dimers **36** and **37** (Scheme 4). No

Scheme 4

31

67

36 and 37
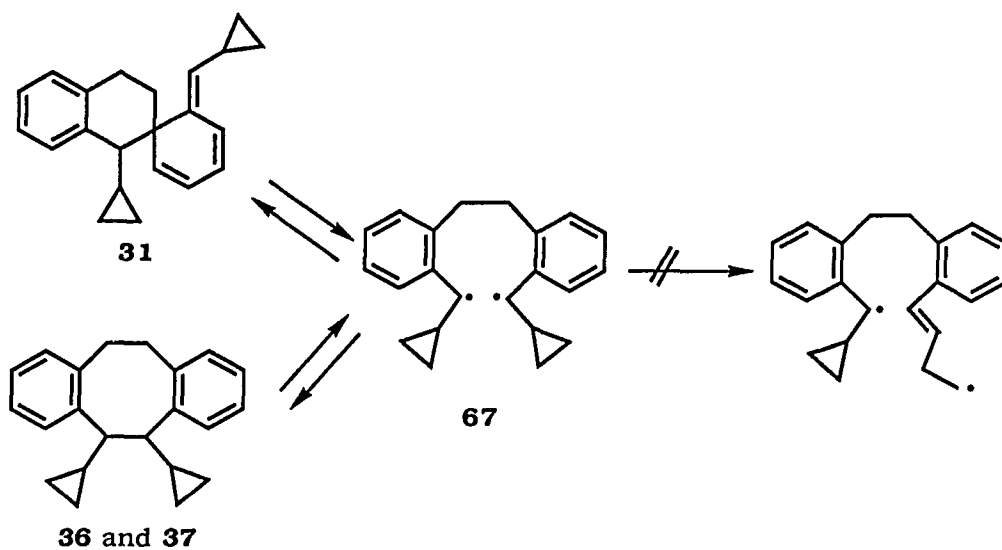
ring opening product was identified by GC/MS analysis. Since the rate constant for the cyclopropyl ring opening of **65** to **66** is measured as 2.7 x 10^5 s^{-1}, we believed that the diradical **67** cyclizes with a rate constant larger than 5 x 10^7 s^{-1}.[31]

The existence of diradical **68** is evidenced by the trapping experiment at 180 °C in thiophenol. When [4+2] dimer **43** was thermolysed in thiophenol at 180 °C, diradical **68** was trapped by hydrogen abstraction from thiophenol and provided the reduction product **45** nearly quantitatively. We attribute this observation to the

68
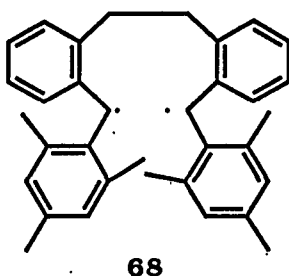
reversible formation of diradical **68** from **43** and **44**, following by trapping of the diradical by thiophenol. In contrast to the thermolysis at high temperature, thermolysis of [4+2] dimer **43** at 80 °C in thiophenol leads to [4+4] dimer **44** quantitatively. No trapping product is observed in the GC/MS analyses. We attribute this observation to the competition between the irreversible [4+4] cyclization and the hydrogen abstraction reaction (Scheme 5). Since the diradical cyclization is far faster than the hydrogen abstraction reaction, the intermediate collapses to the [4+4] product **44** before being trapped by thiophenol. The quenching rate constant for benzyl radical with thiophenol is 3.1x10^5 M^{-1}s^{-1} at 25 °C,[32] and therefore we estimated the cyclization rate constant for **68** to **44** to be larger than 9x10^8 s^{-1}.[33]

129

Scheme 5
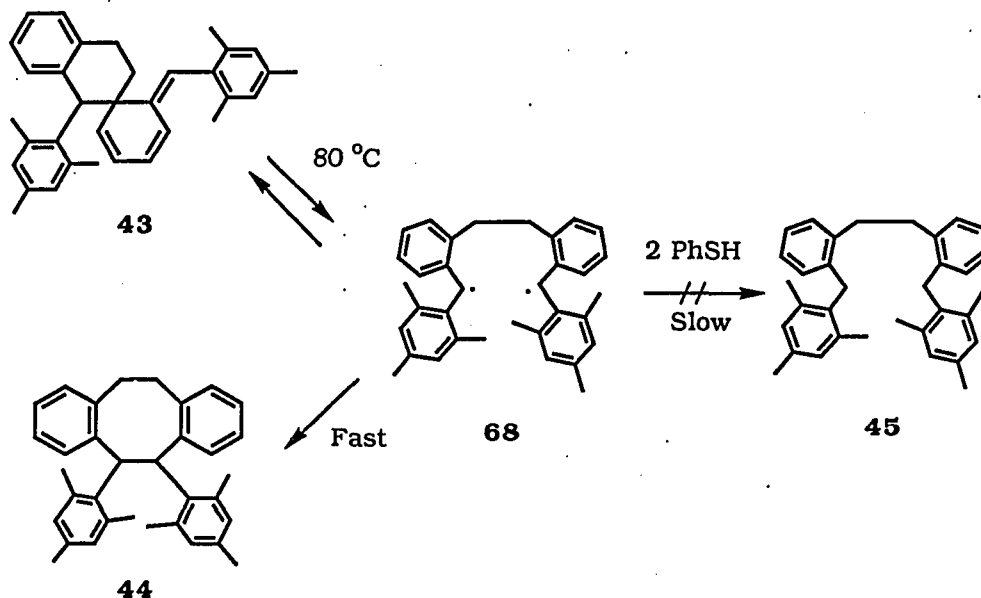
In summary, regioselectivity studies revealed that the Diels-Alder reaction mechanism is consistent with a concerted process while the dimerization mechanism of these o-QDM's is consistent with a stepwise mechanism. On the basis of the similarity of the activation parameters of the parent o-xylylene (1) and those of the α-substituted o-QDM's, we suggest that o-xylylene (1) also dimerizes through a stepwise mechanism. On the basis of a study of the dimer **43** in thiophenol, the cyclization rate constant for the diradical intermediate **68** is estimated to be larger than 9×10^8 s^{-1}.

EXPERIMENTAL SECTION

General experimental procedures were previously described in detail in Section 1. Capillary gas chromatographic analyses for the competitive kinetic experiments were performed using HP5890 Series II gas chromatograph equipped with a 30m DB-1 capillary column (J & W Scientific) using nitrogen as a carrier gas and a flame ionization detector, and HP3396A integrator. The MM-X calculations were performed on a Macintosh II CX computer with PC Model program supplied by Serena Software. Elemental analyses were performed by Spang Microanalytical Laboratory, Eagle Harbour, MI. Acetonitrile and methyl methacrylate for kinetic experiments, and chlorotrimethylsilane for synthesis were distilled before use. Unless otherwise noted the chemicals used in our experiments are commercial available.

Methyl 2-[(trimethylsilyl)methyl]benzoate (17). To a solution of diiso-propylamine (13.2 g, 130 mmol) in THF (100 mL) at -78 °C was slowly added n-butyl-lithium in hexanes (52 mL, 2.5 M, 130 mmol). The mixture was stirred at low temperature for 1 h and a solution of 10.0 g (66.7 mmol) of methyl 2-methylbenzoate (16) and 7.5 g (69 mmol) of chlorotrimethylsilane in THF (50 mL) was then added dropwise. After being stirred for half an hour, the reaction mixture was worked up by addition of water at low temperature. The quenched reaction mixture was warmed to room temperature and extracted with hexanes. The combined extracts was dried over anhydrous Na_2SO_4 and concentrated under reduced pressure to give a crude viscous oil. Vacuum distillation of the crude oil provided essentially pure α–silylated ester 17 (10.5 g, 71 %): bp 131-133 (20 mmHg); IR (neat) 3061, 3204, 2953 (s, C-H), 1722 (s, C=O), 1259 (s, Si-CH3) cm^{-1}; [lit.[34]: IR (neat) 1726 cm^{-1}]; ^{1}H NMR (CDCl3) δ -0.05 (s, 9H), 2.66 (s, 2H), 3.85 (s, 3H), 7.05 (d, J=7.8 Hz, 1H), 7.10 (t, J=7.6 Hz, 1H), 7.33 (dt, J1=1.4 Hz, J2=7.5 Hz, 1H) 7.85 (dd, J1=1.4 Hz, J2= 7.9 Hz, 1H) [lit.[34]: ^{1}H NMR (CDCl3) δ

0.05 (s, 9H), 2.18 (s, 2H) (apparently a typographical error), 3.82 (s, 3H), 6.80-7.75, 7.68-7.88 (m, 4H)]; MS, m/e (relative intensity) 222 (M^+, 25), 221 (30), 207 (100), 118 (95), 90 (20), 89 (20), 73 (70); exact mass m/e 221.10017, calcd for $C_{12}H_{17}OSi$ (M-H) 221.09978.

[2-(Trimethylsilyl)methyl]benzyl alcohol (18). To a suspension of $LiAlH_4$ (1.8g, 47 mmol) in diethyl ether (150 mL) at 0 °C was added dropwise a solution of ester **17** (9.3g, 42 mmol) in diethyl ether (20 mL). After addition, the mixture was stirred for 8 h at ambient temperature. The mixture was then worked up as usual [17] to provide crude alcohol **18**. Distillation of the crude product under reduced pressure gave pure **18** (5.2 g, 64 %): bp 134-136 °C (14 mmHg); IR (neat) 3335 (broad s, OH), 2955 (s, C-H), 1248(s, Si-CH₃) cm^{-1} [lit.[35]: 3320 (s, br), 2954 (s), 1249 (s) cm^{-1}]; ^1H NMR ($CDCl_3$) δ 0.00 (s, 9H), 2.19 (s, 2H), 4.63 (s, 2H), 7.00 (d, J=7.4 Hz, 1H), 7.09 (t, J=7.4 Hz, 1H), 7.17 (t, J=7.4 Hz, 1H), 7.32 (d, J=7 Hz, 1H) [lit.[35]: ^1H NMR δ 0.02 (s, 9H), 2.13 (s, 2H), 2.40 (br s, 1H), 4.45 (s, 2H), 6.77-7.37 (m, 4H)]; MS, m/e (relative intensity) 194 (M^+, 0.1), 105 (10), 104 (100), 91 (3), 75 (18), 73 (26); exact mass m/e 194.11277, calcd for $C_{11}H_{18}OSi$ 194.11269.

2-((Trimethylsilyl)methyl)benzaldehyde (19). To dichloromethane (P_2O_5 dried, 250mL), which was being stirred vigorously and cooled in an ice bath, was added 15.5 g (155 mmol) of CrO_3 and 24.4 g (309 mmol) of pyridine. The reaction is exothermic and the solution became deep red brown in color. After addition of the reagents, the solution was further stirred for 20 min and a solution of alcohol **18** (5.0 g, 26 mmol) in CH_2Cl_2 (20 mL) was added in one portion. After 15 min the solution was decanted and worked up as usual.[18] Chromatography of the crude product on silica gel with hexanes-ethyl acetate (12:1) as the eluent gave pure aldehyde **19** (4.4 g, 90 %): bp 73-75 °C (0.8 mmHg); IR (neat), 2955 (s, C-H), 2729 (w, O=C-H),

1697 (s, C=O) 1249 (s, Si-CH$_3$) cm^{-1} [lit.[35]: IR (neat) 2965 (m), 2730 (w), 1697 (s), 1250

(m) cm^{-1}]; ^{1}H NMR (CDCl$_3$) δ -0.03 (s, 9H), 2.68 (s, 2H), 7.07 (d, J=7.7 Hz, 1H), 7.23 (t,

J=7.5 Hz, 1H), 7.41 (t, J=7.5 Hz, 1H), 7.75 (d, J=7.7 Hz, 1H), 10.16 (s, 1H), [lit.[35]: ^{1}H

NMR δ -0.05 (s, 9H), 2.67 (s, 2H), 6.87-7.40 (m, 3H), 6.87-7.40 (m, 3H), 10.03 (s, 1H)];

MS, m/e (relative intensity) 192 (M$^+$, 40), 177 (60), 73 (100); exact mass m/e 192.09686,

calcd for C$_{11}$H$_{16}$OSi 192.09704.

N-(2-((Trimethylsilyl)methyl)benzylidene))methylamine (20). To a solution

of aldehyde **19** (4.3 g, 22.4 mmol) in benzene (4 mL) was added a solution of

methylamine in benzene (5M, 7 mL, 350 mmol). After being stirred for 10 to 15 min,

the solution became turbid. Azeotropic removal of water from the reaction mixture

completed the formation of **20**. The reaction mixture was then concentrated and

distilled under reduced pressure to give a diastereomeric mixture of **20** (4.3 g, 93 %);

bp 85-87 °C (1 mmHg); IR cm^{-1} (neat), 3068, 2953 (s, C-H), 1645 (C=NMe), 1248 (Si-

CH$_3$); ^{1}H NMR (CDCl$_3$) δ -0.03 (s, 9H), 2.37 (s, 2H), 3.507, 3.502 (2s, 3H), 6.98 (broad d,

J=7.7 Hz, 1H), 7.11 (broad t, J=7.5 Hz, 1H), 7.24 (broad t, J=7.5 Hz, 1H), 7.80 (broad d,

J=7.8 Hz, 1H), 8.493, 8.498 (2s, 1H); MS, m/e (relative intensity) 205 (M$^+$, 30), 204 (100),

190 (98), 132 (15), 73 (72); exact mass m/e 204.12138, 190.10563, calcd for C$_{12}$H$_{18}$NSi

(M-H) 204.12085, C$_{11}$H$_{16}$NSi (M-CH$_3$) 190.10521.

N-[α-[o-((Trimethylsilyl)methyl)phenyl)cyclopropylmethyl]methylamine

(21). Cyclopropyllithium was freshly prepared before use.[20] Amine **21** was prepared in

the following manner. To a solution of imine **20** (2.5g, 12 mmol) in ether (20 mL) at

-10 °C was added the freshly prepared ethereal cyclopropyllithium (20 mL, 24mmol)

under nitrogen. The reaction mixture was then further stirred for 1 h and quenched

with water. The crude **21** was first extracted into diethyl ether and then re-extracted

into acidic aqueous layer with 5 % HCl solution. Neutralization of the acidic extracts

with saturated NaOH solution, extraction of amine **21** from the aqueous layer with hexanes, evaporation of the solvent of the extracts and distillation of the crude product under vacuum gave colorless amine **21** (1.7g, 56 %): bp 120-123 °C (5 mmHg); IR (neat) 3336 (w, N-H), 3067, 2955 (s, C-H), 1248 (s, Si-CH$_3$) cm^{-1}; ^{1}H NMR (CDCl$_3$) δ 0.01 (s, 9H), 0.20 (m, 1H), 0.35 (m, 1H), 0.60 (m, 1H), 1.14 (m, 1H), 1.56 (m, 1H), 2.05-2.22 (ABq, J=14 Hz, 2H), 2.43 (s, 3H), 3.30 (d, J=7.6 Hz, 1H), 6.95 (m, 1H), 7.07(m, 2H), 7.40 (m, 1H); MS, m/e (relative intensity) 247 (M$^+$, 3) 232 (11), 216 (33), 206 (26), 190 (11), 188 (9), 143 (14), 142 (15), 84 (12), 73 (100), 59 (9); exact mass m/e 247.17509, calcd for C$_{15}$H$_{25}$SiN 247.17563.

N-[α–[o–((Trimethylsilyl)methyl)phenyl]neopentyl]methylamine (22). To a solution of imine **20** (4.2 g, 20.5 mmol) in diethyl ether (40 mL) was added 15.2 mL (1.6 M) of t-butyllithium in hexanes at -78 °C. After being stirred for half an hour, the reaction mixture was quenched by addition of water and worked up, in the same manner as described in the preparation of amine **21**, to provide pure amine **22** (4.6 g, 85 %): bp 108-109 °C (2.6 mmHg); IR (neat) 3064, 2952 (s, C-H), 2790 (m, NC-H), 1479 (m), 1247 (s, Si-CH$_3$) cm^{-1}; ^{1}H NMR (CDCl$_3$) δ 0.04 (s, 9H), 0.91 (s, 9H), 2.05 (d, J=14.5 Hz, 1H), 2.21 (s, 3H), 2.40 (d, J=14.5 Hz, 1H), 3.66 (broad s, 1H), 6.99 (m, 1H), 7.05 (m, 2H), 7.32 (m, 1H). The NH signal was not observed in the spectrum. However, a broad peak at 1.46 ppm which may due to the hydrogen bonded H$_2$O with NH groups was observed; MS, m/e 262 (M-H, 0.4) 248 (7), 207 (20), 206 (100), 190 (18), 73 (39); exact mass m/e 262.19852, 248.18345, calcd. for C$_{16}$H$_{28}$NSi (M-H) 262.19914, C$_{15}$H$_{26}$NSi, (M-CH$_3$) 248.18349.

[α-[o-((Trimethylsilyl)methyl)phenyl)cyclopropylmethyl]dimethylamine (23). To a solution of **21** (1.4 g, 5.7 mmol) in CH$_3$CN (30mL) containing 2.4 mL (28 mmol) quantity of aqueous formaldehyde (37%), was added NaBH$_3$CN (0.58 g, 9.1

mmol). After being stirred for 15 min, glacial acetic acid was added to keep the solution neutral. The mixture was then further stirred for 2 h with the pH value kept around seven and then the solvent was evaporated under reduced pressure. The concentrate was quenched by 2N KOH and worked up in a usual manner[21] to give crude amine **21**. Vacuum distillation of the crude amine gave colorless liquid **21** (1.01 g, 68 %): bp 122-124 °C (5 mmHg); IR (neat) 3072, 2953 (s, C-H), 2818, 2773 (m, NMe_2), 1248 (s, Si-CH_3) cm^{-1}; ^1H NMR ($CDCl_3$) δ -0.06 (m, 1H), 0.00 (s, 9H), 0.29 (m, 1H), 0.36 (m, 1H), 0.74 (m, 1H), 1.22 (m, 1H), 2.31 (s, 6H), 2.11, 2.33 (ABq, J=14 Hz, 2H), 2.81 (d, J=9 Hz, 1H), 6.97 (d, J=7.3 Hz, 1H), 7.06 (m, 2H), 7.40 (d, J=7.1 Hz, 1H); MS, m/e (relative intensity) 262 (M$^+$, 10), 246 (4), 220 (24), 216 (18), 188 (5), 143 (10), 142 (11), 129 (6), 98 (13), 73 (100); exact mass m/e 261.19103, calcd. for $C_{16}H_{27}NSi$ (M-H) 261.19128.

N-[α-[o-((Trimethylsilyl)methyl)phenyl]neopentyl]dimethylamine (24).

Amine **24** was prepared, in the same manner as described in the preparation of **23**, from a solution of amine **22** (4.5 g, 17.1 mmol) in CH_3CN (30 mL) containing 7.0 mL (82 mmol) of aqueous formaldehyde (37 %), and $NaBH_3CN$ (1.74 g, 27.7 mmol) to give essentially pure **20** as a colorless liquid. (4.15 g, 88%) : bp 108-109 °C (1.3 mmHg); IR (neat), 3064, 2954 (s, C-H), 2819, 2775 (m, NMe_2), 1250 (s, Si-CH_3) cm^{-1}; ^1H NMR ($CDCl_3$) δ 0.06 (s, 9H), 1.01 (s, 9H), 2.21 (s, 2H), 2.27 (s, 6H), 3.55 (s, 1H), 7.05 (m, 3H), 7.39 (d, J=6.8 Hz, 1H); MS, m/e (relative intensity) 276 (M-H, 0.1), 262 (6), 221 (20), 220 (100), 73 (28); exact mass m/e 276.21418, 262.19938, calcd for $C_{17}H_{30}NSi$ (M-H) 276.21475, $C_{16}H_{28}NSi$ (M-CH_3) 262.19910.

[α-[o-((trimethylsilyl)methyl)phenyl]cyclopropylmethyl]trimethylammonium iodide (14). To a solution of tertiary amine **23** (0.99 g, 3.8mmol) in acetonitrile (15 mL) was added methyl iodide (3.2 g, 23 mmol). The mixture was stirred at room temperature for 24 h in the dark condition and some white precipiate formed. The

completeness of the reaction was confirmed by TLC analysis and the solution was filtered inside the fume-hood. Concentrating the filtrate under reduced pressure gave a batch of yellowish solid. The yellowish solid was then re-dissolved in anhydrous acetone and anything insoluble in the solution was filtered. Hexanes was then added to the filtrate and the crude quaternary ammonium salt **14** precipiated. Recrystallization of the crude solid in a mixture of acetone and hexanes gave essentially crystalline product **14** (1.1 g, 72 %): mp 147-152 °C (decomposed); IR, (mineral oil), 2961 (s, C-H), 1489 (s), 1248 (s, Si-CH$_3$) cm^{-1}; ^{1}H NMR (CD$_3$CN) δ 0.02 (s, 9H), 0.09 (m, 1H), 0.62 (m, 1H), 1.04 (m, 1H), 1.07 (m, 1H), 1.76 (m, 1H), 2.19, 2.45 (ABq, J=14.3 Hz, 2H), 3.07 (s, 9H), 4.26 (d, J=10.3 Hz, 1H), 7.21 (m, 2H), 7.33 (t, J=7.5 Hz, 1H), 7.59 (d, J=8.1 Hz, 1H); MS, FAB m/e (relative intensity) 679 (2 cation + I$^-$, 2), 276 (cation, 33), 217 (100), 73 (64). Anal. calcd for C$_{17}$H$_{30}$NSiI: C, 50.61; H, 7.50; N, 3.47. Found: C, 50.39; H, 7.20; N, 3.64.

[α-[o-((Trimethylsilyl)methyl)phenyl]neopentyl]trimethylammonium

iodide (15). Ammonium salt was prepared from a solution of tertiary amine **24** (4.1g, 14.8mmol) in acetonitrile (40 mL) and methyl iodide (12.6 g, 88.7 mmol), in the same manner as described in the preparation of **14**, to provide pure crystalline product **15** (3.85 g, 62%): mp 141-143 °C (decomposed); IR (mineral oil), 2959 (s, C-H), 1481 (s), 1249 (s, Si-CH$_3$) cm^{-1}; ^{1}H NMR (CD$_3$CN) δ 0.11(s, 9H), 1.23 (s, 9H), 2.27, 2.43 (ABq, J=15.1Hz, 2H), 3.15 (s, 9H), 4.86 (s, 1H), 7.20 (m, 1H), 7.31 (m, 2H), 7.59 (d, J=7.9 Hz, 1H); MS, FAB m/e (relative intensity) 711 (2 Cation + I$^-$, 0.2), 292 (cation, 5), 233 (20), 159 (30), 73 (100). Anal. calcd for C$_{18}$H$_{34}$NSiI: C, 51.54; H, 8.17; N, 3.34. Found : C, 51.56; H, 8.33; N, 3.31.

α-[o-((Trimethylsilyl)methyl)phenyl]mesitylmethanol (26). Mesityl magnesium bromide was freshly prepared by Smith procedure[37] before use. The

prepared Grignard reagent (20 mL in THF, 10 mmol) was then transferred to a solution of aldehyde **19** (1 g, 5.2 mmol) in THF (10 mL) slowly under nitrogen. After addition of the reagent, the mixture was kept under reflux for half an hour and then cooled in an ice bath. Water was added dropwise to quench any excess Grignard reagent. The product was extracted hexanes-ethyl acetate. The combined extracts was dried over anhydrous Na_2SO_4 and concentrated under reduced pressure. Purification of the crude product by silica gel liquid chromatography with hexanes-ethyl acetate (8:1) as the eluent provided 1.26 g (78 %) of **21**; IR (neat) 3545 (s, OH), 2953 (s, C-H), 1248 (s, Si-CH3) cm^{-1}; ^{1}H NMR (CDCl3) δ -0.004 (s, 9H), 1.84 (d, J=5 Hz, 1H), 2.12 (d, J=16 Hz, 1H), 2.22 (s, 6H), 2.26 (d, J=16 Hz, 1H), 2.27 (s, 3H), 6.22 (d, J=5 Hz, 1H), 6.84 (s, 2H), 7.00 (m, 2H) 7.13 (m, 1H), 7.18(d, J=1.8Hz, 1H); MS, m/e (relative intensity) 311 (M$^+$-1, 0.3), 297 (20), 207 (100), 192 (25), 91 (10), 75 (20), 73 (43); exact mass m/e 311.18320, 297.16763, calcd. for $C_{20}H_{27}OSi$ (M-H) 311.18312, $C_{19}H_{25}OSi$ (M-CH3) 297.16747.

[α-[o-((Trimethylsilyl)methyl)phenyl]mesitylmethyl] trichloroacetate (25).
To a solution of alcohol **26** (0.65 g, 2.1 mmol) in benzene (5 mL) containing pyridine (1 g, 13 mmol) at 0 °C was added a solution of trichloroacetyl chloride (1.14 g, 6.3 mmol) in CH_2Cl_2 (10 mL). The mixture was stirred for half an hour and worked up by addition of water. The organic layer was extracted with hexanes, washed with dilute HCl solution and brine, dried over anhydrous Na_2SO_4 and concentrated under reduced pressure to give product **25** quantitatively: IR (neat) 2956 (s, C-H), 1757 (s, C=O), 1248 (s, Si-CH3) cm^{-1}; ^{1}H NMR (CDCl3) δ 0.045 (s, 9H), 2.13 (s, 2H), 2.29 (s, 3H), 2.33 (s, 6H), 6.89 (s, 2H), 7.02 (m, 1H), 7.08 (m, 2H), 7.22 (m, 1H), 7.37 (s, 1H); MS, m/e (relative intensity) 456 (M$^+$, 2), 295 (6), 207 (100), 192 (12), 73 (27); exact mass m/e 456.08475, calcd for $C_{22}H_{27}O_2Cl_3Si$ 456.08495.

Diels-Alder reactions of α-methyl-*o*-xylylene (9) with methyl methacrylate. To a solution of methyl methacylate (53 mg, 0.53 mmol) in acetonitrile (1mL) containing 53 mg (0.16 mmol) of tetrabutylammonium fluoride (TBAF) was added dropwise a solution of quaternary ammonium salt precursor **13** (20 mg, 0.053 mmol) in acetonitrile (2 mL). After addition of the TBAF solution, the mixture was further stirred for 15 min and quenched by addition of water. The products were extracted with hexanes and analysed by GC-MS. Finally, the extract was concentrated and subjected to a silica gel liquid chromatography with hexanes as the eluent and four Diels-Alder adducts were isolated from the dimer mixture: GC analysis condition, column DB1, temperature program, 80 °C, 5 min, 5°C/min (rate), 200 °C, 30 min. Component I ("meta" isomer): GC retention time (relative intensity) 21.6 min (4.6 %); MS, m/e (relative intensity) 218 (M^+, 29), 186 (4), 159 (22), 158 (60), 143 (100), 129 (10), 128 (16), 117 (9). Component II ("ortho" isomer): GC retention time (relative intensity) 22.3 min (34.3 %); MS, m/e 218 (M^+, 34), 186 (6), 159 (37), 158 (100), 143 (54), 129 (14), 128 (17), 118 (40), 117 (35). Component III ("ortho" isomer): GC retention time (relative intensity) 22.5 min (38.8 %) MS, m/e (relative intensity) 218 (M^+, 43), 186 (11), 159 (35), 158 (100), 143 (55), 129 (14), 128 (17), 118 (61), 117 (49). Component IV ("meta" isomer): GC retention time (relative intensity) 22.6 min (3.7 %); MS, m/e (relative intensity) 218 (M^+, 42), 159 (41), 158 (87), 143 (100), 129 (11), 128 (22), 118 (8), 117 (27). ^{1}H NMR analyses of the Diels-Alder adducts: The structural assignment of the components are based on the results of the spin-spin decoupling experiment results of the adduct mixture. The quartet at 3.35 ppm coupled to the major doublet at 1.17 ppm and the quartet at 2.95 ppm coupled to another major doublet at 1.10 ppm suggest that the major two components indeed possess the "ortho" structures which have an benzylic proton only coupled to a methyl substituent. On the basis of this observation,

we assign component II and III as the "ortho" adducts and component I and IV as the "meta" adducts.

Diels-Alder reactions of α–cyclopropyl-*o*-xylylene (10) with methyl methacrylate. The Diels-Alder adducts of **10** was prepared from a solution of methyl methacrylate (107 mg, 1.24 mmol) in acetonitrile (2 mL) containing a 117 mg (0.4 mmol) quantity of TBAF and a solution of quaternary ammonium salt presursor **14** (50 mg, 0.12 mmol) in acetonitrile (4 mL) in the same manner as described previously. The products were by GC-MS and separated through a silica gel liquid chromatography with hexanes as the eluent. A mixture of the major two Diels-Alder regio-isomers were isolated from the minor isomers and identified as the "ortho" adducts by ^{1}H NMR spectroscopy: GC analysis condition, column DB 1, temperature program 120 °C, 5 min, 5 °C/min (rate), 200 °C, 20 min. Component I ("meta" isomer): GC retention time (relative intensity) 14.14 (6.2 %); MS, m/e (relative intensity), 244 (M$^+$, 1), 216 (4), 185 (27), 184 (33), 169 (27), 158 (12), 157 (100), 156 (24), 155 (12), 143 (35), 142 (16), 141 (23), 129 (19), 128 (39), 115 (16), 91 (8). Compoment II ("ortho" isomer): GC retention time (relative intensity) 14.59 min (26.3 %); MS, m/e (relative intensity) 244 (M$^+$, 11), 229 (10), 216 (3), 186 (12), 185 (73), 184 (52), 169 (18), 158 (6), 157 (353), 156 (21), 155 (14), 144 (41), 143 (79), 142 (22), 141 (27), 130 (12), 129 (100), 128 (61), 127 (16), 117 (12), 116 (32), 115 (37), 19 (16). Component III ("ortho" isomer): GC retention time (relative intensity) 14.76 min (25.0 %); MS, m/e (relative intensity) 244 (M$^+$,11), 229 (8), 216 (3), 186 (6), 185 (39), 184 (44), 169 (11), 158(2), 157 (15), 156 (8), 155 (11), 144 (43), 143 (100), 142 (17), 141 (21), 130 (11), 129 (86), 128 (50), 127 (16), 117 (8), 116 (20), 115 (28), 101 (16), 91 (11). Component IV ("meta" iosomer): GC retention time (relative intensity); 15.03 min (5.7 %); MS, m/e (relative intensity) 244 (M$^+$, 11), 186 (7), 185 (43), 184 (20), 169 (25), 158 (4), 157 (32), 156 (14), 155 (13), 144

(19), 143 (100), 142 (20), 141 (25), 130 (9), 129 (30), 128 (41), 127 (10), 115 (21), 91 (10).

^{1}H NMR analyses of the Diels-Alder adducts: The structural assignments of the components are based on the spin-spin decoupled spectrum for a mixture of the major two isomers. The doublet at 2.49 ppm and at 2.17 ppm coupled to the multiplets of the cyclopropyl ring protons at 0.8 ppm comfirm the "ortho" structure for these two major regio-isomers.

Diels-Alder reactions of α-*tert*-butyl-*o*-xylylene (11) with methyl methacrylate. The Diels-Alder adducts of **11** was prepared from a solution of methyl methacrylate (470 mg, 5.5 mmol) in acetonitrile (10 ml) containing 470 mg (1.5 mmol) of TBAF and a solution of quaternary ammonium salt precursor **15** (200 mg, 0.48 mmol) in acetonitrile (10 ml) in the same manner as described previously. The products were analysed by GC-MS and subjected to a silica gel liquid chromatography with hexanes-benzene (4:1) as the eluent and all four regio-isomers were separated and identified by ^{1}H NMR spectroscopy respectively: GC analysis conditions, column DB1, temperature program 120 °C, 5 min, 10°C/min (rate), 200 °C, 20 min. Component I ("meta" isomer): GC retention time (relative intensity) 13.07 min (4.3 %); MS, m/e (relative intensity) 260 (M$^+$, 2), 204 (9), 203 (23), 144 (27), 143 (100), 129 (15), 128 (20), 115 (7), 57 (21). Since the compound was mixed with 20 % of other isomers and could not be isolated in pure form, exact mass experiment has not been performed.; ^{1}H NMR (CDCl$_3$) δ 0.88 (s, 9H), 1.33 (s, 3H), 2.44-2.57(m, 3H), 2.87-2.93 (m, 2H), 3.29 (s, 3H), 6.96-7.35 (m, 4H). Component II ("ortho" isomer): GC retention time (relative intensity) 13.82 min (13.2 %); MS, m/e (relative intensity) 260 (M$^+$, 1), 245 (0.7), 204 (23), 172 (7), 144 (50), 143 (100), 129 (25), 128 (23), 115 (10), 57 (56), 41 (24); exact mass m/e 260.17785, calcd for C$_{17}$H$_{24}$O$_2$ 260.17763; ^{1}H NMR (CDCl$_3$) δ 1.01 (s, 9H), 1.44 (s, 3H), 1.92-2.08 (m, 1H), 2.34-2.44 (m, 1H), 2.84-2.99 (m, 2H), 3.01 (d, J=1.9 Hz, 1H), 3.28

(s, 3H), 6.95-7.10 (m, 4H). The characteristic spin-spin coupling among four protons having chemical shifts at 1.97-2.08, 2.34-2.44, 2.84-2.99 ppm and a single proton having a doublet with a small coupling constant (long range coupling) at 3.01 ppm match the "ortho" structural assignment for this component. Component III ("meta" isomer) GC retention time (relative intensity) 14.20 min (4.2 %); MS, m/e (relative intensity) 260 (M^+, 0.1), 245 (0.2), 204 (23), 172 (9), 144 (59), 143 (100), 129 (23), 128 (23), 115 (8), 57 (36), 41 (17); exact mass m/e 260.17800, calcd for $C_{17}H_{24}O_2$ 260.17763; ^1H NMR ($CDCl_3$) δ 0.85 (s, 3H), 0.90 (s, 9H), 1.94 (ddd, J_1=2.8 Hz, J_2=9.6 Hz, J_3=14.2 Hz, 1H), 2.06 (dd, J_1=7.1 Hz, J_2=14.8 Hz, 1H), 2.57 (dd, J_1=2.8 Hz, J_2=14.8 Hz, 1H), 2.76 (dd, J_1=7.3 Hz, J_2=9.5 Hz, 1H), 3.01 (d, J=14.7 Hz, 1H), 3.75 (s, 3H), 7.03-8.20 (m, 4H). The characteristic AB pattern appearing at 2.57 and 3.01 ppm, and the spin-spin coupling among three protons at 1.94, 2.06, 2.76 ppm suggest the "meta" structure for this component. Component IV ("ortho" isomer): GC retention time (relative intensity) 14.38 min (6.2 %); MS, m/e (relative intensity) 245 (M^+-15, 1), 204 (27), 172 (150), 145 (22), 144 (100), 143 (68), 129 (36), 128 (23), 115 (9), 57 (42), 41 (25); exact mass m/e 245.15458, calcd for $C_{16}H_{21}O_2$ (M-CH_3) 245.15415; ^1H NMR ($CDCl_3$) δ 0.84 (s, 9H), 0.94 (s, 3H), 1.91 (m, 1H), 2.43 (m, 1H), 2.81 (dd, J_1=18.5 Hz, J_2=9.2 Hz, 1H), 2.93 (d, J=1.9 Hz, 1H), 3.00 (dd, J_1=10.8 Hz, J_2= 19.4 Hz, 1H), 3.71 (s, 3H), 7.02-7.15 (m, 4H). The ^1H NMR spectrum with four coupled multiplets at 1.91, 2.43, 2.81, 3.00 ppm and one doublet with a small coupling constant at 2.93 ppm are consistent with the "ortho" structural assignment.

Diels-Alder reactions of α–mesityl-_o_-xylylene (12) with methyl methacrylate. To a solution of methyl methacrylate (5 g, 50 mmol) in acetonitrile (60 mL) containing TBAF (90 mg, 0.29 mmol) was added dropwise a mixture of trichloroacetate **25** (45 mg, 0.1 mmol) and methyl methacrylate (5 g, 50 mmol) in acetonitrile (50 mL).

After addition, the solution was further stirred for 15 min and quenched by addition of water. The products were extracted with hexanes and analysed by GC-MS. Finallly, the solvent was removed under reduced pressure and subjected to a silica gel liquid chromatography with hexenes-benzene (4:1) as the eluent. The Diels-Alder adducts were separated and identified respectively: GC analysis conditions, column DB1, temperature program 120 °C, 5 min, 10 °C/min (rate), 220 °C, 20 min. Component I ("meta" isomer): GC retention time (relative intensity) 22.21 min (4.4 %); MS, m/e (relative intensity) 332 (M^+, 40), 262 (77), 247 (100), 220 (17), 143 (14), 133 (14), 128 (14); ^{1}H NMR (CDCl$_3$) δ 1.35 (s, 3H), 1.70 (s, 3H), 1.79 (dd, J_1=12.6 Hz, J_2=13.2 Hz, 1H), 2.25 (s, 3H), 2.39 (m, 1H), 2.41 (s, 3H), 2.73 (d, J=16.3 Hz, 1H), 3.37 (dd, J_1=2.7 Hz, J_2=16.3 Hz, 1H), 3.64 (s, 3H), 4.63 (dd, J_1=6.2 Hz, J_2=12.5 Hz, 1H), 6.7-7.1 (m, 6H). The typical AB quartet at 2.73 and 3.37 ppm supports the "meta" structural assignment. Component II ("ortho" isomer): GC retention time (relative intensity) 22.4 min (10.7 %); MS, m/e (relative intensity) 332 (M^+, 18), 262 (49), 248 (32), 233 (15), 220 (11), 207 (100), 202 (45), 192 (47), 143 (81), 129 (24), 128 (20); ^{1}H NMR analyses. Since the component II could not be separated in pure form, the ^{1}H NMR spectrum could not be obtained. However, the characteristic benzylic singlet at 4.56 ppm strongly suggests the "ortho" structure for this regio-isomer. Component III ("ortho" isomer): GC retention time (relative intensity) 23.60 min (38.0 %); MS, m/e (relative intensity) 322 (M^+, 16), 275 (10), 263 (24), 262 (98), 247 (12), 207 (100), 202 (25), 192 (37), 143 (65), 128 (16); ^{1}H NMR (CDCl$_3$) δ 1.11 (s, 3H), 1.70 (s, 3H), 1.98 (m, 1H), 2.24 (s, 3H), 2.33 (m, 1H), 2.44 (s, 3H), 2.85 (m, 2H), 3.67 (s, 3H), 5.40 (s, 1H), 6.65-7.15 (m, 6H). The characteristic benzylic singlet at 5.40 ppm strongly supports the "ortho" structure for this regio-isomer. Component IV ("meta" isomer): GC retention time (relative intensity) 24.91 min (4.6 %); MS, m/e (relative intensity) 322 ($M^{+\cdot}$ 12), 247 (39), 207 (10), 202 (30), 192

(11), 143 (100), 128 (11); ^{1}H NMR (CDCl$_3$) δ 1.32 (s, 3H), 1.69 (s, 3H), 2.03 (ddd, J$_1$=2.6 Hz, J$_2$=6.8 Hz, J$_3$=13 Hz, 1H), 2.17 (dd, J$_1$=12.4 Hz, J$_2$=13.5 Hz, 1H), 2.25 (s, 3H), 2.42 (s, 3H), 2.83 (dd, J$_1$=2.5 Hz, J$_2$=16.3 Hz, 1H), 3.19 (d, J=16.1 Hz), 3.70 (s, 3H), 4.60 (dd, J$_1$=7 Hz, J$_2$=12.4 Hz, 1H), 6.6-7.1 (m, 6H). The AB pattern at 2.83 and 3.29 ppm supports the "meta" structural assignment for this regio-isomer.

General procedures for dimerizations of α–substituted o-xylylenes. To a solution of α–substituted o-xylylene precursor (~200 mg) in acetonitrile (10 mL) was added a solution of TBAF (600 mg) in acetonitrile (10 mL). After addition of the TBAF solution, the reaction mixture was further stirred for 15 min and worked up with addition of water. The mixture was extracted with hexanes, dried over anhydrous Na$_2$SO$_4$ and concentrated under reduced pressure. Before the crude dimers were subjected to a silica gel liquid chromatography, a ^{1}H NMR spectrum was collected. Since the [4+2] dimer might be unstable on silica gel and rearrange to give rise to other products, the ^{1}H NMR spectrum of the mixture was used as a standard to identifiy whether the isolated products was included in the original dimer mixture or not. Finally, the dimers were isolated through silica gel liquid chromatography with hexanes as the eluent.

Dimerization products of α–methyl-o-xylylene (9). [4+2] Dimer **27** (yield 66.9 %): ^{1}H NMR (CDCl$_3$) δ 1.07 (d, J=7.1 Hz, 3H), 1.68-1.75 (d, J=7 Hz, 3H; dd, 1H. The absorption of the methyl group overlap with that of a doublet of doublet) 1.93-2.03 (m, 1H), 2.78 (q, J=7.1 Hz, 1H), 2.83-3.00 (m, 2H), 5.18 (q, J=7 Hz, 1H), 5.85-5.95 (m, 3H), 6.42 (d, J=9.5 Hz, 1H), 7.03-7.32 (m, 4H). Two characteristic quartets at 2.78 and 5.18 ppm support the structure assignment for **27**. Decoupling experiments show that four protons at 1.68-1.75, 1.93-2.03 and 2.82-3.00 ppm are coupled with each others. This kind of coupling pattern further supports the assignment for **27**. Mass spectrum could

not be obtained successfully since the dimer polymerizes quickly when it is concentrated. Moreover, this dimer is thermally unstable and decomposed under GC conditions. [4+2] Dimer **28** (yield 9 %): ^{1}H NMR (CDCl$_3$) δ 0.93 (d, J=6.7 Hz, 3H), 1.07 (d, J=7.2 Hz, 3H), 2.18-2.26 (m, 1H), 2.61-2.72 (m, 2H), 2.99 (dd, J$_1$=6.3 Hz, J$_2$=17.3 Hz, 1H), 4.78 (s, 1H), 5.31 (s, 1H), 5.78 (d, J=9.8 Hz, 1H), 5.84 (dd, J$_1$=5.9 Hz, J$_2$=9.4 Hz, 1H), 5.95 (dd, J$_1$=5.8 Hz, J$_2$=9.5 Hz, 1H), 6.12 (d, J=9.3 Hz, 1H), 7.02-7.31 (m, 4H). The characteristic singlets for gem-vinyl protons at 4.78 and 5.31 ppm support the structure of **28**. Moreover, decoupling experiments showed that the multiplets of two protons at 2.61-2.72 ppm collasped to one singlet and one doublet of doublet when the methyl protons at 1.07 ppm were irradiated. It implys the existence of a single proton which is coupled with the methyl group at 1.07 ppm only. This information further comfirms the structural assignment; MS, m/e (relative intensity) 236,(M$^+$, 28), 221 (40), 207 (100), 192 (28), 179 (30), 178 (26), 165 (9), 129 (15), 119 (64), 118 (43), 117 (60), 115 (24), 105 (11), 91 (28), exact mass m/e 236.15615, calcd for C$_{18}$H$_{20}$ 236.15650.

[4+2] Dimer **29** (yield 10 %): ^{1}H NMR (CDCl$_3$) δ 0.87 (d, J=6.6 Hz, 3H), 1.18 (d, J=6.9 Hz, 3H), 1.88 (m, 1H), 2.73-2.84 (m, 3H), 5.03 (s, 1H), 5.28 (s, 1H), 5.50 (d, J=9.7 Hz, 1H), 5.71 (dd, J$_1$=5.0 Hz, J$_2$=9.2 Hz, 1H), 6.11 (dd, J$_1$=5.5 Hz, J$_2$=10.1 Hz, 1H), 6.24 (d, J=9.4 Hz, 1H), 7.06-7.31 (m, 4H). The characteristic singlets at 5.03 and 5.28 ppm are assigned as the gem-vinyl protons of the dimer **29**. Irradiation at 1.18 ppm led to a singlet along with multiplets at 2.73-2.83 ppm. This observation suggests the existence of a single proton coupled with the methyl group at 1.18 ppm only. These ^{1}H NMR patterns confirm the structural assignment of **29**. MS, m/e (relative intensity) 236 (M$^+$, 40), 221 (48), 207 (100), 193 (22), 192 (33), 179 (32), 178 (29), 165 (13), 129 (20), 119 (96), 118 (59), 117 (89), 115 (38), 105 (17), 91 (40), 81 (17), 69 (54); exact mass, m/e, 236.15592, calcd for C$_{18}$H$_{20}$ 236.15650. [4+2] Dimer **30** (yield 9 %): ^{1}H NMR

(CDCl$_3$) δ 1.28-1.34 (m, 4H), 1.79 (d, J=7.0 Hz, 3H), 2.12 (ddd, J$_1$=2.4 Hz, J$_2$=6.0 Hz, J$_3$ = 13.0 Hz, 1H), 2.74 (dd, J$_1$=2.4 Hz, J$_2$=16.0 Hz, 1H), 2.90 (d, J=16.0 Hz, 1H), 3.08 (m, 1H), 5.56 (q, J=7.2 Hz, 1H), 5.78-5.93 (m, 3H), 6.50 (d, J=9.0 Hz, 1H), 7.03 (d, J=7.3 Hz, 1H), 7.11 (t, J=7.5 Hz, 1H), 7.18 (t, J=7.7 Hz, 1H), 7.31 (d, J=7.7 Hz, 1H). The characteristic AB pattern at 2.74 and 2.90 ppm and the vinyl quartet at 5.56 ppm support the structural assignment of **30**; MS, m/e (relatively intensity) 263 (M$^+$, 50), 291 (48), 207 (100), 193 (33), 192 (25), 179 (35), 178 (33), 165 (12), 145 (10), 129 (20), 119 (72), 118 (51), 117 (69), 115 (31), 105 (15), 91 (35), exact mass m/e 236.15629, calcd for C$_{18}$H$_{20}$ 236.15650.

Dimerization products of α-cyclopropyl-*o*-xylylene (10). [4+2] dimer **31** (yield 53 %); ^{1}H NMR (CDCl$_3$) δ 0.08-0.18 (m, 1H), 0.20-0.35 (m, 2H), 0.38-0.51 (m, 2H), 0.70-0.90 (m, 4H), 1.65-1.80 (m, 2H), 2.00 (d, J=9.4 Hz, 1H), 2.21-2.16 (m, 1H), 2.86-3.01 (m, 2H), 4.60 (d, J=9.4 Hz, 1H), 5.84-5.91 (m, 3H), 6.60-6.68 (m, 1H), 7.05-7.20 (m, 4H). The characteristic benzylic doublet at 2.00 ppm and the vinyl doublet at 4.60 ppm support the structural assignment of **31**. [4+2] Dimer **32** (yield 13 %): ^{1}H NMR (CDCl$_3$) δ 0.21-0.35 (m, 3H), 0.38-0.58 (m, 2H), 0.68-0.89 (m, 4H), 1.71-1.91 (m, 4H), 2.68-3.08 (m, 2H), 4.72 (d, J=9.3 Hz, 1H), 5.61 (d, J=9.7 Hz, 1H), 5.81 (m, 1H), 5.94 (dd, J$_1$=5.9 Hz, J$_2$=9.7 Hz, 1H), 6.68 (d, J=9.5 Hz, 1H), 7.06-7.18 (m, 3H), 7.80 (d, J=6.3 Hz, 1H). The vinyl doublet at 4.72 ppm and the benzylic doublet which overlaps with other multiplets support the assignment. In addition, the assignment was also further confirmed by the results of the flash vacuum pyrolysis experiments which is described later. [4+2] Dimer **33** (yield 11%): ^{1}H NMR (CDCl$_3$) δ 0.12-0.21 (m, 1H), 0.23-0.58 (m, 4H), 0.72-0.90 (m, 4H), 1.39-1.48 (t, J=12 Hz, 1H), 1.68-1.81 (m, 1H), 2.05-2.22 (m, 2H), 2.72, 2.83 (ABq, J=16 Hz, 2H), 4.80 (d, J=9.5Hz, 1H), 5.73 (d, J=9.2 Hz, 1H), 5.72-5.83 (m, 2H), 6.66 (d, J=8.5 Hz, 1H), 7.04 (d, J=6.8 Hz, 1H), 7.10-7.22 (m, 2H), 7.77 (d, J=7.6

Hz, 1H). The characteristic doublet at 4.80 ppm and the AB quartet at 2.78 ppm support the structural assignment of **33**.   [4+2] Dimers **34** and **35** (yield 3 and 4 % respectively): A mixture of dimers **34** and **35** was isolated from other isomers on silica gel liquid chromatography. On the basis of the ^{1}H NMR spectrum of the mixture, the structure of the dimers were suggested as **30** and **31**. Their structural assignments are based on (a) the gem-vinyl singlets at 4.90 & 5.18 ppm and 4.36 & 5.01 ppm; (b) benzylic doublet at 1.93 and 2.17 ppm. Moreover, the pyrolysis results also support the assignments since it gives two head-to-tail [4+4] dimers as the major products in flash vacuum pyrolysis.   Head-to-head [4+4] dimer **36**: ^{1}H NMR (CDCl$_3$) δ -0.1-1.4 (m, 10 H); 2.1-2.3 (m, 1H), 2.7-3.1 (m, 3H), 3.2-3.7 (m, 2H), 6.5-7.3 (m, 8H); MS, m/e (relative intensity) 288 (M$^{+\cdot}$ 37), 273 (2), 260 (7), 259 (6), 245 (8), 231 (8), 217 (14), 205 (9), 183 (12), 169 (18), 158 (19), 143 (86), 129 (92), 128 (100), 117 (48), 115 (62), 105 (23), 91 (46).

Head-to-head [4+4] dimer **37**: ^{1}H NMR (CDCl$_3$) δ Signals of the cyclopropyl ring protons cannot be seen clearly since the solution was too dilute and their signals are covered by the proton signals of the hydroncarbon residues from the chromatography solvents, 2.4-2.5 (m, 2H), 2.9-3.0 (m, 4H), 7.0-7.3 (m, 8H); MS, m/e (relative intensity) 288 (M$^+$, 30), 273 (2), 260 (7), 259 (6), 245 (7), 231 (7), 217 (14), 202 (8), 183 (11), 169 (17), 158 (18), 157 (17), 143 (82), 129 (93), 128 (100), 117 (45), 115 (64), 105 (23), 91 (45).

Flash vacuum pyrolyses of dimers 31-35.   Dimers **31-35** were pyrolysed at 540-550 °C under 10^{-5} torr. The pyrolysates were analysed by GC-MS and the results are summarized in Table 12.

Table 12. GC[a]-MS analyses for the flash vacuum pyrolyses of dimers **31-35**

Precursor[b] Dimer	Products			
	Head-to-head [4+4] **36**[c]	Head-to-tail [4+4] **38**[d]	Head-to head [4+4] **37**[e]	Head-to-tal [4+4] **39**[f]
31	83	> 0.5	16	>1
32	45	2	53	---
33	10	23	10	57
34 & 35	8	51	3	38

[a] GC Conditions: Column DB1, temperature program 120 °C, 5 min, 10 °C/min (rate) 200 °C, 35min.
[b] Purity of the dimer is higher than 80%.
[c] Retention time is 26.0 min.
[d] Retention time is 27.0 min.
[e] Retention time is 28.6 min.
[f] Retention time is 30.8 min.

Dimerization products of α-tert-butyl-o-xylylene (11). The [4+2] dimer **40** was separated from the [4+4] dimers **41** and **42** through a AgNO3 treated silica gel column. (1) [4+2] dimer **40** (yield 80 %): ^{1}H NMR (CDCl3) δ 0.89 (s, 9H), 1.19 (s, 9H), 1.78-1.87 (m, 1H), 2.65-2.75 (m, 1H), 2.87 (d, J=1.8 Hz, 1H), 2.93-3.05 (m, 1H), 3.14-3.21 (m, 1H), 5.49 (d, J=9.4 Hz, 1H), 5.54 (s, 1H), 5.56-5.60 (m, 1H), 5.84-5.90 (m, 1H), 6.67 (d, J=9.7 Hz, 1H), 6.90 (d, J=7.5 Hz, 1H), 6.95-7.03 (m, 1H), 7.05-7.14 (m, 2H). The characteristic benzylic doublet with a small coupling constant (long range coupling) at 2.87 ppm and singlet at 5.54 ppm support the structural assigment of **40**. Head-to-head [4+4] dimer **41** (yield 8 %): ^{1}H NMR (CDCl3) δ 0.74 (s, 9H), 1.03 (s, 9H), 2.87-3.17 (m, 4H), 3.28-3.37 (m, 1H), 3.52 (s, 1H), 7.04-7.17 (m, 7H), 7.70-7.73 (m, 1H); MS, m/e (relative intensity) 320 (M+,34), 277 (53), 264 (11), 263 (12), 221 (14), 193 (100), 159 (67), 117 (30), 91 (17), 57 (36); exact mass, m/e 320.25032, calcd for $C_{24}H_{32}$ 320.25040.

Thermally unstable head-to-head [4+4] dimer **42** (yield 12 %): ^{1}H NMR (CDCl3) δ 1.21 (s, 18H), 2.83-3.12 (AA'BB', 4H), 3.24 (s, 2H), 7.05-7.15 (m, 4H), 7.20-7.25 (m, 2H),

7.69-7.74 (m, 2H). Thermally stable head-to-head [4+4] dimer **42** (< 2 %): ^{1}H NMR (CDCl$_3$) δ 0.82 (s, 18H), 2.81-2.88 and 3.27-3.30 (AA'BB', 4H), 3.32 (s, 2H), 7.04-7.19 (m, 8H); MS, m/e (relative intensity) 320 (57), 277 (82), 264 (18), 263 (13), 221 (26), 193 (22), 159 (100), 117 (48), 91 (22), 57 (39); exact mass, m/e, 320.25062 calcd for C$_{24}$H$_{32}$ 320.25040.

Dimerization products of α-mesityl-*o*-xylylene (12). [4+2] Dimer **43** (yield 53 %): ^{1}H NMR (CDCl$_3$) δ 1.70 (s, 3H), 1.86 (dd, J$_1$=5 Hz, J$_2$=13 Hz, 1H), 2.06 (s, 3H), 2.09 (s, 3H), 2.24 (2, 3H), 2.26 (s, 3H), 2.35 (s, 3H), 2.80 (dd, J$_1$=4 Hz, J$_2$=17 Hz, 1H), 3.27-3.42 (m, 2H), 4.87 (s, 1H), 5.33 (d, J= 9.3 Hz, 1H), 5.65-5.80 (m, 3H), 6.09 (s, 1H), 6.73 (s, 1H), 6.80 (s, 2H), 6.84 (d, J=7 Hz, 1H), 6.88 (s, 1H), 6.79 (t, J= 7Hz, 1H), 7.05 (t, J= 7 Hz, 1H), 7.12 (d, J=7 Hz, 1H). Head-to-head [4+4] dimer **44** (yield 47 %): ^{1}H NMR (CDCl$_3$) δ 1.50-2.00 (broad s, 12 H), 2.20 (s, 6H), 3.32-3.74 (AA'BB', 4H), 5.89 (s, 2H), 6.62 (s, 4H), 6.82 (d, J=7 Hz, 2H), 6.92 (t, J=7 Hz, 2H), 7.05 (t, J=7 Hz, 2H), 7.15 (d, J=7 Hz, 2H); MS, m/e (relative intensity) 444 (M$^+$, 15), 429 (5), 324 (9), 309 (23), 233 (61), 221 (27), 207 (100), 204 (36), 192 (11); exact mass m/e 444.28141, calcd for C$_{34}$H$_{36}$ 444.28170.

Thermolysis of dimer 43 in thiophenol. A 20 mg quantity of **43** in thiophenol (3 mL) was thermolysed at 180 °C under a seal tube condition for 2h. After thermolysis, the solution was cooled down to room temperature and 2N NaOH solution was added. The mixture was extracted with hexanes and the extract was washed with two 30-mL portions of 2N NaOH solution and one 30 mL portion of NaHCO$_3$ solutionts, dried over anhydrous Na$_2$SO$_4$, concentrated under reduced pressure and subjected to silica gel liquid chromatography with benzene-hexanes (1:3) as the eluent. The first fraction isolated from the column is diphenyl disulfide and the second fraction is the reduction product **45**. Product **45** cannot be visualized on a TLC

plate by a normal UV visualization process. By use of an aqueous formaldehyde solution with H_2SO_4, product **45** can be thermally decomposed and stained as a very faint spot on a silica gel TLC plate. However, the product can be detected effectively by GC analysis: ^{1}H NMR (CDCl_3) δ 2.21 (s, 12H), 2.23 (s, 6H), 3.14 (s, 4H), 3.97 (s, 4H), 6.53 (d, J=7 Hz, 2H), 6.89 (s, 4H), 7.01 (t, J=7 Hz, 2H), 7.14 (t, J=7 Hz, 2H), 7.24 (d, J=7 Hz, 2H); MS, m/e (relative intensity) 446 (M^+, 55), 326 (33), 223 (100), 206 (76), 193 (48), 178 (18), 143 (13), 133 (22), 120 (13); exact mass m/e 446.29665, calcd for $C_{34}H_{38}$ 446.29735.

Determination of λ_{max} for α-*tert*-butyl-*o*-xylylene (11). A 2-cm path-length UV-visible cell was charged with 3 mL of CH_3CN and 0.1 mL of a 0.1 M TBAF solution. To this was rapidly added 1.0 mL of 10^{-3} M quaternary ammonium salt **15** in CH_3CN and **11** was generated. The cell was shaken once and placed in the optical path of a Perkin-Elmer 7000 Lambda-Array UV-Visible Spectrophotometer. Spectra were recorded every 0.03 min in the spectral range 200-450 nm. From a plot of absorbances versus wavelengths, the λ_{max} was determined. Determination of the λ_{max} values for **1** and **9** was reported by Macius.

Determination of ε_{max} and dimerization rate constants for 9 and 11. The ε_{max} for **9** and **11** were measured by a Canterbury SF 3A Stopped-Flow UV-Visible Spectrophotometer. Several runs were carried out in which the optimum fluoride ion concentration was kept constant but the concentration of the quaternary ammonium salt precursor was varied. The rapid injection of TBAF and precursor solutions into the mixing chamber of stopped-flow UV-visible spectrophotometer generated *o*-QDM's rapidly. The generation and decay of *o*-QDM's were monitored by UV-visible spectrometer. In each experiment, we obtained a maximum absorbance for the *o*-QDM intermediate followed by a second order decay. Assuming that the

quaternary ammonium salt precursor was converted quantitatively to the corresponding o-QDM before much of o-QDM intermediate had dimerized, we obtained the initial concentration of o-QDM. By use of the Beer's law, the ε_{max} for o-QDM was obtained from the linear plot of the maximum absorbances against the initial concentrations of o-QDM intermediate. The extinction coefficients ε_{max} for 9 and 11 are reported in Table 12. By use of the determined extinction coefficients of 9 and 11, the dimerization rate constants of the o-QDM's were evaluated from the second order decay curves obtained from the stopped-flow experiments. Temperature dependent experiments were performed with a stopped-flow mixing cell immersed in a thermal static water bath.

General procedures for the competitive kinetic experiments. Five fast mixing cells, a series of five solutions containing quaternary ammonium salt precursor (1×10^{-3}M), diphenylmethane (4×10^{-4} M) and various amount of methyl methacrylate (3 to 16×10^{-2}M for oQDM 9 and 1 to 5 $\times 10^{-1}$ M for o-QDM 11) in acetonitrile (solution A) and a 0.2 M TBAF solution in acetonitrile (solution B) were prepared. To each of the fast mixing cells were charged a 0.4 mL of solution A and a 0.4 mL of TBAF solution (solution B) respectively. The cells were capped by a ground-glass stopper, sealed with parafin film, attached to the cell holder and immersed into a constant temperature water bath for half an hour until the solution temperature was equilibrated with the bath temperature. The cells were then flipped twice inside the water bath and the solutions A and B were mixed and reacted inside the cells for 15 min. After the reactions were complete, the reaction mixtures were diluted with a 1 mL quantity of CH_2Cl_2 respectively. The diluted mixtures were then subjected to silica gel short columns and the unreacted TBAF was removed. The filtrates were subjected to GC analyses and the yield percentage of the Diels-Alder adducts and dimerization

products were determined. In these experiments, diphenylmethane is employed as an GC internal standard to calibrate the yield percentage of the Diels-Alder adducts. Although the dimers will be decomposed under the GC conditions, the total yield percentage can be determined from the yield percentage of the Diels-Alder adducts. On the basis of the non-linear curve fitting technique, the rate constant ratio for the dimerization to the Diels-Alder reaction was determined. The same procedures were repeated at several different temperatures between 0 °C and 50 °C and the activation parameters were determined. The kinetic studies were performed twice for each system.

REFERENCES

(1)   For reviews, see: (a) Martin, N.; Seoane, C.; Hanack, M. *Org. Prep. Proc. Int.* **1991**, 239. (b) Charlton, J. L.; Alauddin, M. M. *Tetrahedron* **1987**, *43*, 2873. (c) Funk, R. L.; Vollhardt, K. P. C. *Chem. Soc. Rev.* **1980**, *9*, 41. (d) McCullough, J. J. *Acc. Chem. Res.* **1980**, *13*, 270. (e) Oppolzer, W. *Synthesis*, **1978**, 793. (f) Taub, D. In *The Natural Synthesis of Natural Products*; ApSimon, J., Ed.; Wiley-Interscience: New York, **1984**; Vol. 6, pp. 17-37. (h) Ciganek, E. *Org. Reactions.* **1984**, *32*, 72-374.

(2)   Errede, L. A. *J. Am. Chem. Soc.* **1961**, *83*, 949.

(3)   Trahanovsky, W. S.; Cassady, T. J.; Woods, T. L. *J. Am. Chem. Soc.* **1981**, *103*, 6691.

(4)   Chou, C.-H.; Trahanovsky, W. S. *J. Am. Chem. Soc.* **1986**, *108*, 4138.

(5)   Huang Y.-c. J. Ph. D. Dissertation, Iowa State University, **1987**.

(6)   Woodward, R. B.; Hoffmann, R. *J. Am. Chem. Soc.* **1965**, *87*, 395; *Angew. Chem. Int. Ed. Engl.* **1969**, *8*, 781.

(7)   (a) Roth, W. R.; Biermann, M.; Dekker, H.; Jochems, R.; Mosselman, C.; Hermann, H. *Chem. Ber.* **1978**, *111*, 3892. (b) Roth, W. R.; Scholz, B. P. *Chem. Ber.* **1981**, *114*, 3741.

(8)   Michl, J.; Flynn, C. R. *J. Am. Chem. Soc.* **1973**, *95*, 7609; **1974**, *96*, 3280.

(9)   Michl, J.; Tseng, K. L. *J. Am. Chem. Soc.* **1977**, *99*, 4840.

(10)   Kreile, J.; Munzel, N.; Schulz, R.; Schweig, A. *Chem. Phys. Lett.* **1984**, *108*, 609.

(11)   (a) Trahanovsky, W. S.; Chou, C.-H.; Fischer, D. R.; Gerstein, B. C. *J. Am. Chem. Soc.* **1988**, *110*, 6579; paper submitted. (b), Fischer, D. R,. Ph.D. Dissertation, Iowa State University, 1990.

(12)   (a) Trahanovsky, W. S.; Macias, J. R. *J. Am. Chem. Soc.* **1986**, *108*, 6820. (b) Macias, J. P. Ph.D. Dissertation, Iowa State University, 1987.

(13)   Gajewski, J. J.; Peterson, K. B.; Kagel, J. R. *J. Am.. Chem. Soc.* **1987**, *109*, 5545.

(14)   Ito, Y.; Nakatsuka, M.; Saegusa, T. *J. Am. Chem. Soc.* **1982**, *104*, 7609.

(15)   Aono, M.; Terao, Y.; Achiwa, K. *Chem. Lett.* **1985**, 359.

(16)   Clark, R. D.; Jahangir *J. Org. Chem.* **1987**, *52*, 5378.

(17)   Fieser, L. F. and Fieser, M. *Reagents for Organic Synthesis*; John Wiley and Sons: New York, 1967; Vol 1, pp 581-595.

(18)   Ratcliffe, R.; Rodehorst, R. *J. Org. Chem.* **1970**, *35*, 4000.

(19)   Moffett, R. B. *Org. Synthesis Coll. Vol.* **1963**, 4 , 605.

(20)   Seyferth, D.; Cohen, H. M. *J. Organomet. Chem.* **1963**, *1*, 15.

(21)   Borch, R. F.; Hassid, A. I. *J. Org. Chem.* **1972**, *37*, 1673.

(22)   Brown, R. C. F. *Pyrolysis Methods in Organic Chemistry*; Academic: New York, **1980**, Chapter 2

(23)   Arshinova, R. R. *Russ. Chem. Rev.* **1988**, *57*, 1142.

(24)   For MM-X molecular mechanic computation methods, see Carey, F. A; Sundberg, R. J. *Advanced Organic Chemistry 3ed.* Plenum: New York and London, **1990**, Part A, p118-119 and references cited therein.

(25)   (a) Tinner, U.; Espenson, T. H. *J. Organomet. Chem.* **1981**, *212*, 43.

(b) Christian, S. D. ; Tucker, E. E. *American Laboratory* **1982**, Aug, 35; **1982**, sept, 31.

(26)   (a) Kahn, S. D.; Pau, C. F.; Overman, L. E.; Hehre, W. J. *J. Am. Chem. Soc.* **1986**, *108*, 7381. (b) Konovalov, A. I.; Kiselve, V. D. *Russ. Chem. Rev.* **1989**, *58*, 230 and references cited therein.

(27) Sustmann, R.; Daute; P.; Sauer, R.; Sommer, A.; Trahanovsky, W. S. *Chem. Ber.* **1989**, *122*, 1551.

(28) The preference of exo or endo stereoisomer has not been determined

(29) Scaiano, J. C.; Johnston, L. J. *Chem. Rev.* **1989**, *81*, 521.

(30) Masnovi, J.; Samsel, E. G.; Bullock, R. M. *J. Chem. Soc. Chem. Commun.* **1989**, 1044.

(31) Assuming that the rate of diradical cyclization is at least 100 folds faster than that of the cyclopropane ring opening reaction.

(32) Franz, J. A.; Naushadali, K. S.; Alanjjar, M. S. *J. Org. Chem.* **1986**, *51*, 19.

(33) The estimation is based on the assumption that the rate of the diradical cyclization is at least 100 folds faster than that of the thiophenol hydrogen abstraction reaction. The concentration of thiophenol which is equal to 14.4 M at 25 °C is estimated from the thiophenol density at room temperature.

(34) Shih, C.; Swenton, J. S. *J. Org. Chem.* **1982**, *47*, 2668.

(35) Smith, L. I. *Org. Synthesis Coll. Vol.* **1943**, *2*, 360.

APPENDIX

Table A-1. Absorbance values for various concentration of [9]

[9], M	Absorbance of [9]				
	Trial 1	Trial 2	Trial 3	Trial 4	Average
0	0	0	0	0	0
1.775E-04	0.1364	0.1361	0.1326	0.1254	0.1326
3.829E-04	0.2574	0.2606	0.2612	0.2592	0.2596
6.850E-04	0.4592	0.4578	0.4589	0.4599	0.4590

Table A-2. Kinetic data for α–methyl-o-xylylene (9) dimerization measured at 15.50 °C in CH$_3$CN

Time, s	Absorbance	[9], M	[9]$^{-1}$, M^{-1}
0.05	0.2845	4.28E-04	2.33E+03
0.10	0.2564	3.86E-04	2.59E+03
0.15	0.2322	3.50E-04	2.86E+03
0.20	0.2103	3.17E-04	3.16E+03
0.25	0.1909	2.88E-04	3.48E+03
0.30	0.1752	2.64E-04	3.79E+03
0.35	0.1611	2.43E-04	4.12E+03
0.40	0.1491	2.25E-04	4.45E+03
0.45	0.1380	2.08E-04	4.81E+03
0.50	0.1288	1.94E-04	5.16E+03
0.55	0.1211	1.82E-04	5.48E+03
0.60	0.1139	1.72E-04	5.83E+03
0.65	0.1077	1.62E-04	6.17E+03
0.70	0.1016	1.53E-04	6.54E+03
0.75	0.0960	1.45E-04	6.92E+03
0.80	0.0920	1.39E-04	7.22E+03
0.85	0.0876	1.32E-04	7.58E+03
0.90	0.0841	1.27E-04	7.90E+03
0.95	0.0798	1.20E-04	8.32E+03
1.00	0.0772	1.16E-04	8.60E+03

Table A-3. Kinetic data for α–methyl-o-xylylene (9) dimerization measured at 15.50 °C in CH₃CN

Time, s	Absorbance	[9], M	[9]$^{-1}$,M^{-1}
0.05	0.2823	4.25E-04	2.35E+03
0.10	0.2550	3.84E-04	2.60E+03
0.15	0.2299	3.46E-04	2.89E+03
0.20	0.2082	3.14E-04	3.19E+03
0.25	0.1895	2.85E-04	3.50E+03
0.30	0.1739	2.62E-04	3.82E+03
0.35	0.1598	2.41E-04	4.16E+03
0.40	0.1475	2.22E-04	4.50E+03
0.45	0.1360	2.05E-04	4.88E+03
0.50	0.1282	1.93E-04	5.18E+03
0.55	0.1197	1.80E-04	5.55E+03
0.60	0.1122	1.69E-04	5.92E+03
0.65	0.1068	1.61E-04	6.22E+03
0.70	0.1007	1.52E-04	6.59E+03
0.75	0.0951	1.43E-04	6.98E+03
0.80	0.0907	1.37E-04	7.32E+03
0.85	0.0868	1.31E-04	7.65E+03
0.90	0.0829	1.25E-04	8.01E+03
0.95	0.0798	1.20E-04	8.32E+03
1.00	0.0768	1.16E-04	8.65E+03

Table A-4. Kinetic data for α–methyl-o-xylylene (9) dimerization measured at 15.50 °C in CH_3CN

Time, s	Absorbance	[9], M	[9],M
0.05	0.2817	4.24E-04	2.36E+03
0.10	0.2533	3.81E-04	2.62E+03
0.15	0.2288	3.45E-04	2.90E+03
0.20	0.2072	3.12E-04	3.20E+03
0.25	0.1890	2.85E-04	3.51E+03
0.30	0.1726	2.60E-04	3.85E+03
0.35	0.1585	2.39E-04	4.19E+03
0.40	0.1472	2.22E-04	4.51E+03
0.45	0.1357	2.04E-04	4.89E+03
0.50	0.1270	1.91E-04	5.23E+03
0.55	0.1194	1.80E-04	5.56E+03
0.60	0.1123	1.69E-04	5.91E+03
0.65	0.1057	1.59E-04	6.28E+03
0.70	0.0997	1.50E-04	6.66E+03
0.75	0.0953	1.44E-04	6.97E+03
0.80	0.0905	1.36E-04	7.34E+03
0.85	0.0858	1.29E-04	7.74E+03
0.90	0.0823	1.24E-04	8.07E+03
0.95	0.0789	1.19E-04	8.42E+03
1.00	0.0754	1.14E-04	8.81E+03

Table A-5. Kinetic data for α–methyl-*o*-xylylene (**9**) dimerization measured at
23.80 °C in CH_3CN

Time, s	Absorbance	[9], M	$[9]^{-1}$, M^{-1}
0.05	0.2993	4.51E-04	2.22E+03
0.10	0.2570	3.87E-04	2.58E+03
0.15	0.2223	3.35E-04	2.99E+03
0.20	0.1957	2.95E-04	3.39E+03
0.25	0.1740	2.62E-04	3.82E+03
0.30	0.1573	2.37E-04	4.22E+03
0.35	0.1439	2.17E-04	4.61E+03
0.40	0.1313	1.98E-04	5.06E+03
0.45	0.1213	1.83E-04	5.47E+03
0.50	0.1129	1.70E-04	5.88E+03
0.55	0.1047	1.58E-04	6.34E+03
0.60	0.0990	1.49E-04	6.71E+03
0.65	0.0935	1.41E-04	7.10E+03
0.70	0.0883	1.33E-04	7.52E+03
0.75	0.0836	1.26E-04	7.94E+03
0.80	0.0789	1.19E-04	8.42E+03
0.85	0.0752	1.13E-04	8.83E+03

Table A-6. Kinetic data for α–methyl-o-xylylene (9) dimerization measured at
23.80 °C in CH_3CN

Time, s	Absorbance	[9], M	$[9]^{-1}, M^{-1}$
0.05	0.2988	4.50E-04	2.22E+03
0.10	0.2551	3.84E-04	2.60E+03
0.15	0.2209	3.33E-04	3.01E+03
0.20	0.1945	2.93E-04	3.41E+03
0.25	0.1736	2.61E-04	3.82E+03
0.30	0.1566	2.36E-04	4.24E+03
0.35	0.1420	2.14E-04	4.68E+03
0.40	0.1306	1.97E-04	5.08E+03
0.45	0.1210	1.82E-04	5.49E+03
0.50	0.1122	1.69E-04	5.92E+03
0.55	0.1047	1.58E-04	6.34E+03
0.60	0.0988	1.49E-04	6.72E+03
0.65	0.0929	1.40E-04	7.15E+03
0.70	0.0874	1.32E-04	7.60E+03
0.75	0.0837	1.26E-04	7.93E+03
0.80	0.0793	1.19E-04	8.37E+03
0.85	0.0750	1.13E-04	8.85E+03

Table A-7. Kinetic data for α–methyl-*o*-xylylene (9) dimerization measured at 23.80 °C in CH₃CN

Time, s	Absorbance	[9], M	[9],M
0.05	0.3055	4.60E-04	2.17E+03
0.10	0.2612	3.93E-04	2.54E+03
0.15	0.2256	3.40E-04	2.94E+03
0.20	0.1989	3.00E-04	3.34E+03
0.25	0.1770	2.67E-04	3.75E+03
0.30	0.1594	2.40E-04	4.17E+03
0.35	0.1448	2.18E-04	4.59E+03
0.40	0.1318	1.98E-04	5.04E+03
0.45	0.1228	1.85E-04	5.41E+03
0.50	0.1140	1.72E-04	5.82E+03
0.55	0.1054	1.59E-04	6.30E+03
0.60	0.0991	1.49E-04	6.70E+03
0.65	0.0939	1.41E-04	7.07E+03
0.70	0.0887	1.34E-04	7.49E+03
0.75	0.0837	1.26E-04	7.93E+03
0.80	0.0793	1.19E-04	8.37E+03
0.85	0.0760	1.14E-04	8.74E+03

Table A-8. Kinetic data for α–methyl-*o*-xylylene **(9)** dimerization measured at 30.40 °C in CH_3CN

Time, s	Absorbance	[9], M	$[9]^{-1}$, M^{-1}
0.050	0.3075	4.63E-04	2.16E+03
0.075	0.2785	4.19E-04	2.38E+03
0.100	0.2541	3.83E-04	2.61E+03
0.125	0.2330	3.51E-04	2.85E+03
0.150	0.2158	3.25E-04	3.08E+03
0.175	0.1989	3.00E-04	3.34E+03
0.200	0.1862	2.80E-04	3.57E+03
0.225	0.1743	2.63E-04	3.81E+03
0.250	0.1654	2.49E-04	4.01E+03
0.275	0.1554	2.34E-04	4.27E+03
0.300	0.1482	2.23E-04	4.48E+03
0.325	0.1406	2.12E-04	4.72E+03
0.350	0.1332	2.01E-04	4.98E+03
0.375	0.1267	1.91E-04	5.24E+03
0.400	0.1215	1.83E-04	5.47E+03
0.425	0.1175	1.77E-04	5.65E+03
0.450	0.1124	1.69E-04	5.91E+03
0.475	0.1081	1.63E-04	6.14E+03
0.500	0.1043	1.57E-04	6.37E+03
0.525	0.1005	1.51E-04	6.61E+03
0.550	0.0975	1.47E-04	6.81E+03

Table A-8.   Continued

Time, s	Absorbance	[9], M	$[9]^{-1}, M^{-1}$
0.575	0.0937	1.41E-04	7.09E+03
0.600	0.0904	1.36E-04	7.35E+03
0.625	0.0878	1.32E-04	7.56E+03
0.650	0.0852	1.28E-04	7.79E+03
0.675	0.0827	1.25E-04	8.03E+03

Table A-9. Kinetic data for α–methyl-o-xylylene (9) dimerization measured at 30.40 °C in CH$_3$CN

Time, s	Absorbance	[9], M	[9]$^{-1}$, M^{-1}
0.050	0.3108	4.68E-04	2.14E+03
0.075	0.2800	4.22E-04	2.37E+03
0.100	0.2550	3.84E-04	2.60E+03
0.125	0.2339	3.52E-04	2.84E+03
0.150	0.2158	3.25E-04	3.08E+03
0.175	0.2003	3.02E-04	3.32E+03
0.200	0.1867	2.81E-04	3.56E+03
0.225	0.1744	2.63E-04	3.81E+03
0.250	0.1647	2.48E-04	4.03E+03
0.275	0.1547	2.33E-04	4.29E+03
0.300	0.1471	2.22E-04	4.51E+03
0.325	0.1400	2.11E-04	4.74E+03
0.350	0.1338	2.02E-04	4.96E+03
0.375	0.1269	1.91E-04	5.23E+03
0.400	0.1213	1.83E-04	5.47E+03
0.425	0.1162	1.75E-04	5.71E+03
0.450	0.1123	1.69E-04	5.91E+03
0.475	0.1073	1.62E-04	6.19E+03
0.500	0.1038	1.56E-04	6.40E+03
0.525	0.1000	1.51E-04	6.64E+03
0.550	0.0963	1.45E-04	6.90E+03

Table A-9 Continued

Time, s	Absorbance	[9], M	$[9]^{-1}, M^{-1}$
0.575	0.0925	1.39E-04	7.18E+03
0.600	0.0907	1.37E-04	7.32E+03
0.625	0.0874	1.32E-04	7.60E+03
0.650	0.0841	1.27E-04	7.90E+03
0.675	0.0823	1.24E-04	8.07E+03

Table A-10. Kinetic data for α–methyl-o-xylylene (9) dimerization measured at 30.40 °C in CH_3CN

Time, s	Absorbance	[9], M	$[9]^{-1}, M^{-1}$
0.050	0.3038	4.58E-04	2.19E+03
0.075	0.2759	4.16E-04	2.41E+03
0.100	0.2519	3.79E-04	2.64E+03
0.125	0.2311	3.48E-04	2.87E+03
0.150	0.2128	3.20E-04	3.12E+03
0.175	0.1980	2.98E-04	3.35E+03
0.200	0.1845	2.78E-04	3.60E+03
0.225	0.1733	2.61E-04	3.83E+03
0.250	0.1632	2.46E-04	4.07E+03
0.275	0.1538	2.32E-04	4.32E+03
0.300	0.1462	2.20E-04	4.54E+03
0.325	0.1388	2.09E-04	4.78E+03
0.350	0.1319	1.99E-04	5.03E+03
0.375	0.1258	1.89E-04	5.28E+03
0.400	0.1207	1.82E-04	5.50E+03
0.425	0.1164	1.75E-04	5.70E+03
0.450	0.1110	1.67E-04	5.98E+03
0.475	0.1072	1.61E-04	6.19E+03
0.500	0.1022	1.54E-04	6.50E+03
0.525	0.0992	1.49E-04	6.69E+03
0.550	0.0951	1.43E-04	6.98E+03

Table A-10. Continued

Time, s	Absorbance	[5], M	[5]$^{-1}$, M^{-1}
0.575	0.0933	1.41E-04	7.12E+03
0.600	0.0896	1.35E-04	7.41E+03
0.625	0.0874	1.32E-04	7.60E+03
0.650	0.0834	1.26E-04	7.96E+03
0.675	0.0820	1.23E-04	8.10E+03

Table A-11. Kinetic data for α–methyl-o-xylylene (9) dimerization measured at 38.40 °C in CH_3CN

Time, s	Absorbance	[9], M	$[9]^{-1}, M^{-1}$
0.050	0.3277	4.94E-04	2.03E+03
0.075	0.2899	4.37E-04	2.29E+03
0.100	0.2583	3.89E-04	2.57E+03
0.125	0.2337	3.52E-04	2.84E+03
0.150	0.2131	3.21E-04	3.12E+03
0.175	0.1949	2.94E-04	3.41E+03
0.200	0.1808	2.72E-04	3.67E+03
0.225	0.1676	2.52E-04	3.96E+03
0.250	0.1564	2.36E-04	4.25E+03
0.275	0.1463	2.20E-04	4.54E+03
0.300	0.1392	2.10E-04	4.77E+03
0.325	0.1314	1.98E-04	5.05E+03
0.350	0.1237	1.86E-04	5.37E+03
0.375	0.1177	1.77E-04	5.64E+03
0.400	0.1114	1.68E-04	5.96E+03
0.425	0.1066	1.61E-04	6.23E+03
0.450	0.1026	1.55E-04	6.47E+03
0.475	0.0983	1.48E-04	6.75E+03
0.500	0.0944	1.42E-04	7.03E+03
0.525	0.0908	1.37E-04	7.31E+03
0.550	0.0873	1.31E-04	7.61E+03

Table A-11. Continued

Time, s	Absorbance	[9], M	$[9]^{-1}, M^{-1}$
0.575	0.0849	1.28E-04	7.82E+03
0.600	0.0818	1.23E-04	8.12E+03
0.625	0.0784	1.18E-04	8.47E+03
0.650	0.0760	1.14E-04	8.74E+03
0.675	0.0736	1.11E-04	9.02E+03

Table A-12. Kinetic data for α–methyl-o-xylylene (9) dimerization measured at 38.40 °C in CH_3CN

Time, s	Absorbance	[9], M	$[9]^{-1}, M^{-1}$
0.050	0.3247	4.89E-04	2.04E+03
0.075	0.2871	4.32E-04	2.31E+03
0.100	0.2556	3.85E-04	2.60E+03
0.125	0.2316	3.49E-04	2.87E+03
0.150	0.2115	3.19E-04	3.14E+03
0.175	0.1942	2.92E-04	3.42E+03
0.200	0.1792	2.70E-04	3.71E+03
0.225	0.1673	2.52E-04	3.97E+03
0.250	0.1561	2.35E-04	4.25E+03
0.275	0.1472	2.22E-04	4.51E+03
0.300	0.1384	2.08E-04	4.80E+03
0.325	0.1318	1.98E-04	5.04E+03
0.350	0.1237	1.86E-04	5.37E+03
0.375	0.1177	1.77E-04	5.64E+03
0.400	0.1121	1.69E-04	5.92E+03
0.425	0.1077	1.62E-04	6.17E+03
0.450	0.1022	1.54E-04	6.50E+03
0.475	0.0990	1.49E-04	6.71E+03
0.500	0.0947	1.43E-04	7.01E+03
0.525	0.0911	1.37E-04	7.29E+03
0.550	0.0876	1.32E-04	7.58E+03

Table A-12. Continued

Time, s	Absorbance	[9], M	$[9]^{-1}$, M^{-1}
0.575	0.0845	1.27E-04	7.86E+03
0.600	0.0814	1.23E-04	8.16E+03
0.625	0.0789	1.19E-04	8.42E+03
0.650	0.0759	1.14E-04	8.75E+03
0.675	0.0742	1.12E-04	8.95E+03

Table A-13. Kinetic data for α–methyl-*o*-xylylene (9) dimerization measured at 38.40 °C in CH$_3$CN

Time, s	Absorbance	[9], M	[9]$^{-1}$, M^{-1}
0.050	0.3327	5.01E-04	2.00E+03
0.075	0.2922	4.40E-04	2.27E+03
0.100	0.2609	3.93E-04	2.55E+03
0.125	0.2342	3.53E-04	2.84E+03
0.150	0.2150	3.24E-04	3.09E+03
0.175	0.1962	2.95E-04	3.38E+03
0.200	0.1808	2.72E-04	3.67E+03
0.225	0.1692	2.55E-04	3.92E+03
0.250	0.1580	2.38E-04	4.20E+03
0.275	0.1474	2.22E-04	4.50E+03
0.300	0.1399	2.11E-04	4.75E+03
0.325	0.1317	1.98E-04	5.04E+03
0.350	0.1251	1.88E-04	5.31E+03
0.375	0.1183	1.78E-04	5.61E+03
0.400	0.1135	1.71E-04	5.85E+03
0.425	0.1076	1.62E-04	6.17E+03
0.450	0.1036	1.56E-04	6.41E+03
0.475	0.0982	1.48E-04	6.76E+03
0.500	0.0950	1.43E-04	6.99E+03
0.525	0.0914	1.38E-04	7.26E+03
0.550	0.0886	1.33E-04	7.49E+03

Table A-13. Continued

Time, s	Absorbance	[9], M	$[9]^{-1}, M^{-1}$
0.575	0.0851	1.28E-04	7.80E+03
0.600	0.0820	1.23E-04	8.10E+03
0.625	0.0796	1.20E-04	8.34E+03
0.650	0.0772	1.16E-04	8.60E+03
0.675	0.0741	1.12E-04	8.96E+03

Table A-14. Kinetic data for α–methyl-o-xylylene (9) dimerization measured at 45.60 °C in CH$_3$CN

Time, s	Absorbance	[9], M	[9]$^{-1}$, M^{-1}
0.050	0.3423	5.16E-04	1.94E+03
0.075	0.2956	4.45E-04	2.25E+03
0.100	0.2585	3.89E-04	2.57E+03
0.125	0.2303	3.47E-04	2.88E+03
0.150	0.2070	3.12E-04	3.21E+03
0.175	0.1882	2.83E-04	3.53E+03
0.200	0.1731	2.61E-04	3.84E+03
0.225	0.1593	2.40E-04	4.17E+03
0.250	0.1475	2.22E-04	4.50E+03
0.275	0.1379	2.08E-04	4.82E+03
0.300	0.1292	1.95E-04	5.14E+03
0.325	0.1215	1.83E-04	5.47E+03
0.350	0.1149	1.73E-04	5.78E+03
0.375	0.1082	1.63E-04	6.14E+03
0.400	0.1029	1.55E-04	6.45E+03
0.425	0.0983	1.48E-04	6.75E+03
0.450	0.0921	1.39E-04	7.21E+03
0.475	0.0897	1.35E-04	7.40E+03
0.500	0.0843	1.27E-04	7.88E+03
0.525	0.0813	1.22E-04	8.17E+03
0.550	0.0777	1.17E-04	8.55E+03

Table A-15. Kinetic data for α–methyl-*o*-xylylene (**9**) dimerization measured at 45.60 °C in CH_3CN

Time, s	Absorbance	[9], M	$[9]^{-1}, M^{-1}$
0.050	0.3465	5.22E-04	1.92E+03
0.075	0.2972	4.48E-04	2.23E+03
0.100	0.2615	3.94E-04	2.54E+03
0.125	0.2322	3.50E-04	2.86E+03
0.150	0.2088	3.14E-04	3.18E+03
0.175	0.1900	2.86E-04	3.49E+03
0.200	0.1744	2.63E-04	3.81E+03
0.225	0.1602	2.41E-04	4.14E+03
0.250	0.1488	2.24E-04	4.46E+03
0.275	0.1387	2.09E-04	4.79E+03
0.300	0.1305	1.97E-04	5.09E+03
0.325	0.1220	1.84E-04	5.44E+03
0.350	0.1151	1.73E-04	5.77E+03
0.375	0.1097	1.65E-04	6.05E+03
0.400	0.1037	1.56E-04	6.40E+03
0.425	0.0981	1.48E-04	6.77E+03
0.450	0.0936	1.41E-04	7.09E+03
0.475	0.0895	1.35E-04	7.42E+03
0.500	0.0861	1.30E-04	7.71E+03
0.525	0.0821	1.24E-04	8.09E+03
0.550	0.0798	1.20E-04	8.32E+03

Table A-16. Kinetic data for α–methyl-o-xylylene (9) dimerization measured at 45.60 °C in CH_3CN

Time, s	Absorbance	[9], M	$[9]^{-1}, M^{-1}$
0.050	0.3397	5.12E-04	1.95E+03
0.075	0.2929	4.41E-04	2.27E+03
0.100	0.2566	3.86E-04	2.59E+03
0.125	0.2272	3.42E-04	2.92E+03
0.150	0.2059	3.10E-04	3.22E+03
0.175	0.1864	2.81E-04	3.56E+03
0.200	0.1710	2.58E-04	3.88E+03
0.225	0.1574	2.37E-04	4.22E+03
0.250	0.1468	2.21E-04	4.52E+03
0.275	0.1365	2.06E-04	4.86E+03
0.300	0.1279	1.93E-04	5.19E+03
0.325	0.1209	1.82E-04	5.49E+03
0.350	0.1141	1.72E-04	5.82E+03
0.375	0.1080	1.63E-04	6.15E+03
0.400	0.1020	1.54E-04	6.51E+03
0.425	0.0968	1.46E-04	6.86E+03
0.450	0.0927	1.40E-04	7.16E+03
0.475	0.0890	1.34E-04	7.46E+03
0.500	0.0846	1.27E-04	7.85E+03
0.525	0.0813	1.22E-04	8.17E+03
0.550	0.0776	1.17E-04	8.56E+03

Table A-17. Rate constants for the dimerization of **9** at various temperatures

Temperature, °C	Dimerization rate constant k_2 for **9**, $M^{-1}s^{-1}$			
	Trial 1	Trial 2	Trial 3	Average
15.5	6784	6731	6875	6797±73
23.8	8262	8252	8295	8270±23
30.4	9418	9500	9536	9485±60
38.4	11208	11036	11082	11109±89
45.6	13014	12902	12875	12930±73

Table B-1.   Absorbance values for various concentration of [11]

[7], M	Absorbance of [7]		
	Trial 1	Trial 2	Average
0	0.000	0.000	0.000 [a]
3.31E-04	0.283	0.281	0.282 [a]
4.01E-04	0.336	0.341	0.339 [a]
5.75E-04	0.456	0.453	0.454 [b]
7.10E-04	0.539	0.535	0.537 [b]

[a]   The extinction coefficient is determined from these data

[b]   Since the rate for the generation of o-QDM **11** at higher precursor concentration is slower, the maximum absorbance of **11** at these concentrations deviate from the Beer's law. Therefore, these data are ignored in the determination of the extinction coefficient of **11**.

Table B-2. Kinetic data for α–*tert*-butyl-*o*-xylylene (**11**) dimerization measured at 14.75 °C in CH_3CN

Time, s	Absorbance	[11], M	$[11]^{-1}, M^{-1}$
0.00	0.3936	4.65E-04	2.15E+03
1.00	0.2931	3.46E-04	2.89E+03
2.00	0.2325	2.75E-04	3.64E+03
3.00	0.1916	2.26E-04	4.42E+03
4.00	0.1632	1.93E-04	5.19E+03
5.00	0.1421	1.68E-04	5.96E+03
6.00	0.1258	1.49E-04	6.73E+03
7.00	0.1127	1.33E-04	7.51E+03
8.00	0.1024	1.21E-04	8.27E+03
9.00	0.0928	1.10E-04	9.13E+03
10.00	0.0861	1.02E-04	9.84E+03
11.00	0.0795	9.39E-05	1.07E+04
12.00	0.0744	8.79E-05	1.14E+04
13.00	0.0690	8.15E-05	1.23E+04
14.00	0.0641	7.57E-05	1.32E+04
15.00	0.0611	7.22E-05	1.39E+04
16.00	0.0575	6.79E-05	1.47E+04

Table B-3. Kinetic data for α-*tert*-butyl-*o*-xylylene (**11**) dimerization measured at 14.75 °C in CH_3CN

Times, S	Absorbance	[11], M	$[11]^{-1}$, M^{-1}
0.00	0.3880	4.58E-04	2.18E+03
1.00	0.2908	3.43E-04	2.91E+03
2.00	0.2308	2.73E-04	3.67E+03
3.00	0.1900	2.24E-04	4.46E+03
4.00	0.1630	1.92E-04	5.20E+03
5.00	0.1418	1.67E-04	5.97E+03
6.00	0.1263	1.49E-04	6.70E+03
7.00	0.1123	1.33E-04	7.54E+03
8.00	0.1021	1.21E-04	8.29E+03
9.00	0.0928	1.10E-04	9.13E+03
10.00	0.0861	1.02E-04	9.84E+03
11.00	0.0788	9.31E-05	1.07E+04
12.00	0.0741	8.75E-05	1.14E+04
13.00	0.0697	8.23E-05	1.21E+04
14.00	0.0650	7.68E-05	1.30E+04
15.00	0.0607	7.17E-05	1.40E+04
16.00	0.0578	6.83E-05	1.47E+04

Table B-4. Kinetic data for α–*tert*-butyl-*o*-xylylene (11) dimerization measured at 14.75 °C in CH_3CN

Time, s	Absorbance	[11], M	$[11]^{-1}$, M^{-1}
0.00	0.3903	4.61E-04	2.17E+03
1.00	0.2911	3.44E-04	2.91E+03
2.00	0.2308	2.73E-04	3.67E+03
3.00	0.1892	2.23E-04	4.48E+03
4.00	0.1618	1.91E-04	5.23E+03
5.00	0.1408	1.66E-04	6.01E+03
6.00	0.1238	1.46E-04	6.84E+03
7.00	0.1121	1.32E-04	7.55E+03
8.00	0.1012	1.20E-04	8.37E+03
9.00	0.0912	1.08E-04	9.29E+03
10.00	0.0839	9.91E-05	1.01E+04
11.00	0.0781	9.22E-05	1.08E+04
12.00	0.0723	8.54E-05	1.17E+04
13.00	0.0683	8.07E-05	1.24E+04
14.00	0.0636	7.51E-05	1.33E+04
15.00	0.0603	7.12E-05	1.40E+04
16.00	0.0561	6.62E-05	1.51E+04

Table B-5. Kinetic data for α–*tert*-butyl-*o*-xylylene (11) dimerization measured at 23.85 °C in CH_3CN

Time, s	Absorbance	[11], M	[11]$^{-1}$, M^{-1}
0.00	0.3917	4.63E-04	2.16E+03
1.00	0.2718	3.21E-04	3.12E+03
2.00	0.2060	2.43E-04	4.11E+03
3.00	0.1664	1.97E-04	5.09E+03
4.00	0.1392	1.64E-04	6.08E+03
5.00	0.1194	1.41E-04	7.09E+03
6.00	0.1036	1.22E-04	8.17E+03
7.00	0.0925	1.09E-04	9.15E+03
8.00	0.0830	9.80E-05	1.02E+04
9.00	0.0753	8.89E-05	1.12E+04
10.00	0.0691	8.16E-05	1.23E+04
11.00	0.0630	7.44E-05	1.34E+04
12.00	0.0585	6.91E-05	1.45E+04

Table B-6. Kinetic data for α–*tert*-butyl-*o*-xylylene (11) dimerization measured at 23.85 °C in CH_3CN

Time, s	Absorbance	[11], M	$[11]^{-1}$, M^{-1}
0.00	0.3924	4.63E-04	2.16E+03
1.00	0.2701	3.19E-04	3.14E+03
2.00	0.2062	2.44E-04	4.11E+03
3.00	0.1658	1.96E-04	5.11E+03
4.00	0.1389	1.64E-04	6.10E+03
5.00	0.1202	1.42E-04	7.04E+03
6.00	0.1048	1.24E-04	8.08E+03
7.00	0.0929	1.10E-04	9.12E+03
8.00	0.0834	9.85E-05	1.02E+04
9.00	0.0747	8.82E-05	1.13E+04
10.00	0.0678	8.01E-05	1.25E+04
11.00	0.0623	7.36E-05	1.36E+04
12.00	0.0585	6.91E-05	1.45E+04

Table B-7. Kinetic data for α–*tert*-butyl-*o*-xylylene (**11**) dimerization measured at 23.85 °C in CH$_3$CN

Time, s	Absorbance	[11], M	[11]$^{-1}$,M^{-1}
0.00	0.3920	4.63E-04	2.16E+03
1.00	0.2722	3.21E-04	3.11E+03
2.00	0.2052	2.42E-04	4.13E+03
3.00	0.1667	1.97E-04	5.08E+03
4.00	0.1390	1.64E-04	6.09E+03
5.00	0.1192	1.41E-04	7.10E+03
6.00	0.1047	1.24E-04	8.09E+03
7.00	0.0925	1.09E-04	9.15E+03
8.00	0.0833	9.84E-05	1.02E+04
9.00	0.0753	8.89E-05	1.12E+04
10.00	0.0690	8.15E-05	1.23E+04
11.00	0.0635	7.50E-05	1.33E+04
12.00	0.0581	6.86E-05	1.46E+04

Table B-8. Kinetic data for α–*tert*-butyl-*o*-xylylene (**11**) dimerization measured at 29.65 °C in CH_3CN

Time, s	Absorbance	[11], M	$[11]^{-1}$, M^{-1}
0.00	0.4054	4.79E-04	2.09E+03
0.80	0.2838	3.35E-04	2.98E+03
1.60	0.2187	2.58E-04	3.87E+03
2.40	0.1781	2.10E-04	4.75E+03
3.20	0.1500	1.77E-04	5.65E+03
4.00	0.1278	1.51E-04	6.63E+03
4.80	0.1125	1.33E-04	7.53E+03
5.60	0.1002	1.18E-04	8.45E+03
6.40	0.0900	1.06E-04	9.41E+03
7.20	0.0828	9.78E-05	1.02E+04
8.00	0.0749	8.85E-05	1.13E+04
8.80	0.0689	8.14E-05	1.23E+04
9.60	0.0640	7.56E-05	1.32E+04
10.40	0.0594	7.01E-05	1.43E+04

Table B-9. Kinetic data for α–*tert*-butyl-o-xylylene (**11**) dimerization measured at 29.65 °C in CH_3CN

Time, s	Absorbance	[11], M	[11]$^{-1}$, M^{-1}
0.00	0.4129	4.88E-04	2.05E+03
0.80	0.2904	3.43E-04	2.92E+03
1.60	0.2215	2.62E-04	3.82E+03
2.40	0.1802	2.13E-04	4.70E+03
3.20	0.1511	1.78E-04	5.60E+03
4.00	0.1296	1.53E-04	6.53E+03
4.80	0.1131	1.34E-04	7.49E+03
5.60	0.1005	1.19E-04	8.43E+03
6.40	0.0902	1.07E-04	9.39E+03
7.20	0.0819	9.67E-05	1.03E+04
8.00	0.0748	8.83E-05	1.13E+04
8.80	0.0698	8.24E-05	1.21E+04
9.60	0.0642	7.58E-05	1.32E+04
10.40	0.0596	7.04E-05	1.42E+04

Table B-10. Kinetic data for α–*tert*-butyl-*o*-xylylene (**11**) dimerization measured at 29.65 °C in CH_3CN

Time, s	Absorbance	[11], M	$[11]^{-1} \cdot M^{-1}$
0.00	0.4006	4.73E-04	2.11E+03
0.80	0.2826	3.34E-04	3.00E+03
1.60	0.2175	2.57E-04	3.89E+03
2.40	0.1760	2.08E-04	4.81E+03
3.20	0.1488	1.76E-04	5.69E+03
4.00	0.1273	1.50E-04	6.65E+03
4.80	0.1117	1.32E-04	7.58E+03
5.60	0.0997	1.18E-04	8.49E+03
6.40	0.0895	1.06E-04	9.46E+03
7.20	0.0819	9.67E-05	1.03E+04
8.00	0.0747	8.82E-05	1.13E+04
8.80	0.0690	8.15E-05	1.23E+04
9.60	0.0647	7.64E-05	1.31E+04
10.40	0.0602	7.11E-05	1.41E+04

Table B-11. Kinetic data for α-*tert*-butyl-*o*-xylylene (**11**) dimerization
measured at 37.10 °C in CH_3CN

Time, s	Absorbance	[11], M	$[11]^{-1}$, M^{-1}
0.00	0.4010	4.74E-04	2.11E+03
0.80	0.2669	3.16E-04	3.17E+03
1.60	0.2003	2.36E-04	4.23E+03
2.40	0.1589	1.88E-04	5.32E+03
3.20	0.1323	1.57E-04	6.39E+03
4.00	0.1122	1.32E-04	7.55E+03
4.80	0.0940	1.16E-04	8.61E+03
5.60	0.0845	9.81E-05	1.02E+04
6.40	0.0758	8.68E-05	1.15E+04
7.20	0.0683	7.99E-05	1.25E+04
8.00	0.0622	7.35E-05	1.36E+04

Table B-12. Kinetic data for α–*tert*-butyl-*o*-xylylene (**11**) dimerization measured at 37.10 °C in CH_3CN

Time, s	Absorbance	[11], M	$[11]^{-1}$, M^{-1}
0.00	0.4010	4.74E-04	2.11E+03
0.80	0.2669	3.15E-04	3.17E+03
1.60	0.2003	2.37E-04	4.22E+03
2.40	0.1589	1.88E-04	5.32E+03
3.20	0.1323	1.56E-04	6.39E+03
4.00	0.1122	1.33E-04	7.54E+03
4.80	0.0940	1.11E-04	9.00E+03
5.60	0.0845	9.99E-05	1.00E+04
6.40	0.0758	8.96E-05	1.12E+04
7.20	0.0683	8.07E-05	1.24E+04
8.00	0.0622	7.35E-05	1.36E+04

Table B-13. Kinetic data for α–*tert*-butyl-*o*-xylylene (**11**) dimerization measured at 37.10 °C in CH_3CN

Time, s	Absorbance	[11], M	[11^{-1}, M^{-1}
0.00	0.3976	4.70E-04	2.13E+03
0.80	0.2656	3.14E-04	3.19E+03
1.60	0.1989	2.35E-04	4.26E+03
2.40	0.1584	1.87E-04	5.35E+03
3.20	0.1313	1.55E-04	6.45E+03
4.00	0.1055	1.25E-04	8.03E+03
4.80	0.0954	1.13E-04	8.88E+03
5.60	0.0838	9.90E-05	1.01E+04
6.40	0.0751	8.87E-05	1.13E+04
7.20	0.0680	8.03E-05	1.25E+04
8.00	0.0618	7.30E-05	1.37E+04

Table B-14. Kinetic data for α–*tert*-butyl-*o*-xylylene (11) dimerization measured at 44.45 °C in CH₃CN

Time, s	Absorbance	[11], M	[11]$^{-1}$, M^{-1}
0.00	0.3936	4.65E-04	2.15E+03
0.40	0.3069	3.62E-04	2.76E+03
0.80	0.2515	2.97E-04	3.37E+03
1.20	0.2124	2.51E-04	3.99E+03
1.60	0.1837	2.17E-04	4.61E+03
2.00	0.1616	1.91E-04	5.24E+03
2.40	0.1439	1.70E-04	5.88E+03
2.80	0.1296	1.53E-04	6.53E+03
3.20	0.1189	1.40E-04	7.12E+03
3.60	0.1021	1.21E-04	8.29E+03
4.00	0.0943	1.11E-04	8.98E+03
4.40	0.0898	1.06E-04	9.43E+03
4.80	0.0847	1.00E-04	1.00E+04
5.20	0.0790	9.33E-05	1.07E+04
5.60	0.0750	8.86E-05	1.13E+04
6.00	0.0707	8.35E-05	1.20E+04
6.40	0.0670	7.91E-05	1.26E+04
6.80	0.0643	7.59E-05	1.32E+04

Table B-15. Kinetic data for α-*tert*-butyl-*o*-xylylene (11) dimerization measured at 44.45 °C in CH_3CN

Time, s	Absorbance	[11], M	$[11]^{-1}$, M^{-1}
0.00	0.4209	4.97E-04	2.01E+03
0.40	0.3260	3.85E-04	2.60E+03
0.80	0.2637	3.11E-04	3.21E+03
1.20	0.2208	2.61E-04	3.84E+03
1.60	0.1902	2.25E-04	4.45E+03
2.00	0.1666	1.97E-04	5.08E+03
2.40	0.1474	1.74E-04	5.74E+03
2.80	0.1119	1.32E-04	7.57E+03 [a]
3.20	0.1022	1.21E-04	8.29E+03 [a]
3.60	0.1002	1.18E-04	8.45E+03 [a]
4.00	0.0953	1.13E-04	8.89E+03
4.40	0.0885	1.05E-04	9.57E+03
4.80	0.0824	9.73E-05	1.03E+04
5.20	0.0780	9.21E-05	1.09E+04
5.60	0.0740	8.74E-05	1.14E+04
6.00	0.0697	8.23E-05	1.21E+04
6.40	0.0666	7.86E-05	1.27E+04
6.80	0.0624	7.37E-05	1.36E+04

[a]   These data deviate from the second order decay curve of **11** and are ignored in the linear regression for the rate constant determination

Table B-16. Kinetic data for α-*tert*-butyl-*o*-xylylene (**11**) dimerization
measured at 44.45 °C in CH_3CN

Time, s	Absorbance	[11], M	[11]$^{-1}$, M^{-1}
0.00	0.4044	4.78E-04	2.09E+03
0.40	0.3111	3.67E-04	2.72E+03
0.80	0.2536	2.99E-04	3.34E+03
1.20	0.2138	2.52E-04	3.96E+03
1.60	0.1841	2.17E-04	4.60E+03
2.00	0.1623	1.92E-04	5.22E+03
2.40	0.1295	1.53E-04	6.54E+03 [a]
2.80	0.1095	1.29E-04	7.73E+03 [a]
3.20	0.1082	1.28E-04	7.83E+03 [a]
3.60	0.1022	1.21E-04	8.29E+03
4.00	0.0953	1.13E-04	8.89E+03
4.40	0.0888	1.05E-04	9.54E+03
4.80	0.0822	9.71E-05	1.03E+04
5.20	0.0750	8.86E-05	1.13E+04
5.60	0.0710	8.38E-05	1.19E+04
6.00	0.0673	7.95E-05	1.26E+04
6.40	0.0636	7.51E-05	1.33E+04
6.80	0.0618	7.30E-05	1.37E+04

[a] These data deviate from the second order decay curve of **11** and are ignored in the linear regression for the rate constant determination

Table B-17. Rate constants for the dimerization of **11** at various temperatures

Temperature, °C	Dimerization rate constant k_2 for **11**, $M^{-1}S^{-1}$			
	Trial 1	Trial 2	Trial 3	average
14.75	7.860E+02	7.696E+02	7.908E+02	782 ± 11
23.85	1.027E+03	1.036E+03	1.027E+03	1029 ± 5
29.65	1.147E+03	1.168E+03	1.154E+03	1156 ± 10
37.10	1.463E+03	1.445E+03	1.454E+03	1454 ± 9
44.45	1.657E+03	1.763E+03	1.725E+03	1715 ± 53

Table C-1. Compositions of the solution A for **9** (Trial 1)

Solution A	volume, mL	Concentration		
		Methyl methacrylate, M	Precursor **9**, M	Diphenyl-methane , M
1	10	3.009×10^{-2}	1.079×10^{-3}	3.971×10^{-4}
2	10	6.019×10^{-2}	1.079×10^{-3}	3.971×10^{-4}
3	10	9.028×10^{-2}	1.079×10^{-3}	3.971×10^{-4}
4	10	12.04×10^{-2}	1.079×10^{-3}	3.971×10^{-4}
5	10	15.05×10^{-2}	1.079×10^{-3}	3.971×10^{-4}

Table C-2. Compositions of the solution A for **9** (Trial 2)

Solution A	volume, mL	Concentration		
		Methyl methacrylate, M	Precursor **9**, M	Diphenyl-methane , M
1	10	3.251×10^{-2}	1.045×10^{-3}	4.589×10^{-4}
2	10	6.502×10^{-2}	1.045×10^{-3}	4.589×10^{-4}
3	10	9.753×10^{-2}	1.045×10^{-3}	4.589×10^{-4}
4	10	12.04×10^{-2}	1.045×10^{-3}	4.589×10^{-4}
5	10	16.25×10^{-2}	1.045×10^{-3}	4.589×10^{-4}

Table C-3. Kinetic data for competition experiments[a] of dimerization and Diels-Alder reaction of o-QDM **9** at 0.20 °C

[MMA][b], 10^{-2}M	D_2/DA^c(exptl.)	D_2/DA^c (calcd.[d])
1.505	4.678±0.070	4.264
3.009	2.535±0.037	2.432
4.514	1.738±0.029	1.749
6.019	1.343±0.017	1.382
7.523	1.070±0.004	1.151

a   The data are derived from solution A listed in Table XIII.
b   The concentration of methyl methacrylate which is equal to one half of the original concentration after being mixed with equal volume of TBAF solution.
c   The final dimerization products to Diels-Alder adducts ratio.
d   The ratio is calculated on the basis of the rate constant ratio found by a non-linear curve fitting from the experimental data. The rate constant ratio $k_2/k_{DA}=476\pm16$.

Table C-4. Kinetic data for competition experiments[a] of dimerization and Diels-Alder reaction of o-QDM **9** at 8.40 °C

[MMA][b], 10^{-2}M	D_2/DA^c(exptl.)	D_2/DA^c (calcd.[d])
1.626	4.064±0.115	3.685
3.251	2.253±0.079	2.101
4.877	1.450±0.032	1.510
6.024	1.293±0.018	1.270
8.128	0.8950±0.045	0.9915

a The data are derived from solution A listed in Table XIV.
b The concentration of methyl methacrylate which is equal to one half of the original concentration after being mixed with equal volume of TBAF solution.
c The final dimerization products to Diels-Alder adducts ratio.
d The ratio is calculated on the basis of the rate constant ratio found by a non-linear curve fitting from the experimental data. The rate constant ratio k_2/k_{DA}=440±18.

Table C-5.   Kinetic data for competition experiments[a] of dimerization and Diels-Alder reaction of o-QDM **9** at 17.70 °C

[MMA][b], 10^{-2}M	D_2/DA^c(exptl.)	D_2/DA^c (calcd.[d])
1.505	3.972±0.074	3.612
3.009	2.135±0.013	2.059
4.514	1.454±0.009	1.480
6.019	1.145±0.056	1.168
7.523	0.9072±0.034	0.9714

a   The data are derived from solution A listed in Table XIII.
b   The concentration of methyl methacrylate which is equal to one half of the original concentration after being mixed with equal volume of TBAF solution.
c   The final dimerization products to Diels-Alder adducts ratio.
d   The ratio is calculated on the basis of the rate constant ratio found by a non-linear curve fitting from the experimental data. The rate constant ratio $k_2/k_{DA}=385\pm13$.

Table C-6. Kinetic data for competition experiments[a] of dimerization and Diels-Alder reaction of o-QDM **9** at 21.30 °C

$[MMA]^b$, 10^{-2}M	D_2/DA^c(exptl.)	D_2/DA^c (calcd.[d])
1.505	3.747±0.172	3.481
3.009	2.061±0.040	1.984
4.514	1.400±0.062	1.425
6.019	1.110±0.043	1.125
7.523	0.879±0.002	0.935

a   The data are derived from solution A listed in Table XIII.
b· The concentration of methyl methacrylate which is equal to one half of the original concentration after being mixed with equal volume of TBAF solution.
c   The final dimerization products to Diels-Alder adducts ratio
d   The ratio is calculated on the basis of the rate constant ratio found by a non-linear curve fitting from the experimental data. The rate constant ratio $k_2/k_{DA}=367\pm11$.

Table C-7. Kinetic data for competition experiments[a] of dimerization and Diels-Alder reaction of o-QDM **9** at 29.00 °C

[MMA][b], 10^{-2}M	D_2/DA^c(exptl.)	D_2/DA^c (calcd.[d])
1.626	3.477±0.084	2.934
3.251	1.835±0.077	1.671
4.877	1.133±0.078	1.199
6.024	1.065±0.021	1.007
8.128	0.671±0.074	0.784

a The data are derived from solution A listed in Table XIV.
b The concentration of methyl methacrylate which is equal to one half of the original concentration after being mixed with equal volume of TBAF solution.
c The final dimerization products to Diels-Alder adducts ratio.
d The ratio is calculated on the basis of the rate constant ratio found by a non-linear curve fitting from the experimental data. The rate constant ratio $k_2/k_{DA}=332\pm23$.

Table C-8. Kinetic data for competition experiments[a] of dimerization and Diels-Alder reaction of o-QDM **9** at 32.50 °C

[MMA][b], 10^{-2}M	D_2/DA^c(exptl.)	D_2/DA^c (calcd.[d])
1.505	3.297±0.134	3.076
3.009	1.818±0.079	1.753
4.514	1.281±0.032	1.258
6.019	0.9702±0.018	0.9917
7.523	0.8235±0.045	0.8235

a The data are derived from solution A listed in Table XIII.
b The concentration of methyl methacrylate which is equal to one half of the original concentration after being mixed with equal volume of TBAF solution.
c The final dimerization products to Diels-Alder adducts ratio.
d The ratio is calculated on the basis of the rate constant ratio found by a non-linear curve fitting from the experimental data. The rate constant ratio k_2/k_{DA}=315±10.

Table D-1. Compositions of the solution A for **11** (Trial 1)

| Solution A | volume, mL | Concentration | | |
		Methyl methacrylate, M	Precursor **11**, M	Diphenyl-methane , M
1	10	1.288×10^{-1}	1.026×10^{-3}	4.779×10^{-4}
2	10	2.040×10^{-1}	1.026×10^{-3}	4.779×10^{-4}
3	10	2.959×10^{-1}	1.026×10^{-3}	4.779×10^{-4}
4	10	3.720×10^{-1}	1.026×10^{-3}	4.779×10^{-4}
5	10	5.331×10^{-1}	1.026×10^{-3}	4.779×10^{-4}

Table D-2. Compositions of the solution A for **11** (Trial 2)

| Solution A | volume, mL | Concentration | | |
		Methyl methacrylate, M	Precursor **11**, M	Diphenyl-methane , M
1	10	1.157×10^{-1}	1.180×10^{-3}	5.231×10^{-4}
2	10	2.054×10^{-1}	1.180×10^{-3}	5.231×10^{-4}
3	10	2.844×10^{-1}	1.180×10^{-3}	5.231×10^{-4}
4	10	3.632×10^{-1}	1.180×10^{-3}	5.231×10^{-4}
5	10	5.288×10^{-1}	1.180×10^{-3}	5.231×10^{-4}

Table D-3   Kinetic data for competition experiments[a] of dimerization and Diels-Alder reaction of o-QDM **11** at 2.90 °C

[MMA][b], 10^{-1}M	D_2/DA^c(exptl.)	D_2/DA^c (calcd.[d])
0.644	5.126±0.119	5.172
1.020	3.614±0.198	3.561
1.480	2.730±0.015	2.633
1.860	2.261±0.025	2.188
2.665	1.529±0.020	1.630

a   The data are derived from solution A listed in Table XV.
b   The concentration of methyl methacrylate which is equal to one half of the original concentration after being mixed with equal volume of TBAF solution.
c   The final dimerization products to Diels-Alder adducts ratio.
d   The ratio is calculated on the basis of the rate constant ratio found by a non-linear curve fitting from the experimental data. The rate constant ratio k_2/k_{DA}=2692±62.

Table D-4. Kinetic data for competition experiments[a] of dimerization and Diels-Alder reaction of o-QDM **11** at 3.40 °C

[MMA][b], 10^{-1}M	D_2/DA^c(exptl.)	D_2/DA^c (calcd.[d])
0.578	6.664±0.183	6.176
1.027	3.995±0.097	3.871
1.422	2.949±0.092	2.973
1.816	2.240±0.116	2.439
2.644	1.809±0.018	1.797

[a] The data are derived from solution A listed in Table XVI.
[b] The concentration of methyl methacrylate which is equal to one half of the original concentration after being mixed with equal volume of TBAF solution.
[c] The final dimerization products to Diels-Alder adducts ratio.
[d] The ratio is calculated on the basis of the rate constant ratio found by a non-linear curve fitting from the experimental data. The rate constant ratio $k_2/k_{DA}=2618\pm86$.

Table D-5   Kinetic data for competition experiments[a] of dimerization and
Diels-Alder reaction of o-QDM **11** at 10.10 °C

[MMA][b], 10^{-1}M	D_2/DA^c(exptl.)	D_2/DA^c (calcd.[d])
0.644	4.198±0.008	4.268
1.020	2.963±0.052	2.939
1.480	2.149±0.005	2.173
1.860	1.875±0.007	1.805
2.665	1.323±0.002	1.343

a   The data are derived from solution A listed in Table XV.
b   The concentration of methyl methacrylate which is equal to one half of the original
concentration after being mixed with equal volume of TBAF solution.
c   The final dimerization products to Diels-Alder adducts ratio.
d   The ratio is calculated on the basis of the rate constant ratio found by a non-linear
curve fitting from the experimental data. The rate constant ratio k_2/k_{DA}=2126±27.

Table D-6 Kinetic data for competition experiments[a] of dimerization and Diels-Alder reaction of o-QDM **11** at 15.80 °C

[MMA][b], 10^{-1}M	D_2/DA^c(exptl.)	D_2/DA^c (calcd.[d])
0.578	5.057±0.196	5.025
1.027	3.194±0.062	3.152
1.422	2.406±0.023	2.421
1.816	2.009±0.051	1.985
2.644	1.427±0.001	1.461

a. The data are derived from solution A listed in Table XVI.
b The concentration of methyl methacrylate which is equal to one half of the original concentration after being mixed with equal volume of TBAF solution.
c The final dimerization products to Diels-Alder adducts ratio.
d The ratio is calculated on the basis of the rate constant ratio found by a non-linear curve fitting from the experimental data. The rate constant ratio k_2/k_{DA}=2029±17.

Table D-7. Kinetic data for competition experiments[a] of dimerization and Diels-Alder reaction of o-QDM **11** at 23.10 °C

[MMA][b], 10^{-1}M	D_2/DA^c(exptl.)	D_2/DA^c (calcd.[d])
0.644	3.598±0.044	3.558
1.020	2.540±0.043	2.451
1.480	1.847±0.039	1.811
1.860	1.439±0.083	1.516
2.665	1.110±0.044	1.117

[a] The data are derived from solution A listed in Table XV.
[b] The concentration of methyl methacrylate which is equal to one half of the original concentration after being mixed with equal volume of TBAF solution.
[c] The final dimerization products to Diels-Alder adducts ratio.
[d] The ratio is calculated on the basis of the rate constant ratio found by a non-linear curve fitting from the experimental data. The rate constant ratio k_2/k_{DA}=1699±32.

Table D-8. Kinetic data for competition experiments[a] of dimerization and Diels-Alder reaction of o-QDM **11** at 32.90 °C

[MMA][b], 10^{-1}M	D_2/DA^c(exptl.)	D_2/DA^c (calcd.[d])
0.578	3.662±0.005	3.645
1.027	2..341±0.060	2.287
1.422	1.776±0.038	1.756
1.816	1.397±0.022	1.438
2.644	1.047±0.041	1.055

a   The data are derived from solution A listed in Table XVI.
b   The concentration of methyl methacrylate which is equal to one half of the original concentration after being mixed with equal volume of TBAF solution.
c   The final dimerization products to Diels-Alder adducts ratio.
d   The ratio is calculated on the basis of the rate constant ratio found by a non-linear curve fitting from the experimental data. The rate constant ratio $k_2/k_{DA}=1366\pm15$.

Table D-9. Kinetic data for competition experiments[a] of dimerization and Diels-Alder reaction of o-QDM **11** at 33.35 °C

[MMA][b], 10^{-1}M	D_2/DA^c(exptl.)	D_2/DA^c(calcd.[d])
0.644	3.122±0.047	2.861
1.020	2.100±0.060	2.019
1.480	1.442±0.012	1.491
1.860	1.191±0.021	1.236
2.665	0.8847±0.008	0.9164

a   The data are derived from solution A listed in Table XV.
b   The concentration of methyl methacrylate which is equal to one half of the original concentration after being mixed with equal volume of TBAF solution.
c   The final dimerization products to Diels-Alder adducts ratio.
d   The ratio is calculated on the basis of the rate constant ratio found by a non-linear curve fitting from the experimental data. The rate constant ratio k_2/k_{DA}=1332±34.
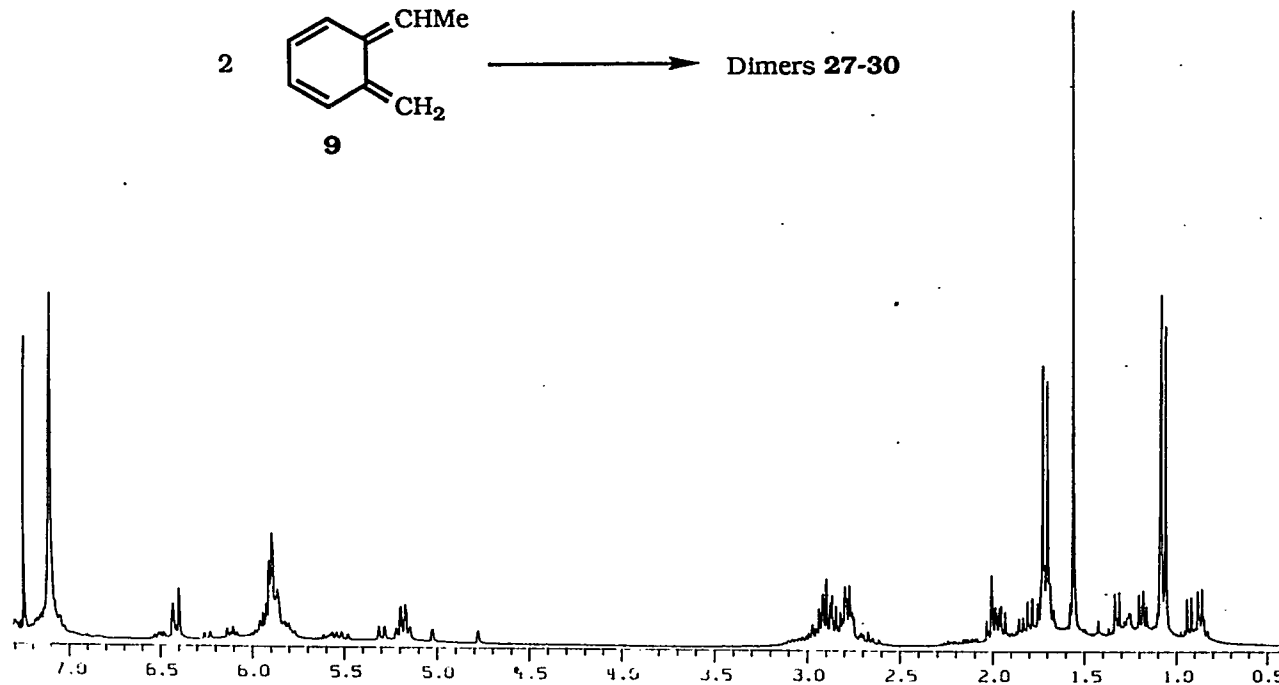
Figure A-1. ^{1}H NMR spectrum (300 MHz, CDCl$_3$) of the dimer mixture of α–methyl-o-xylylene (9).
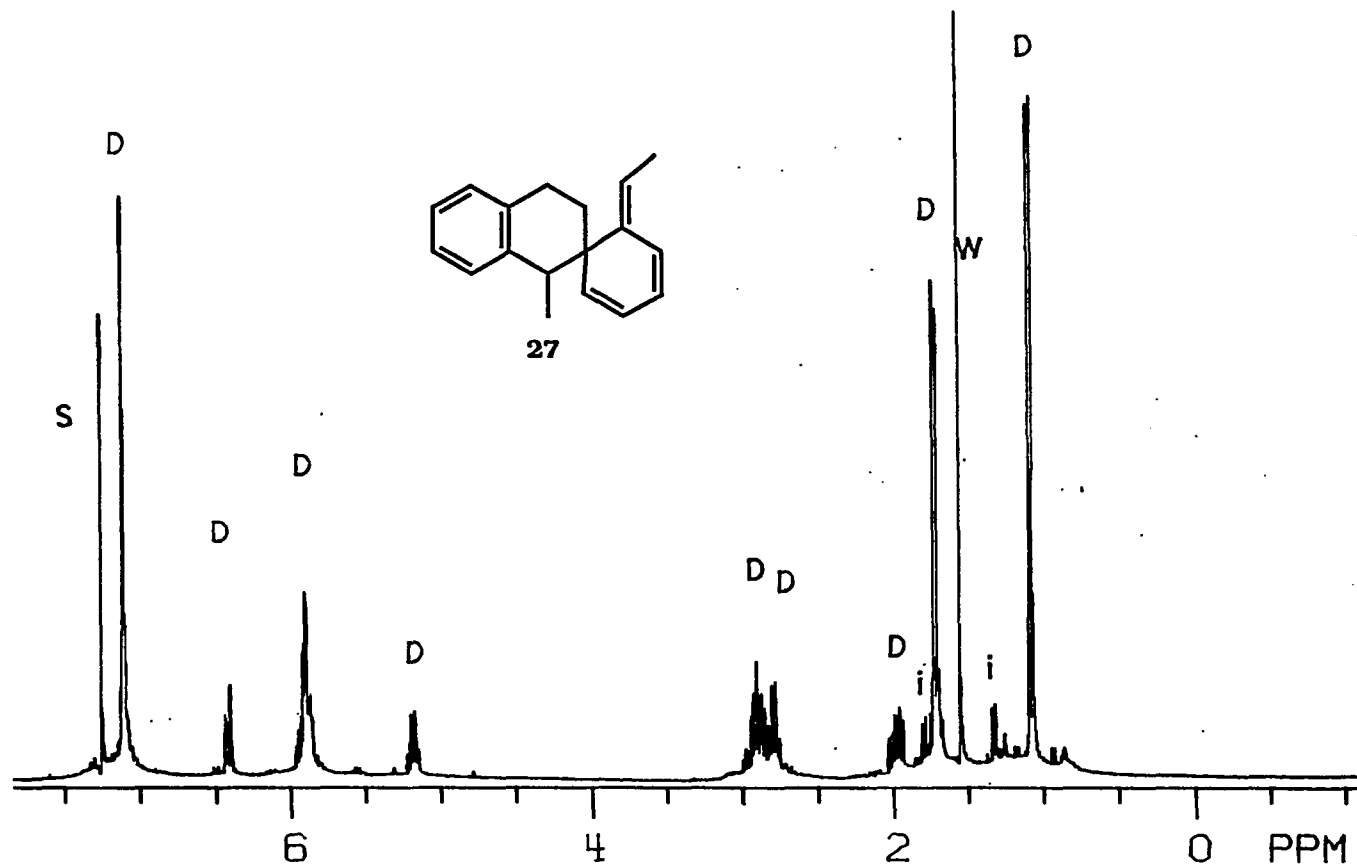
Figure A-2. ^{1}H NMR spectrum (300 MHz, CDCl$_3$) of the [4+2] dimer **27** of α–methyl-o-xylylene (**9**) (s: chloroform, w: H$_2$O, i: impurities, D: dimer **27**).

Figure A-3. ^{1}H NMR spectrum (300 MHz, CDCl$_3$) of the [4+2] dimer **28** of α–methyl-*o*-xylylene (**9**) (s: chloroform, w: H$_2$O, H: high boiling residue from hexanes, the eluent, i: impurities, D: dimer **28**).
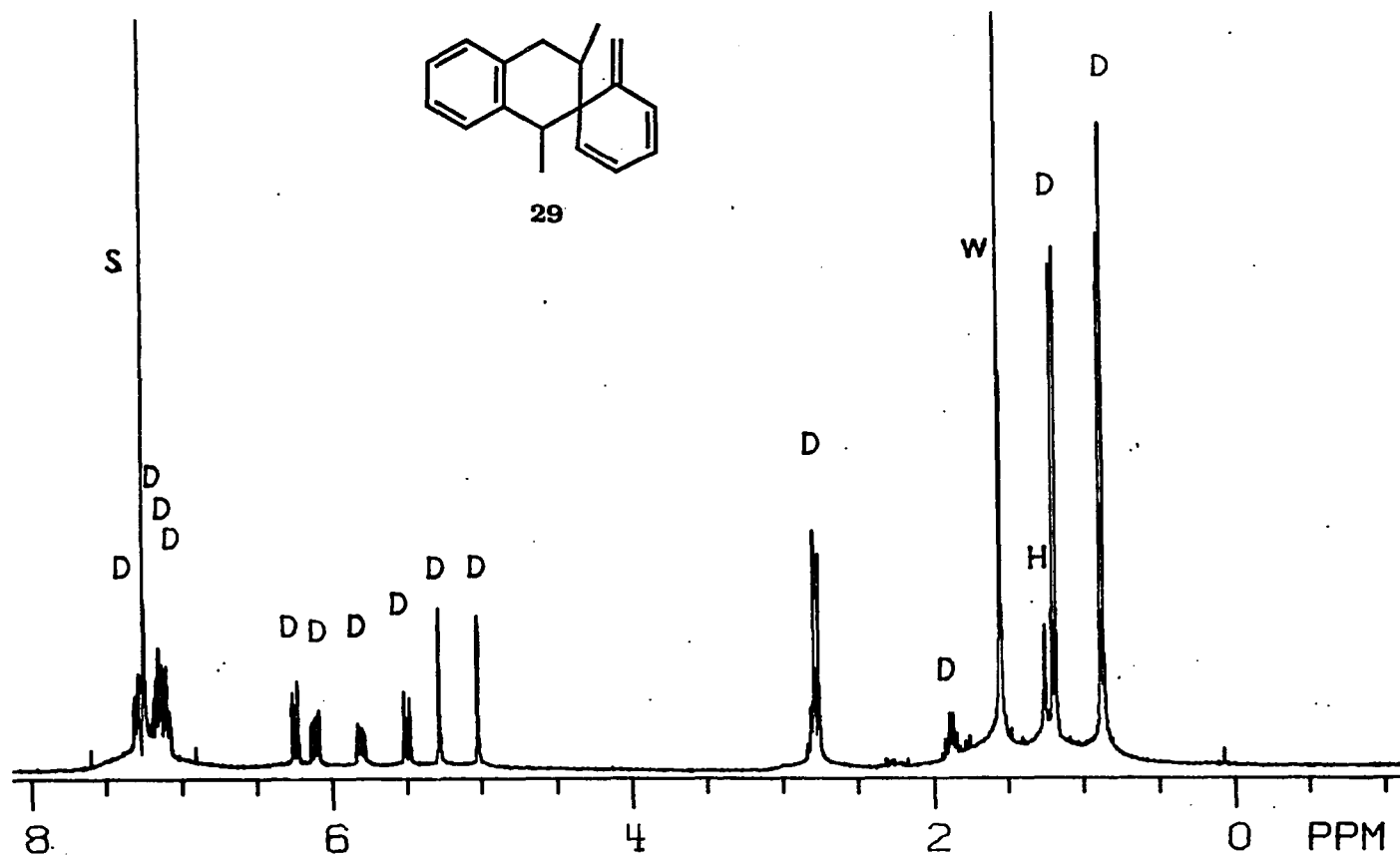
Figure A-4. ^{1}H NMR spectrum (300 MHz, CDCl$_3$) of the [4+2] dimer **29** of α–methyl-o-xylylene (**9**) (s: chloroform, w: H$_2$O, H: high boiling residue from hexanes, the eluent, D: dimer **29**).
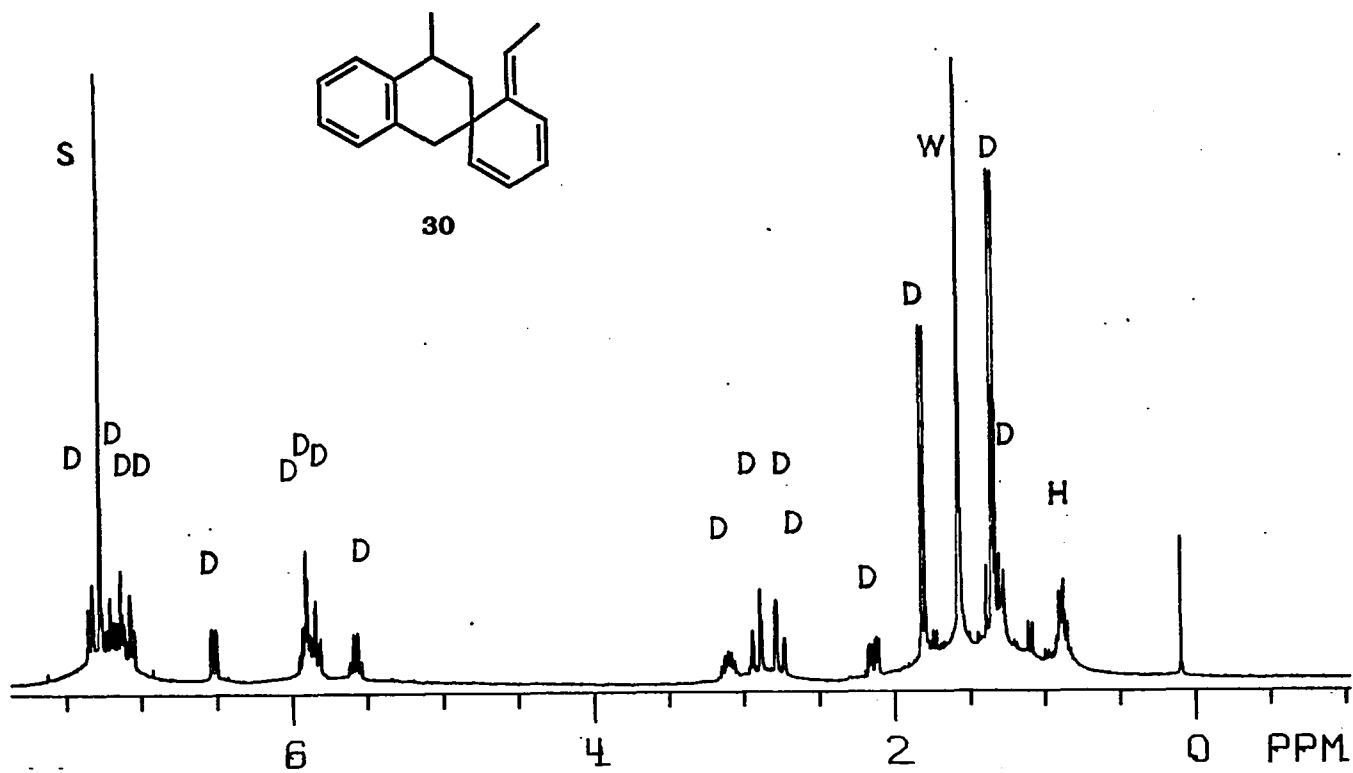
Figure A-5. ^{1}H NMR spectrum (300 MHz, CDCl_3) of the [4+2] dimer **30** of α–methyl-o-xylylene (**9**) (s: chloroform, w: H_2O, H: high boiling residue from hexanes, the eluent, D: dimer **30**).
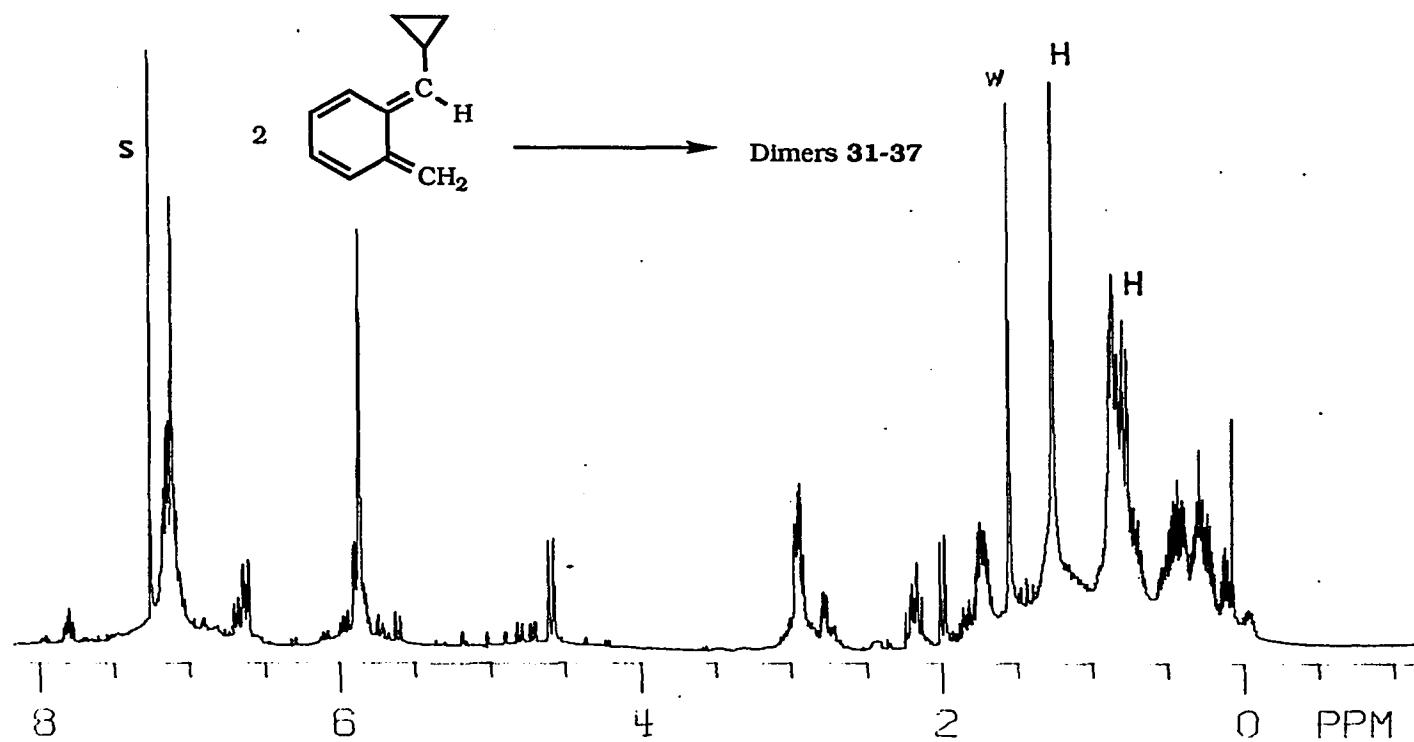
Figure A-6. ^{1}H NMR spectrum (300 MHz, CDCl$_3$) of the dimer mixture of α–cyclopropyl-o-xylylene (**10**) (s: chloroform, w: H$_2$O, H: high boiling residue from hexanes, the eluent).
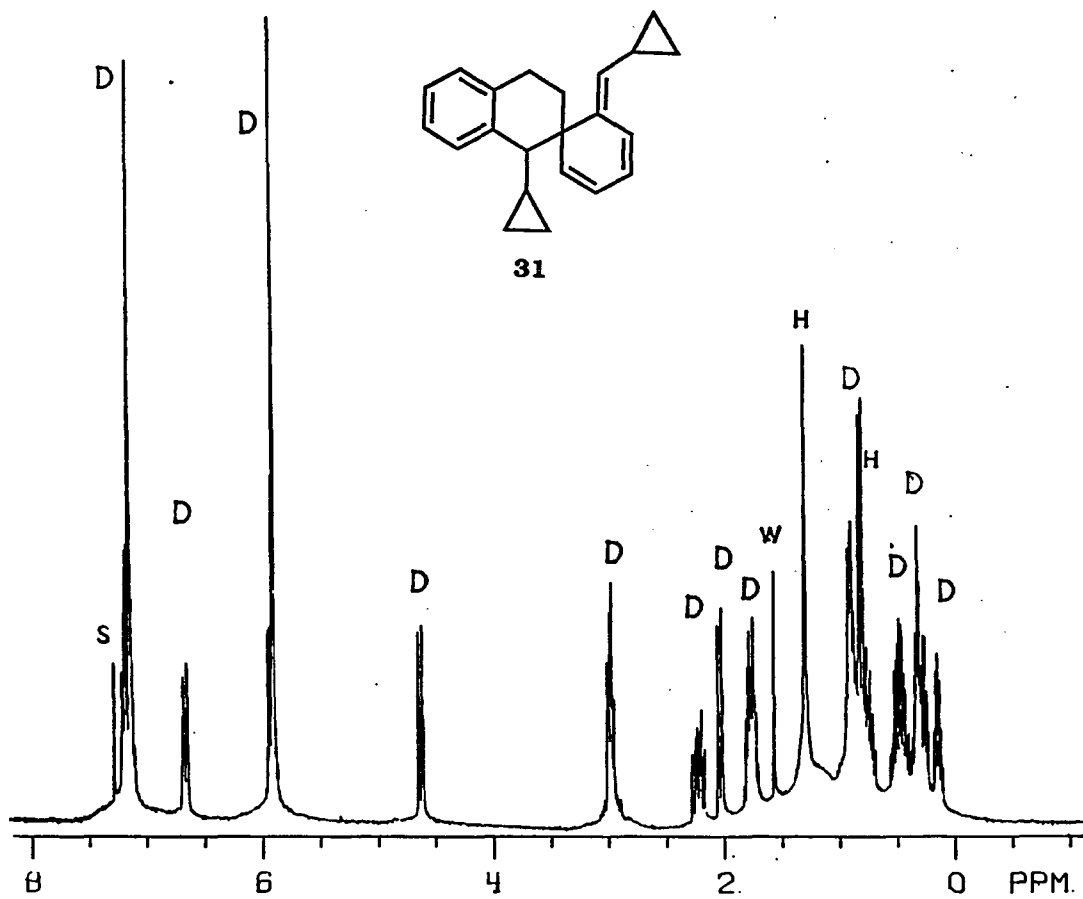
Figure A-7.   ¹H NMR spectrum (300 MHz, CDCl₃) of the [4+2] dimer **31** of α–cyclopropyl-o-xylylene (**10**) (s: chloroform, w: H₂O, H: high boiling residue from hexanes, the eluent, D: dimer **31**).
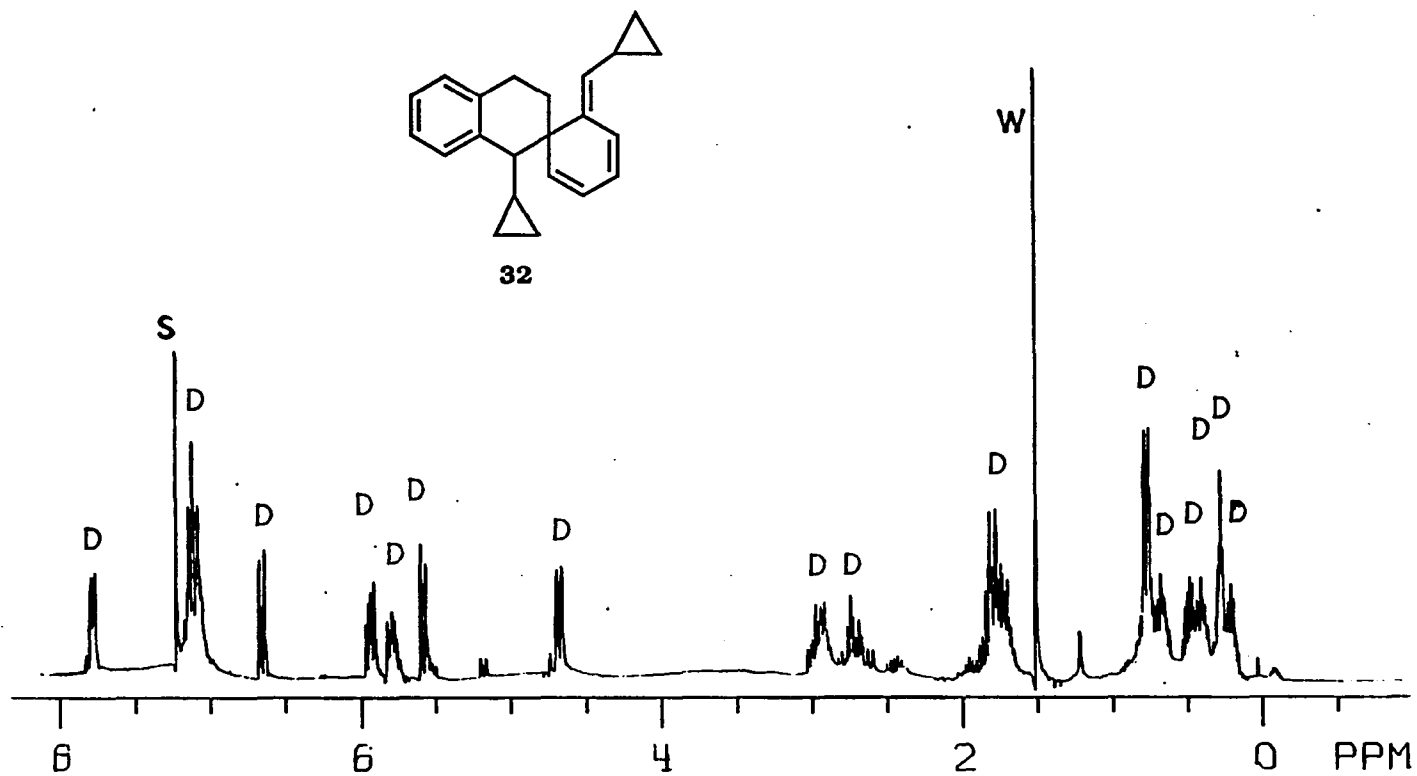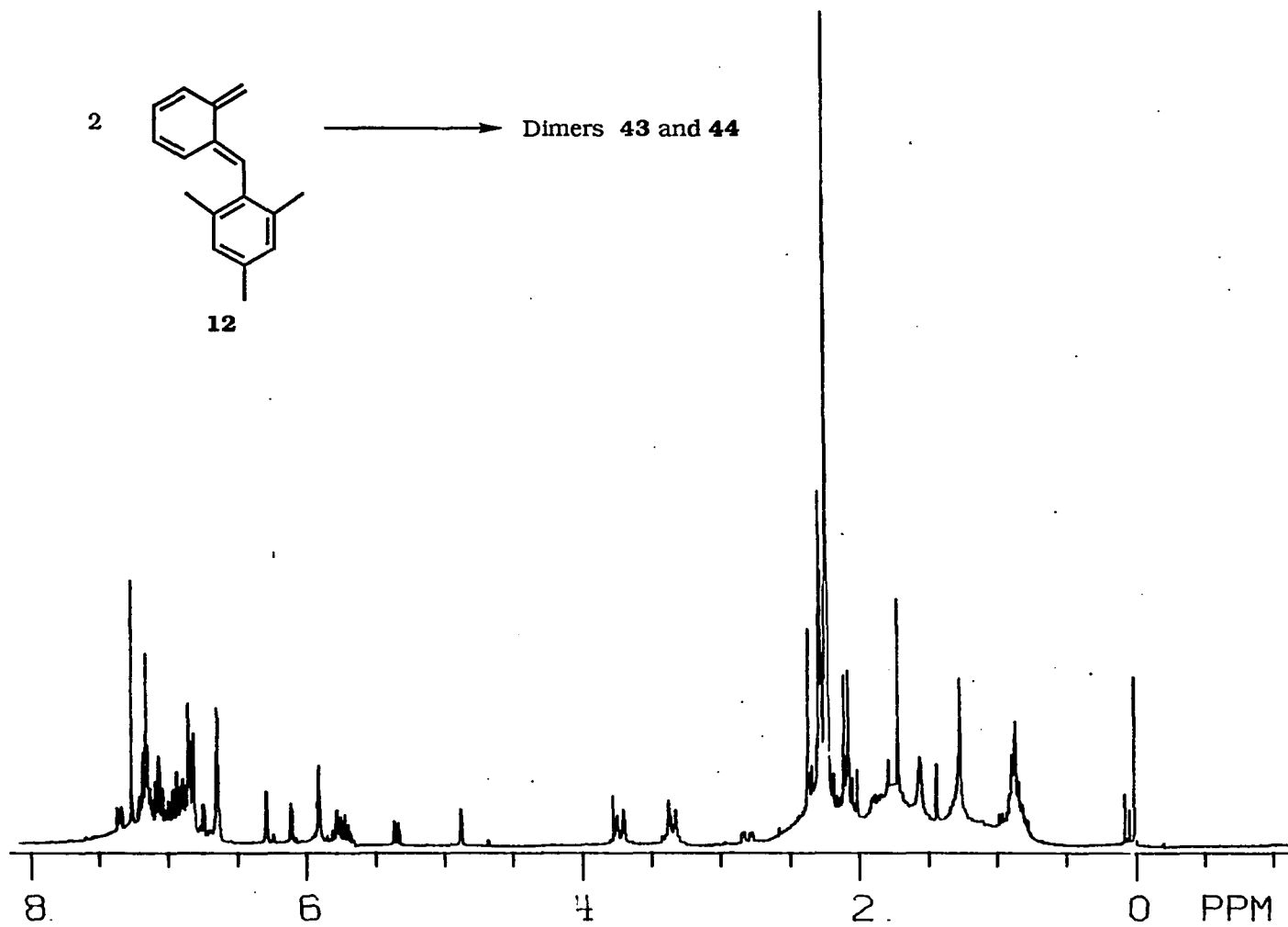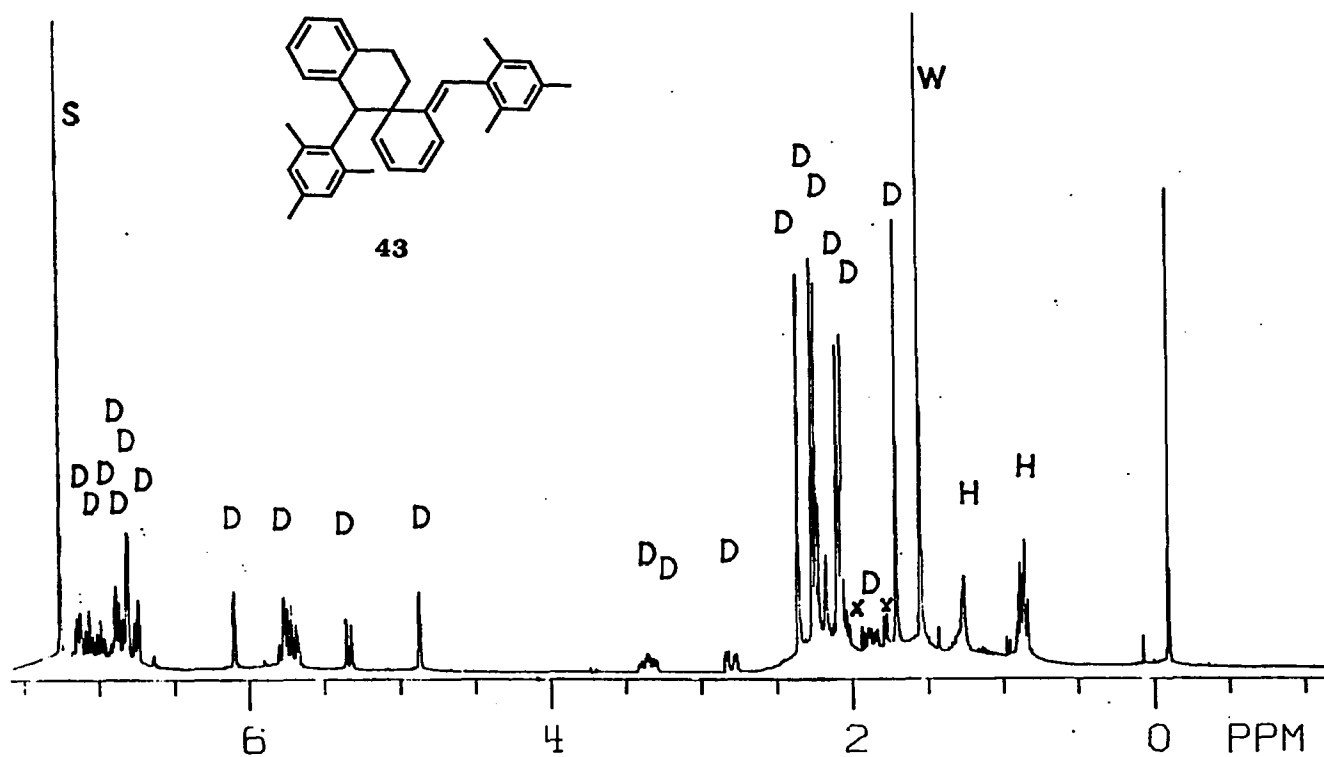
Figure A-8. ^{1}H NMR spectrum (300 MHz, CDCl$_3$) of the [4+2] dimer **32** of α–cyclopropyl-*o*-xylylene (**10**) (s: chloroform, w: H$_2$O, H: high boiling residue from hexanes, the eluent, D: dimer **32**).
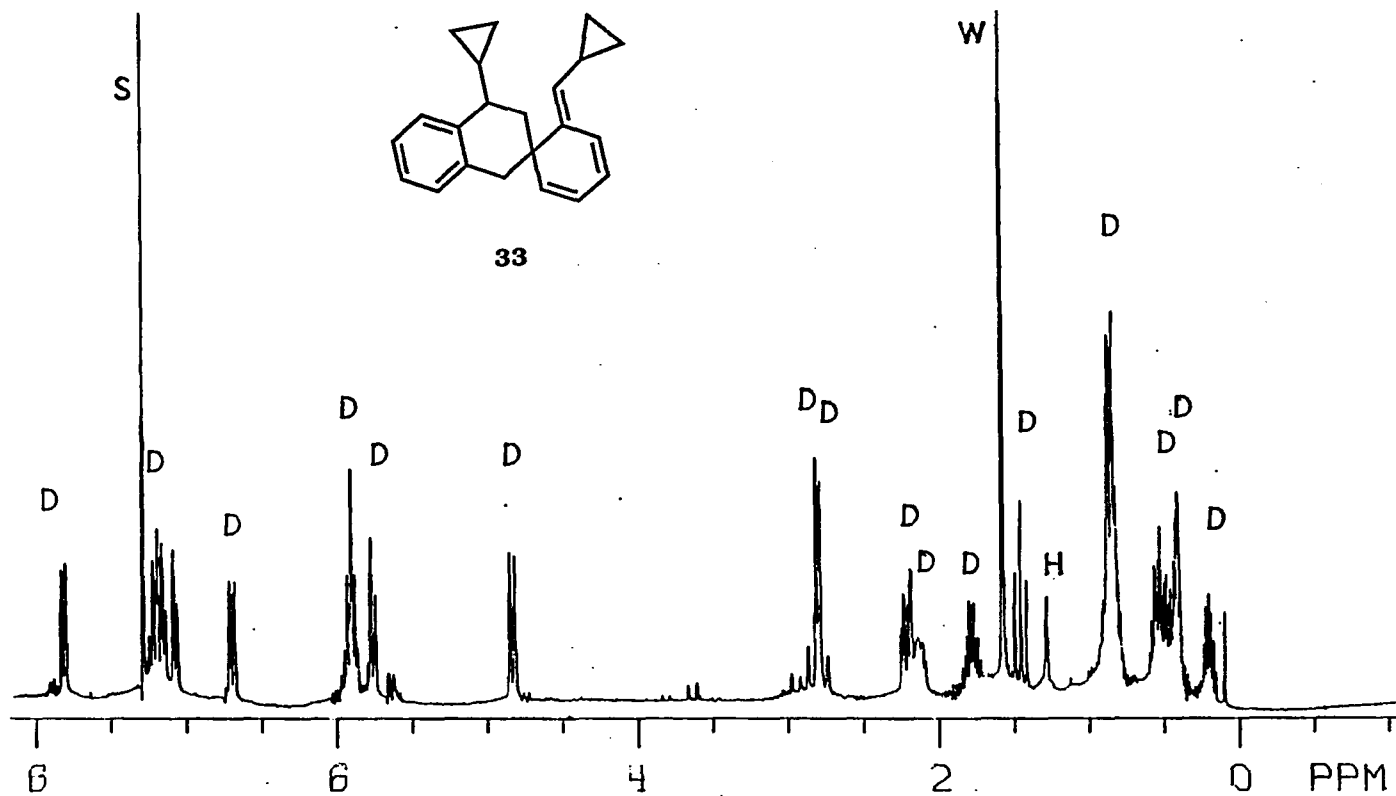
Figure A-9. ^{1}H NMR spectrum (300 MHz, CDCl$_3$) of the [4+2] dimer **33** of α–cyclopropyl-o-xylylene (**10**) (s: chloroform, w: H$_2$O, H: high boiling residue from hexanes, the eluent, D: dimer **33**).

34 + 35

A   A

A′   A′

X   X′

W

6.5   6.0   5.5   5.0   4.5   4.0   3.5   3.0   2.5   2.0   1.5
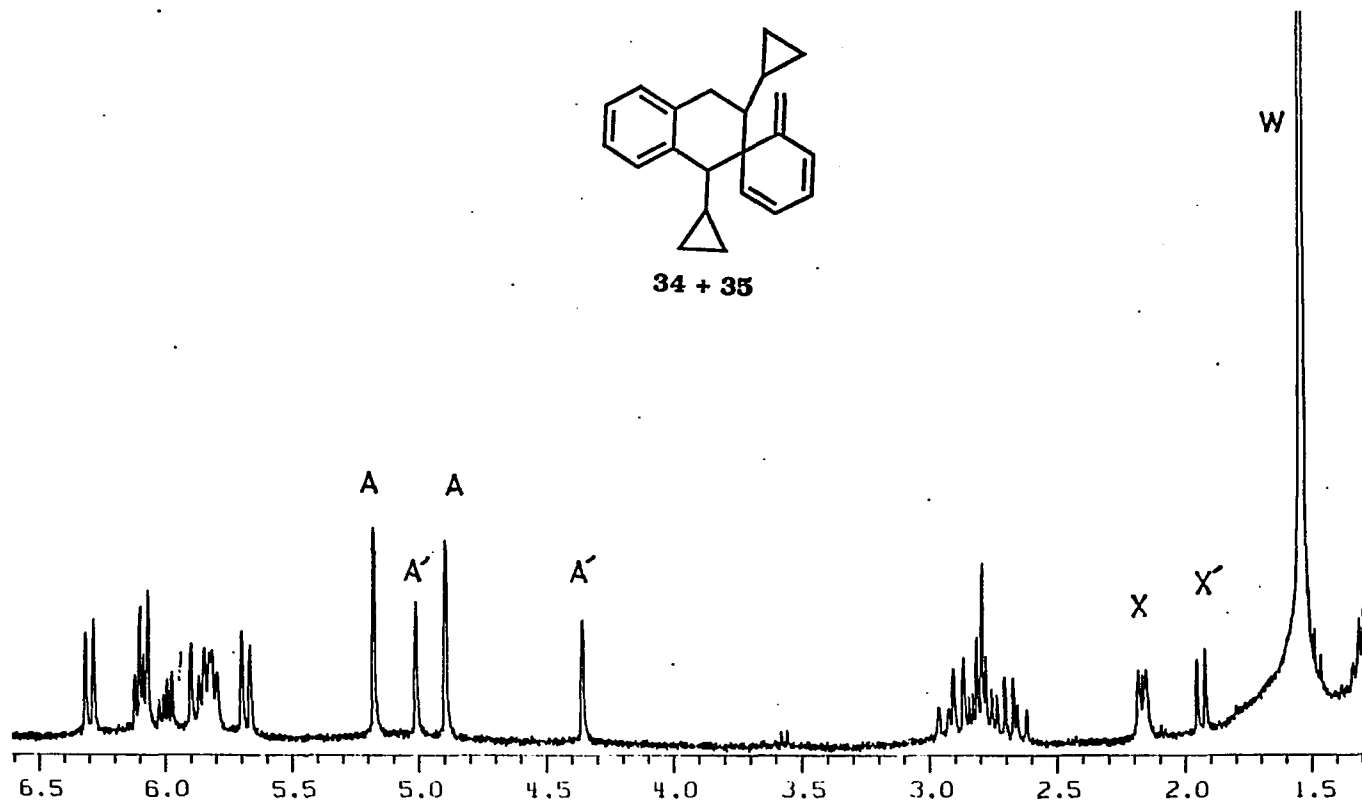
Figure A-10. ^{1}H NMR spectrum (300 MHz, olefin to alphatic region, CDCl$_3$) of the [4+2] dimer **34** and **35** of α–cyclopropyl-o-xylylene **(10)** (w: H$_2$O, A or A': exo-methylene protons of **34** and **35**, X or X': benzylic protons adjacent to the cyclopropyl group).
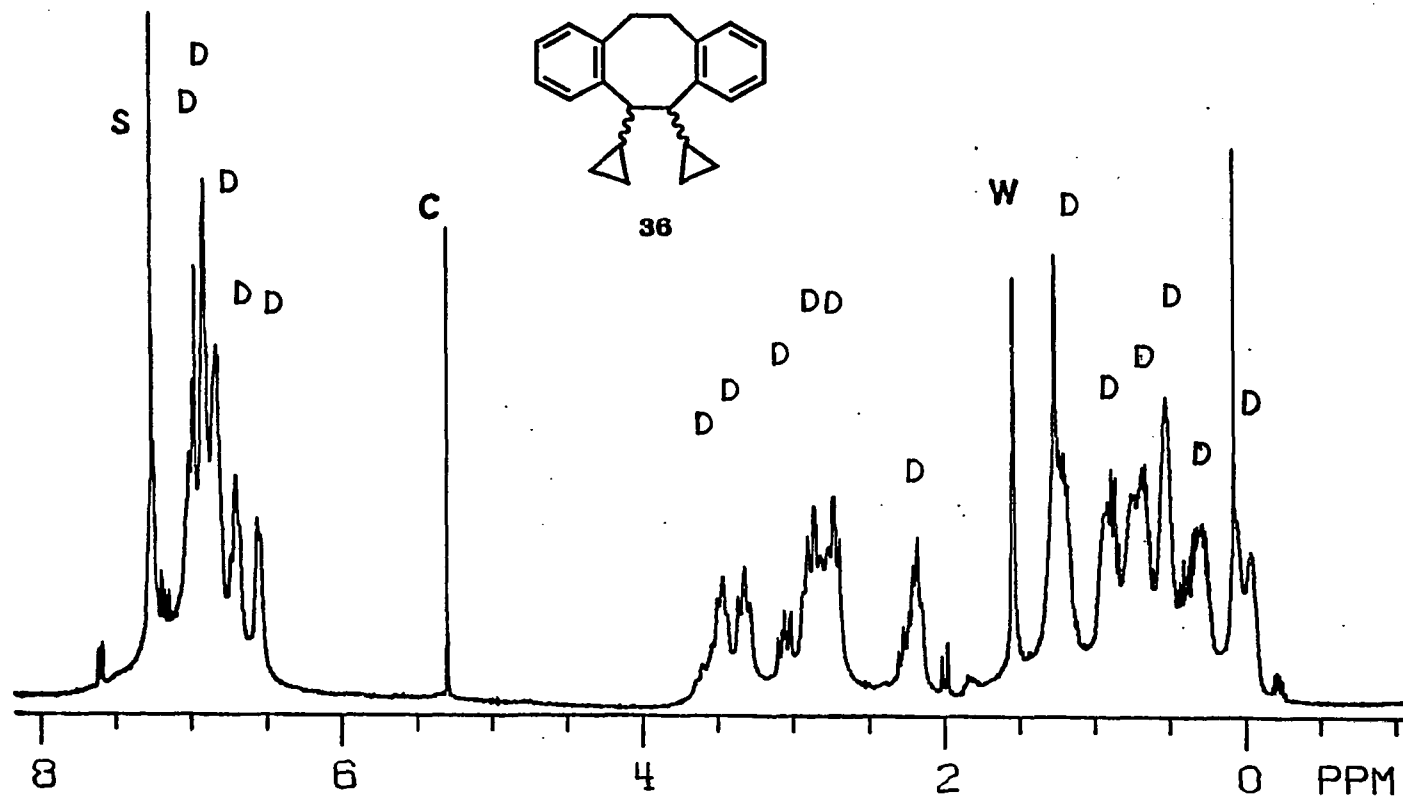
Figure A-11. ^{1}H NMR spectrum (300 MHz, CDCl₃) of the [4+4] dimer **36** of α-cyclopropyl-*o*-xylylene (**10**) (s: chloroform, w: H₂O, H: high boiling residue from hexanes, the eluent, D: dimer **36**. Some cyclopropyl ring proton signals are covered by the signals of high boiling hydrocarbons).
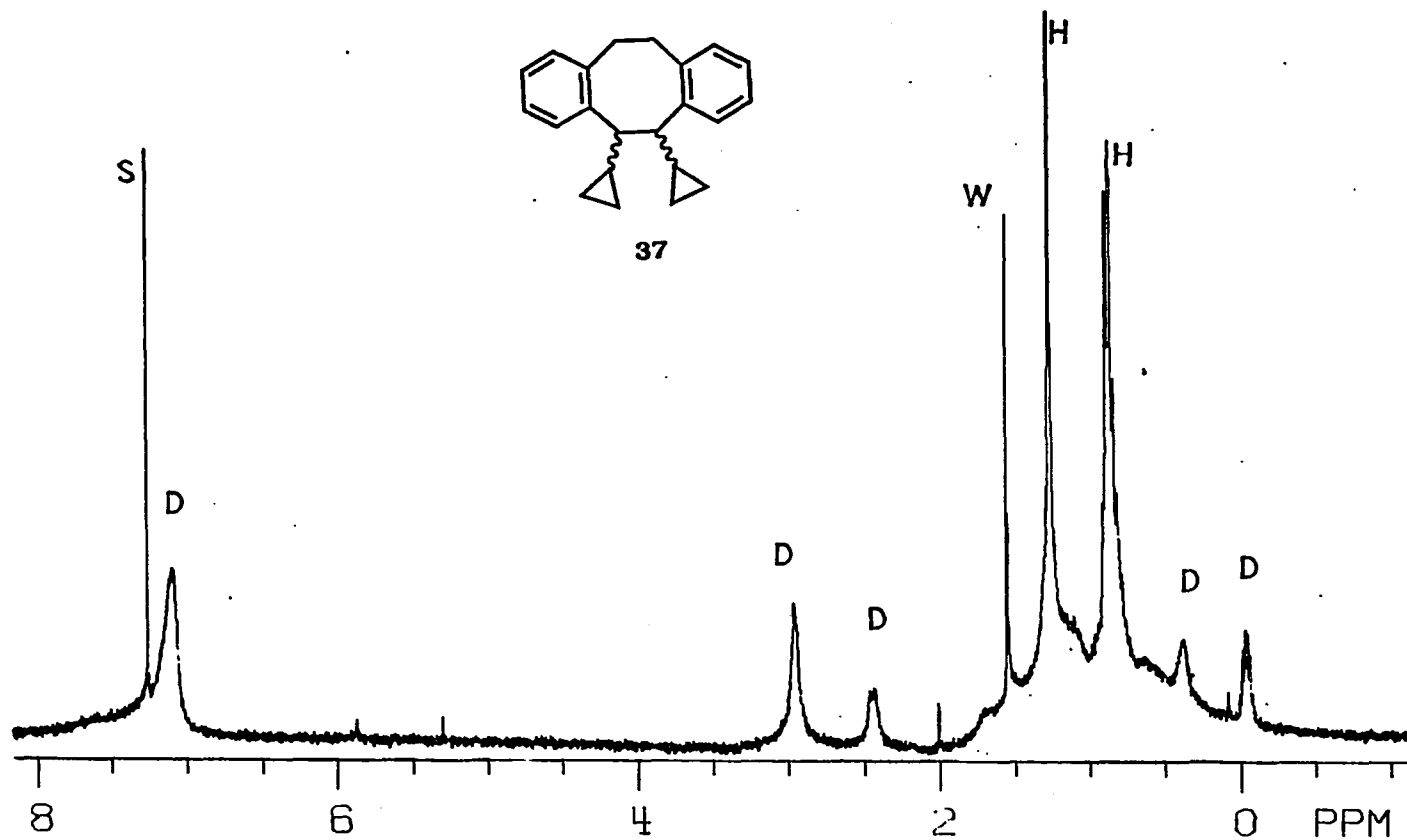
Figure A-12. ^{1}H NMR spectrum (300 MHz, CDCl$_3$) of the [4+4] dimer **37** of α–cyclopropyl-o-xylylene (**10**) (s: chloroform, c: dichloroform, w: H$_2$O, H: high boiling residue from hexanes, the eluent, D: dimer **37**).
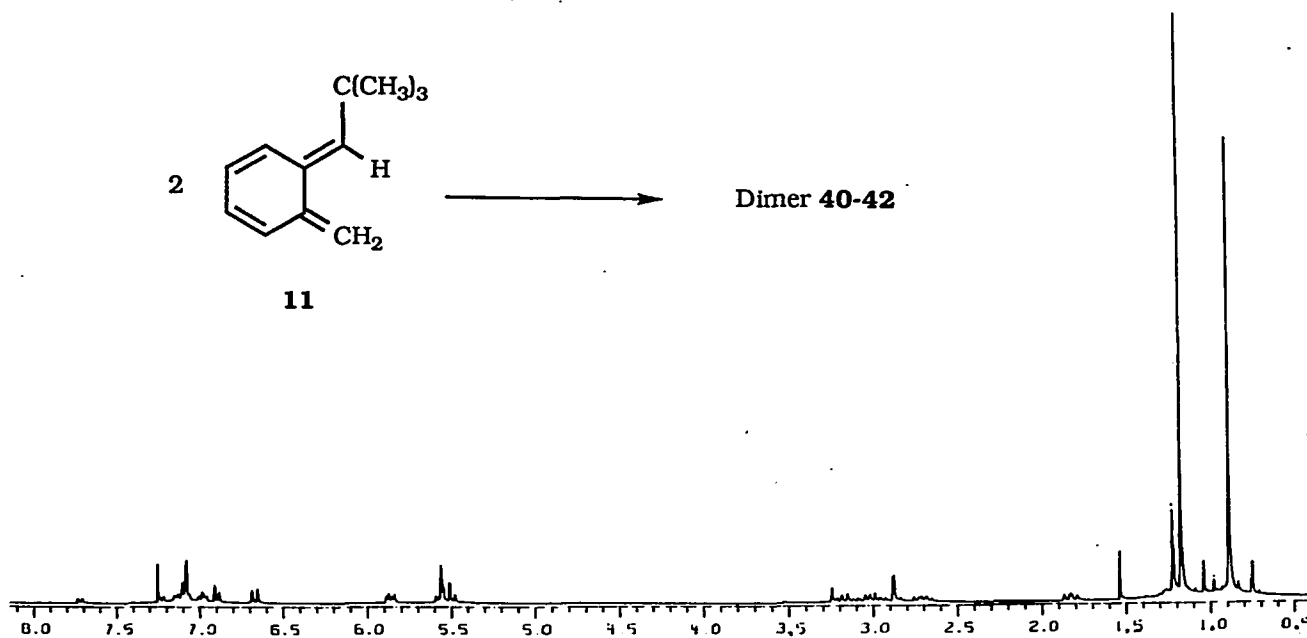
Figure A-13. ^{1}H NMR spectrum (300 MHz, CDCl$_3$) of the dimer mixture of α–*tert*-butyl-*o*-xylylene (**11**).

Compound **40**
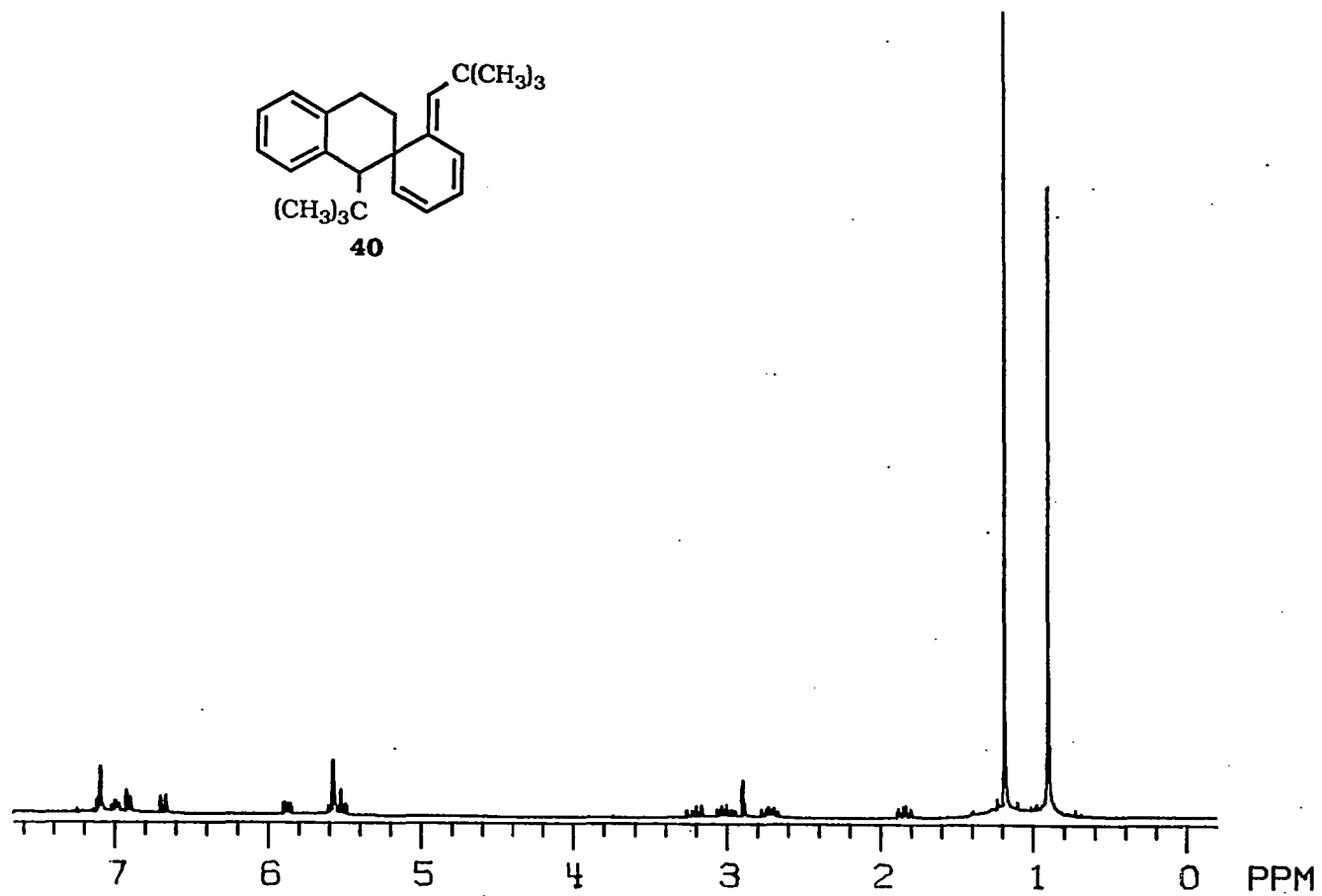
Figure A-14. ^{1}H NMR spectrum (300 MHz, CDCl₃) of the [4+2] dimer **40** of α–*tert*-butyl-*o*-xylylene (**11**).

The structure shown (compound **41**) has substituents (CH₃)₃C and C(CH₃)₃ labeled as $(CH_3)_3C$ and $C(CH_3)_3$.

41
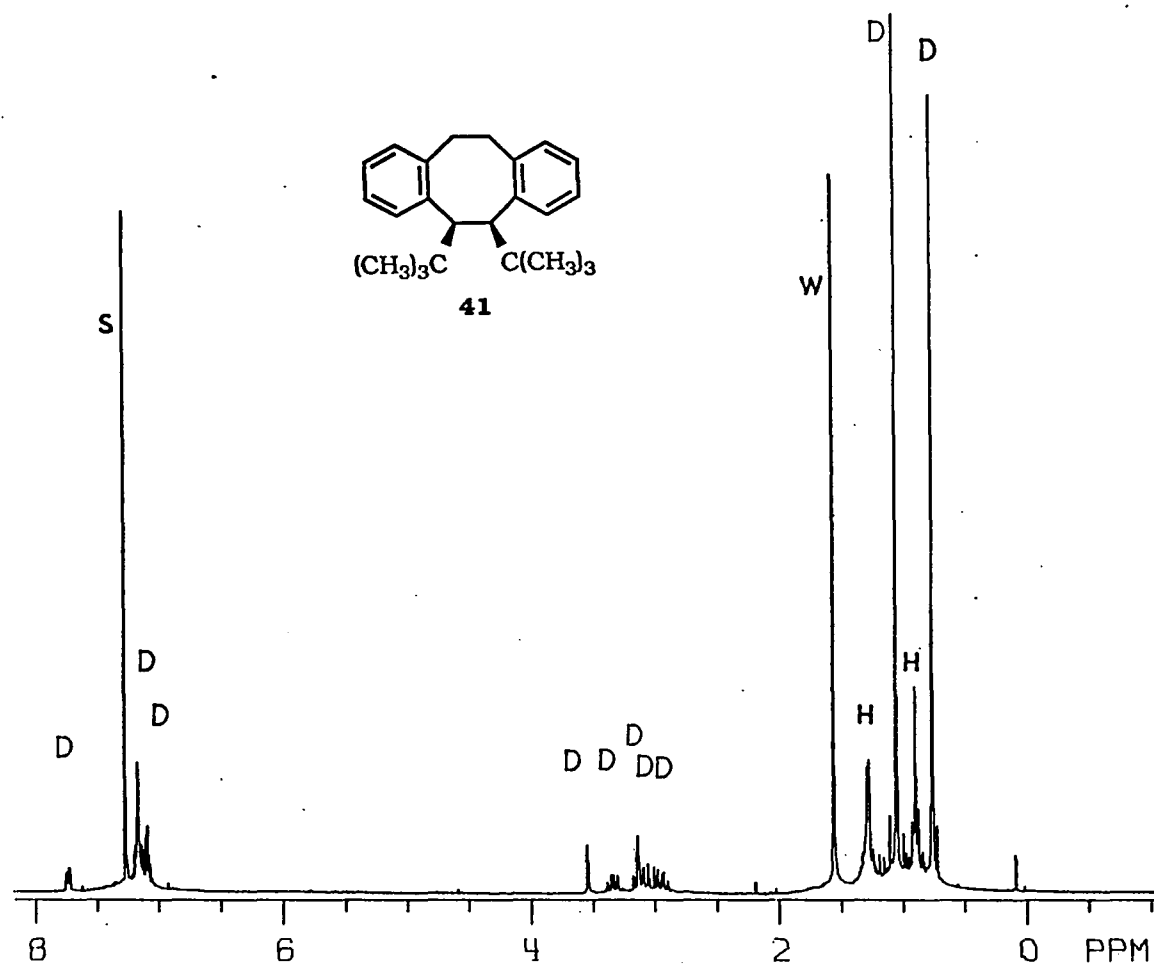
Figure A-15. ^{1}H NMR spectrum (300 MHz, CDCl₃) of the [4+4] dimer **41** of α–*tert*-butyl-*o*-xylylene (**11**) (s: chloroform, w: H₂O, H: high boiling residue from hexanes, the eluent, D: dimer **41**).
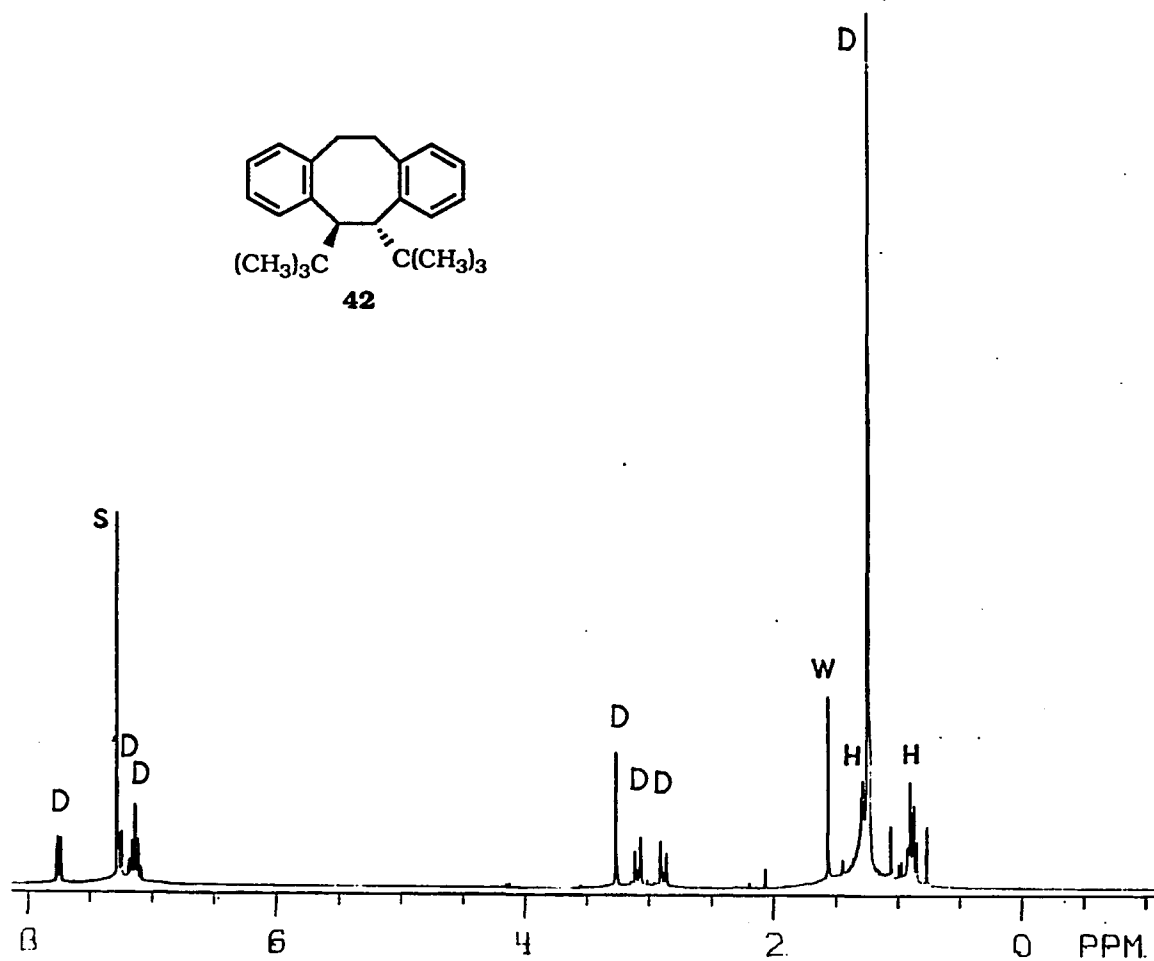
Figure A-16. ^{1}H NMR spectrum (300 MHz, CDCl$_3$) of the thermally less stable [4+4] dimer **42** of α–*tert*-butyl-*o*-xylylene (**11**) (s: chloroform, w: H$_2$O, X: impurities, D: dimer **42**).
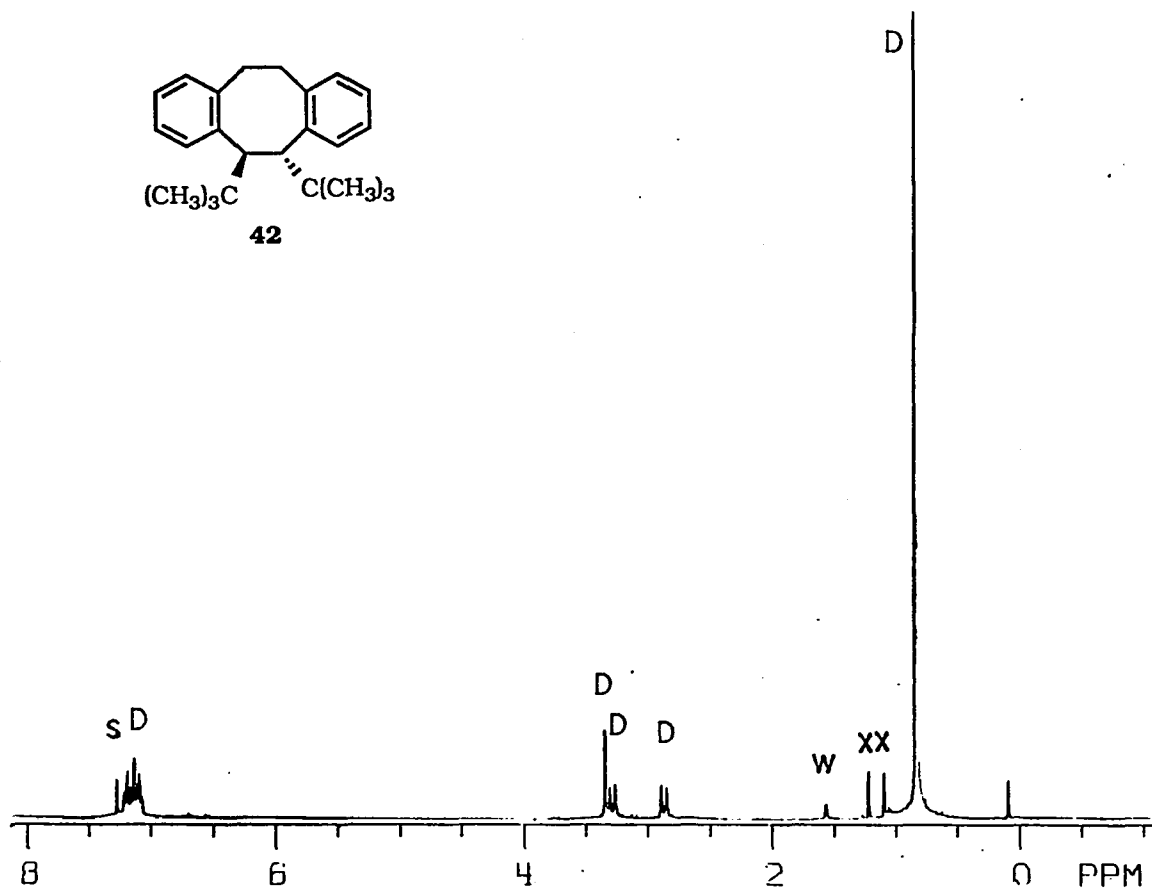
Figure A-17. ^{1}H NMR spectrum (300 MHz, CDCl₃) of the thermally more stable [4+4] dimer **42** of α–*tert*-butyl-*o*-xylylene (**11**) (s: chloroform, w: H₂O, H: high boiling residue from hexanes, the eluent, D: dimer **42**).

2

Dimers **43** and **44**

12

8.   6   4   2   0 PPM

Figure A-18. ^{1}H NMR spectrum (300 MHz, CDCl$_3$) of the dimer mixture of α–mesityl-*o*-xylylene (**12**).

Figure A-19. ^{1}H NMR spectrum (300 MHz, CDCl$_3$) of the [4+2] dimer **43** of α–mesityl-*o*-xylylene (**12**) (s: chloroform, w: H$_2$O, H: high boiling residue from hexanes, the eluent, D: dimer **43**).
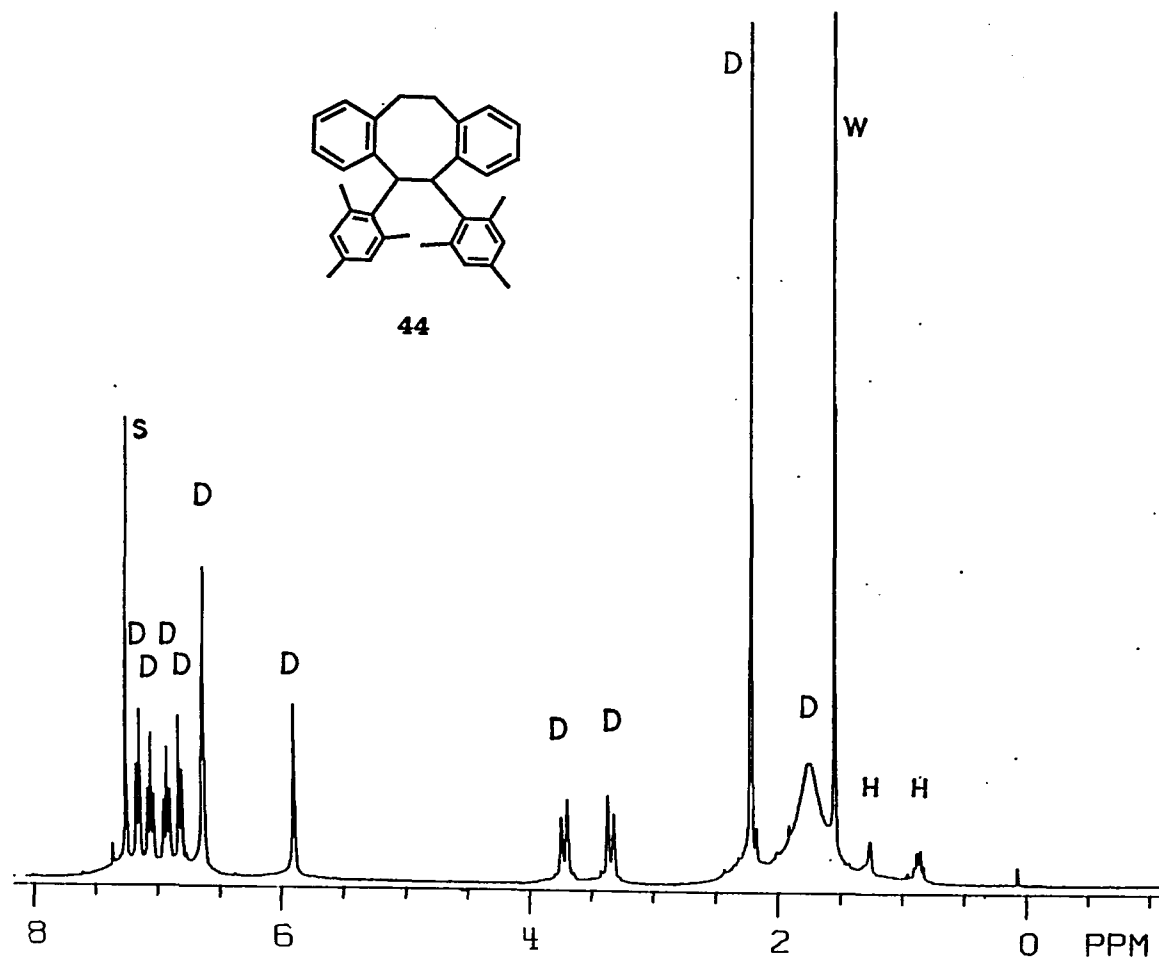
Figure A-20 ^{1}H NMR spectrum (300 MHz, CDCl$_3$) of the [4+4] dimer **44** of α–mesityl-*o*-xylylene (**12**) (s: chloroform, w: H$_2$O, H: high boiling residue from hexanes, D: dimer **44**).
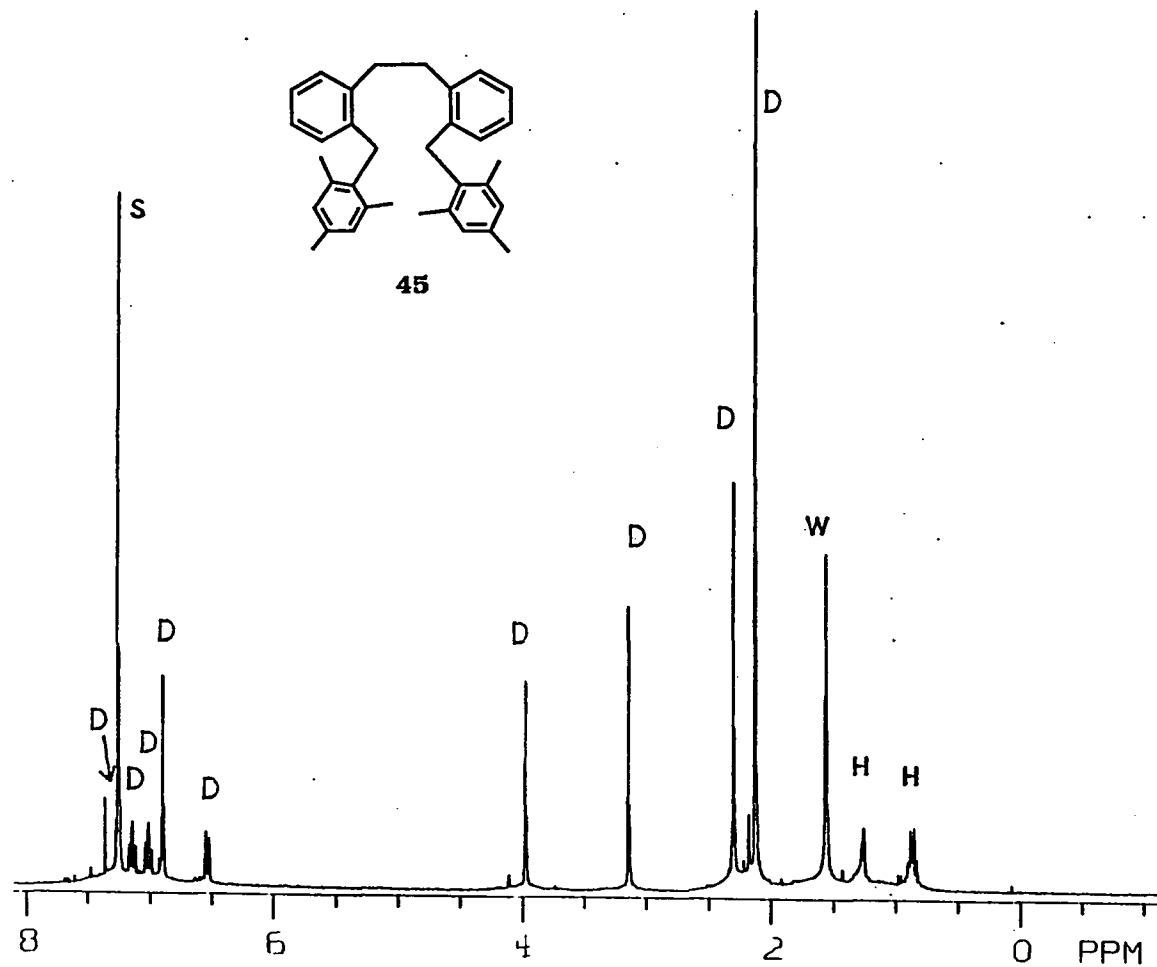
Figure A-21 ^{1}H NMR spectrum (300 MHz, CDCl₃) of the reduction product **45** in the thermolysis of [4+2] dimer **43** in thiophenol at 180 °C in a sealed tube condition (s: chloroform, w: H₂O, H: high boiling residue from hexanes, D: dimer **45**).
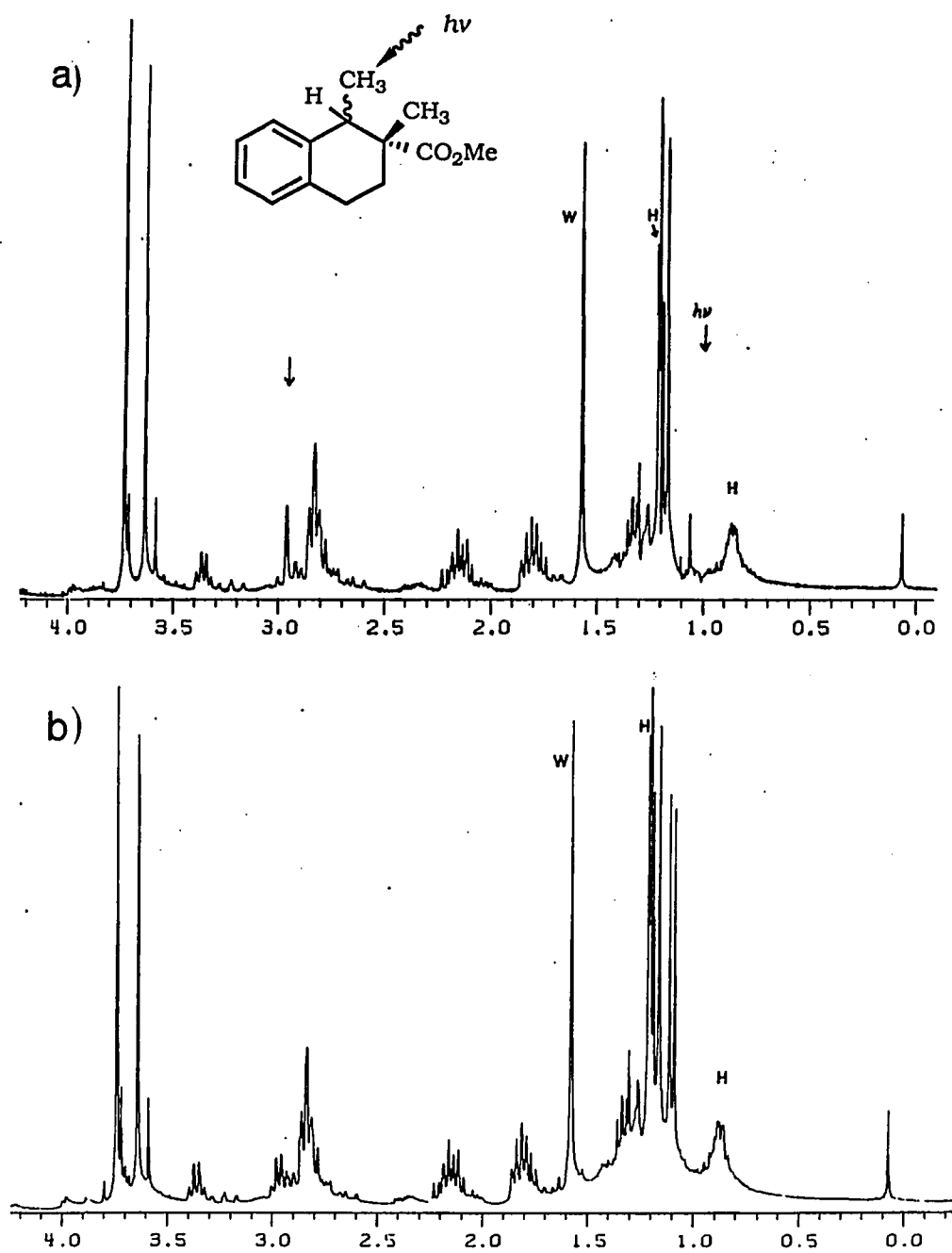
Figure A-22   Closeup of the aliphatic region of the ^{1}H NMR spectrum (300
MHz, CDCl$_3$) of the Diels-Alder reaction products of
α-methyl-*o*-xylylene (9) and methyl methacrylate. (a) Spin-spin
decoupling with irradiation at the methyl proton at 1.09 ppm.
(b) Normal.
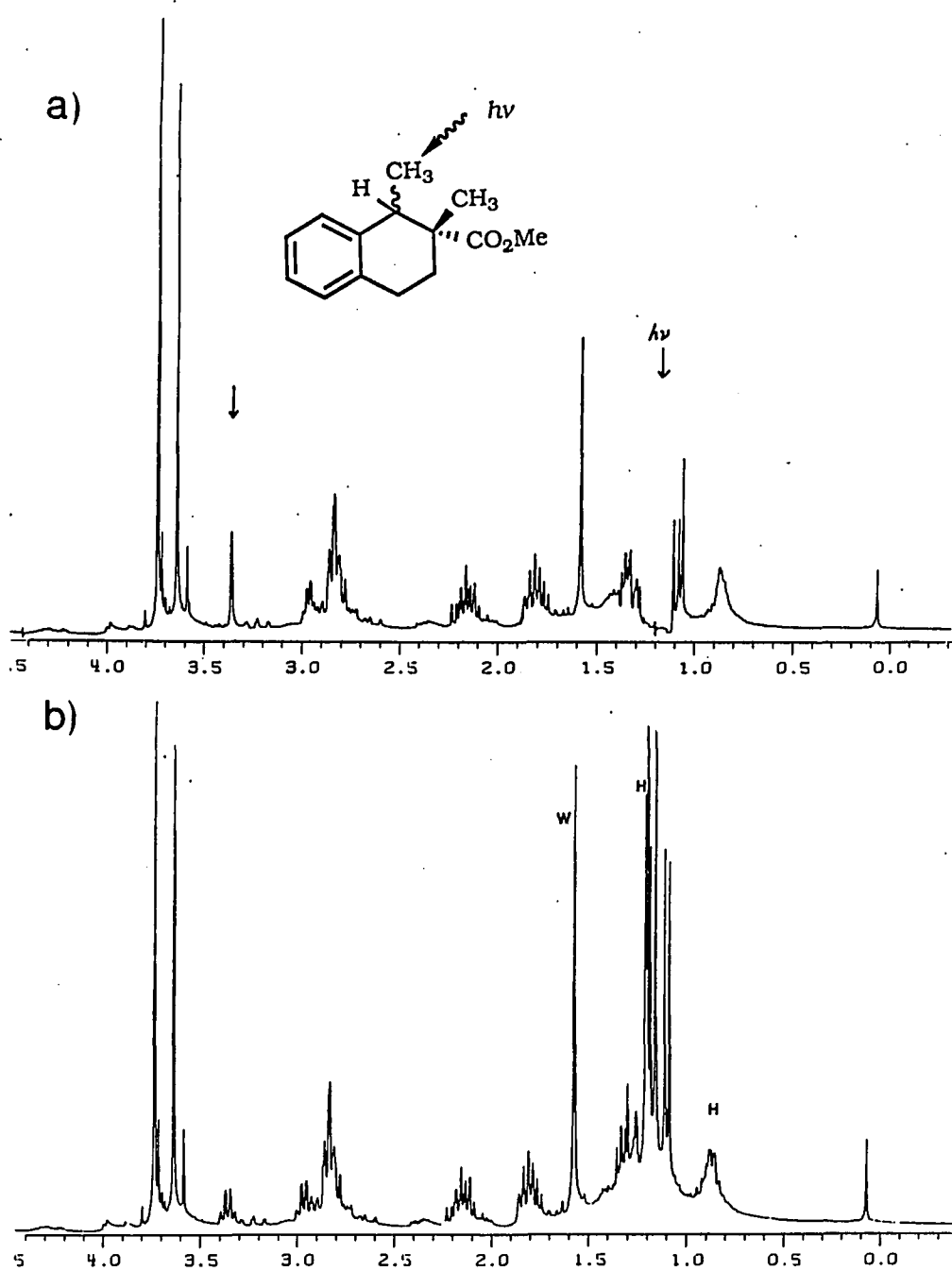
Figure A-23   Closeup of the aliphatic region of the ^{1}H NMR spectrum (300 MHz, CDCl$_3$) of the Diels-Alder reaction products of α–methyl-o-xylylene (9) and methyl methacrylate. (a) Spin-spin decoupling with irradiation at the methyl proton at 1.18 ppm. (b) Normal.
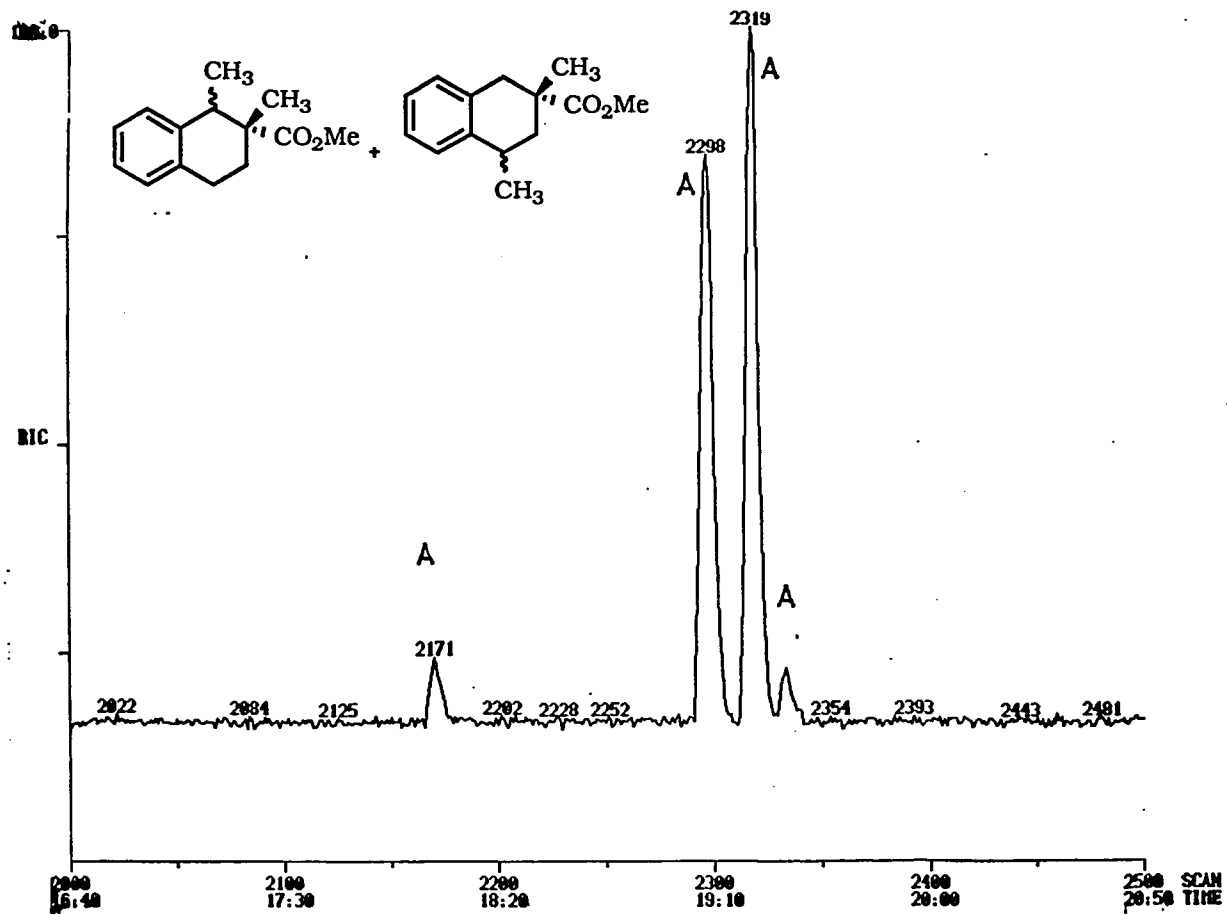
Figure A-24   Gas chromatograph (DB1, temperature program 80 °C, 5 °C/min, 250 °C) of the Diels-Alder reaction products of α–methyl-o-xylylene (9) and methyl methacrylate (A: Diels-Alder adducts).
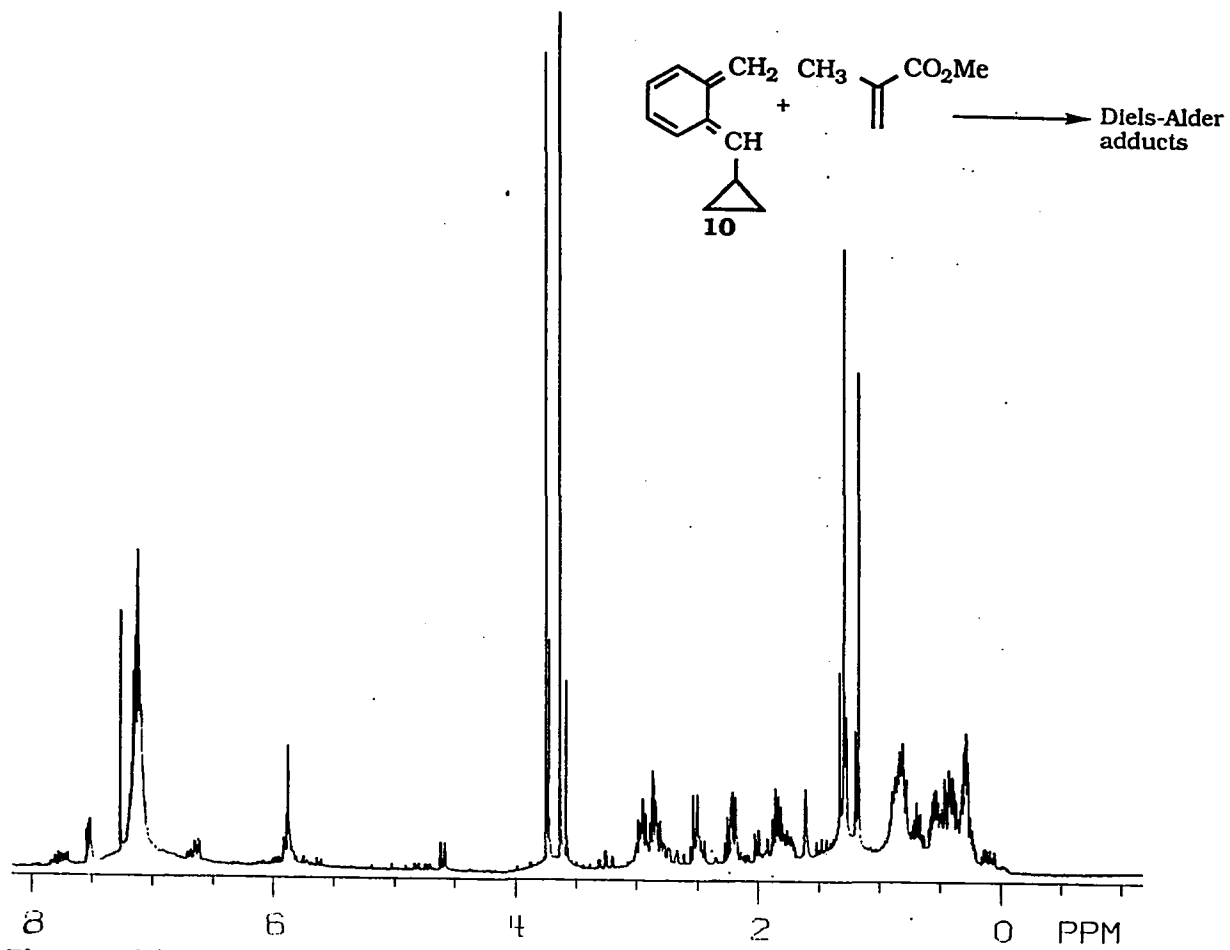
Figure A-25   ¹H NMR spectrum (300 MHz, CDCl₃) of the Diels-Alder reaction products of α–cyclopropyl-o-xylylene (10).
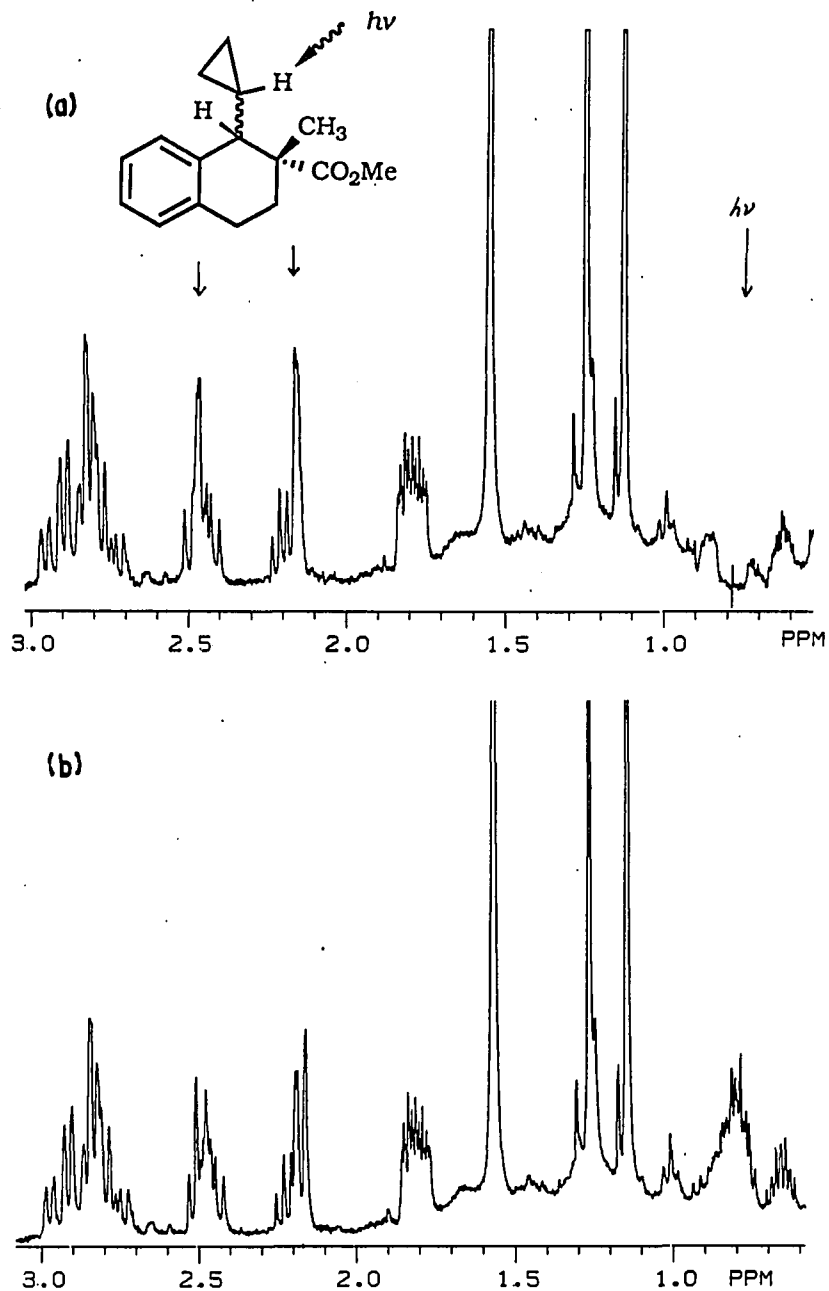
Figure A-26   Closeup of the aliphatic region of the ^{1}H NMR spectrum (300 MHz, CDCl$_3$) of the major two Diels-Alder adducts of α–cyclopropyl-o-xylylene (**10**) and methyl methacrylate. (a) Spin-spin decoupling with irradiation at the cyclopropyl-ring proton at 0.08 ppm. (b) Normal.
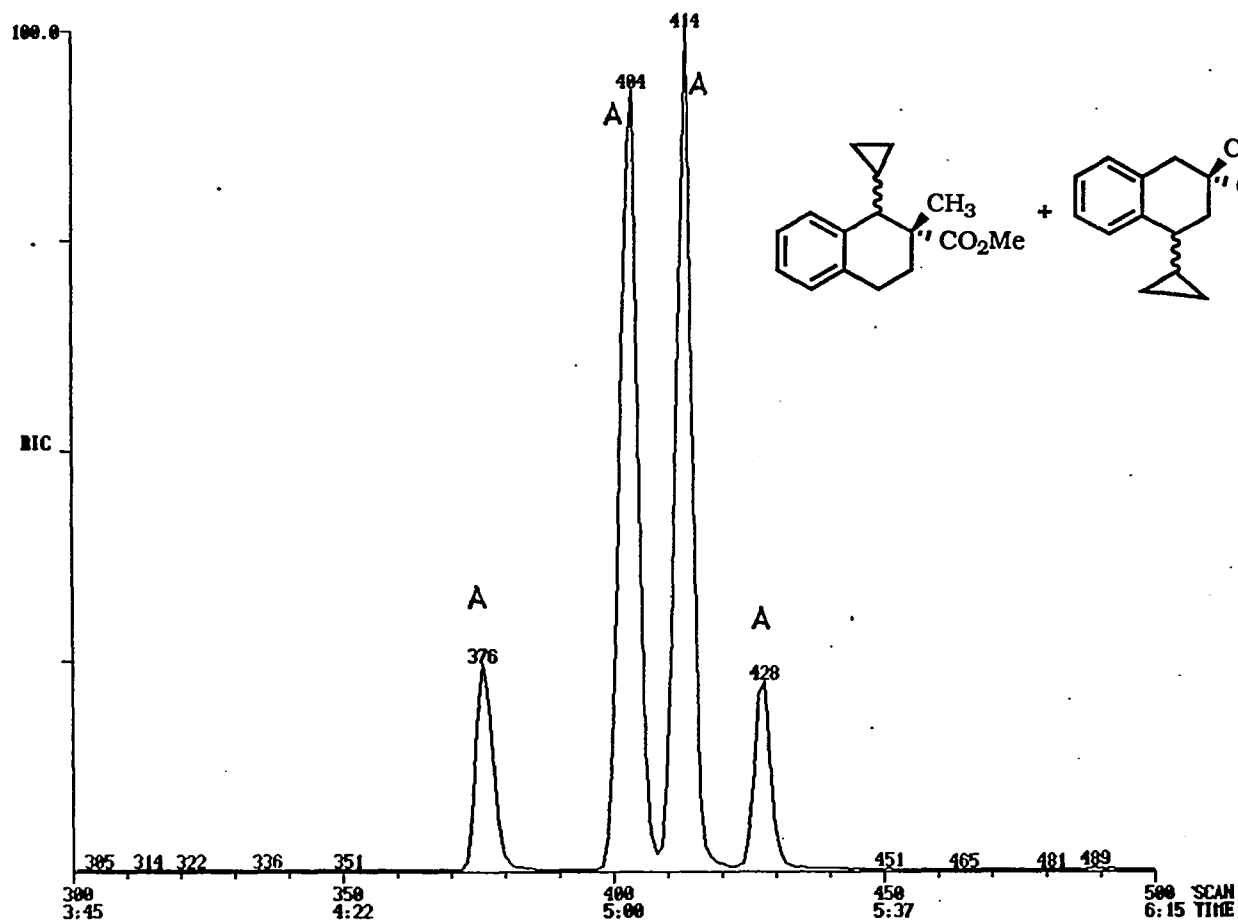
Figure A-27   Gas chromatograph (DB1, temperature program 200 °C) of the Diels-Alder
reaction products of α–cyclopropyl-o-xylylene (**10**) and methyl methacrylate (A:
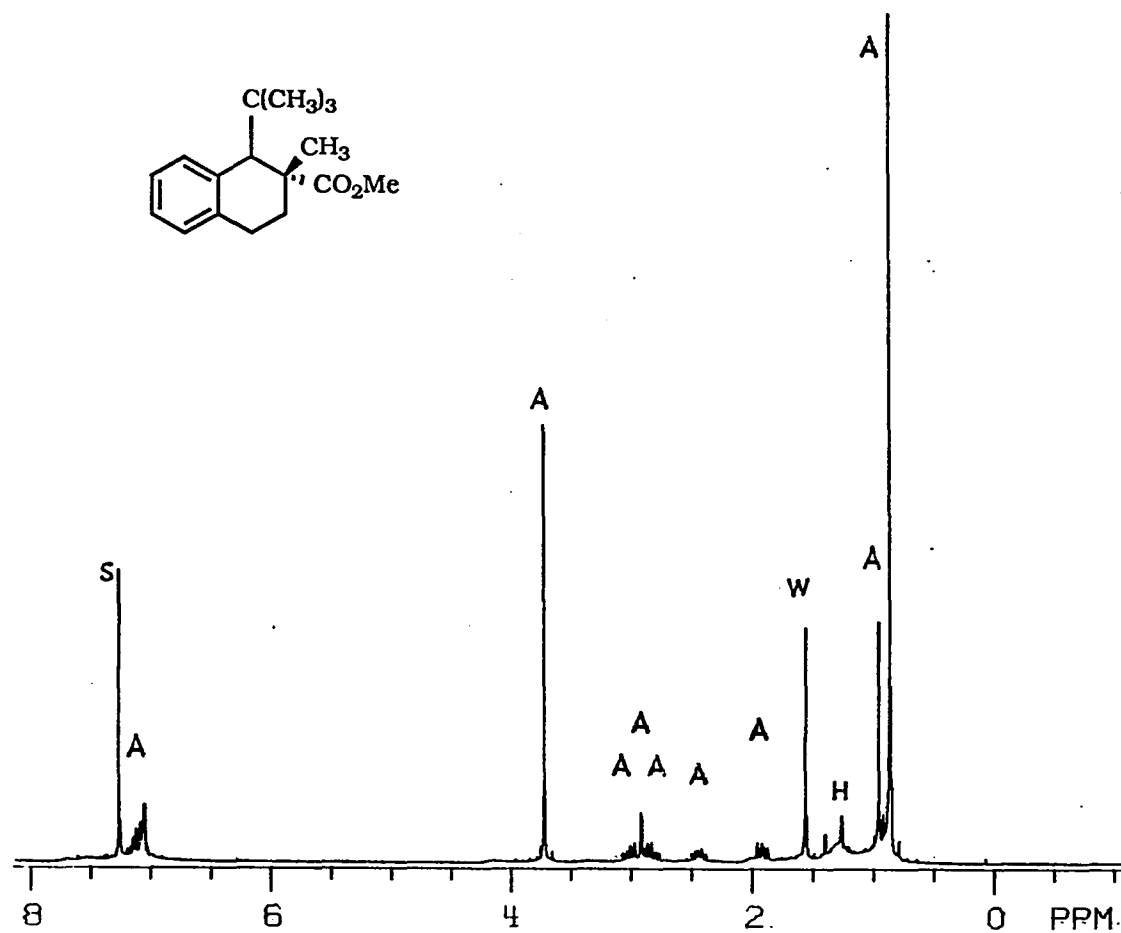Diels-Alder adducts).
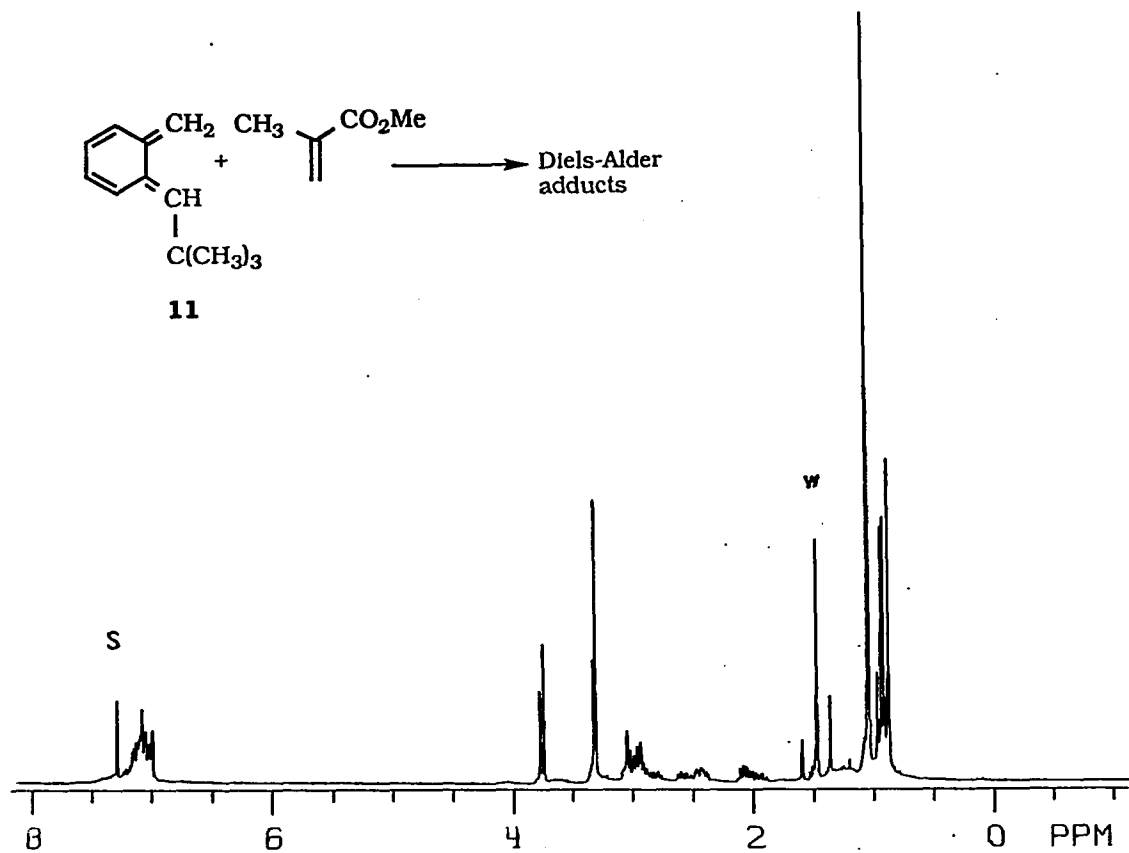
Figure A-28 ^{1}H NMR spectrum (300 MHz, CDCl$_3$) of the Diels-Alder reaction products of α–*tert*-butyl-*o*-xylylene (**11**) and methyl methacrylate (s: chloroform, w: H$_2$O).
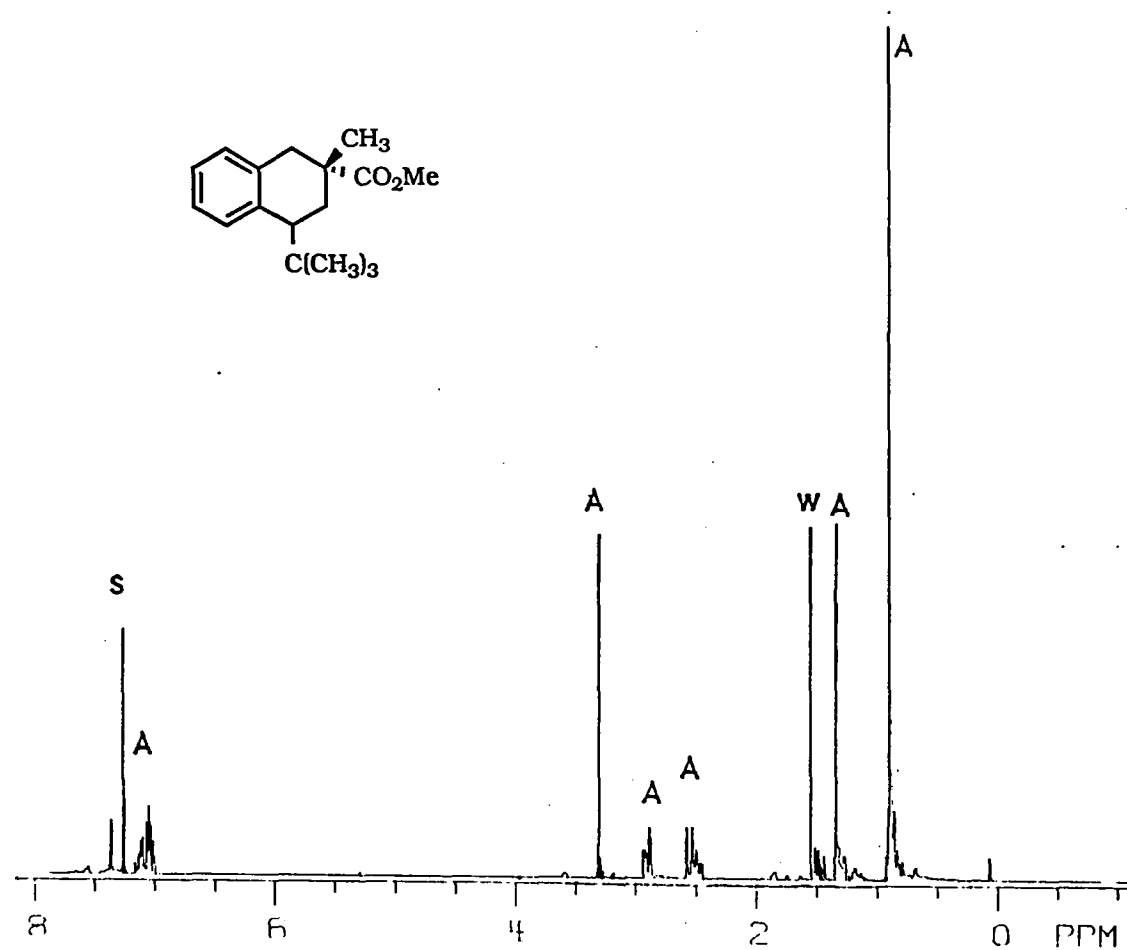
Figure A-29 ^{1}H NMR spectrum (300 MHz, CDCl$_3$) of component 1 of Diels-Alder reaction products of α–*tert*-butyl-*o*-xylylene (**11**) and methyl methacrylate (s: chloroform, w: H$_2$O, A: Diels-Alder adducts).
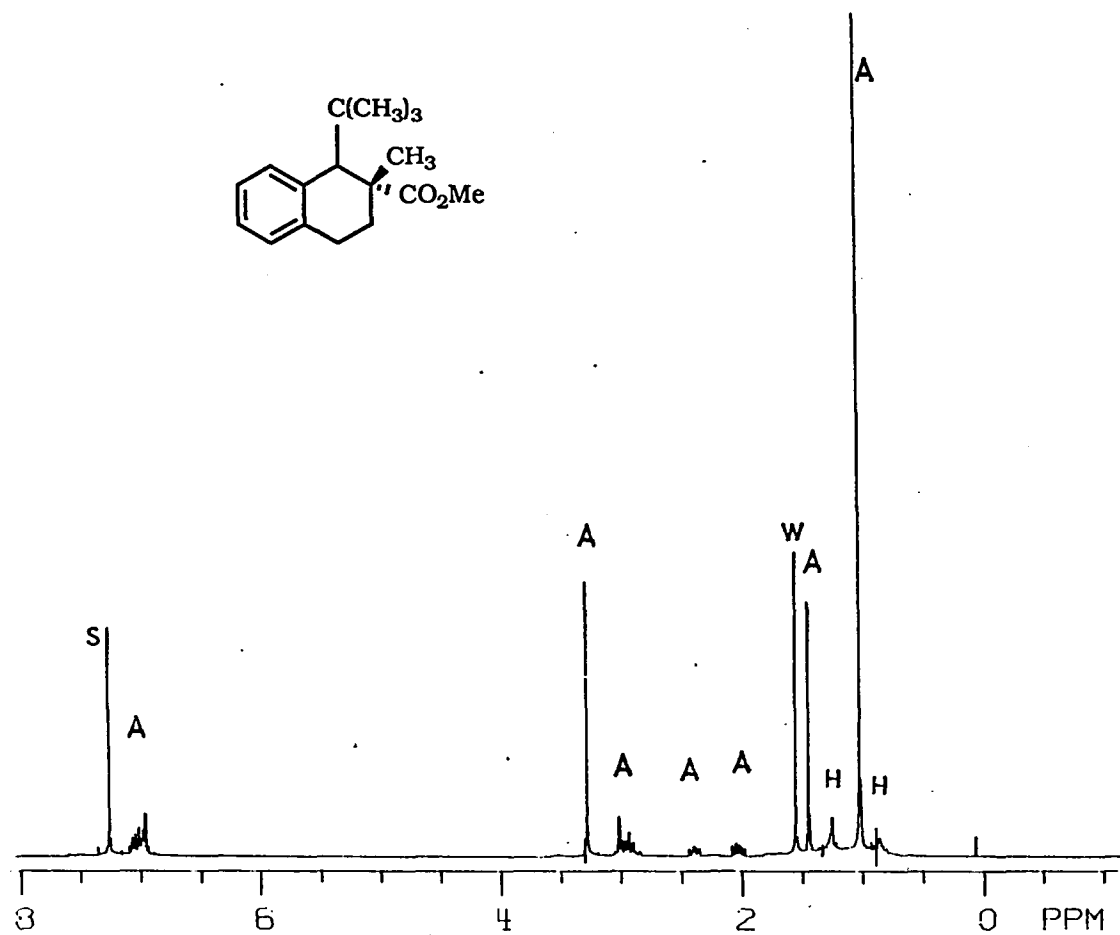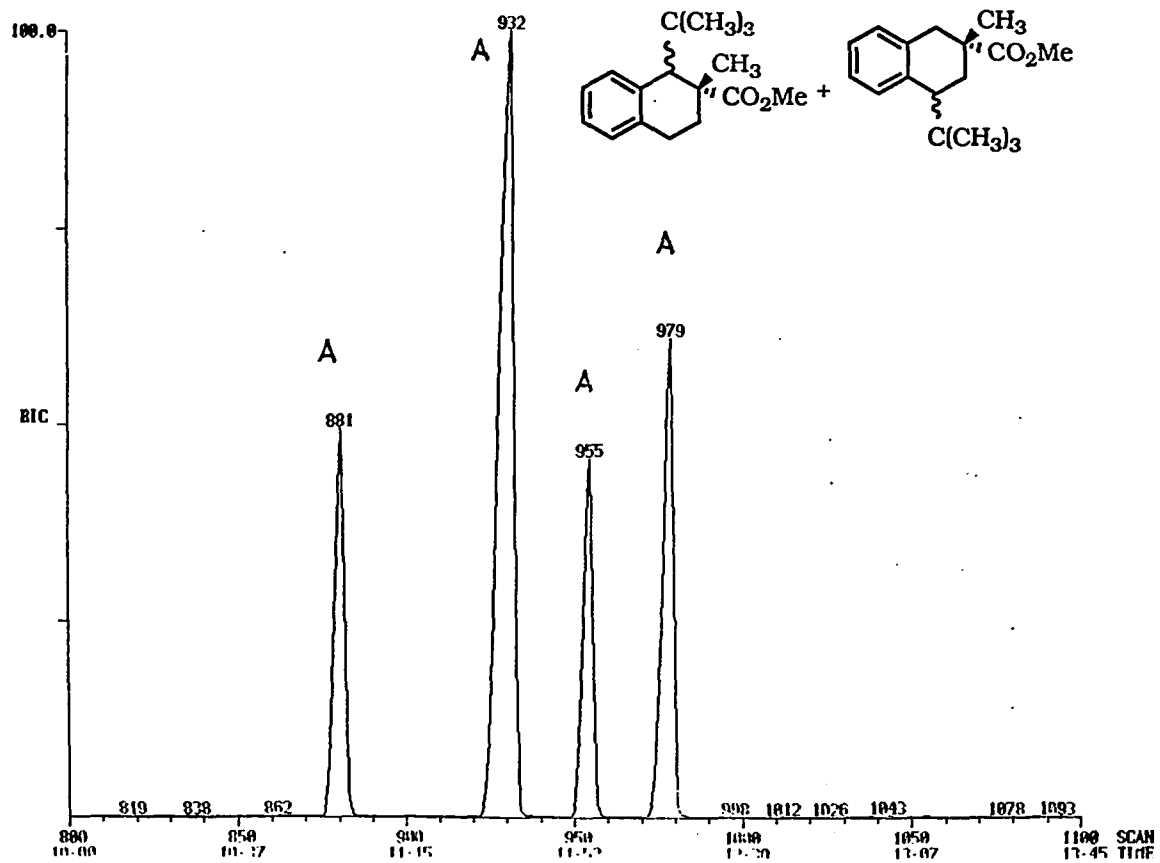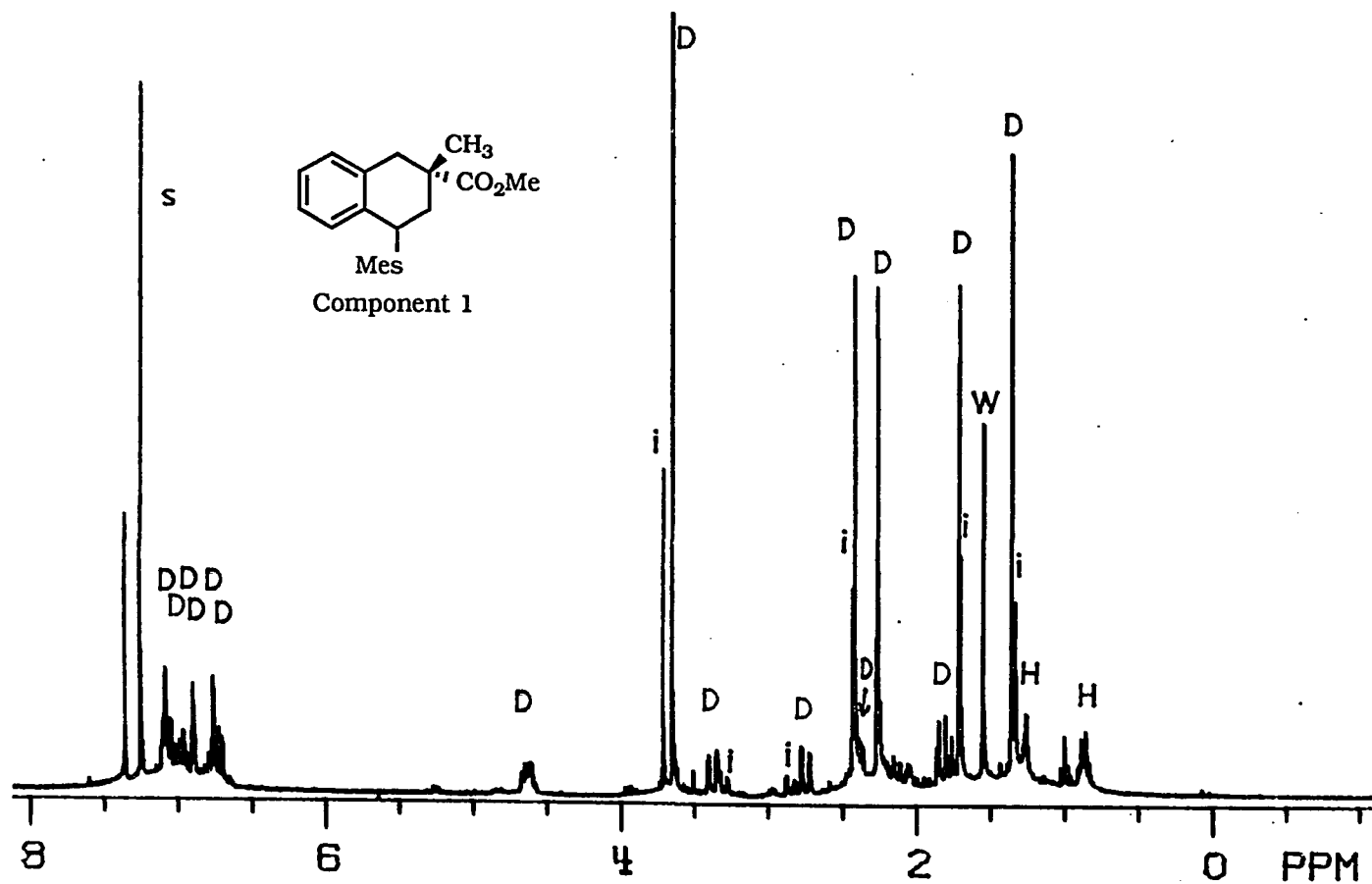
Figure A-30 ^{1}H NMR spectrum (300 MHz, CDCl$_3$) of component 2 of Diels-Alder reaction products of α–*tert*-butyl-*o*-xylylene (**11**) and methyl methacrylate (s: chloroform, w: H$_2$O, H: high boiling hydrocarbon from the chromatography eluent, hexanes, A: Diels-Alder adducts).
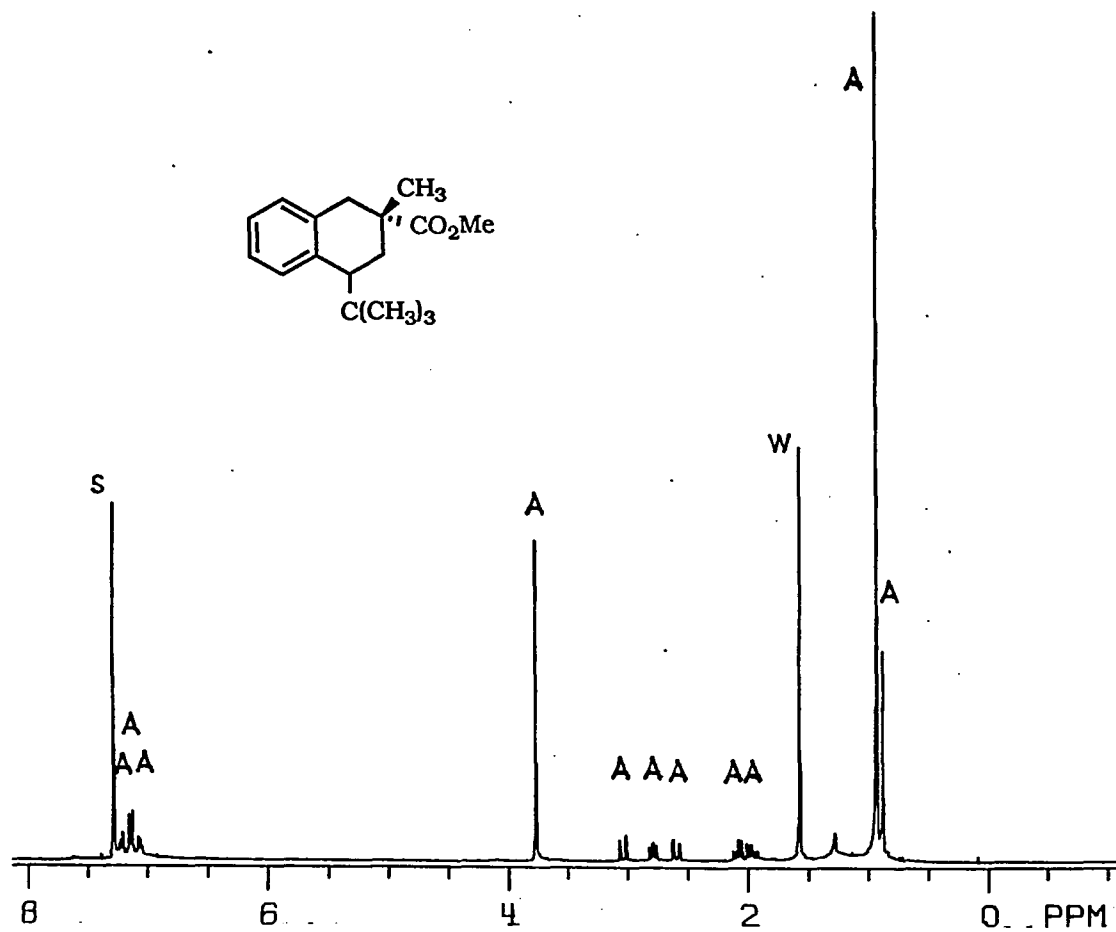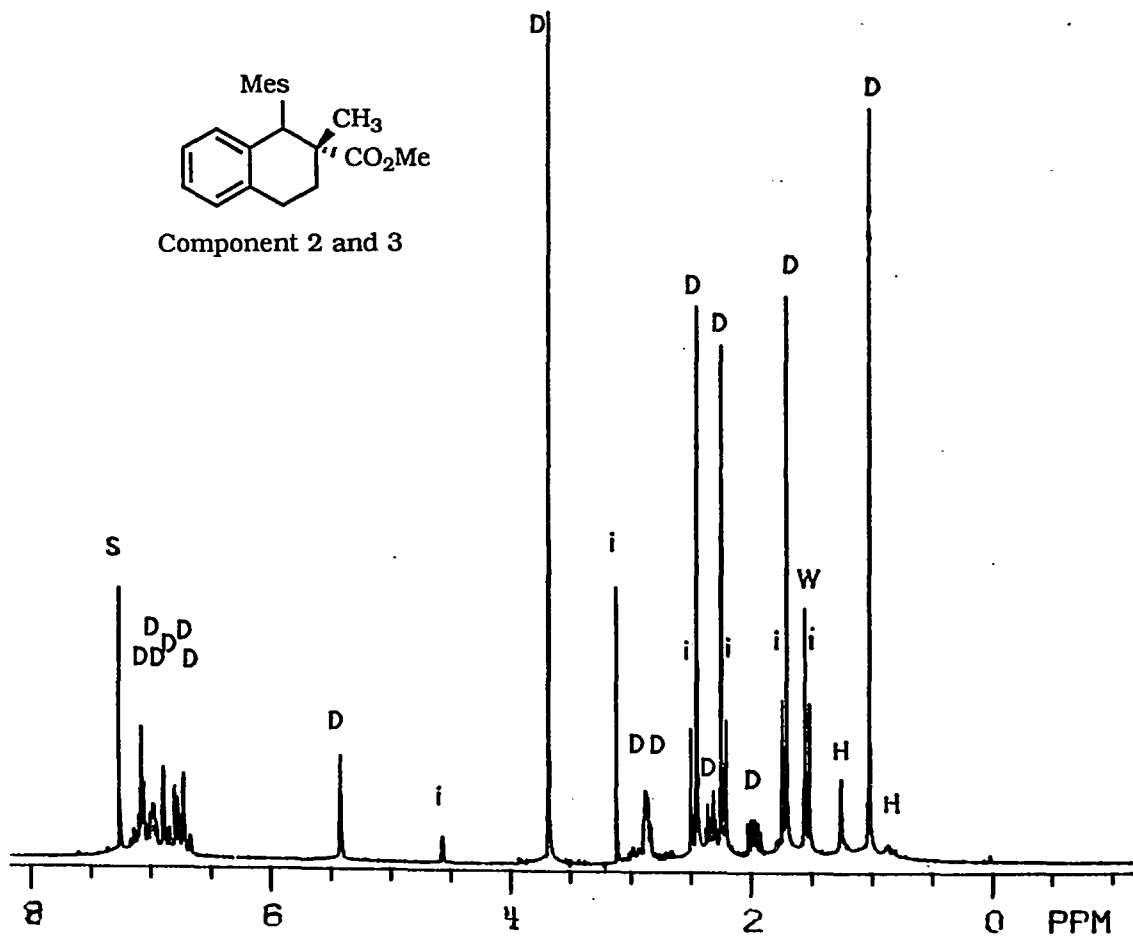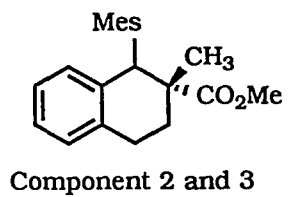
**Figure A-31**   ^{1}H NMR spectrum (300 MHz, CDCl3) of component 3 of Diels-Alder reaction products of α–*tert*-butyl-*o*-xylylene (**11**) and methyl methacrylate (s: chloroform, w: H2O, A: Diels-Alder adducts).

Figure A-32 ^{1}H NMR spectrum (300 MHz, CDCl$_3$) of component 4 of Diels-Alder reaction products of α–*tert*-butyl-*o*-xylylene (**11**) and methyl methacrylate (s: chloroform, w: H$_2$O, A: Diels-Alder adducts).

Figure A-33   Gas chromatograph (DB1, temperature program 100 °C, 10 °C/min, 250 °C) of the Diels-Alder reaction products of α–mesityl-o-xylylene (11) and methyl methacrylate (D: Diels-Alder adducts).

Figure A-34 ^{1}H NMR spectrum (300 MHz, CDCl$_3$) of component 1, (contaminated with 30 % of component 4) of Diels-Alder reaction products of α–mesityl-o-xylylene (12) and methyl methacrylate (s: chloroform, w: H$_2$O, H: high boiling hydrocarbons from the chromatography eluent, hexanes, i: component 4, D: component 1).

Figure A-35 ^{1}H NMR spectrum (300 MHz, CDCl$_3$) of a mixture component 2 and 3 of Diels-Alder reaction products of α–mesityl-o-xylylene (**12**) and methyl methacrylate (s: chloroform, w: H$_2$O, H: high boiling hydrocarbons from the chromatography eluent, hexanes, D: conponent 3, i, component 4).

Figure A-36 ^{1}H NMR spectrum (300 MHz, CDCl$_3$) of component 4 of the Diels-Alder reaction products of α–mesityl-o-xylylene (**12**) and methyl methacrylate (s: chloroform, w: H$_2$O, H: high boiling hydrocarbons from the chromatography eluent, hexanes, D: component 4, X: impurities).
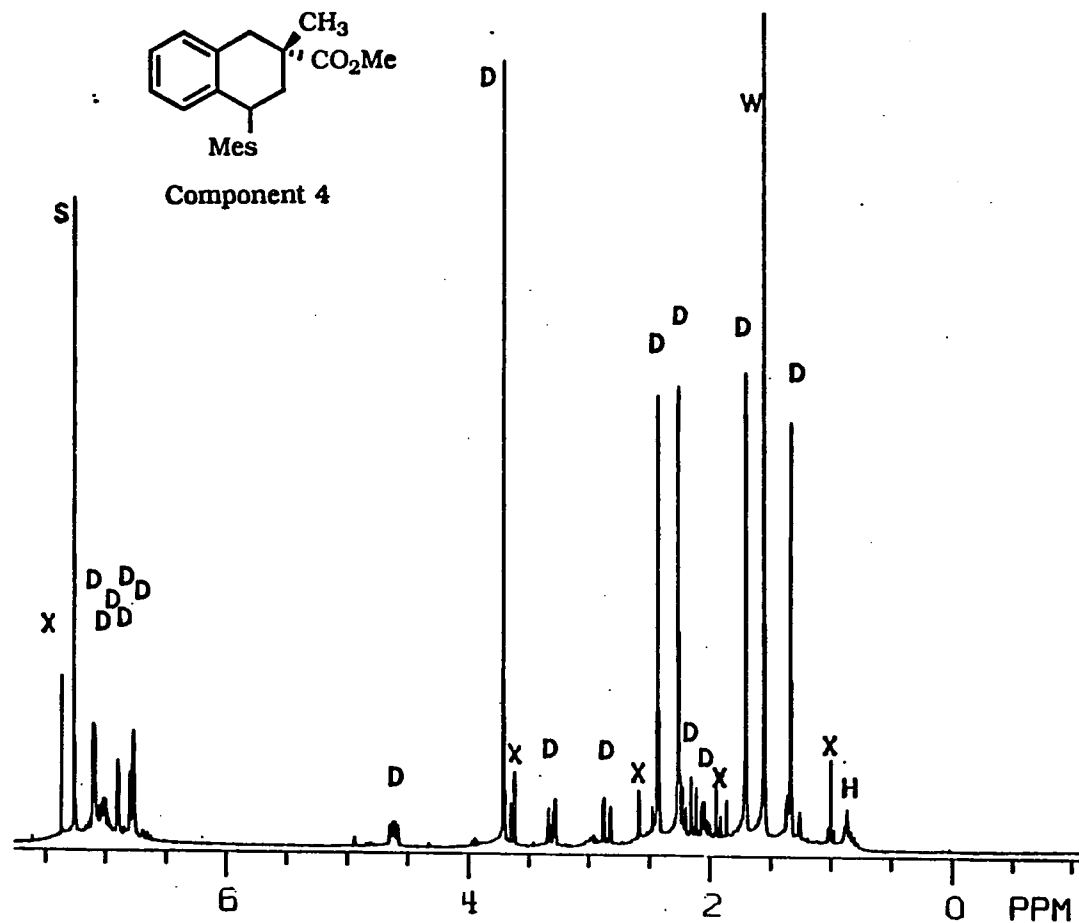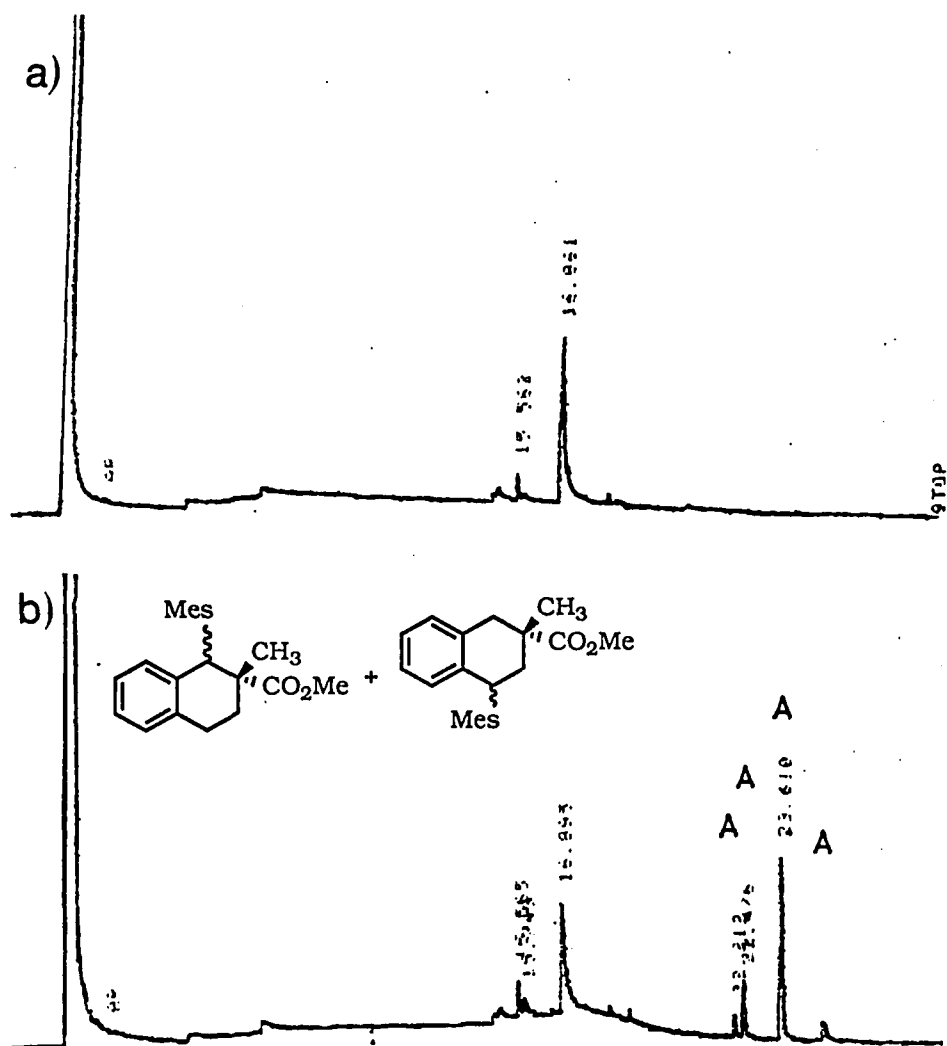
Figure A-37   Gas chromatograph (DB1, temperature program 120 °C, 5 min, 10 °C/min, 200 °C, 10 min) of the Diels-Alder reaction products of α–mesityl-o-xylylene (**12**) and methyl methacrylate: (a) without methyl methacrylate, (b) with methyl methacrylate (A: Diels-Alder adducts).
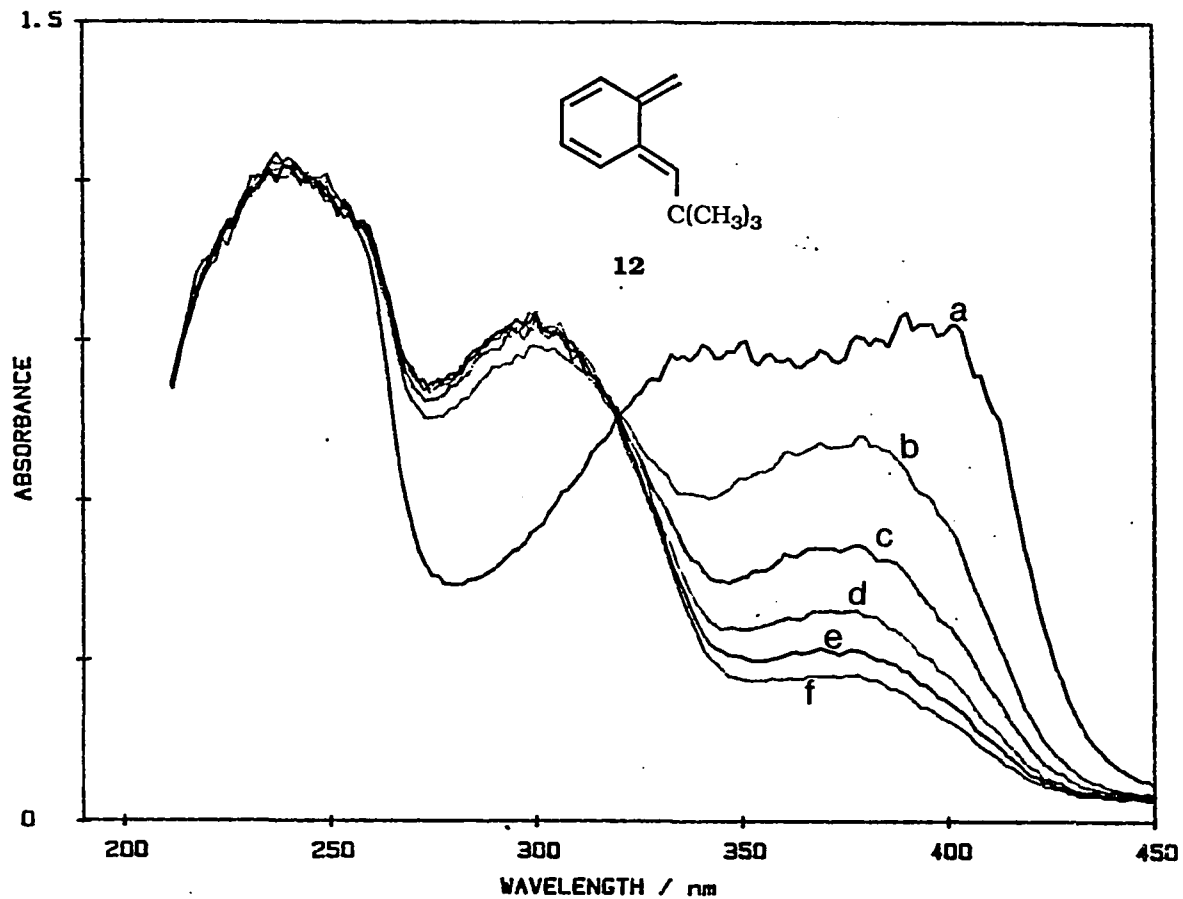
Figure A-38   UV-visable spectra of α–*tert*-butyl-*o*-xylylene **(11)** and its subsequent dimerization at room temperature. (a) t = 0 min, (b) t = 0.09 min, (c) t = 0.27 min, (d) 0.36 min, (e) 0.45 min, (f) 0.54 min.
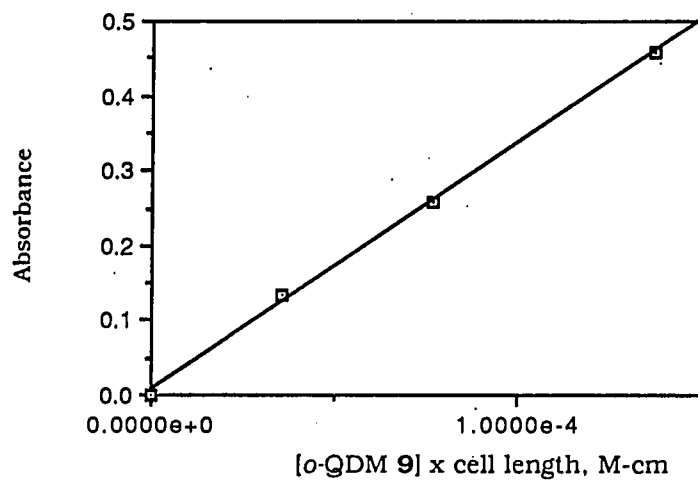
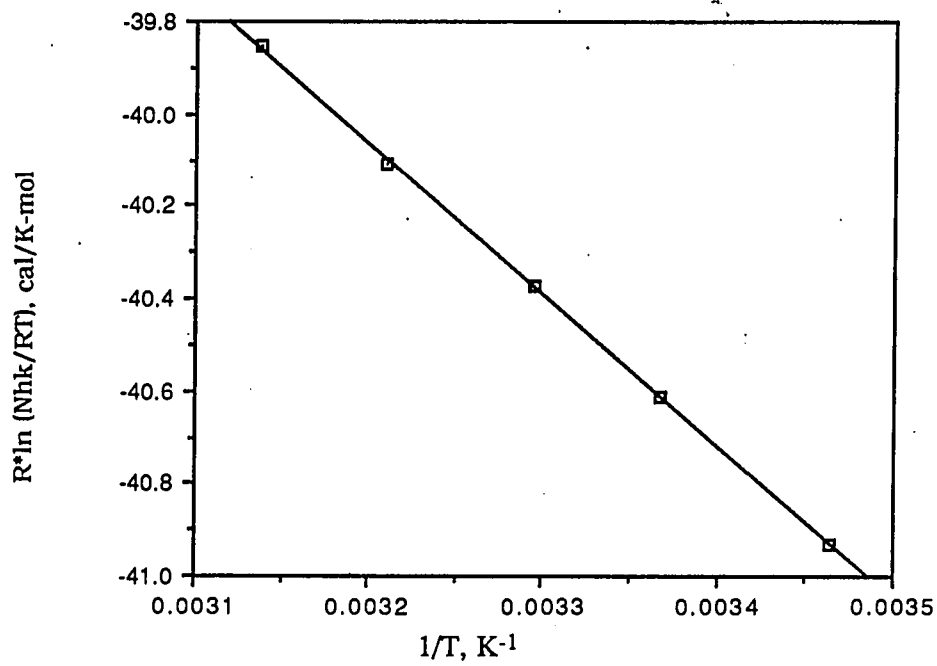**Figure A-39.**   The Beer's plot for α-methyl-*o*-xylylene (**9**).

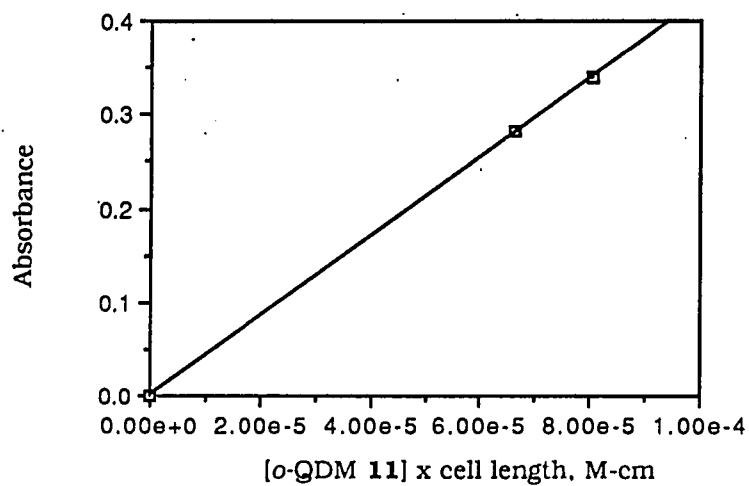**Figure A-40.**   Eyring plot for the dimerization of α-methyl-*o*-xylylene (**9**)

Figure A-41.   The Beer's plot for α–*tert*-butyl-*o*-xylylene (**11**)
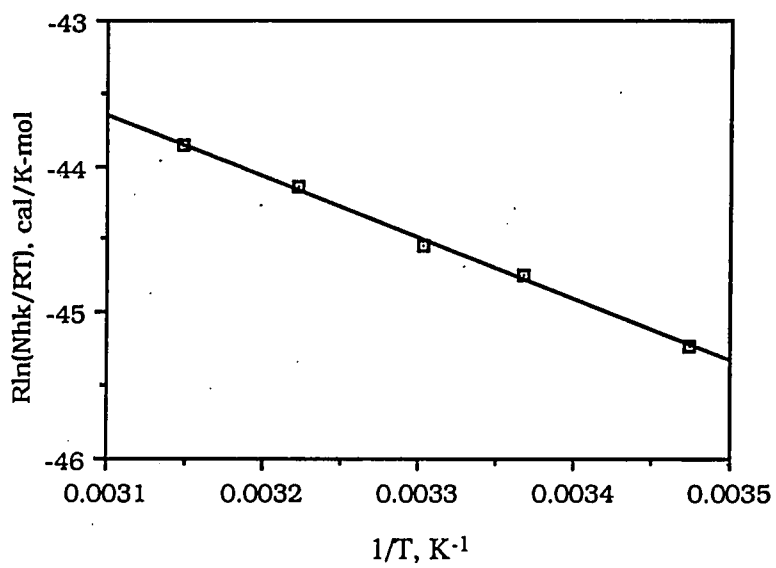
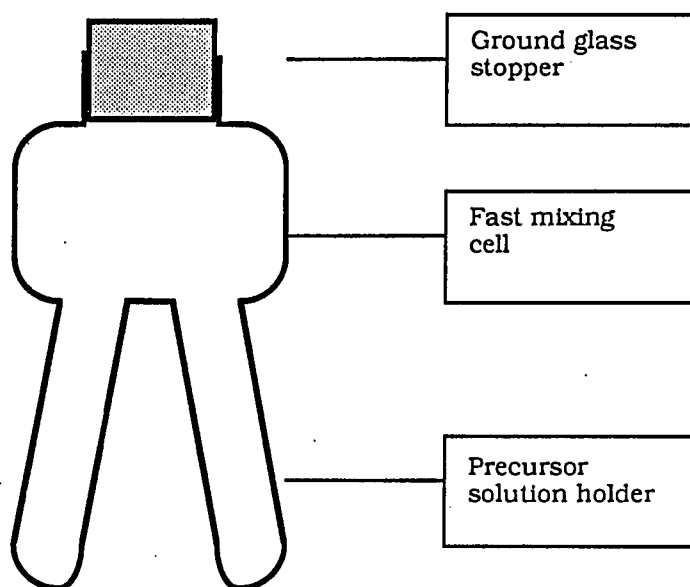**Figure A-42**   Eyring plot for the dimerization of α-*tert*-butyl-*o*-xylylene (11).

Figure A-43.   The fast mixing cell used in the competition experiment
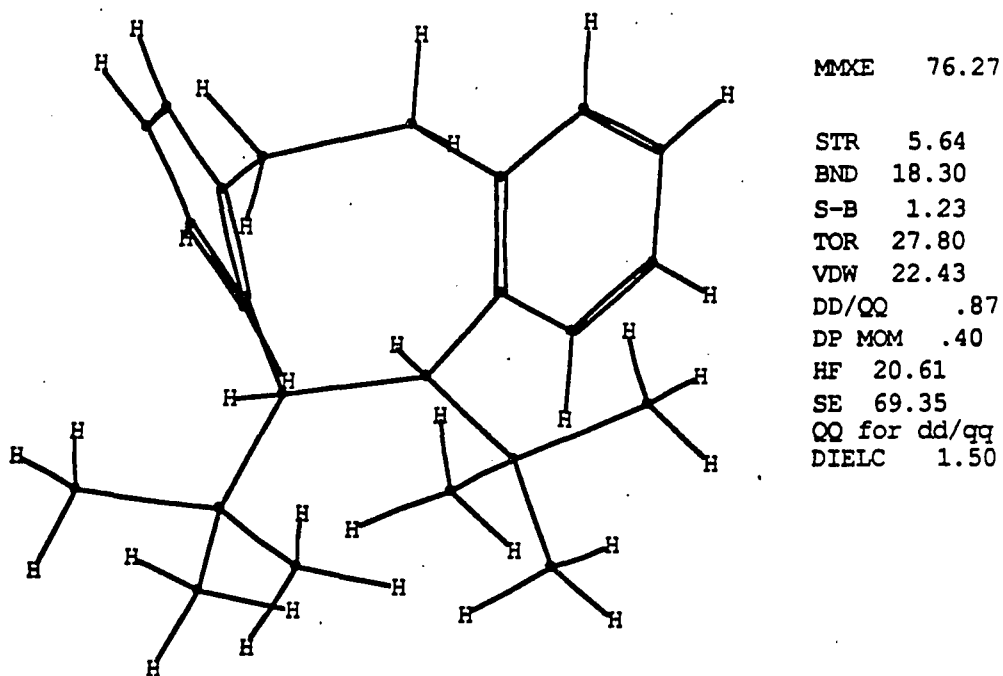for the Diels-Alder reaction and the dimerization of o-QDM

MMXE   76.27

STR   5.64
BND   18.30
S-B   1.23
TOR   27.80
VDW   22.43
DD/QQ   .87
DP MOM   .40
HF   20.61
SE   69.35
QQ for dd/qq
DIELC   1.50

Figure 44.   The thermodynamically-stable conformation, predicted by MM-X
calculations, of *cis*-[4+4] dimer **42**.

MMXE   67.51

STR   5.41
BND   18.12
S-B   1.15
TOR ~ 22.52
VDW   19.46
DD/QQ   .85
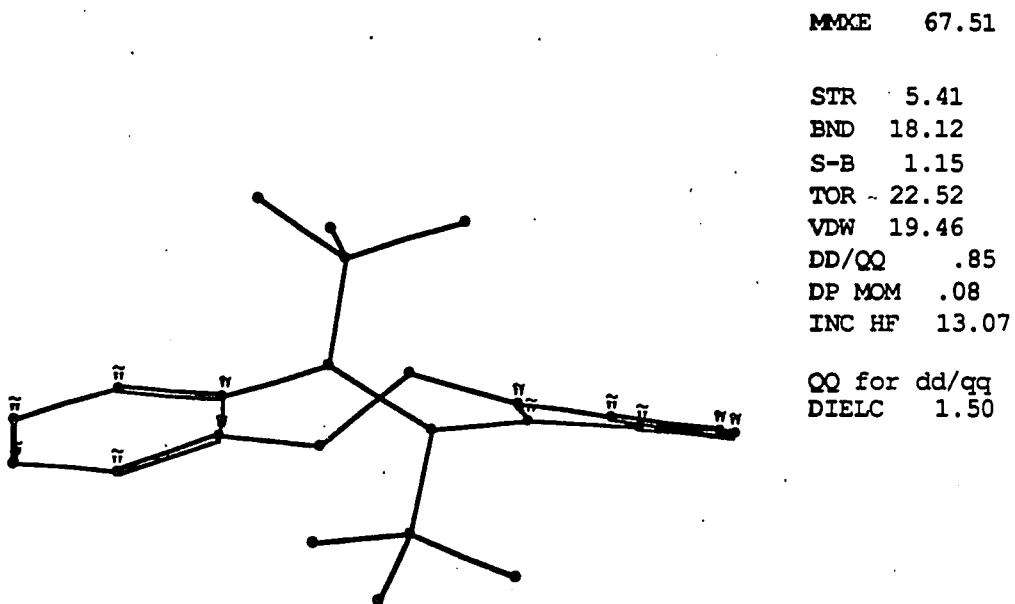DP MOM   .08
INC HF   13.07

QQ for dd/qq
DIELC   1.50

Figure 45. The thermodynamically stable conformation, predicted by MM-X
calculations, of the *trans*-[4+4] dimer **43.**

GENERAL SUMMARY

Effects of the α–substitutions on the termini of the reactive diene unit of o-quinodimethanes revealed a non-concerted mechanism for furan-based and benzene-based o-quinodimethane (o-QDM) dimerizations.

In section one, the co-existence of the cisoid (8) and transoid (9) transition states in the diradical formation step is evidenced by the stereochemistry of the dimers. In view of the results of the furan-based o-QDM dimerizations, we believe that the regioselectivity in the diradical cyclization step is controlled mainly by the interaction between the active sites on the furan moieties in the diradical ring closure step, not by the internal bond rotations of the carbon chain of the diradical intermediate.

In section two, we found that the trend of the regioselectivity, along the size of the α–substituents, of benzene-based o-QDM dimerizations is opposite to that of the Diels-Alder reactions. On the basis of the trends, we suggest that the Diels-Alder reaction mechanism of benzene-based o-QDM's is concerted while the dimerization mechanism of benzene-based o-QDM's is stepwise. Because of their similar activation parameters, we propose that the parent o-xylylene (1') and other o-xylylenes 9'-12' dimerize via a similar two step, diradical mechanism.

ACKNOWLEDGEMENTS